Post-Translational Protein Modifications involved in Exo- and Endocytosis of Synaptic Vesicles

Dissertation

for the award of the degree

“Doctor rerum naturalium”

of the Georg-August-Universität Göttingen

within the doctoral program

“Biomolecules: Structure-Function-Dynamics”

of the Georg-August University School of Science (GAUSS)

submitted by

Ivan Silbern

from Tschebarkul, Russia

Göttingen, 2021

Thesis Committee

Prof. Dr. Henning Urlaub	Bioanalytical Mass Spectrometry Max-Planck Institute for Biophysical Chemistry, Göttingen; Institute for Clinical Chemistry University Medical Center, Göttingen
Prof. Dr. Reinhard Jahn	Laboratory of Neurobiology Max-Planck Institute for Biophysical Chemistry, Göttingen
Prof. Dr. Silvio O. Rizzoli	Department of Neuro- and Sensory Physiology, University Medical Center Göttingen

Members of the Examination Board

Reviewer	
Prof. Dr. Henning Urlaub	Bioanalytical Mass Spectrometry Max-Planck Institute for Biophysical Chemistry, Göttingen; Institute for Clinical Chemistry University Medical Center, Göttingen
Second Reviewer	
Prof. Dr. Reinhard Jahn	Laboratory of Neurobiology Max-Planck Institute for Biophysical Chemistry, Göttingen

Further members of the Examination Board

Prof. Dr. Silvio O. Rizzoli	Department of Neuro- and Sensory Physiology, University Medical Center Göttingen
Prof. Dr. Nils Brose	Department of Molecular Neurobiology, Max Planck Institute of Experimental Medicine, Göttingen
Prof. Dr. Tobias Moser	Institute for Auditory Neuroscience and InnerEarLab, University Medical Center Göttingen
Dr. Alexander Stein	Research Group Membrane Protein Biochemistry, Max Planck Institute for Biophysical Chemistry, Göttingen

Date of oral examination: 13th of October 2021

~ Dedicated to my daughter Margarita ~

Abstract

Neurotransmitter release is a key step that enables information flow between the pre- and post-synapse. However, regulation of the neurotransmitter release remains an intricate and widely unexplored matter despite recent advances in the understanding of the neurotransmitter release machinery and the analysis of the synaptic proteome and protein modifications. Indeed, post-translational protein modifications such as phosphorylation are suitable to quickly fine-tune the neurotransmitter release “in place” via affecting tertiary protein structures and protein-protein interactions, and globally, via modulating signaling pathways. Here, the investigations were focused on the dependence of protein phosphorylation in synaptosomes on the synaptic vesicle (SV) cycling, determining kinase-substrate interactions, and modulatory effects of selected sites on exo- and endocytosis.

The analysis of synaptic phosphoproteome was conducted using TiO_2-based enrichment of phosphorylated peptides with subsequent chemical labeling by isobaric mass tags (TMT) and a mass spectrometry-based quantification. Synaptosomes were employed as a functional model of a synapse as they contain the required neurotransmitter release machinery and respond to stimulation. First, the applicability of electrical stimulation was tested. The field-stimulation evoked reproducible glutamate release that was significantly suppressed in the absence of Ca^{2+}, though it remained uncertain, to which degree the release is governed by exocytosis. Therefore, another approach using a KCl-induced depolarization and treatment with botulinum neurotoxins (BoNTs) was used to identify phosphorylation events that depend on SV cycling. BoNTs cleave specifically SNARE proteins and thus block exocytosis and SV cycling, but do not impede Ca^{2+}-influx evoked by the plasma membrane depolarization. Comparison of phosphorylation events in synaptosomes stimulated in the presence of Ca^{2+}, EGTA (0 net Ca^{2+}) or pre-treated with BoNTs identified sites that were differentially phosphorylated following BoNT treatment, *i.e.*, SV-cycling-dependent sites, and sites that were differentially phosphorylated when comparing Ca and EGTA conditions, but did not change under BoNT treatment, *i.e.*, primarily Ca^{2+}-dependent sites. Further differential expression analysis revealed that BoNT-treatment mostly caused de-phosphorylation of synaptic proteins. A kinase-substrate analysis showed that >25% of BoNT-responsive sites are predicted MAPK substrates and <9% are putative CaMKII targets. In contrast, >20% of primarily Ca^{2+}-dependent sites are presumably regulated by CaMKII, which corroborates Ca^{2+}-dependence of these phosphorylation events. SV-cycling-dependent phosphorylation sites on syntaxin-1 (T21/T23-*Stx1*), synaptobrevin (S75-*Vamp2*), and cannabinoid receptor-1 (S314/T322-*Cnr1*) were further investigated for their impact on exo- and endocytosis. In collaboration with Dr. Eugenio Fornasiero and Prof. Dr. Silvio O. Rizzoli, corresponding phosphomimetic and non-phosphorylatable variants of the proteins were expressed in

cultured hippocampal neurons. Imaging of the pH-sensor pHluorine coupled to synaptobrevin-2 revealed that the expression of phosphomimetic and non-phosphorylatable sites affected exo- and endocytosis in neurons.

This work is first to investigate the electrical stimulation in relation to the Ca^{2+}-dependent neurotransmitter release and exocytosis in synaptosomes. It further provides a comprehensive draft of synaptosomal phosphoproteome and is first to demonstrate its global dependence on an active SV cycling. The analysis of cultured hippocampal neurons expressing non-phosphorylatable and phosphomimetic mutants of pre-synaptic proteins syntaxin-1, synaptobrevin-2, and cannabinoid receptor-1 further demonstrates that the identified SV-cycling-dependent sites affect exo- and endocytosis.

Table of contents

List of figures

List of tables

Acknowledgments

First of all, I would like to express my gratitude to my supervisor, Prof. Dr. Henning Urlaub for his trust and continuous support during my PhD time and previously during the Master's studies. I have learnt a lot about mass spec and life while being a part of your group! Here I would also like to thank Dr. Christof Lenz who was the first to introduce me to the peculiarities of working in a proteomics lab and Dr. Kuan-Ting Pan who always helped me to navigate and advance projects I was working on.

Furthermore, I would like to thank cordially Prof. Dr. Reinhard Jahn for advising me during the PhD time and being open to my questions. Here I would also like to thank all members of the Neurobiology lab and the group of Dr. Alexander Stein for their willingness to share materials, instruments, lab space and, most important, their expertise. Especially, I would like to thank Dr. Mahdokht Kohansal Nodehi, a former PhD student of Prof. Dr. Jahn, who shared her preliminary work on electrical stimulation with me.

I would like to take this opportunity to thank sincerely Prof. Dr. Rizzoli and Dr. Eugenio Fornasiero for their advices and willingness to help, as well as for a great collaboration. I would also like to express my gratitude to Prof. Dr. Tobias Moser, Prof. Dr. Nils Brose, and Dr. Alexander Stein for their willingness to serve on my examination board.

My warmest thanks go to all members of the Bioanalytical mass spectrometry group for the lively environment and (though sometimes heated) discussions. In particular, I would like to thank former, current, and occasional "inhabitants of the cave": Sofia Ainatzi, Dr. Yanlong Li, Dr. Fan Pan, Dr. Christof Lenz, Uwe Plessmann, Dr. Ralf Pflanz, Dr. Kuan-Ting Pan, Fanni Bazsó, as well as Dr. Alexandar Chernev. I would like to address my special thanks to Dr. Momchil Ninov, Dr. Iwan Parfentev, and Sofia Ainatzi for helping me with synaptosomal preparations and with reviewing this thesis. Furthermore, I would like to thank Monika Raabe, Annika Reinelt, Uwe Plessmann, Dr. Sabine König, Dr. Ralf Pflanz, and Dr. Olex Dybkov for an excellent support in all technical (and beyond) questions, as well as Sascha Krause and Thomas Gundlach for taking care of lab animals.

Last but not least I would like to greatly thank my family, my mum, dad, my brother Sascha and my wife Daria for being always on my side, supporting me during my studies and forgiving me my late hours at work. Your sacrifice meant a lot to me!

Abbreviations

AAV	adeno-associated virus
ACN	acetonitrile
ADBE	activity-dependent bulk endocytosis
AGC	automatic gain control (depending on context)
AGC	protein kinase A, G, C kinase group
AKAP	A-kinase anchoring proteins
AMPA	α-amino-3-hydroxy-5-methyl-4-isoxazolepropionic acid
AMPAR	α-amino-3-hydroxy-5-methyl-4-isoxazolepropionic acid receptor
AMPK	AMP-activated protein kinase
AP	action potential
AP1	adaptor protein 1
AP2	adaptor protein 2
AP3	adaptor protein 3
AP180	adaptor protein 180
aPKC	atypical protein kinase C
BAR	Bin-Amphiphysin-Rvs domain
BCKDK	branched chain ketoacid dehydrogenase kinase
BoNT	botulinum neurotoxin
bRP	basic reversed-phase chromatography
BSA	bovine serum albumin
CAA	chloroacetamide
CAMK	calcium-calmodulin dependent kinases
CaMKII	calcium-calmodulin kinase 2
cAMP	adenosine 3′, 5′-monophosphate
CDK	cyclin-dependent kinase
CDK5	cyclin-dependent kinase 5
CDKL	cyclin-dependent-like kinase
CK1	casein kinase 1
CK2	casein kinase 2
CLK	SRPK1 and Clk/Sty protein kinase
CME	clathrin-mediated endocytosis
CMGC	CDK, MAP, GSK, CDKL kinase group
CNQX	6-cyano-7-nitroquinoxaline-2,3-dione
cPKC	conventional protein kinase C
CREB1	CAMP responsive element binding protein 1

DAG	diacylglycerol
D-AP5	2-amino-5-phosphonopentanoic acid
DAPK	death associated protein kinase
DC	direct current
DDA	data-dependent acquisition
EGTA	ethylene glycol-bis(β-aminoethyl ether)-N,N,N′,N′-tetraacetic acid
ERK	extracellular signal-regulated kinase
ESI	electrospray ionisation
FA	formic acid
FAK	focal adhesion kinase
FC	fold change
FDR	false discovery rate
FHA	forkhead-associated domain
GABA	γ-aminobutyric acid
GAP	GTPase-activating protein
GEF	Guanine nucleotide exchanging factor
GluDH	glutamate dehydrogenase
GO	gene ontology
GRK	G protein coupled receptor kinase
GSEA	gene set enrichment analysis
GSK3	glycogen synthase kinase 3
HCD	high energy collisional dissociation
IMAC	immobilized-metal-ion affinity chromatography
ITR	inverted terminal repeat (sequence)
JNK	c-Jun amino-terminal kinases
LC	liquid chromatography
LC-MS/MS	liquid chromatography - tandem mass spectrometry
LTD	long-term depression
LTP	long-term potentiation
MAGUK	membrane-associated guanylate kinase
MALDI	matrix-assisted laser desorption
MAP2K	mitogen activated protein kinase kinase
MAPK	mitogen activated protein kinase
MAPKAPK	MAP kinase activated protein kinase
MAPKK	mitogen activated protein kinase kinase
MAPKKK	mitogen activated protein kinase kinase kinase
MARK	microtubule associated kinase

MAST	microtubule-associated serine/threonine-protein kinase
MaxIT	maximum injection time
Mnk	MAPK-interacting protein kinase
MOAC	metal-oxide affinity chromatography
MS	mass spectrometry or mass spectrum, depending on context
MS/MS	tandem mass spectrum
MS1	survey mass spectrum
MS2	tandem mass spectrum
NCE	normalized collision energy
NDR	nuclear dbf2-related kinase
NEK	NIMA-related kinase
NIMA	never in mitosis A
NMDA	methyl-d-aspartate
NMDAR	N-methyl-d-aspartate receptor
nPKC	novel protein kinase C
NSF	*N*-ethylmaleimide-sensitive factor
PAK	p21 activated kinase
PDHK	pyruvate dehydrogenase kinase
PFA	paraformaldehyde
$PI(4,5)P_2$	phosphatidylinositol (4,5)-bisphosphate
PKA	protein kinase A
PKB	protein kinase B
PKC	protein kinase C
PKD	protein kinase D
PKGcGK	cGMP-dependent protein kinase
PNGase F	peptide-N(4)-(N-acetyl-beta-glucosaminyl)asparagine amidase
POI	protein of interest
PP1	protein phosphatase 1
PP2A	protein phosphatase 2A
PP2B	protein phosphatase 2B
PSD	post-synaptic density
PSM	peptide-spectrum match
PTB	phosphotyrosin-binding domain
PTM	post-translational protein modification
PTP	protein tyrosine phosphatase
QIK	Qin-induced kinase
RAS	rat sarcoma gene

RF	radio frequency
RIM	regulating synaptic membrane exocytosis protein
ROCK	Rho-associated protein kinase
RP	reserved pool
RRP	readily releasable pool
RSK	ribosomal S6 kinase
RT	room temperature
SGK	serum and glucocorticoid regulated kinase
SH2	Src homology 2 domain
SH3	Src homology 3 domain
SHANK	SH3 and multiple ankyrin repeat domains
SNAP	soluble NSF-attachment protein
SNAP-25	Synaptosomal-associated 25 kDa protein
SNARE	N-ethylmaleimide-sensitive factor-attachment protein receptors
SRPK1	serine/arginine-rich protein-specific kinase 1
STE	“sterile” serine/threonine protein kinases
STLK	STE20-like serine/threonine protein kinase
SV	synaptic vesicle
TANK	TRAF family member-associated NF-kappa-B activator
TBK	TANK-binding kinase
TCEP	tris(2 carboxyethyl)phosphine
TEAB	triethylammonium bicarbonate buffer
TFE	trifluoroethanol
TK	tyrosine kinase
TKL	tyrosine-like kinase
TMT	tandem mass tags
TMT6	TMTsixplex isobaric labeling reagents
TRAF	tumor necrosis factor receptor-associated factor
TTBK	tau-tubulin kinase
ULK	Unc-51 like autophagy activating kinase
V-ATPase	vacuolar proton ATPase
VGLUT1	vesicular glutamate transporter 1
VT	vesicular transporter
Wnk	with no lysine (K) kinase
WT	wild type

1. Introduction

1.1 Chemical synapse

Synapses are special types of cellular contacts that enable directed information transfer between cells. Here I refer to the “synapse” meaning specifically the chemical synapse in the central nervous tissue. Other synapse types, *e.g.*, the electrical synapse and the immunological synapse are not considered in this work due to their different organization and function. Although synapses represent highly specialized sites of intercellular communication, synapse-like structures has appeared early during the evolution before the nervous system could be defined as such (1). On electron micrographs a typical synapse appears as an electron-dense structure at the contact zone between two plasma membranes, the pre- and the post-synapse, separated by a thin synaptic cleft (exemplified in **Figure 1.1A**).

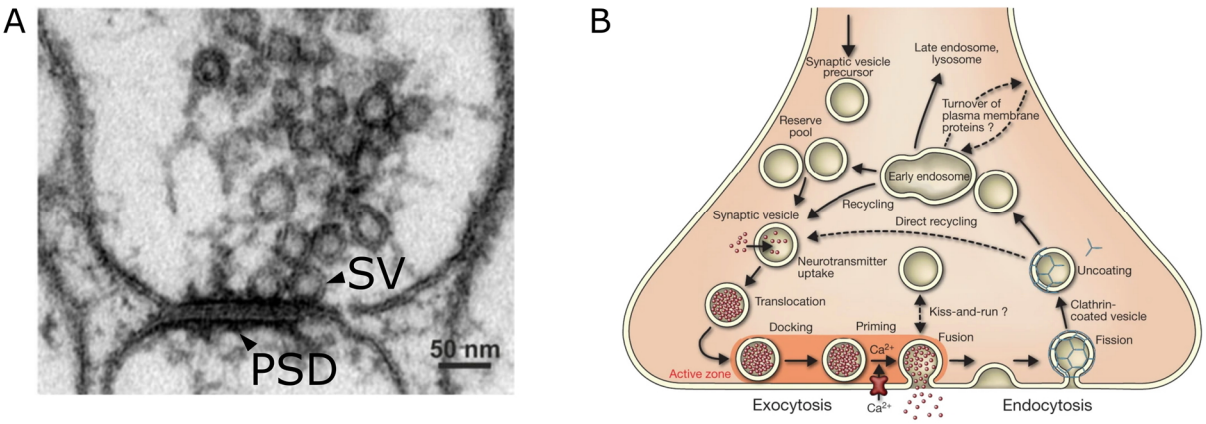

Figure 1.1: Nerve terminal and synaptic vesicle cycling. (A) *An electron micrograph of a nerve terminal. The pre-synapse (upper part) can be recognized by the presence of synaptic vesicles (SV) and the post-synapse (lower part) by the post-synaptic density (PSD) at the place of the contact with the pre-synapse. The micrograph is adapted from Guzman et al (2).* ***(B)*** *Proposed steps of SV cycling: i) SVs fuse with the plasma membrane and release their content in the synaptic cleft via exocytosis; ii) SVs are recycled via endocytotic mechanisms and prepared for the next round of endocytosis (refilled with the neurotransmitter, docked and primed at the active zone). The figure is adapted from Jahn and Fasshauer (3).*

The pre-synaptic compartment can be readily distinguished by the presence of synaptic vesicles (SVs) - spherical membrane-enclosed structures filled with neurotransmitter. Upon fusion with the plasma membrane, SVs release their content into the synaptic cleft thus mediating chemical signal transmission. SVs are decorated with proteins required for SV trafficking, such as synaptobrevins (*Vamp1, Vamp2*), small GTP-binding proteins *Rab3a-c, etc.*; as well as proteins responsible for the composition of intravesicular fluid, such as ion channels (*e.g.*, chloride channels *Clcn3, Clcn7*), transporters (*e.g.*, glutamate transporters

VGLUT1 (*Slc17a7*), VGLUT2 (*Slc17*a6)), and the vacuolar H^+-ATPase. SVs further contain proteins that are engaged in interactions with other proteins and presumably fulfil regulatory functions, such as a Ca^{2+}-sensor synaptotagmin (*Syt1*), a chaperone protein *Dnaj5* and synapsins (*Syn1-3*) (4).

The site of SVs release represents a structurally organized electron-dense matrix also known as the active zone (5, 6). Large multi-domain proteins such as bassoon (*Bsn*) and piccolo (*Pclo*), as well as RIM proteins (*Rims1-4*), RIM-binding proteins (*Rimbp1-3*), ERC proteins (*Erc1-2*), liprins (*Ppfia1-4*), and Munc13 (*Unc13a, b, c*) tether different pre-synaptic components such as SVs, cytoskeleton proteins, channels, receptors, and, therefore, orchestrate the turnover of SVs, *i.e.,* SV cycling (7).

The hallmark of the post-synaptic compartment is the electron-dense structure at the plasma membrane also known as the post-synaptic density (PSD) (8). Scaffolding proteins such as PSD-95 (*Dlg4*), membrane-associated guanylate kinase (MAGUK) proteins (*Mpp2-4*), SH3 and multiple ankyrin repeat domains (SHANK) proteins (*Shank1-3*)*, etc*. hold together proteins of other functional classes, *e.g.,* ionotropic glutamate receptors NMDA (*Grin1, Grin2a-d, Grin3a, b*) and AMPA (*Gria1-4*), ion channels, cell adhesion molecules, and cytoskeletal proteins (9). Also, regulatory proteins, such as calcium-calmodulin-dependent kinases are typically associated with the PSD (10). This definitive organization enables the controlled propagation and the modulation of the signal arriving from the pre-synaptic part.

1.1.1 Electro-chemical coupling

An important moment in the synapse physiology is the transformation of an electrical signal into the chemical, *i.e.*, neurotransmitter release. In a simplified view, biological membranes, *e.g.*, the synaptic plasma membrane, represent an electrical capacitor, which consists of a non-conducting lipid bilayer (membrane) separating two conducting media filling the extra- and intracellular space. At rest, the synaptic membrane is negatively charged (~ -70 mV) as compared to the extracellular fluid (11). An electric field across the membrane generates the driving force for the positive ions (Na^+, K^+, Ca^{2+}) to enter the intracellular space and force negative ions (Cl^-, HCO_2^-, $H_2PO_4^-$) in the opposite direction. On the other hand, the uneven distribution of ions between the extra- and intracellular fluids forces the ions to follow their concentration gradient. For each ion, an equilibrium membrane potential at which the electrical and chemical driving forces would cancel each other can be calculated using the Nernst equation (12):

$$E_{eq} = \frac{RT}{zF} ln \frac{[Ion]_{ex}}{[Ion]_{in}} \text{ (1)},$$

where $[Ion]_{ex}$ and $[Ion]_{in}$ are the extra- and intracellular concentrations of an ion, respectively, R is the gas constant (~8.314 $J \cdot K^{-1}$ mol^{-1}), T is the temperature in Kelvin (K), z is the ionic charge, and F is the Faraday's constant (~96480 $C \cdot mol^{-1}$). Ionic concentrations and corresponding equilibrium potentials for K^+, Na^+, Ca^{2+}, and Cl^- in a typical mammalian cell are listed in Table 1.1 (adapted from *Graziane and Dong* (11)).

Table 1.1: Ionic concentrations and equilibrium potentials (adapted from Graziane and Dong (11))

Ion	$[Ion]_{in}$ **/ mM**	$[Ion]_{ex}$ **/ mM**	E_{eq} **(37°C) / mV**
K^+	140	5	-89.7
Na^+	5-15	145	+61.1 – +90.7
Ca^{2+}	1-2	2.2-5	+136 – +145
Cl^-	4	110	-89

The resting membrane potential (E_m) can be calculated using Goldman–Hodgkin–Katz equation (13, 14) when considering the equilibrium potentials and corresponding membrane permeability for each ion. For the monovalent cations (M^+) and anions (A^-) the equation has the following form:

$$E_m = \frac{RT}{F} \ln\left(\frac{\sum_i^n P_{M_i^+}[M_i^+]_{ex} + \sum_j^m P_{A_j^-}[A_j^-]_{in}}{\sum_i^n P_{M_i^+}[M_i^+]_{in} + \sum_j^m P_{A_j^-}[A_j^-]_{ex}}\right) \qquad (2),$$

where P is the membrane permeability for a given ion.

The difference in the ionic concentrations between the extra- and intracellular space is maintained due to the selective membrane permeability for ions and the activity of transporters (15). The most important transporters in the plasma membrane are:

1. Na^+/K^+-ATPase (encoded by *Atp1a1-4* (catalytic α-subunit) and *Atp1b1-4* (auxiliary β-subunit)), exchanges three Na^+ inside the cell against two K^+ from the outside of the cell thus contributing to the charge disparity between extra- and intracellular space (16).
2. Na^+/Ca^{2+}-exchanger (*Slc8a1-3*) utilizes the energy accumulated in Na^+ concentration gradient. It preserves low intracellular Ca^{2+} concentration as it drives one Ca^{2+} outwards in exchange for three Na^+ from the extracellular space (17).
3. Ca^{2+}-ATPase is present in the plasma membrane (*Atp2b1-4*) and endoplasmic reticulum (*Atp2a1-3*). It actively pumps Ca^{2+} out of the cytosol into extracellular space or endoplasmic reticulum (18).
4. HCO_3^-/Cl^--exchangers (*Slc4a1-3, Slc4a8, Slc4a10*) keep the intracellular concentration of Cl^- low. The exchange is Na^+ dependent (19).

5. $Na^+/K^+/Cl^-$ - co-transporter (*Slc12a2*) pumps Na^+, K^+, and two Cl^- into the cytosol, thus contributing to the Cl^--homeostasis (20).
6. K^+/Cl^--co-transporter (*Slc12a5-6)* drives one K^+ and one Cl^- outwards, thereby maintaining low intracellular Cl^- concentration (21).

Specialized ion channels, most importantly, Ca^{2+}, Na^+, and K^+-channels, govern the ionic permeability of the membrane. At the pre-synapse, Ca^{2+}-channels clustered at the active zone (represented by the P/Q- or N-type Ca^{2+}-channels) trigger the fast neurotransmitter release as discussed below (s. section 1.1.2.1). The pore-forming α_1-subunits identify the family of Ca^{2+}-channels. For $Ca_V2.1$-3 channels, these subunits are encoded by *Cacna1a, Cacna1b,* and *Cacn1e* genes, respectively (22).The Ca^{2+}-influx is commonly generated through P/Q- ($Ca_V2.1$) or N-type ($Ca_V2.2$) Ca^{2+}-channels, whereas other types such as R-type ($Ca_V2.3$), L-type ($Ca_V1.1$-4) Ca^{2+}-channels play a minor role in the triggering of the neurotransmitter release (23). Auxiliary subunits $\alpha_2\delta$ (*Cacna2d1-4*), β (*Cacnb1-4*), and γ (*Cacng1-9*) can be present in different combinations and presumably modulate the function of Ca^{2+}-channels (24). Na^+-channels are abundant at the neuron's body and in the axon, while the amount and diversity of Na^+-channels at the pre-synapse are rather sparse (25). $Na_V1.2$ (*Scn2a*) and $Na_V1.6$ (*Scn*8a) are the most probable channel type at the axon terminals (26, 27). The limited number of Na^+-channel at the pre-synapse allows to control the shape of arriving signals and consequently the Ca^{2+}-inflow (27, 28). In contrast to Na^+-channels, K^+-channel family is exceptionally diverse and encompasses ~70 genes. The channels differ in their structural organization, function and gating mechanisms (29). The most common K^+-channel subunits found at the pre-synapse are of $K_V1.1$ (*Kcna1*) and $K_V1.2$ (*Kcna2*) type (25, 30). They belong to low-voltage-gated-channels that activate at modest depolarizations near the resting membrane potential thus preventing aberrant firing (31). The high-voltage-activated K_V3 channels (*Kcnc1-3*) located at the pre-synapse become conductive at significant depolarizations (around 0 mV) and are required to achieve a quick repolarization (32). The role of other types of voltage- and ligand-gated K^+-channels present at the pre-synapse is less established, however, their involvement in the regulation of synaptic transmission is generally recognized (33).

In the current view, activity of electrogenic transporters such as Na^+/K^+-ATPase and K^+ leakage through low-voltage-gated K^+-channels maintains the plasma membrane potential at approx. -70 mV at rest (11). Arrival of a depolarization wave – an action potential (AP) – from the proximal part of the axon leads to the depolarization of the pre-synaptic plasma membrane, opening of the voltage-gated Ca^{2+}-channels, Ca^{2+}-influx into the cytosol, SV exocytosis and neurotransmitter release. The involvement of Na^+-channels in the active propagation of the action potential at the nerve terminals remains debatable. It is assumed

that APs spread passively from the preterminal part of the axon to its terminus, while Na^+-channels located in the pre-synapse may modulate this process (27). Opening of the high-voltage-gated K^+-channels helps to repolarize the membrane quickly thus allowing for repetitive firing (32).

1.1.2 SV cycling

The process of SV cycling can be broadly divided into two functional steps: i) SV fusion with the plasma membrane via the process of exocytosis, and ii) SV recycling (**Figure 1.1B**). The latter includes SV material retrieval via endocytosis, and the preparation for the next round of SV cycling, *i.e.*, refilling with the neurotransmitter, SV tethering, docking, and priming. Each step of SV cycling is governed by distinct multiprotein complexes, of which the most important members are listed below.

1.1.2.1 Exocytosis

As a part of the SV cycling process, exocytosis is responsible for SV fusion with the plasma membrane and the active release of neurotransmitters. In the current interpretation, Ca^{2+} ions are the natural trigger of this process (34). Depolarization of the pre-synaptic membrane increases the open state probability of voltage-gated Ca^{2+}-channels clustered at the active zone resulting in the influx of Ca^{2+}-ions into the pre-synapse following the electrochemical gradient (35). SVs near the plasma membrane are “primed” for the fusion via soluble *N*-ethylmaleimide-sensitive factor-attachment protein receptors (SNARE). SNARE proteins form a core complex, which includes SV membrane-standing protein synaptobrevin (*Vamp2*) and plasma-membrane-standing proteins syntaxin-1 (*Stx1a*), and SNAP-25 (*Snap25*). Interaction of these proteins act as a “molecular zipper” that brings fusing membranes into a close proximity with each other (36, 37). Other proteins such as complexins (*Cplx1-3*), Munc18 (*Stxbp1*), and SV membrane-anchored protein synaptotagmin-1 (*Syt1*) interact with the SNARE and probably regulate the stability of the whole complex (38-40). Moreover, synaptotagmin-1 acts as a Ca^{2+}-sensor that can interact with negatively charged phospholipids of the plasma membrane upon Ca^{2+}-binding (41). This interaction may destabilize the complex and lead to complete zippering of the pre-assembled SNARE complex. The latter may provide required mechanical force to pull the plasma membrane and a SV into close proximity, leading to the formation of a fusion pore or its expansion (42). Other proteins might affect the complex formation. For instance, Tomosyn (*Stxbp5*) and amysin (*Stxbp6*) are able to substitute synaptobrevin in the complex thus preventing the formation of functional SNARE complexes (43, 44). Similarly, the interaction of synaptobrevin with another SV protein synaptophysin (*Syp*) may sequester the number of vesicular SNARE molecules available for the fusion (45).

Following the fusion of the membranes, the SNARE complex remains anchored in the plasma membrane. Vesicle-fusing ATPase NSF (*Nsf*) and its adaptors α/β/γ-SNAPs (*Napa, b, g*) dissociate the complex under ATP consumption (36). The energy stored in monomeric SNAREs can ignite the next round of SV fusion (46).

1.1.1.2 SV Recycling

The persistent firing of the synapse necessitates recycling mechanisms that replenish the SV pool and maintain the composition and integrity of the pre-synaptic plasma membrane. The recycling process begins with the separation of the membrane material of fused SVs and the plasma membrane via the process of endocytosis. Several endocytotic mechanisms have been described that rely on partially overlapping protein machinery and most probably co-exist in the synapse (47). At least four types of endocytosis have been described: clathrin-mediated endocytosis (CME), “kiss-and-run”, “ultrafast endocytosis”, and activity-dependent bulk endocytosis (ADBE) (48). The molecular machinery and the key steps are best described for CME (49). It begins with the binding of clathrin adaptor proteins such as adaptor protein (AP) 2 (*Ap2a1, Ap2a2, Ap2b1, Ap2m1, Ap2s1*), AP180 (*Snap91*), epsin (*Epn1, Epn2*), F-BAR domain protein (*Fcho2)* to cytosolic domains of SV proteins in the context of phosphatidylinositol(4,5)-bisphosphate ($PI(4,5)P_2$)-rich plasma membrane (50-54). The adaptors recruit light (*Clta, Cltb*) and heavy (*Cltc*) chains of clathrin, which form a basket-like structure around the invaginating membrane also known as “coated pit” (55). In the next step, a GTPase dynamin (*Dnm1*) mediates the fission of the pit (56). Endophilins (*Sh3gl1, 2*) recruit a phosphatase synaptojanin-1 (*Synj1*) that dephosphorylates $PI(4,5)P_2$ and thus promotes detachment of the adaptor proteins (57, 58). The disassembly of clathrin is further mediated by the ATPase Hsc70 (*Hspa8*) and its co-factor auxilin (*Dnaj6*) (59, 60). Other proteins are involved at different steps and take part in the control of the CME machinery. For instance, intersectin (*Itsn1, Itsn2*), *Eps15*, and dynamin-binding protein (*Dnmbp*) serve as platforms for attachment of other proteins (61-63). Cell division control protein 42 homolog (*Cdc42*) and neuronal Wiskott-Aldrich syndrome protein (*Wasl*) regulate the actin cytoskeleton dynamics (64). Myc box-dependent-interacting protein 1 (*Bin1*), amphiphysin (*Amph*), and *Dnmbp* can further be implicated in the membrane curvature formation (65-67).

CME is a relatively slow process in the minute time range (68). In contrast, other types of endocytosis are much faster (< 10 s) and do not require a clathrin coat. SVs that do not fuse completely with the plasma membrane are thought to undergo “kiss-and-run” endocytosis (69). Such SVs release their neurotransmitter content through a transient nanometer-wide pore (70). SVs remain within the active zone and preserve their membrane composition, which makes them quickly available (within 10 s) for the next round of SV cycling (71). Even

a faster mode of endocytosis (“ultrafast endocytosis”) was described that happens within 500 ms. It appears as membrane invaginations flanking the active zone and probably represents a mechanism which allows to rapidly restore the membrane surface following a brief but intense stimulus (72, 73). Some key proteins of CME seem to participate in the ultrafast endocytosis, *e.g.,* synaptojanin-1, endophilin-A, and dynamin-1 (72, 74). Longer stimulation is able to trigger ADBE (75). It retrieves large areas of membranes that form intracellular endosomes within 1-2 s, which is probably a compensatory mechanism to retrieve excessive membrane material (76). The molecular mechanisms of ADBE and SV reformation from endosome-like structures generated via fast endocytosis are not entirely understood. Several reports show that ADBE and SV regeneration require dynamin-1 dephosphorylation by the calcium-activated phosphatase calcineurin (*Ppp3ca-c, Ppp3r1, 2*) and the lipid-deforming activity of syndapin-1 (*Pacsin1*) (77-79). Further, the process of SV retrieval from the endosome-like structures relies on SV protein recognition by adaptor protein complexes involved in CME, *i.e.,* AP2 (80), or its endosomal cognates AP1 and AP3 (81). Therefore, it cannot be excluded that, at least some, SVs are recycled via early/sorting endosomes (82).

The regeneration of SVs requires the filling of SV with neurotransmitters. The driving force for this filling is the electrochemical gradient generated by the vacuolar proton ATPase (V-ATPase). V-ATPase is the largest multi-subunit protein complex of SVs encoded by *Atp6v* gene family (83). V-ATPase consists of two main domains, V_0 and V_1. The peripheral complex V_1 possesses the ATPase activity, while the transmembrane complex V_0 translocates H^+ through the SV membrane into SV lumen (84). Vesicular transporters (VTs) in the SV membrane utilize this proton gradient to fill SVs with respective neurotransmitter molecules. The transporter type determines the type of the neurotransmitter stored in SV, and it is assumed that, in accordance with the Dale’s principle (85), the majority of SVs contain a single type of neurotransmitter (86). However, a recent study has shown that ~36% of SVs carry two distinct VTs, which renders the possibility for neurotransmitter co-release from the same synapse. For example, ~34% of all SVs contained glutamate transporter 1 (VGLUT1, *Slc17a7*) and the zinc transporter-3 (*Slc30a3*), while ~2% accounted for 27 other combination (87).

The regenerated SVs are recruited to the active zone where they are prepared for fusion following a series of successive “priming” reactions. The key role in the SV tethering and docking is attributed to the active zone proteins such as RIM proteins, calcium-dependent secretion activator 1 (*Cadps)*, and Munc13 (88, 89). The role of SNARE proteins in the priming reactions is still under investigation. Although some data suggest an existence of

partially assembled SNARE complexes, the molecular mechanism of the SNARE arrest in the pre-zipped form is yet to be elucidated (3, 90).

1.1.3 Synaptosomes as a model of synapse

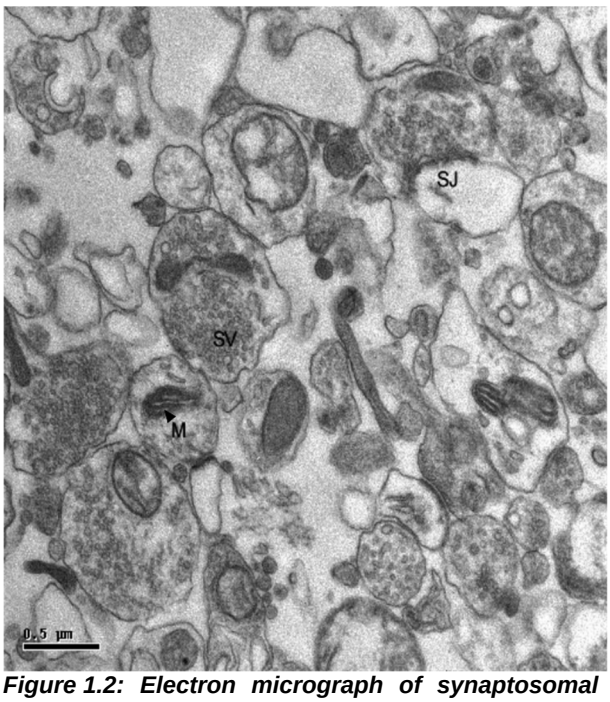

Figure 1.2: Electron micrograph of synaptosomal fraction. *Synaptosomes are membrane-enclosed structures that contain synaptic vesicles (SV), mitochondria (M). In some cases, post-synaptic compartment remains attached via synaptic junction (SJ). Bar, 0.5 mm. Adapted from Schrimpf et al (91).*

Synaptosomes represent pinched-off nerve terminals that can be isolated following a gentle homogenization of the brain tissue and differential and gradient centrifugation. First synaptosomes were isolated by Victor Whittaker as reported in 1958 (92). Their subsequent characterization showed that synaptosomes are membrane-enclosed nerve terminals whose membrane reseals during the homogenization process (93). Synaptosomes contain all the machinery needed for the neurotransmitter release (94). Being of ~500-900 nm in diameter, they contain SVs and mitochondria (**Figure 1.2**) (93, 95). Over time, multiple protocols for synaptosomes preparation have been developed. The core procedure, however, remained unchanged: i) brain tissue is homogenized using a Teflon/glass homogenizer in an isotonic sucrose/low-salt buffer; ii) the homogenate is clarified from nuclei and debris yielding a crude suspension S1; iii) synaptosomes are precipitated by differential centrifugation yielding a crude synaptosomal pellet P2; and iv) synaptosomes are further purified by differential centrifugation in discontinuous sucrose, Ficoll, or Percoll gradients (96). Of note, purified synaptosomes following the described procedure still contain residuals of neuronal or glial membranes, free mitochondria, or myelin. ~15% of synaptosomes contain an attached post-synaptic membrane (97). Despite this fact, only self-enclosed axonal terminals are capable of maintaining membrane potential and ATP levels needed for the neurotransmitter release and SV cycling (98, 99).

Due to the small size of synaptosomes, they are not amenable to electrophysiological measurements, *i.e.*, patch-clamp. Moreover, synaptosomes most probably lose the most axonal Na^+-channels during preparation and are not able to generate classical action potential (96). Nonetheless, fluorimetry-based methods have been found useful in studying

neurotransmitter release and synaptosomal functionality. In particular, the glutamate release assay became a method of choice to assess the functionality of synaptosomal preparation (100). The assay utilizes the conversion of glutamate to ketoglutarate by glutamate dehydrogenase (GluDH). The concomitant conversion of NADP to NADPH can be monitored as an increase of NADPH-specific emission at 440 nm wavelength. In order to conduct the assay, GluDH and NADP need to be externally added to the synaptosomal suspension. Glutamate being the most common type of the neurotransmitter in the central nervous system is released from synaptosomes following their stimulation/depolarization. Other fluorescence-based assays utilizing fluorescence dyes allowed to monitor i) cytosolic free Ca^{2+} (Fura-2 (101)), ii) membrane potential ($DiSC_2$ (102)), and iii) endocytosis (FM-dyes (103) and acridine orange (104)). Accordingly, it was shown that synaptosomes are able to maintain the polarization of the plasma membrane and cover their energy demands via glycolysis and oxidative phosphorylation (98). They hold the cytoplasmic Ca^{2+}-levels at ~100-200 nM (101) and can release neurotransmitter in a Ca^{2+}-dependent manner via exocytosis and subsequent SV recycling (99).

In order to study the neurotransmitter release, different stimulation protocols have been developed. Unlike neuronal cell cultures, electrical field stimulation of synaptosomes did not find broad acceptance (96) with only a few early studies reporting electrical stimulation of synaptosomes (105-112). Most of them applied a long (>10 min) intense (100 Hz) stimulation (105-111), while few used 10 Hz stimulation (112). Despite the observed release of glutamate, aspartate, and GABA by electrically stimulated synaptosomes (105), it remained unclear whether the release is driven by the exocytosis. For example, tetanus toxin (in action similar to botulinum neurotoxins, s. below) reduced the liberation of glycine but not glutamate or other neurotransmitters, which poses a question whether the exocytotic machinery is involved in the neurotransmitter release following the electrical stimulation (113). On the other hand, increased accumulation of an isotope ^{45}Ca by synaptosomes during the course of the stimulation speaks for a possibility of a Ca^{2+}-driven neurotransmitter release (111, 112).

Due to the uncertainties associated with the electrical stimulation, currently, chemical methods are commonly used for synaptosomal stimulation. For instance, the addition of KCl to the external buffer to lift $[K^+]_{ex}$ to 30-100 mM has been proven a reliable method to achieve strong depolarization of synaptosomal membrane and glutamate release (114). However, the method has been criticized for it causes a persistent depolarization of the synaptosomal membrane leading to a strong increase in intracellular Ca^{2+}-concentration (up to 400 nM) (114). The latter leads to the activation of Na^+/Ca^{2+}-ATPase, increased energy demand and reversal of the Na^+-coupled transporter of the plasma membrane, *e.g.*, Na^+/glutamate

transporter (115). To overcome the non-physiological clamp-depolarization of the plasma membrane, blocker of potassium channels such as 4-aminopyridine or dendrotoxin were introduced (116). It is hypothesized that the blockage of K^+-channels causes a moderate increase in the membrane potential. A spontaneous opening of Na^+-channels can further depolarize the membrane leading to the neurotransmitter release. This view is supported by the fact that 4-aminopyridine evoked release is sensitive to Na^+-channel blockers, *i.e.,* tetrodotoxin (117).

Apart from tetrodotoxin, other chemicals and toxins can be applied to synaptosomes for studying their effects on the neurotransmitter release. For instance, Ca^{2+}-dependence of the neurotransmitter release can be demonstrated using a metal chelator ethylene glycol-bis(β-aminoethyl ether)-N,N,N′,N′-tetraacetic acid (EGTA): incubation of synaptosomes with 0.2-1 mM of EGTA greatly reduced the amount of the released glutamate following KCl-induced depolarization (100, 104, 118). In a similar way, application of Ca^{2+}-channel inhibitors Cd^{2+} or ω-conotoxin can efficiently block neurotransmitter release (119). The remaining Ca^{2+}-independent release could be attributed to the leakage of the cytoplasmic glutamate via the glutamate transporter of the plasma membrane (118). The necessity of SNARE proteins for the neurotransmitter release can be demonstrated by the use of botulinum neurotoxins (BoNTs) – a group of exceptionally specific SNARE proteases (120). Application of BoNTs efficiently blocks SV exocytosis without compromising Ca^{2+}-influx or synaptosomal bioenergetics (121, 122).

1.1.4 SV pools

Despite similar ultrastructure and composition, SVs constitute different populations or pools, which can be distinguished by how fast they release neurotransmitter in response to stimulation (123). Primed SVs compose a so-called “readily releasable” SV pool (RRP) and are the first to release neurotransmitter, *i.e.,* possess the highest release probability (123). An intense stimulation (2 s stimulation at 20 Hz in hippocampal cell cultures) can deplete this pool, which leads to a significant drop of the neurotransmitter release or the use-dependent depression (124, 125). However, it seems that RRP is not homogeneous, and primed SVs can exhibit different release probabilities. The later might be interpreted as distinct subpopulations of “fully primed” and “incompletely primed” SVs (126, 127). The vacancies in the RRP can be replenished via SV recycling mechanisms such as CME or “kiss-and run” (128, 129) or via recruitment from the recycling pool. The latter is responsible for the continuous neurotransmitter release under moderate (physiological) stimulation (123). In contrast to a stimulation-reluctant “reserve” pool, the recycling pool is considered to contain mobile, recently endocytosed SVs (130, 131). As indicated above, the reserve pool (at least ~50% of total SVs) contain SVs that are engaged into SV cycling only during

phases of intense stimulation (123), although experiments using dynamin knockouts indicate that the reverse pool can be recruited for the release even under low-frequency stimulation if the other SV pools are depleted (132). Since intense stimulation also triggers bulk endocytosis, it is tempting to speculate that SVs regenerated through budding from endosome-like structures contribute to the reserve pool in the first place. However, the existence of distinct recycling routes for different SV pool has not been sufficiently shown (131). Of note, the balance between the pools determines the releasable amount of neurotransmitter and, therefore, the synaptic strength. The activity-dependent modulation of the neurotransmitter release at the pre-synaptic part and the regulation of the evoked response at the post-synapse constitute what is known as synaptic plasticity. Different forms of pre- and post-synaptic plasticity have been described that are generally referred to as long and short potentiation/depression (133). It is assumed that synaptic plasticity plays key roles in learning and memory formation. Various cellular processes contribute to the plasticity and protein phosphorylation is one of the underlying molecular mechanisms.

1.2 Post-translational modifications of proteins

Post-translational modifications (PTMs) of proteins are covalent modifications of the polypeptide chain that occur during or after the synthesis and affect the functioning of the modified protein. Among post-translational protein modifications such as glycosylation, acetylation, methylation *etc.*, phosphorylation of serine (S), threonine (T) or tyrosine (Y) is one of the most prominent PTMs – it is estimated that up to 25% proteins annotated in the Swiss-Prot database (134) might carry this modification (135).

1.2.1 Protein phosphorylation

Reversible phosphorylation/dephosphorylation of proteins has been long recognized regulating protein activity, localization in the cell, and protein-protein interactions (136). The first *in vitro* phosphorylation of casein by a liver enzyme was described by *Burnet and Kennedy* (137). The authors also noted that the incorporation of a phosphate into the protein could be almost solely attributed to the phosphorylation of serine hydroxyl groups. The latter indeed aligns with the fact that serine is the most frequently phosphorylated amino acid, followed by threonine and tyrosine (135). Other amino acids such as lysine, arginine, and histidine can be also a site of phosphorylation; however, their role in the signaling pathways in eukaryotes is less established (138, 139).

Phosphorylation of a protein can have different consequences for the activity of that protein and the whole cell. Thus, introduction of a negative charge has an impact on the conformation and consequently the enzymatic activity of a protein. For example, autophosphorylation of a Ca^{2+}/calmodulin-dependent protein kinase 2 (CaMKII) renders its

activity even in the absence of Ca^{2+} (140, 141). Phosphorylation can further affect the interaction with other proteins. Thus, specialized proteins and protein domains that can recognize phosphorylation sites play a central role in the intracellular signaling pathways. Among them are 14-3-3 proteins (*Ywhb, Ywhe, Ywhg-h, Ywhq, Ywhz*), WW domains, forkhead-associated (FHA) domains, and WD40 repeats/LRR modules that bind phosphorylated serine or threonine residues (142). Phosphorylated tyrosine residues are recognized by Src homology 2 (SH2), phosphotyrosin-binding (PTB), and C2 domains of protein kinase C β/θ (PKCβ, θ), *etc.* (143).

1.2.2 Kinase activity at the synapse

Protein phosphorylation is extensively involved in the cellular signaling pathways – almost every signaling pathway involves kinase and/or phosphatase. In Humans, more than 400 proteins (potentially) possess kinase activity, *i.e.*, the ability to transfer a γ-phosphate group of an ATP molecule onto its substrate. Kinases are able to recognize the amino acid sequences – linear motifs – surrounding the phosphorylation site. Consensus sequences of the kinase linear motifs as well as sequence similarities in the kinase domain can be used for kinase classification (144, 145). AGC (Protein kinases A, G, and C (PKA, B, C)), CMGC, (cyclin-dependent kinase (CDKs), mitogen-activated kinase (MAPK), glycogen synthase kinase (GSK), and CLK) CAMK (Ca^{2+}/calmodulin-dependent kinases (CAMKI and CAMKII)), CK1 (casein kinase 1), STE (“sterile” serine/threonine protein kinases), TK and TKL (tyrosine- and tyrosine-like kinases) constitute the main groups of kinases.

In the synapse, it has been proposed that the kinase activity is associated with changes in synaptic signal transmission or synaptic strength, such as long-term potentiation and depression (LTP and LTD, respectively). Although LTP and LTD can be both, pre- and post-synaptic phenomena, these processes were best studied in the post-synapse (146). A brief overview of the most prominent kinases located in the synapse is given below.

1.2.2.1 Calcium/calmodulin-dependent protein kinase II (CaMKII)

CaMKII is a serine/threonine kinase, which is very abundant (1-2% of total protein in the brain) in the pre- and, especially, post-synapse. *Camk2a, b, d,* and *g* genes encode α, β, δ, and γ forms of CaMKII, respectively. The catalytically active enzyme is formed by twelve subunits (147). The protein sequence contains four main regions, the catalytic domain, the auto-inhibitory domain, the variable region, and the self-association domain (148). Peculiar is the (auto)regulation of the CaMKII activity: binding of Ca^{2+}/calmodulin to the autoinhibitory domain releases the active site of the enzyme from binding the pseudo-substrate sequence of the auto-inhibitory domain. It further exposes a regulatory site (T286 in *Camk2a*) that can be autophosphorylated. The latter locks the kinase in the active state (140, 141). Two other

autophosphorylation sites (T305 and T306 in *Camk2a*) inhibit re-association of CaMKII and Ca^{2+}/calmodulin and, therefore, re-activation of CaMKII upon phosphorylation (149).

CaMKII has been extensively studied in the post-synapse, where it is thought to induce LTP via phosphorylation of AMPA (*Gria1-4*) and NMDA (*Grin1, Grin2a-d, Grin3a-b*) receptors (150, 151), and Ras/Rap GTPase-activating protein SynGAP (*Syngap1*) (152). In the pre-synapse, it was shown to phosphorylate an SV-associated protein synapsin-1 (*Syn1*) at S603 (153). Phosphorylation affects synapsin-1 interaction with actin cytoskeleton, which subsequently regulates the size of SV cycling pool (154, 155). Experiments with CaMKII inhibitors and injections of CaMKII itself demonstrated its importance for the pre-synaptic plasticity (156). Moreover, it was also shown that CaMKII may regulate the pool of docked SVs, and this regulation does not depend on its enzymatic activity (157) and might be a result of its F-acting bundling capabilities (158).

1.2.2.2 Mitogen-activated protein kinases (MAPK)

MAPK represent a group of serine/threonine kinases expressed in neuronal and non-neuronal cells. These kinases are often involved into response to extracellular stimuli such as growth factors that affect cell proliferation, differentiation, and survival. MAPK-signaling is organized in cascades: a basic module consists of MAP kinase kinase kinase (MAPKKK) that phosphorylates and activates MAP kinase kinase (MAPKK), which activates the downstream MAP kinase (MAPK).The MAPKKK and MAPKK levels are mainly responsible for the signal transmission, while MAPK phosphorylate a large number of substrates (159). There are four main cascades distinguished by their MAPK component: i) extracellular signal-regulated kinase (ERK) 1 and 2 (*Mapk3*, *Mapk1,* respectively), ii) ERK5 (*Mapk7*), iii) c-Jun amino-terminal kinases (JNK) 1-3 (*Mapk8-10*), and iv) p38 (*Mapk11-14*) (160).

The classical cascade starts with the production of an active GTP-bound form of the small protein Ras in response to the extracellular stimuli. GTP-Ras triggers activation of MAPKKK Raf (*Raf1*), which activates MAPK/ERK kinase (MEK) 1/2 (*Map2k1-2*), which further phosphorylates ERK1/2 (159). Dual phosphorylation of ERK1 at T203 and Y205 (in mouse/rat) and ERK2 at T183 and Y185 (in mouse/rat) induces their full activation (161). ERK1/2 are “proline-directed” kinases: they phosphorylate serine or threonine adjacent to proline. The most common consensus sequences for substrate recognition are P-X-S/T-P or S/T-P, where X is any amino acid (162).

High levels of ERK1/2 were found in the adult brain (163) and the and the ERK1/2 activation was observed following glutamate receptor stimulation and synaptic activity (164, 165). The ERK activation in the synapse is presumably Ras-dependent and mediated via Ca^{2+}-dependent activation or inhibition of guanine nucleotide exchange factors (GEFs) and

GTPase activating factors (GAPs), though an exact mechanism is to be elucidated (166-168). Studies including MEK inhibitors have demonstrated the importance of MAPK for different forms of synaptic plasticity (reviewed in (169)). ERK substrates that can modulate the synaptic functioning include C-terminal domain of K_V4.2 (*Kcnd2*) K^+-channel (170) and synapsin-1 phosphorylation at S62, S67, and S549 (positions in rat *Syn1*) (171). The long-lasting effects of MAPK activation are probably mediated via transcriptional activation (172, 173).

1.2.2.3 Protein kinase A (PKA)

PKA is a family of adenosine 3′, 5′-monophosphate (cAMP)-activated serine/threonine protein kinases. While inactive, PKA holoenzyme consists of two catalytic and two regulatory subunits. In humans, *Prkaca, Prkacb,* and *Prkacg* genes encode for catalytic subunits. Two types of regulatory subunits are encoded by *Prkar1a, b* (Type I) and *Prkar2a, b* (Type II), respectively. Binding of cAMP to a regulatory subunit cause its conformational change and release of the catalytic subunit (174). The PKA activity depends, therefore, on the cAMP levels and adenylate cyclase (*Adcy1-9*) activity, though recent data suggest that the holoenzyme can exhibit kinase activity at basal cAMP levels without subunit dissociation (175). The latter mechanism may rely on the interaction of Type II regulatory subunit with A-kinase anchoring proteins (AKAPs, in particular *Akap5*). Importantly, AKAPs are able to anchor PKA to cytoskeletal and/or organellar proteins. In the synapse, AKAPs may bring it close to the plasma membrane and SV fusion sites where it may regulate the neurotransmitter release via phosphorylation of Rim1 at S413 (176, 177) , SNAP25 at T138 (178), and C-terminus of complexins (179) and others (180). Furthermore, a neuron specific signal-transduction cascade from cAMP/PAK to MAPK has been discussed (181).

1.2.2.4 Protein kinase C (PKC)

PKC comprises a family of serine/threonine kinases that contain a similar catalytic domain but differ in their regulatory domains (isoenzymes). Three major PKC groups were described: i) conventional PKC (cPKC, including α, β, and γ enzymes encoded by *Prkca, Prkcb,* and *Prkcg,* respectively); ii) novel PKC (nPKC, including δ, θ, ϵ, and η forms encoded by *Prkcd, Prkcq, Prkce,* and *Prkch,* respectively); iii) atypical PKC (aPKC, including ζ and ι encoded by *Prkcz, Prkci,* respectively) (182). All PKC isoforms contain one or two C1 domains that binds to diacylglycerol (DAG), however, only cPKC and nPKC are DAG-dependent. Conventional and novel PKC further contain a C2 or a C2-like domain that binds Ca^{2+} and acts as a Ca^{2+}-sensor (only in the case of cPKC). Atypical PKCs require neither Ca^{2+} nor DAG, but could be stimulated by phosphatidylserine (183). Following synthesis, PKCs become phosphorylated at conserved amino acid residues: for *Prkcb* these are T500, T641, and S660 (the last two autophosphorylated) (184). Following the phosphorylation, the

kinase can adopt an autoinhibited conformation. Elevated concentrations of Ca^{2+} and DAG induce conformational changes that lead to the PKC translocation to the plasma membrane and releasing of the catalytic domain from the pseudosubstrate binding (182). At the synapse, PKC activity has been found modulating synaptic strength (185). SNAP25 (S187), Munc18-1 (S313), and synaptotagmin-1 (T112) were identified as PKC substrates. The phosphorylation of these and other PKC substrates might contribute to the regulation of the neurotransmitter release (186-188).

1.2.2.5 Cyclin-dependent kinase 5 (CDK5)

CDK5 (*Cdk5*) is a member of the cyclin-dependent kinase family, but unlike other CDKs, its function is not primarily focused on the regulation of the cell cycle, but rather on the regulation of a variety of other cellular processes in neurons as well as other cell types (189). Another hallmark that distinguishes CDK5 from other members of the CDK family is its dependence on non-cyclin activators, p35 (*Cdk5r1*) or p39 (*Cdk5r2*) (190-193). The localization of CDK5 activators might represent the mechanism of spatial restriction of the kinase activity of the ubiquitously expressed CDK5 (193). Further regulation mechanism include p35 phosphorylation at S8 and T138 by CDK5 itself that leads to the proteasome-dependent degradation of p35 (194). Moreover, phosphorylation of CDK5 at Y15 by tyrosine-kinases Abl (*Abl*) and Fyn (*Fyn*) increases its catalytic activity (195, 196).

Several synaptic targets were identified that can convey the role of CDK5 in the synapse organization and plasticity. For instance, it has been shown to phosphorylate S549 and S551 of synapsin-1 (rat) which correlates with the reduced actin filament binding of that protein (171, 197). CDK5 may regulate endocytosis itself via phosphorylation of Munc18-1 at T574 (198, 199) and P/Q type Ca^{2+}-channels (200). Furthermore, CDK5 phosphorylates amphiphysin at multiple sites (S262, S272, S276, S285, and T310) (201, 202), dynamin-1 at S778 (203), and synaptojanin at S1144 (204). The three proteins are also known as “dephosphins” because they undergo dephosphorylation by a phosphatase calcineurin – an essential process for SV endocytosis (205). The re-phosphorylation of dephosphins by CDK5 indicates an important role the kinase plays in the regulation of SV endocytosis (206).

1.2.2.6 Glycogen synthase kinase 3 (GSK3)

GSK3 is a constitutively active and ubiquitously expressed serine/threonine kinase. It exists in two isoforms, GSK3α (*Gsk3a*) and GSK3β (*Gsk3b*). GSK3 is a proline-directed kinase that exhibits a weak affinity to substrates containing proline next to serine/threonine (207). However, a common requirement for GSK3-mediated phosphorylation is a pre-phosphorylated serine/threonine at the +4 position relatively to the to the target site (S/T-X-X-X-pS/pT, where pS/pT is a pre-phosphorylated serine or threonine) (208). GSK3 can perform a sequential phosphorylation of closely located S/T residues since the recently

phosphorylated serine/threonine acts as a pre-primed site for the following S/T residue. The latter can be observed in the case of glycogen synthase (*Gys1*-S653, S649, S645, and S641) and β-catenin (*Ctnnb1*-T41, S37, S33) (207). GSK3 phosphorylation at an N-terminal serine (*Gsk3a*-S21/*Gsk3b*-S9) turns it into a pre-phosphorylated substrate, or pseudosubstrate, thus reducing GSK3 activity (209). Several signaling cascades can mediate this phosphorylation, including CaMKII following an increase in the cytosolic Ca^{2+} concentration (210).

In the pre-synapse, GSK3 can regulate exocytosis via phosphorylation of P/Q-type Ca^{2+}-channels (211). It participates in re-phosphorylation of dephosphins, whereby CDK5 acts as a pre-priming kinase for GSK3 (203). Furthermore, GSK3 is implicated in the abnormal phosphorylation of microtubule-binding protein tau (*Mapt*), thus contributing to the neurofibrillary tangles formation in Alzheimer's disease (212).

1.2.2.7 Casein kinase 1 (CK1)

CK1 is a monomeric serine/threonine kinase encoded by six distinct genes in humans, *Csnk1a1, Csnk1d, Csnk1e,* and *Csnk1g1-3*. Similarly to GSK3, CK1 prefers pre-phosphorylated substrates and exhibit affinity to acidic or phosphorylated residues in the -3 position (213). CK1 is implicated in controlling circadian rhythms (214, 215), membrane trafficking (216), cytoskeleton maintenance (217), *etc*. Via interfering with Wnt signaling, it is involved into the regulation of synapse stability and development (218, 219). Moreover, it can phosphorylate tau protein (*Mapt*), which might affect its aggregation (220). Altogether, it renders CK1 importance in neurodegenerative diseases, especially in Alzheimer disease (221).

1.2.2.8 Casein kinase 2 (CK2)

CK2 is a ubiquitously expressed serine/threonine kinase. The holoenzyme consists of two catalytic (α and α', encoded by *Csnk2a1* and *Csnk2a2,* respectively) and a non-catalytic β subunit (*Csnk2b*). CK2 is constitutively active and its localization to different compartments and cooperation with other proteins can confer the substrate specificity (222, 223). CKII (auto)phosphorylation can further regulate its activity (224). Thus, CKII phosphorylation at Y250 correlates with an increase enzymatic activity (225). Experiments have shown CK2 involvement into synapse organization and plasticity (226, 227). Syntaxin-1a (*Stx1a*-S14), and NMDA receptor (*Grin2b*-S1480) are among CK2 targets and their phosphorylation may contribute to the synaptic plasticity (223, 228-230).

1.2.2.9 p21-activated kinase 1 (PAK1)

PAK1 (*Pak1*) is a serine/threonine kinase which that interact with the activated forms of small GTPases, namely cell division control protein 42 homolog (*Cdc42*) or *Ras*-related C3

botulinum toxin substrate 1 (*Rac1*) (231). Binding of *Cdc42* or *Rac1* drives PAK autophosphorylation and subsequent activation. This interaction renders PAK involvement into regulation of cytoskeleton, *e.g.*, loss of actin stress fibers (232), and cell morphology (233). Moreover, PAK is capable of activating MAPK by phosphorylating MAPKKK *Raf1* (234).

1.2.3 Phosphatase activity at the synapse

Phosphatases catalyze the removal of the phosphate group from the substrate, *i.e.*, proteins or lipids. The human genome encodes ~200 phosphatases that can be categorized into six phosphatase super-families based on the sequence similarity of the catalytic domain (235). Protein tyrosine phosphatases (PTPs) is the most abundant group (> 100 genes (235)). It contains phosphatases that are more specific in their action and have a weak sequence preference towards their targets. Some members of this family are known as dual-specificity phosphatases (DUSP) and can remove the phosphate group from Y, S, and T residues (236). For example, MAPK phosphatases (MKP) represent an important sub-group of PTPs that can dephosphorylate Y and T in the activation loop of MAPK. A much smaller family, PPP, includes only 13 genes (235), but contains important serine/threonine phosphatases for the synapse plasticity, such as Protein phosphatase 1 (PP1), 2A (PP2A), and 2B (PP2B, Calcineurin) (237). In contrast to kinases, the substrate targeting of serine/threonine phosphatases is governed by adaptor proteins or auxiliary domains rather than via docking motifs (235). Absence of clearly defined docking motifs, overlapping substrates and signaling pathways make it challenging to pinpoint functional phosphatase-substrate interaction.

1.2.3.1 Protein phosphatase 1 (PP1)

PP1 is a ubiquitously expressed and a highly abundant phosphatase. *Ppp1ca, Ppp1cb, Ppp1cc* genes to the four distinct catalytic subunits (α, β/δ, γ1, γ2) via alternative splicing. There is a plethora of regulatory subunits that define the substrate specificity and the subcellular localization of the phosphatase. Prominent regulators of PP1 function are neurabin-1 (*Ppp1r9a*) and neurabin-2 or spinophilin (*Ppp1r9b*) that anchor PP1 via modular binding motifs to F-actin – a very abundant cytoskeleton protein of the nerve terminals (238). The PP1-neurabin/spinophilin interaction has been shown to be important for postsynaptic LTD in hippocampus (239, 240), which may act via PP1-mediated dephosphorylation of AMPA receptors (241). Phosphorylation of neurabin-1 at S461 by PKA and neurabin-2 at S100 by CaMKII may represent the mechanisms of attenuating PP1 activity (242-244).

Further prominent regulators of PP1 activity are inhibitor-1 (*Ppp1r1a*) and dopamine- and cAMP-regulated phosphoprotein 32 (DARPP-32, *Ppp1r1b*). Increased levels of cAMP and

PKA-mediated phosphorylation makes these proteins to potent inhibitors of PP1. Interestingly, phosphorylation at distinct residues such as *Ppp1r1a*-S67, T75 or *Ppp1r1b*-T75, which may be accomplished by CDK5, results in the attenuation of PKA activity (245-247).

1.2.3.2 Protein phosphatase 2A (PP2A)

PP2A holoenzyme consists of a catalytic subunit (*Ppp2ca*) associated with a scaffolding PR65 (*Ppp2r1a*) subunit, which coordinates the association of the catalytic subunit with a variety of regulatory B subunits (248). The number of possible holoenzyme compositions is estimated at ~75 (238). A conditional knockout experiment in mice has shown that PP2 loss affects synaptic transmission and plasticity in hippocampus (249). Previous stimulation experiment demonstrated that LTP induction correlates with the decrease of PP2A activity and the phosphorylation of its 55 kDa Bα subunit (*Ppp2r2a*) by CaMKII (250). Further reports have shown that B55-PP2A dephosphorylates protein tau (*Mapt*) at multiple sites (251-253). An intricate mechanism coordinating PKA, PP1, and PP2 activity was proposed by *Ahn et al* (254). Authors showed that PKA-mediated phosphorylation of B56δ subunit (*Ppp2r5d*) has an activating effect on PP2A, which in turns dephosphorylates T75 on PP1 inhibitory subunit *Ppp1r1b* leading to PP1 inhibition.

1.2.3.3 Protein phosphatase 2B (PP2B, Calcineurin)

Similar to PP1, calcineurin holoenzyme consists of a catalytic subunit (*Ppp3ca, Ppp3cb, or Ppp3cc*) and a regulatory subunit (*Ppp3r1 or Ppp3r2*). Calcineurin is fully activated following binding of Ca^{2+}/calmodulin to its catalytic subunit and the concurrent binding of Ca^{2+} to its regulatory subunit (255, 256). It is assumed that due to high affinity of calcineurin to Ca^{2+}/calmodulin, initial increase of the cytosolic Ca^{2+} concentration activates calcineurin before Ca^{2+}/calmodulin dependent kinases (257). The latter is particularly important given that the phosphatase activity of calcineurin is required in SV endocytosis (258). Calcineurin acts as a Ca^{2+}-sensor and dephosphorylates dynamin-1, amphiphysin, synaptojanin, AP180, epsin, and eps15 during different steps of SV endocytosis (205). Other cellular effects of calcineurin activation can be mediated via dephosphorylation of PP1 inhibior-1 and DARPP-31 leading to disinhibition of PP1 (259). Due to the calcineurin-mediated PP1 activation, it is not always possible to distinguish a direct and a PP1-mediated effect of calcineurin on protein dephosphorylation. Accordingly, further calcineurin substrates include microtubule-associated proteins *Map2, Mapt,* and tubulin itself. (260). Their dephosphorylation aid the assembly and stabilization of microtubules (260, 261). Calcineurin may further mediate dephosphorylation of known PKC substrates such as the myristoylated alanine-rich C kinase substrate (*Marcks*), neurogranin (*Nrgn)* and neuromodulin (*Gap43*). Dephosphorylation of these proteins enhance their affinity towards

calmodulin (Ca^{2+}/calmodulin for *Marcks)* and impact actin cytoskeleton cross-linking by *Marcks* and synaptogenesis by *Ngrn* and *Gap43* (262). Moreover, calcineurin may be involved in regulation of SV pools via synapsin-1 dephosphorylation (197).

1.3 Mass-spectrometric analysis of peptides, proteins, and PTMs

Recent technological advances and development of mass spectrometry (MS) instrumentation have enabled large-scale identification and quantification of proteins and PTMs. In the following, I give a brief overview of the main principles underlying MS-based analysis of peptides, proteins, and PTMs.

1.3.1. Instrumentation and working principle

First mass spectrometers have appeared already in the beginning of the 20th century, but for many years, the application of the technique was restricted to studying atoms and small molecules. Only after the invention of the soft ionization techniques electrospray ionization (ESI) (263) and matrix-assisted laser desorption (MALDI) (264, 265) in the mid-1980s, mass spectrometers became widely used for the analysis of large labile organic molecules such as proteins and peptides (266). Nowadays, mass spectrometry became an inevitable tool for biochemical studies and studies aimed at a comprehensive system-wide description of protein content, *i.e.*, proteomics studies.

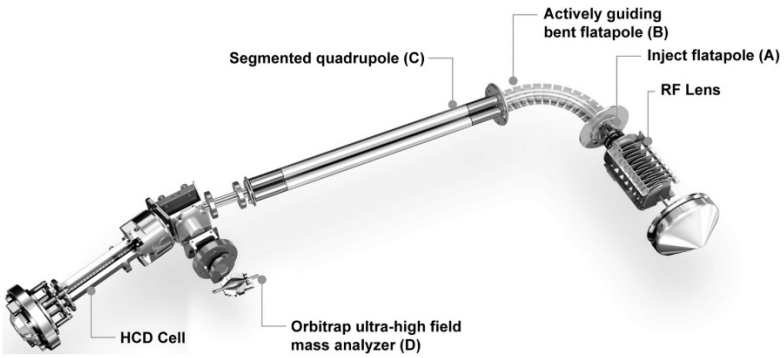

Figure 1.3: Ion path of the Q Exactive HF mass spectrometer*. RF lens, inject flatopole* ***(A),*** *and actively guiding bent flatopole* ***(B)*** *guide, focus and pre-filter ions entering the mass spectrometer. Segmented quadrupole* ***(C)*** *functions as a selective mass filter. Masses of intact precursor ions and fragment ions produced in the HCD cell are analyzed by the Orbitrap* ***(D****). The figure is adapted from Scheltema et al* ***(267).***

A conventional mass spectrometer requires an ion source, mass analyzer and, depending on the implementation, a detector. Usually, it is operated under vacuum, and ionized particles are guided by magnetic and/or electric fields. Ions are directed from an ion source to a mass analyzer where the separation of ions according to their mass-to-charge ratio (*m/z*) takes place. A Time-of-flight or quadrupole mass-analyzer further require a detector, which determines the intensity of the ions. A result of the ion detection is a mass spectrum (MS): a list of observed *m/z* and corresponding intensities. (268). An ion path of an ESI – hybrid quadrupole – Orbitrap mass spectrometer as implemented in the Thermo

Fisher Scientific Q Exactive HF mass spectrometer is illustrated in **Figure 1.3** (267). Mass spectrometers applied in this work utilize similar construction principles and elements.

Mass spectrometers are designed to measure charged molecules or ions. In an ESI ion source, an analyte is sprayed under high voltage (>1 kV) through a fine emitter into the inlet of a mass spectrometer. It is assumed that the ionization of larger molecular ions, *e.g.,* peptide ions, is achieved through passive solvent evaporation from small droplets containing only one analyte ion (269). Initially, the high potential difference between the needle and the inlet of the mass spectrometer results in generation of charged droplets with a charge density approaching its theoretical limit, the Rayleigh limit. Solvent evaporation further increases the charge density resulting in the generation of even smaller droplets that are emitted from a Taylor Cone formed on the original droplet. This process leads to a very fine liquid dispersion and a further release of molecular ions due to the solvent evaporation (269).

The initial parts of the ion route, *i.e.,* the RF lens, injection flatopole and the bent flatopole focus the ion beam and act as initial pre-filter to remove neutral molecules, solvent droplets, and ion clusters, as well as to reduce the kinetic energy of ions via collisional cooling (270). Transmitted ions are further filtered by a segmented quadrupole (267). A quadrupole mass analyzer is constructed of four pairwise connected parallel metal rods. By varying the radio frequency (RF) voltage and direct current (DC) voltage applied to the rod pairs, it is possible to stabilize a path of selected ions, while trajectories of other ions end up in collision with the rods (271). The quadrupole is followed by a short octapole that conducts ions into the C-trap connected to the terminal quadrupole that acts as a collision chamber (a high energy collision dissociation or HCD cell (272)). Here, ions become activated through the collision with nitrogen gas molecules filling the collision chamber. A portion of the collision energy is converted into internal energy resulting in the bond breakage and fragmentation. Peptide ions typically break along their amine/peptide bond, which produces a series of ions, *i.e., y* and *b* fragment ions as illustrated in **Figure 1.4** (273). Fragment ions can be trapped inside the HCD cell, pushed back into the C-trap and ejected into the Orbitrap analyzer (270).

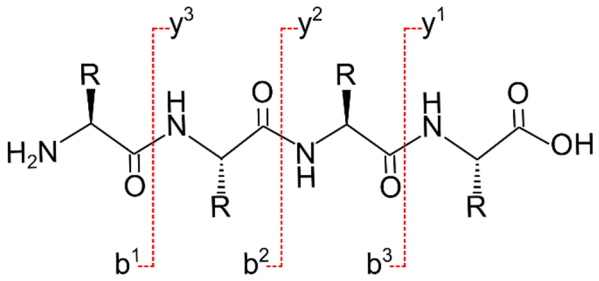

Figure 1.4: Nomenclature of y and b fragment ions. *In an HCD cell, y and b ions are the common fragment ions that arise due to the breakage of the peptide bond. B ions contain an intact N-terminus, and y ions an intact C-terminus of a peptide. The fragments are numbered consecutively with the increasing mass (274, 275). R denotes an amino acid side chain.*

Orbitrap acts as both a mass analyzer and a detector providing *m/z* and the signal intensity of an ion. It consists of two cup-shaped outer electrodes and one spindle-like central electrode (276). Ions injected into the space between the electrodes oscillate harmonically along the central (axial) electrode. Mass-to-charge ratios and the intensities of ions can be calculated based on the frequency of these oscillations using Fourier transformation. Because the axial frequency does not depend on the initial energy and the spatial spread of ions, it allows for a high resolution (>100,000) and an accurate mass detection (277).

1.3.2. Sample Preparation for Mass Spectrometry (MS)

Currently, there are two main branches in mass spectrometric protein analysis. In a conventional *bottom-up* experiment, proteins are cleaved by an endoproteinase and resulting peptides are subjected to a mass spectrometry analysis. Information about proteins is inferred from the pool of identified peptides. An alternative workflow known as *top-down* proteomics aims at analyzing non-cleaved proteins. Since peptides are more amenable for an MS analysis due to a limited set of charge states, uniform fragmentation and better detection limits, the bottom-up approach allows for a large-scale analysis and identification of thousands of proteins in complex samples. (278). Trypsin is a widely used proteinase that cleaves at the C-terminus of arginine (R) or lysine (K). Tryptic peptides often contain 7-20 amino acids and carry one of the basic amino acids at their C-terminus. At low pH, the basic residues are positively charged, which improves the ionization properties and the “flyability” of a peptide. Therefore, it is common to operate the liquid chromatography (LC) coupled to a mass spectrometer at low pH. Supplements such as formic acid (FA) act as H^+ donors and facilitate the ionization of peptides. During ESI, peptides typically acquire two or more H^+, which results in multiply charged peptide ions that can be analyzed by a mass spectrometer operated in a positive ionization mode. Moreover, specific cleavage sites simplify the subsequent peptide identification, since it reduces the number of theoretical peptides that can fit to an MS spectrum (273).

When analyzing PTMs, additional enrichment methods are usually required, since post-translationally modified peptides, *e.g.*, phosphopeptides, are underrepresented in complex

samples. Common enrichment strategies employ immobilized-metal-ion affinity chromatography (IMAC (279)) and metal-oxide affinity chromatography (MOAC (280)). The enrichment is conducted at low pH, which facilitates the protonated state of carboxyl groups of acidic amino acids (D and E) and of the peptide C terminus. In contrast, phosphate groups remain deprotonated due to their different pKa values. As a result, phosphate groups become complexed by the metal oxide or metal ion on the solid phase forming an enrichable complex (281).

When speaking about identifying and quantifying proteins in a biological sample, one often has to deal with thousands of different proteins. To decrease the complexity of the sample and improve coverage of identified proteins and peptides in a *bottom-up* MS experiment, different protein and peptide fractionation approaches have been developed. In particular, chromatographic techniques using a C18-based reversed-phase stationary phase has proven useful for efficient peptide separation (282). Off-line pre-fractionation at basic pH (bRP) can be successfully combined with an on-line (directly coupled to a mass spectrometer, LC-MS/MS) reversed-phase chromatography at acidic pH (283, 284). Thus, the general scheme for the sample preparation includes the following steps: i) protein digestion using specific endoproteinase (*e.g.,* trypsin); ii) optional: enrichment of modified peptides for PTM analysis; iii) off-line pre-fractionation using bRP to reduce sample complexity; iv) sample analysis using LC-MS/MS.

1.3.3. Data-Dependent Acquisition

After passing an ion source, ionized peptides are subjected to a survey scan (MS1) to determine their *m/z* ratio and intensity. In a top N mode, N of the most intense peaks (precursors) are sequentially selected by quadrupole for fragmentation in a collision cell (an HCD cell, s. above). Identification of precursor fragments allows for a confident precursor identification based on its fragmentation pattern (285).

Due to the preselection of precursor ions based on their intensity, this type of MS/MS acquisition is known as data-dependent acquisition (DDA). Acquisition in this mode produces pairs of MS1-precursors and corresponding MS2-fragment spectra, and a narrow *m/z* window used for precursor selection assures that fragments observed in MS2 originate from a selected precursor ion. The fragmentation patterns can be matched against theoretical MS/MS spectra, resulting in peptide-spectrum matches (PSMs) (273).

However, the drawback of DDA is that by selecting N precursors, it introduces a stochastic and irreproducible component into MS/MS acquisition. Furthermore, as the decision which MS/MS spectra will be acquired is mostly based on the precursor intensity, peptides present

in low amounts (such as phosphorylated peptides) might be completely masked by highly-abundant peptides resulting in precursor undersampling (286).

1.3.4 Identification of peptides and proteins

An acquired tandem MS/MS spectrum is a record of *m/z* of fragment ions and corresponding ion intensities. An MS/MS spectrum further contains the information about its parent or "precursor" ion, *i.e.*, its *m/z* and charge (deduced from the isotopic distribution of the precursor ion). A common approach for peptide identification based on MS/MS spectra is the automated database search (287). This approach utilizes protein sequence databases – collections of amino acid sequences of proteins that extensively covers proteins potentially present in the analyzed sample. Protein sequences are *in silico* digested in accordance with specified cleavage rules (cleavage after K or R for trypsin), and the mass of the peptide precursor and its theoretical fragments (*b*- and *y*-ions) are calculated. In the case of possible (variable) modifications such as phosphorylation, a precursor mass and masses of theoretical fragment ions are computed separately considering all possible positions of the modification within the peptide sequence. Acquired MS/MS spectra are matched against the theoretical spectra. Certain mass deviations (tolerances) between the observed *m/z* of an ion and calculated *m/z* are allowed for the match to be reported. Each match is scored, and the best peptide-spectrum match (PSM) is assigned to the spectrum.

In the case of phosphorylated peptides, it is important to not only identify the peptide, but also to localize the phosphate group. The latter is in particular challenging if there are several S/T/Y amino acids in the peptide sequence and a peptide is multiply phosphorylated. Therefore, a confident PTM localization requires rich fragmentation pattern and characteristic fragment ions containing either an intact phosphate (+80 Da) or neutral losses of H_3PO_4 (-98 Da) or HPO_3 (-80 Da). Based on the observed fragment ions, probabilities for each phosphorylated site are calculated and expressed in percent. Usually, only phosphorylated sites with the localization probability > 75% are considered for further analysis (first-class phosphorylated sites) (288).

In order to find a minimal acceptable score and to prevent accumulation of false assignments, one makes use of decoy sequences (289). Decoy sequences are non-existing peptide sequences, which are generated, for example, via reversal of the existing peptide sequences in the database. When comparing the distribution of PSM scores for existing peptides (S_{PSM}) *vs.* the distribution of scores for a priori false positive matches to decoy sequences (S_{dec}), it is possible to derive a cut-off score S_{cut}, such that the list of reported PSMs with $S_{PSM} \geq S_{cut}$ will contain no more than N false positives (290). The tolerated

proportion of false positives (also known as the false discovery rate, FDR) is commonly set to 1%.

In the bottom-up proteomics, the information about the proteins is inferred based on the pool of all identified peptides (291). Since there are peptides that are shared between proteins, a common approach is to organize proteins in a minimal number of protein groups according to the principle of parsimony (291, 292). Thus, each protein group contains proteins that share one or more peptides. Protein groups are distinguished from each other based on peptides that are unique for a given protein group. A leading protein is a characteristic protein that contains the most peptides assigned to its protein group. Shared peptides are usually distributed in “all-or-nothing” principle, *i.e.*, the protein group with the maximum number of peptides becomes all shared peptides assigned. The peptide scores of the assigned peptides are combined into a protein score and the FDR is calculated again on the protein group level (290). The FDR has to be controlled at each level separately since false assignments at a lower level (*e.g.,* peptide level), tend to inflate identifications at a higher level (293).

1.3.5 Protein quantification using a label-free and an isobaric-tag labeling approach

MS based proteomics allows not only identification of proteins, peptides, and PTMs, but it can be applied to compare their abundances in different samples. Quantitative approaches can be broadly categorized in label-free and chemical labeling-based methods (294). I discuss in brief a classical label-free approach and an isobaric-tag labeling, as they are both utilized in this work.

The label-free approach utilized by MaxQuant (295) relies on quantification of the precursor signal in MS1 survey scans (296). In a standard DDA method, MS1 survey scans are repeated after a certain time interval or following a fixed number of MS/MS acquisitions, depending on a chromatographic setup, usually, every 2-3 seconds. If the chromatographic elution of a peptide takes 30 s and MS1 scans are conducted every 3 s, there are approx. 10 time points that can be used to reconstruct the elution profile of a precursor. Area under the curve correlates with the peptide abundance and is suitable for quantitative comparisons (297).

An alternative approach to peptide quantification utilizes isobaric labels such as tandem mass tags (TMT) (298). TMT reagents consist of an amine-reactive NHS-ester group, a mass normalizer, and an MS/MS reporter. Each reagent has the same nominal mass but differs in the distribution of ^{13}C and ^{15}N isotopes between the mass reporter and the mass normalizer. TMT reagents are highly reactive towards primary amines, *i.e.*, N-termini and lysine side chains of peptides. After labeling with TMT reagents, different peptide samples

are pooled and analyzed as a single sample. Due to the isobaric nature of the TMT reagents, precursor signals are indistinguishable in MS1. Only the precursor fragmentation leads to generation of reporter ions with distinct masses. Intensities of the reporter ions in the MS/MS spectrum are used for quantitative comparison of peptide abundances in the labeled samples (299).

The advantages of TMT-labeling technique *vs.* label-free approach is in that i) it reduces the technical variance and minimizes the problem of missing values because the peptide samples are processed as one following the labeling and pooling; ii) it is better compatible with pre-fractionation techniques resulting in a deeper proteome coverage, since the reporter ion intensities and not the elution profiles of peptide ions are used for quantification; iii) it boosts sensitivity because intensities of low-abundant peptides are combined in MS1, which increases their chance to be selected for MS/MS. The disadvantages of the labeling approach lie in the cost of the reagents, the lower dynamic range, and the inaccuracy in depicting large changes due to the co-isolation of other precursor ions leading to “ratio compression” (300). A development on an SPS-MS3 acquisition method (301) allowed to alleviate the “ratio compression” problem, although at the cost of the reduced sensitivity (300). Therefore, an experimenter can select a suitable method to prioritize the quantification accuracy or the sensitivity depending on the scientific question.

It has to be noted that in a *bottom-up* proteomics the lowest quantitative level is either the precursor (MS1 peak area, label free quantification) or a PSM (reporter ion intensity, TMT), while the desired quantification levels are often peptides or proteins. Several precursors or PSMs may identify the same peptide and several peptides may originate from a single protein. This requires, therefore, a summarization of quantitative values obtained at the lowest quantitative level. Different sophisticated algorithms have been suggested that propagate quantitative values up to peptide or protein level (302, 303), though simple mean, median or sum of precursor/reporter ion intensities being still common summarization methods (304).

1.3.6 Post-processing of quantitative proteomics data

Label-free or label-based protein quantitative data enable, in the first place, a relative quantification of peptide and/or protein abundances (294). The peptide intensity observed in an ESI-LC-MS/MS setup is dependent not only on the peptide abundance, but also on its physical and chemical properties. Therefore, a direct comparison of LC-MS/MS intensities of different peptides/proteins would require additional correction steps and use of calibration curves of standards in pre-defined amounts (305). In contrast, intensity comparison of the same peptide/protein allow for a direct estimation of changes in peptide/protein abundance

in different samples. Such differences are conveniently expressed as $log_2(I_2 / I_1)$ and known as log_2-fold changes (log2FC), where *I* is a peptide/protein intensity in the sample 1 or 2, respectively (306). Accordingly, Log2FC of 1 means a two-fold increase in the intensity in the sample 2 as compared to the sample 1, while a value of -1 corresponds to a two-fold intensity decrease in the sample 2 *vs.* sample 1.

When comparing peptide/protein abundances in two or more samples, it is important to correct for possible systematic errors that arise during sample preparation, *i.e.,* errors in the estimation of the protein concentration and errors associated with liquid handling, and result in unequal protein amounts being analyzed (307). Normalization strategies using median subtraction and its extended version, Tukey's median polishing, proved useful and robust methods for intensity normalization in proteomics (308). These normalization strategies are based on the assumption that abundancies of the majority of peptides/proteins are not changed between the samples.

In the following, log2FC are tested to be significantly different from 0 (no abundance difference), *e.g.*, using a one-sample t-test. Other methods were developed to improve differential analysis in large genomic or transcriptomic data such as microarrays (309), and were further adapted to the analysis of proteomics data (310). For example, *limma* (311) offers an extended functionality, as it supports complex experimental designs via linear models. Further, it augments the statistical power of a test via correcting individual peptide/protein variances by the global variance within the data set utilizing a Bayesian framework, which is in particular beneficial for experiments with low number of replicates (311, 312).

While performing a differential expression analysis, it is important to control the number of false discoveries, since given the number of peptides and proteins quantified in a typical proteomics experiment, some of them might appear differentially expressed just by chance. For large-scale experiments such as a proteomics experiment, statistical methods were developed that estimates a false discovery rate among a list of differentially expressed peptides/proteins (313-315). FDR is commonly expressed in a form of *q*-values, which can take values between zero and one and are similar in this way to *p*-values. One can define a *q*-value threshold, *e.g.*, 0.01, that can be used to list significant tests with the desired FDR level (here 1%). This approach is convenient, as defining a *q*-value threshold resembles hypothesis rejection based on a *p*-value.

1.3.7 Systems analysis of proteomics data

A differential expression analysis commonly produces a list of differentially expressed peptides or proteins. In a case of a phosphoproteomics study, this might be a list of

differentially phosphorylated amino acid positions (sites) of proteins. A systems analysis is a next step towards understanding how observed changes might impact cellular processes, pathways, *etc*. (316). For this, proteins are assigned to hierarchically structured terms (gene ontologies) that concisely describe a molecular or biological function or a cellular localization of proteins (317). By using statistical testing (usually a Fisher's exact test) it is possible to assess which categories are particularly enriched among differentially expressed proteins as compared to some background (usually, a whole proteome or its subset). A fold enrichment and a *p*-value are returned for each term. *P*-values can be corrected for multiple testing using one of the approaches described above. A result is a list of significantly enriched terms that can be further refined analytically depending on the biological context (316). A similar approach can be applied for pathway analysis (318, 319) or analysis of protein domains (320) and sequence motifs (321). Furthermore, using specialized databases such as String (322), one can query interaction partners of regulated proteins and explore how they are interconnected. Together with the sequence motif analysis, this information, for example, is utilized to predict kinase-substrates relationships for identified phosphorylated sites (144, 323). Nonetheless, one needs to be aware that the analysis is not unbiased (316). Potential sources of bias are the automated annotation and lack of detailed inspection by an expert; overlapping, redundant, too general or too specific categories; problems with the data transfer from one biological system to another; domination of a few extensively studied and, therefore, well annotated proteins over the majority of a rather poorly described proteins, *etc*. To partially alleviate these problems, a curated pathway database Reactome (319) or a synapse-specific expert-curated database SynGO (324) have been developed . Moreover, consulting experimentally validated data such as provided in the PhosphoSitePlus (325) database can further enhance the credibility of the analysis.

2 Aim of the thesis

An accumulating evidence suggests that kinases and phosphatases play an important role in the synapse physiology and that protein phosphorylation may modulate the neurotransmitter release, and, therefore, the synaptic strength. It is widely accepted that the increase in the cytosolic Ca^{2+} concentration is the main trigger of the phosphoproteome changes in the synapse. The main goal of this thesis is to demarcate phosphorylation events that depend on active SV cycling from those that are primarily triggered by the Ca^{2+}-influx due to the membrane depolarization. Such separation would offer a new point of view at the protein phosphorylation in the synapse and propose sites that exert a direct modulatory role on the neurotransmitter release. To achieve this, several steps had to be made. First, a stimulation protocol had to be established that would either allow for an active SV cycling with low net Ca^{2+}-influx or abolish SV cycling while preserving the Ca^{2+}-influx. For this, the applicability of electrical field stimulation as a potentially milder stimulation in comparison to chemical stimulation protocols and BoNT as a potent and very specific blocker of exocytosis and, therefore, of a complete SV cycling, were investigated. Second, a selection and optimization of suitable sample preparation techniques for MS-based analysis were carried out to achieve a comprehensive identification and quantification of the synaptic phosphoproteome. Thus, application of TMT-labeling techniques together with pre-fractionation techniques and MS2 and SPS-MS3-based quantifications allowed for a comprehensive analysis of the synaptosomal phosphoproteome. Third, based on the differential expression analysis and predicted substrate-kinase interactions, the demarcation of the SV cycling dependent and primarily Ca^{2+}-dependent phosphorylation sites and their association with different kinase groups was achieved. Finally, selected SV-dependent phosphorylated sites had to be tested for their modulatory effects on the exo- and endocytosis. In cooperation with Prof. Silvio O. Rizzoli and Dr. Eugenio Fornasiero, modulatory effects of SV cycling dependent phosphorylation sites on syntaxin-1, synaptobrevin-2, and cannabinoid receptor-1 were demonstrated in cultured hippocampal neurons.

3 Preliminary Methods

3.1 Ethical statement

All animal experiments were conducted in accordance with the national law of the Federal Republic of Germany. For details s. section 5.4.1

3.2 Synaptosome preparation

Synaptosomes were prepared as described in section 5.4.3.

3.3 Electrical stimulation of synaptosomes

1.5 mL of synaptosomal suspension in a sodium-containing buffer (1 mg of synaptosomal protein per 1 mL buffer) were kept at 37°C in a thermostated quartz cuvette (119F-10-40, 3.5 mL, Hellma Analytics, Mühllheim, Germany) under constant stirring as described for the glutamate release assay in section 5.4.4. Platinum electrodes of 1 mm diameter were inserted at the two opposite corners (distance $\sqrt{2}$ cm) reaching the bottom of the cuvette. Stimulation was applied using square pulses of alternating polarity generated by A385 Stimulus Isolator in a combination with an A310 Accupulser Stimulator (both from World Precision Instruments, Sarasota, USA) and monitored using an oscilloscope (PCSGU250, Velleman, Gavere, Belgium). Following stimulation parameters were applied if not stated otherwise: 15 ms pulse width, one pulse per 100 ms (10 Hz), 15 mA nominal current, voltage at a peak ~2.5 V, stimulus duration 120 s.

3.4 BoNT-treatment and glutamate release assay

BoNT-treatment and glutamate release assay were performed as described in section 5.4.4. Electrical stimulation was used instead of KCl-stimulation.

3.5 Treatment with Cd^{2+}, ω-conotoxin, and bafilomycin A_1

Chemicals/toxins were added to synaptosomes resuspended in sodium buffer and pre-incubated at 37°C for at least 5 min. 20 mM $CdCl_2$ stock solution (Merck, Taufkirchen, Germany) in water was added to synaptosomes 5 min prior to the first or the second (repeated) electrical stimulation. A final concentration of 20 or 60 µM of $CdCl_2$ was used. Ω-Conotoxin MVCII (Alomone Labs, Jerusalem, Israel) was dissolved in 1% (v/v) ethanol/water at the concentration of 1 mM. The toxin was added to synaptosomes to a final concentration of 1 or 2 µM, 10 min prior to the first or the second electrical stimulation. Stock solution of 0.1 mM bafilomycin A_1 (Abcam, Cambridge, UK) in 1% (v/v) DMSO in water was added to synaptosomes to reach a final concentration of 300 nM. The toxin was added 10 min before the stimulation, if not stated otherwise.

3.6 Acridine orange fluorescence assay

The acridine orange fluorescence assay was conducted following the previously published protocol (104). In brief, stock solution of 1.5 mM acridine orange in water was added to synaptosomes to reach a final concentration of 5 µM. Synaptosomes were incubated for 10 min at 37°C in a thermostated quartz cuvette as described for the glutamate release assay. The AO fluorescence was monitored at 490 nm excitation and 530 nm emission wavelengths. For stimulations including bafilomycin A1 treatment, the toxin was added ~5 s prior the stimulation (electrical stimulation or KCl).

3.7 Fura-2 assay

Fura-2 assay was set up as described in section 5.4.13. The Fura-2 fluorescence was measured in synaptosomes pre-incubated in sodium buffer without extra Ca^{2+} (zero net Ca^{2+} or "background"). Then, $CaCl_2$ was added to reach a final concentration of 1.3 mM and the fluorescence was recorded for further 3 min. Synaptosomes were then stimulated using a repeated electrical stimulation separated by a 2 min pause, and then stimulated with 50 mM KCl. The maximum and minimum Fura-2 signal was determined following lysis with 2% SDS and subsequent quenching with 100 mM EGTA, respectively. Cytoplasmic Ca^{2+} concentration was calculated as described in (101) assuming K_d (Ca/fura-2) = 224 nM.

3.8 Analysis of fluorescence data

The fluorescence data were analyzed in R programming language for statistical computing. Glutamate release assay and AO fluorescence data were collected as two data points every 3-4 s seconds. A fluorescence signal (S) was corrected by the fluctuations in the lamp current (R) and the corrected signal S/R was used for further analysis. An average of the two data points was computed, and the data were smoothed using rolling truncated mean of seven data points (trim parameter of 0.3) to remove excessive fluctuations of the signal. Fluorescence *f* was normalized by the fluorescence prior to the first electrical stimulation, f_0. The change in the normalized fluorescence before and after stimulation were assessed as $f/f_0(after) - f/f_0(before)$, where $f/f_0(before)$ is the normalized fluorescence at the start of the stimulation, and $f/f_0(after)$ is the median fluorescence of the first 60 s after the stimulation was aborted. In the case of KCl stimulation, the fluorescence at 2 min after adding KCl was used.

3.9 MS sample preparation

1.7 mg synaptosomes were resuspended in sodium buffer at a concentration of 1 mg of synaptosomal protein per 1 mL. The synaptosomes were prepared for electrical stimulation as described before. Aliquots of the synaptosomal suspension corresponding to 200 µg of

synaptosomal proteins were collected during, prior, or after the stimulation and immediately lysed in equal volume of lysis buffer (4% (wt/v) SDS, 1 mM EDTA, 20 mM TCEP, 80 mM CAA, 100 mM HEPES, in water, supplemented with 2 × Halt protease and phosphatase inhibitor cocktail), pre-warmed at 95°C. Four kinetic experiments were conducted and six samples were collected for each kinetic at the following time points: 1) 0 s (before stimulation), 2-4) 10 s, 30 s, 60 s after the stimulation started, 5) ~5 s after the stimulation ended, 6) 60 s after the end of the stimulation. The samples were further processed as described in section 5.4.4 and section 5.4.5. Following the digestion and prior to enrichment of phosphorylated peptides, samples were labeled with TMT6 labeling reagents. After the labeling, materials of each two kinetics were combined, resulting in two TMT6-labeled samples. Subsequent sample preparation followed protocols in the sections 5.4.5 and 5.4.6

3.10 LC-MS/MS

The LC-MS/MS acquisition followed the LC set up and parameters described in section 5.4.7. BRP fractions of the enriched phosphorylated peptides and the whole proteome were acquired in duplicates or as single injections, respectively, using Fusion Tribrid mass spectrometer (Thermo Fisher Scientific, Waltham, USA). Phosphorylated peptides were eluted using a linear gradient consisting of the following steps: i) increase from 2% to 7% buffer B for 4 min; ii) increase from 7% to 32% over 86 min; iii) from 32% to 50% over 28 min; iv) wash at 90% over 5 min and v) equilibration at 2% over 5 min. The elution gradient for the whole proteome was as follows: i) 5-8% over 4 min; ii) 8-34% over 86 min; iii) 34-50% over 28 min; iv, v) wash and equilibration as described above. MS was operated in positive data-dependent SPS-MS3 (301) mode. MS1 survey scans of 350-2000 *m/z* range were acquired at the resolution of 120,000, automated gain control target (AGC) of 1e6 and the maximum injection time (MaxIT) of 50 ms. Precursor ions of charge states 2-7 were selected for fragmentation using normalized collision energy (NCE) of 38%. MS2 scans were acquired in Orbitrap at the resolution of 30,000 (phosphorylated peptides) or 15,000 (whole proteome), AGC target of 5e5 and MaxIT of 200 ms (phosphorylated peptides) or 54 ms (whole proteome). 10 most intense fragment ions were subjected to HCD-fragmentation using NCE of 50%. SPS-MS3 spectra were acquired at the resolution of 50,000, using AGC target of 2.5e5 and the MaxIT of 200 ms (phosphorylated peptides) or 86 ms (whole proteome).

3.11 Data Analysis

Data analysis was conducted as described in section 5.4.8 with a few exceptions. In MaxQuant, the quantification was based on reporter ion intensities in SPS-MS3 scans. The reporter ion intensities were $\log_2$-transformed and normalized using median polishing, and

the intensity of the first channel (0 s time point) was subtracted from the other channels. Phosphorylation sites showing a Pearson correlation of the two kinetic measurements > 0.6 and a minimum absolute log_2 intensity fold change at any time point of 0.585 were subjected to hierarchical clustering using *hclust* function and Euclidean distances in R.

4 Preliminary Results

As mentioned before, chemical agents such as KCl and 4-AP are commonly used to stimulate neurotransmitter release from synaptosomes. One of the drawbacks of this stimulation is that the stimulating agent cannot be easily removed from the system. This mode of stimulation is non-physiologically strong and results in a significant increase in the cytoplasmic Ca^{2+} concentration. The latter activates Ca^{2+}-dependent kinases and phosphatases, however, it remains unclear, to which extent this activity is relevant for a normal SV cycling process. In order to study phosphorylation events that are closely related to SV cycling, the applicability of electrical stimulation to evoke neurotransmitter release was investigated.

According to early reports, field-stimulation of synaptosomes in suspension caused glutamate liberation monitored by the glutamate release assay. However, high frequency stimulation with short pulses similar to one used in earlier synaptosomal studies (0.4 ms pulses at 100 Hz (105)) or the one commonly applied in neuronal cell cultures (1-2 ms pulses at 20 Hz (123)) did not produce a measurable glutamate release using moderate currents (<15 mA/mL). When applying stronger currents, glutamate release in 1.3 mM Ca^{2+}-containing incubation medium (in the following referred to as Ca) almost did not differ from glutamate release in Ca^{2+}-free incubation media containing 0.5 mM EGTA (in the following referred to as EGTA). Reducing the stimulation frequency and prolonging the pulse duration allowed for a reproducible Ca^{2+}-dependent glutamate release (**Figure 4.1A**). The release was proportional to the pulse width and applied current: when using shorter pulses, a stronger current was required to evoke similar glutamate release (**Figure 4.1B**). Following stimulations were conducted using 15 ms pulses of alternating polarity delivered every 100 ms (10 Hz). Glutamate release halted after the stimulation was aborted. Repeated stimulation of the same synaptosome suspension evoke a reproducible release (s. repeated stimulations in **Figure 4.1D-F**). These observations imply that the membrane remained intact after the electrical stimulation. Accordingly, an earlier study did not find any significant development of heat or reactive oxygen species at the electrodes that might cause synaptosome damage and thus explain the neurotransmitter release (109). However, a Fura-2 assay could not reveal any increase in the cytoplasmic Ca^{2+} concentration that is attributable to electrical stimulation (**Figure 4.1C**). More strikingly, treatment of

synaptosomes with a combination of botulinum neurotoxins (BoNT) A and D did not hamper the glutamate release; though the toxin treatment caused a significant suppression of the release following KCl-induced depolarization (**Figure 4.1D**). Application of Ca^{2+}-channel blockers Cd^{2+} (20 µM) or ω-conotoxin MVCII (1 or 2 µM) caused a decrease of 11%, 29%, and 12%, respectively (**Figure 4.1E, F**). Interestingly, no decline was observed after the application of 60 µM $CdCl_2$ or 2 µM of the ω-conotoxin in the first stimulation replicate. When using acridine orange (AO) that is trapped in SVs and illuminate after the release, electrical stimulation did not prevent the decay of AO-fluorescence due to the gradual accumulation of the dye inside SVs. In contrast, 50 mM KCl caused a spike-like increase in the fluorescence (**Figure 4.1G**). Application of electrical stimulation together with 300 nM bafilomycin A_1 that inhibits v-ATPase and thus prevents AO trapping in SVs, showed the same rate of AO leakage as the application of bafilomycin A_1 alone, meaning that electrical stimulation did not accelerate the liberation of AO (**Figure 4.1H)**. When using the glutamate release assay, pre-incubation of synaptosomes with 300 nM bafilomycin A_1 resulted in a 15-16% lower glutamate release, while it decreased the KCl-evoked release by 54% (**Figure 4.1I**). Taken together, these observations do not allow to exclude that the glutamate release evoked by electrical stimulation may be generated by some non-exocytotic mechanisms. In contrast, the proportion of the glutamate released via exocytosis is probably below 30%. The reversal of the glutamate transporter of the plasma membrane might be the non-exocytotic pathway that constitutes the observed glutamate release.

Phosphoproteomics analysis of electrically stimulated synaptosomes revealed that a few phosphorylation sites undergo up- (**Figure 4.2A, B**, cluster 1) or down-regulation (cluster 2) during the stimulation. Among affected proteins, there are proteins involved in the cytoskeleton regulation (**Figure 4.2C**), *e.g.*, microtubule-associated protein 1a (*Map1a*), and tau (*Mapt*), tau tubulin kinase (*Ttbk1*), Protein kinase C and casein kinase substrate in neurons protein 1 (*Pacsin1*), and Erythrocyte membrane protein band 4.1-like 3 (*Epb41l3*). Another prominent group contain proteins involved into signaling pathways, kinases, ubiquitin-ligases and their modifiers: Adenomatous polyposis coli protein (*Apc*); Serine/threonine-protein kinase BRSK2 (*Brsk2*); CaMKII (*Camk2a, b, g*); Serine/threonine-protein kinase DCLK2 (*Dclk2*); A-kinase anchor protein 12 (*Akap12*); MAP kinase-activating death domain protein (*Madd*); PKA (*Prkaa1*); Protein phosphatase 1 regulatory subunit 7 (*Ppp1r7*); Neural precursor cell-expressed, developmentally down-regulated 4-like, E3 ubiquitin protein ligase (*Nedd4l*); *etc*. The latter group implies regulation through signaling pathways operating via CaMKII, MAPK, PKA, Wnt, PP1, and ubiquitination. Next, phosphorylated sites on Ca^{2+}, K^+, and Na^+-channel proteins are affected (*Cacnb4*, *Kcna2*, and *Scn1a*, respectively). Last but not least, several proteins involved in SV cycling are

affected, including, protein bassoon (*Bsn*), piccolo (*Pclo*), caskin-1 (*Caskin1*), DnaJ homolog subfamily C member 5 (*Dnja5*), DnaJ heat shock protein family (Hsp40) member C6 (*Dnaj6*), clathrin light chain A (*Clta*), AP2 complex subunit alpha (*Ap2a1*), amphiphysin (*Amph*), *etc*. Interestingly, S449/S551 sites on synapsin-1 follow the down-regulation pattern (**Figure 4.2D**). These sites on synpasin-1 were previously shown to be a target of MAPK and their dephosphorylation increased a pool of available SVs (171). These observations imply that electrical stimulation might induce adaptation processes in synaptosomes. However, it remains to be elucidated, to which degree this effect is achieved due the stimulation of SV cycling. In the following **chapter 5**, I introduce another approach to study SV cycling dependent phosphorylation events, which is based on KCl-stimulation and BoNT-treatment. The results of this approach are presented in the following manuscript (326), which constitutes a significant part of this thesis, and my own contribution is stated in detail in Author's contribution statement.

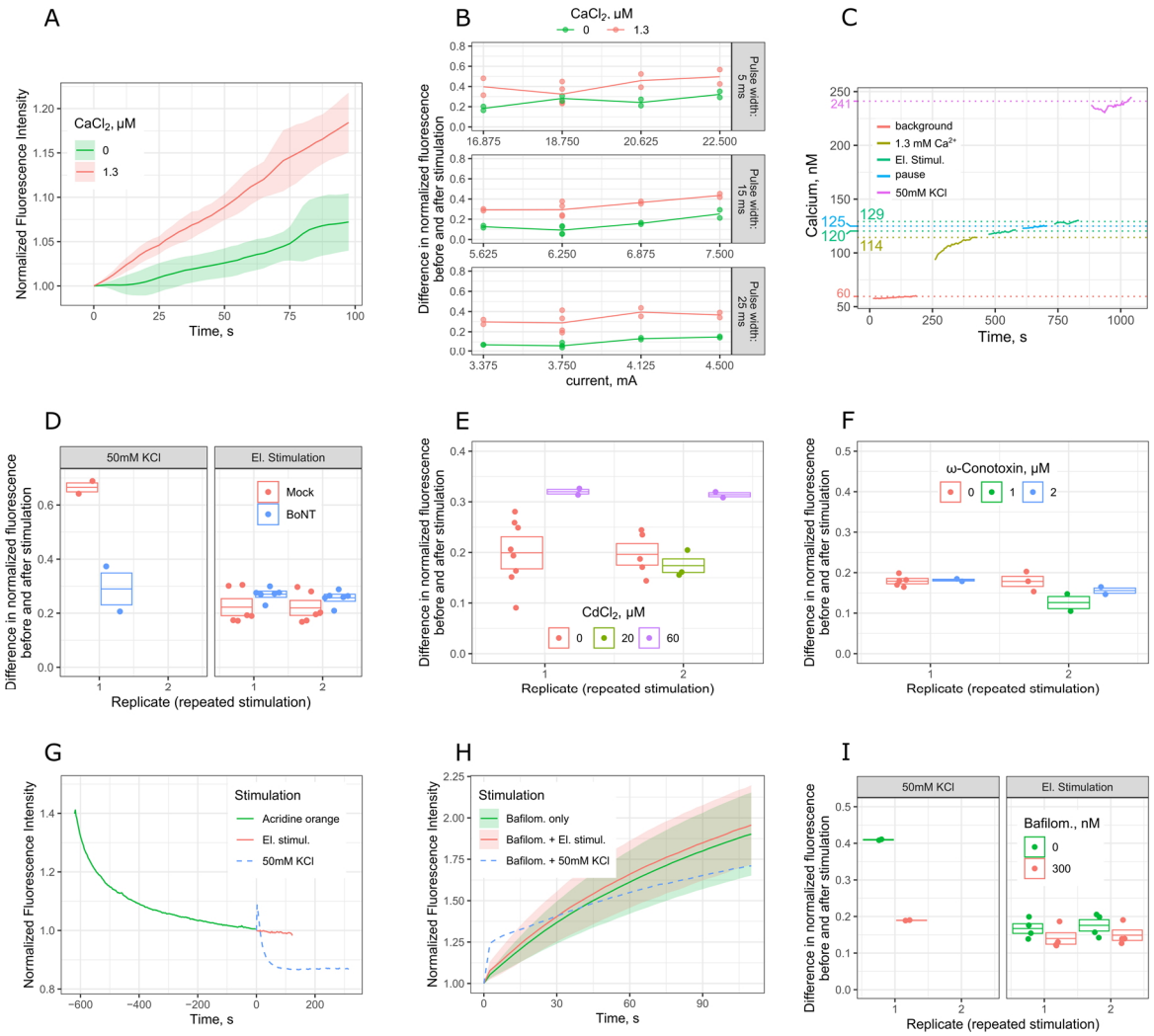

Figure 4.1: Electrical stimulation of synaptosomes. *Synaptosomes in suspension (1.5 mg synaptosomal proteins, at a concentration of 1 mg/mL) were electrically stimulated for 2 min using 15 ms square pulses of alternating polarity at a frequency of 10 Hz and 15 mA current if not stated otherwise. (**A**) Glutamate release during the stimulation in the presence of 0 (0.5 mM EGTA) or 1.3 mM Ca^{2+}. Lines represent means and areas represent standard deviations (N = 4). (**B**) Testing stimulation parameters. Conditions same as in (A)**.** (**C**) Fura-2 assay, a representative replicate. "Background" corresponds to 0 mM Ca^{2+} (no $CaCl_2$ added). (**D**) Glutamate release following treatment with heat-inactivated (Mock) or active BoNT A and D. Stimulation using 50 mM KCl or electrical stimulation. (**E**) Glutamate release following treatment with 0, 20, or 60 µM $CdCl_2$ and electrical stimulation. (**F**) Glutamate release following treatment with 0, 1, or 2 µM ω-conotoxin MVIIC and electrical stimulation. (**G**) Acridine orange (AO) fluorescence, a representative replicate. Synaptosomes were pre-incubated with AO (green solid line) and then stimulated with 50 mM KCl (blue dashed line) or electrically (red solid line). (**H**) AO fluorescence following addition of 300 nM bafilomycin A_1 and 50 mM KCl (blue dashed line), electrical stimulation (red solid line) or no stimulation (green solid line). Synaptosomes were pre-loaded with AO as in (G). Lines represent means and areas represent standard deviations (N = 7 (Bafilom. only), 6 (El. Stimul.), or 5 (50 mM KCl)). (**I**) Glutamate release following pre-incubation with 300 nM bafilomicyn A_1 and stimulation using 50 mM KCl or the electrical stimulation.*

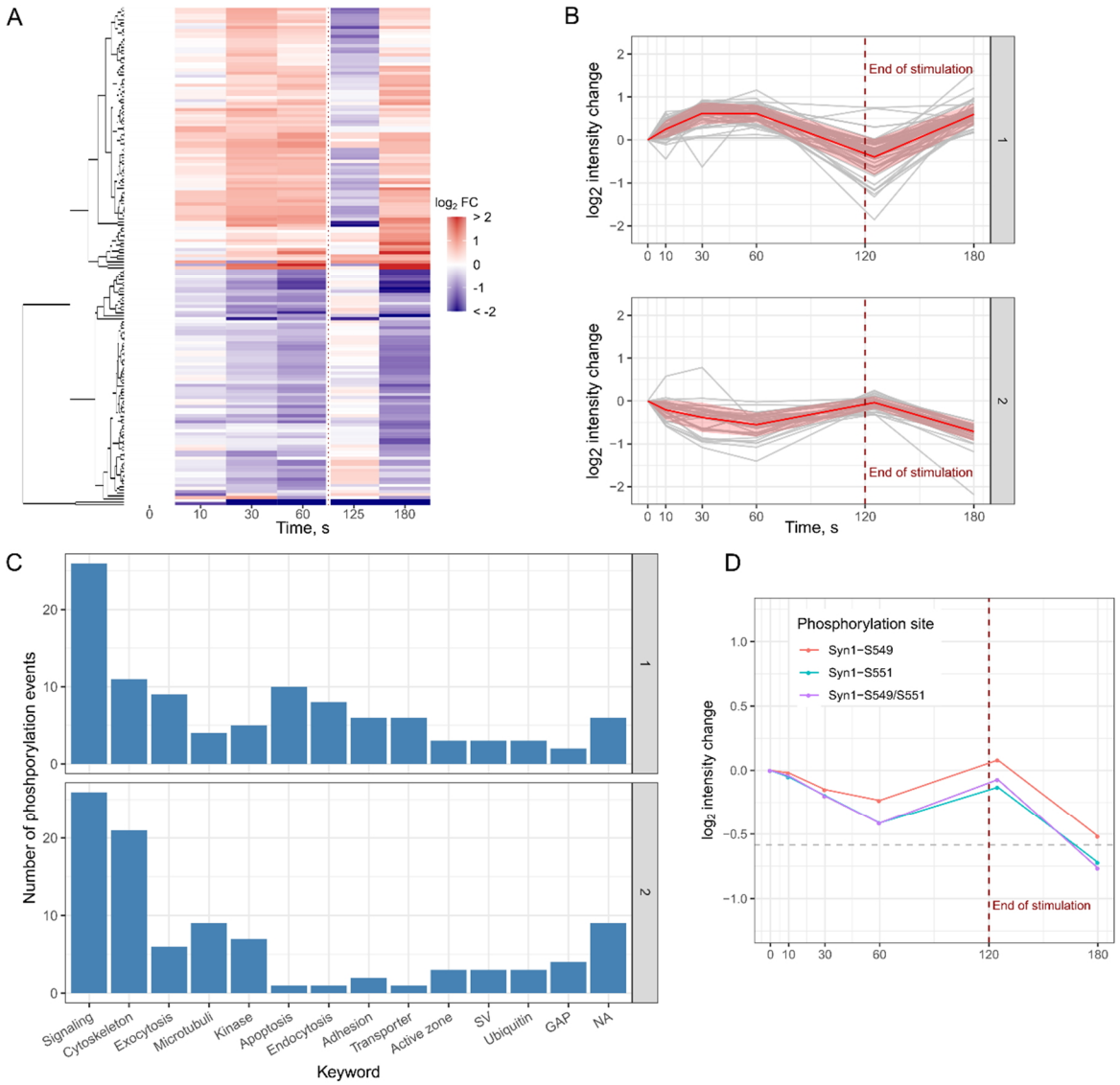

Figure 4.2: Phosphoproteomics analysis of electrically stimulated synaptosomes. *Synaptosomes in suspension (1.5 mg synaptosomal proteins, at a concentration of 1 mg/mL) were electrically stimulated for 2 min using 15 ms square pulses of alternating polarity at a frequency of 10 Hz and 15 mA. Six time points were collected: right before stimulation (0 s), during the stimulation (10 s, 30 s, and 60 s), right after the stimulation (~125 s), and one minute after the stimulation (180 s). The data are based on two kinetic measurements. Each kinetic is an average of two independent stimulation experiments. (**A**) Heat map of phosphorylation events showing Pearson correlation of >0.6 and a minimum absolute log_2FC of 0.585 at any time point as compared to the 0 s time point. A dotted line represents an end of the electrical stimulation. Color code represents log_2FC as compared ot the 0 s time point. The events are hierarchically clustered (s. dendrogram) based on the Euclidian distance. (**B**) Representation of the two main clusters from (A). Grey lines depict single phosphorylation events (log_2FC). Red line represents an average of all events in the cluster. Red area is a mean ± SD. (**C**) Keywords describing protein function/localization were assigned to proteins containing phosphorylation sites in the clusters 1 and 2. The keyword assignments were performed manually based on the information from available literature. 1-4 keywords were assigned per protein. Bars display a number of phosphorylation events per keyword per cluster, NA ~ not annotated. (**D**) Kinetics of selected singly (S449 and S551) and doubly (S449/S551) phosphorylated sites on synapsin-1. A grey dashed line represents a minimum log_2FC threshold of 0.585.*

5 Protein phosphorylation in depolarized synaptosomes: Dissecting primary effects of calcium from synaptic vesicle cycling[1]

Ivan Silbern[1, 2], Kuan-Ting Pan[2, #], Maksims Fiosins[3, 4], Stefan Bonn[3, 4], Silvio O. Rizzoli[5, 6], Eugenio F. Fornasiero[5, §], Henning Urlaub[1, 2 §], Reinhard Jahn[7, 8, §]

[1]Institute of Clinical Chemistry, University Medical Center Göttingen, D-37075 Göttingen, Germany;

[2]Bioanalytical Mass Spectrometry Group, Max Planck Institute for Biophysical Chemistry, D-37077 Göttingen, Germany;

[3]German Center for Neurodegenerative Diseases, D-72076 Tübingen, Germany;

[4]Institute for Medical Systems Biology, University Medical Center Hamburg-Eppendorf, D-20246 Hamburg, Germany;

[5]Department of Neuro- and Sensory Physiology, University Medical Center Göttingen, D-37073, Göttingen, Germany;

[6]Cluster of Excellence "Multiscale Bioimaging: from Molecular Machines to Networks of Excitable Cells" (MBExC), University of Göttingen, D-37075 Göttingen, Germany;

[7]Laboratory of Neurobiology, Max Planck Institute for Biophysical Chemistry, D-37077 Göttingen, Germany;

[8]University of Göttingen, D-37073 Göttingen, Germany;

[#]Current affiliation: Frankfurt Cancer Institute, Goethe University, D-60596, Frankfurt am Main, Germany; Hematology/Oncology, Department of Medicine II, Johann Wolfgang Goethe University, D-60590 Frankfurt am Main, Germany.

[§]Corresponding Authors: RJ (rjahn@gwdg.de), HU (henning.urlaub@mpibpc.mpg.de), EF (efornas@gwdg.de)

[1] The manuscript is represented as published in the "Molecular & Cellular Proteomics" with the exception of the reference list, which is merged with the reference list of this thesis. The joint list of references is presented at the end of this work. The references number in the manuscript are updated to match the merged list of references. Similarly, numbers of figures and tables are adjusted to align the figure and table numbering in the thesis.

5.1 Author's contribution

Figure 5.1	I**.S.**, K.T.P. H.U and R.J. conceptualized the experiments using synaptosomes. **I.S.** performed experiments and data analysis.
Figure 5.2	**I.S.** performed synaptosome preparation, stimulation experiments, BoNT-treatment, phosphopepeptide enrichment, and MS acquisition. **I.S.** performed differential expression analysis (B, C), kinase-substrate analysis (E, F) and comparison to previous studies (A, D) under supervision of K.T.P and H.U.
Figure 5.3	**I.S.** performed GO term enrichment analysis under the supervision of H.U and R.J.
Figure 5.4	**I.S.** categorized data in (A, B) and performed the enrichment analysis in (C) under the supervision of H.U, R.J, and S.O.R. **I.S.** performed the enrichment analysis in (D) following pilot analysis by M.F and S.B.
Figure 5.5	**I.S.** conducted protein annotations under the supervision of R.J.
Figure 5.6	E.F. and S.O.R. conceptualized experiments based on the phosphoproteome data. E.F. performed all experiments and analyzed data.
Figure 5.S1	**I.S.** isolated synaptosomes and conducted fluorimetric measurements
Figure 5.S2-S18	**I.S.** analyzed and categorized data under the supervision of K.T.P and H.U.
Figure 5.S19	**I.S.** performed protein extraction, and MS analysis. **I.S.** analyzed data under the supervision of K.T.P and H.U.
Figure 5.S20	**I.S.** performed BoNT treatment, phosphopeptide enrichment, MS sample preparation and MS analysis. **I.S.** analyzed data under the supervision of H.U.
Figure 5.S21	**I.S.** performed synaptosome preparation, stimulation experiments, BoNT treatment, MS sample preparation and MS analysis. **I.S.** analyzed data under the supervision of H.U.

5.1 Abbreviations

AAV	adeno-associated virus
ACN	acetonitrile
AGC	protein kinase A, G, C kinase group
AGC	automatic gain control
AMPAR	α-amino-3-hydroxy-5-methyl-4-isoxazolepropionic acid receptor
AP	action potential
BoNT	botulinum neurotoxin
bRP	basic reversed-phase chromatography
CAA	chloroacetamide
CaMKII	calcium-calmodulin kinase 2
CDK	cyclin-dependent kinase
CK1	casein kinase 1
CK2	casein kinase 2
CLK	SRPK1 and Clk/Sty protein kinase
CMGC	CDK, MAP, GSK, CDKL kinase group
CREB1	CAMP responsive element binding protein 1
DAPK	death associated protein kinase
FA	formic acid
GABA	γ-aminobutyric acid
GluDH	glutamate dehydrogenase
GO	gene ontology
GRK	G protein coupled receptor kinase
GSK3	glycogen synthase kinase 3
ITR	inverted terminal repeat (sequence)
MAPK	mitogen activated protein kinase
NMDAR	N-methyl-d-aspartate receptor
PAK	p21 activated kinase
PKC	protein kinase C
PNGase F	peptide-N(4)-(N-acetyl-beta-glucosaminyl)asparagine amidase
POI	protein of interest
PP1	protein phosphatase 1
RAS	rat sarcoma gene
RT	room temperature
SNARE	N-ethylmaleimide-sensitive factor-attachment protein receptors
STE	“sterile” serine/threonine protein kinases

SV	synaptic vesicle
TCEP	tris(2 carboxyethyl)phosphine
TEAB	triethylammonium bicarbonate buffer
TFE	trifluoroethanol

5.2 Abstract

Synaptic transmission is mediated by the regulated exocytosis of synaptic vesicles. When the presynaptic membrane is depolarized by an incoming action potential, voltage-gated calcium channels open, resulting in the influx of calcium ions that triggers the fusion of synaptic vesicles (SVs) with the plasma membrane. SVs are recycled by endocytosis. Phosphorylation of synaptic proteins plays a major role in these processes, and several studies have shown that the synaptic phosphoproteome changes rapidly in response to depolarization. However, it is unclear which of these changes are directly linked to SV cycling and which might regulate other presynaptic functions that are also controlled by calcium-dependent kinases and phosphatases. To address this question, we analyzed changes in the phosphoproteome using rat synaptosomes in which exocytosis was blocked with botulinum neurotoxins (BoNTs) while depolarization induced calcium influx remained unchanged. BoNT-treatment significantly alters the response of the synaptic phoshoproteome to depolarization and results in reduced phosphorylation levels when compared with stimulation of synaptosomes by depolarization with KCl alone. We dissect the primary Ca^{2+}-dependent phosphorylation from SV cycling dependent phosphorylation and confirm an effect of such SV-cycling-dependent phosphorylation events on syntaxin-1a-T21/T23, Vamp2-S75, and cannabinoid receptor-1-S314/T322 on exo- and endocytosis in cultured hippocampal neurons.

5.3 Introduction

In the nervous system, synapses represent specialized cellular junctions that are able to transmit signals from the pre- to the postsynaptic neuron. Signaling is mediated by the release of neurotransmitter molecules that are stored in the presynaptic compartment (327). When an action potential arrives in the nerve terminal, the presynaptic membrane depolarizes, which elicits a rapid influx of calcium ions through voltage-dependent calcium channels clustered around the active zone, an electron-dense protein complex connecting the presynaptic release site with the neurotransmitter receptors in the postsynaptic membrane (35). Major protein constituents of the active zone include RIM proteins, RIM-binding protein and Munc13, as well as bassoon, piccolo, and liprins. Among other functions, these proteins are required for the clustering of calcium-channels and govern the priming and docking of SVs. The calcium ions entering the presynapse are recognized by the calcium-sensor synaptotagmin 1 that triggers exocytosis by lowering the energy barrier for fusion. Exocytotic fusion itself is accomplished by soluble *N*-ethylmaleimide-sensitive factor-attachment protein receptors (SNARE) (36, 38, 328). This process requires additional cytoplasmic proteins, such as Munc18 and complexins, which modulate the efficiency of SNARE zippering (39, 40).

In order to sustain continuous neurotransmitter release and to maintain the structure and composition of the plasma membrane, fused SVs are retrieved by endocytosis, followed by rapid regeneration of SV precursors that are filled with neurotransmitters and prepared for the next round of neurotransmitter release. It is still debated which mechanisms are primarily responsible for endocytosis and recycling, with several occurring in parallel (49, 69, 72, 75, 329-332). The classical pathway of clathrin-mediated endocytosis requires coordinated actions of a protein machinery responsible for coat formation, invagination, and formation of a coated pit, followed by scission, removal of the vesicle from the plasma membrane, and disassembly of the clathrin coat. Key proteins involved in these steps include, among others, clathrin adaptor proteins (AP2, AP180), clathrin itself, the GTPase dynamin-1, the phosphatase synaptojanin-1, endophilins, and related proteins, as well as the clathrin uncoating ATPase Hsc70 and its cofactor auxilin (48). Finally, re-endocytosed SVs are filled with the respective neurotransmitter by specific vesicular neurotransmitter transporters that are fueled by the activity of a vacuolar proton pump (333). In this article, we refer to SV cycling as a multistep process, which includes SV fusion with the plasma membrane mediated by the exocytotic machinery (exocytosis) and SV recycling through available endocytotic mechanisms (endocytosis), followed by the steps in which SVs become ready for the next round of SV cycle (*i.e.*, refilling of the neurotransmitter, SV priming and docking).

An increasing body of data suggests that the basic exo-endocytotic machinery is fine-tuned by regulatory control mechanisms that mainly operate by phosphorylations and dephosphorylations of proteins involved in the SV cycle. In particular, calcium plays an important role not only as a trigger of exocytosis, but also as a modulator of kinase and phosphatase activity in the presynapse (334). Calcium/calmodulin-dependent kinase 2 (CaMKII) residing in synapses is one of the major targets activated by calcium influx (156, 335-337). Its first known substrate was the SV resident protein synapsin-1, and it is now established that its phosphorylation influences the available pool of SV for exocytosis (154, 155, 338). Other kinases such as protein kinase C (PKC) and cyclin-dependent kinase 5 (CDK5) have been shown to be important for SV endocytosis and control, together with the calcium-dependent protein phosphatase calcineurin, the phosphorylation status of many endocytosis-associated proteins such as dynamin-1, amphiphysin, and AP180 (201, 206, 339-346). Mitogen-activated protein kinases (MAPK) appear to operate on parallel pathways as these can regulate synaptic plasticity either by directly modifying synaptic proteins (347, 348) or by affecting gene expression (349, 350), thereby contributing to both rapid and long-lasting modulatory effects.

Earlier phosphoproteomics studies have shown systematic changes in phosphorylation of synaptic proteins caused by depolarization-evoked calcium influx, and they have pointed to involvement of CaMKII and MAP kinases in this process (351, 352). However, it remains elusive, which of the observed phosphorylation changes caused by calcium influx have a direct functional impact on SV cycling. Indeed, following the initial discovery of synapsin-1 phosphorylation, many studies have demonstrated that phosphorylation of specific synaptic proteins at specific sites does have an impact on exo- or endocytosis. For instance, phosphorylation of SNARE proteins (*Snap25*-S187, *Stx1a*-S14, S188, *Vamp2*-T35, S75), as well as of the SNARE-interacting protein Munc18 (*Stxbp1*-S313), can indeed interfere with the formation of the SNARE complex, which results in altered exocytosis (353-358). Munc18 phosphorylation can further be a result of the MAP kinase activation due to cannabinoid receptor-1 signaling (347); the latter was also shown to bear a phosphorylation site (*Cnr1*-S317) that is controlled by PKC (359).

However, it remains to be established which of the vast amount of phosphosite changes observed in recent phosphoproteomic studies are dependent on the membrane trafficking steps of the SV cycle and which are, while being targeted by the activated network of kinases and phosphatases, not directly related to exo-endocytotic cycling. Changes in the protein conformation that accompany assembly and disassembly of multimolecular protein complexes during SV cycling may alter the accessibility of phosphorylation sites as well as the availability of docking sites for kinases and phosphatases. To address this issue, we

conducted a quantitative phosphoproteome analysis using synaptosomes as a functional model of the synapse. Synaptosomes contain the complete SV cycling machinery, can maintain the membrane potential and ATP at physiological levels, and respond to depolarization by Ca^{2+}dependent neurotransmitter release (98, 99, 115, 360). To differentiate between calcium-induced changes and phosphorylation events that are directly connected to SV cycling, we utilized botulinum neurotoxins. These bacterial protein toxins represent a group of endoproteinases that selectively cleave individual SNARE proteins and thus block exocytosis and, consequently, SV recycling without compromising Ca^{2+} influx or synaptosomal ATP-levels (121, 122). We stimulated mock- and BoNT-treated synaptosomes with potassium chloride, which is known to elicit dose-dependent Ca^{2+}-influx and neurotransmitter release (100, 361). By quantitatively monitoring changes of phosphorylation sites of synaptosomal proteins, we found that BoNT-treatment affects almost 1500 phosphorylation sites implying that they are directly dependent on SV cycling. Strikingly, most of the sites show reduced phosphorylation intensity in depolarized synaptosomes following BoNT treatment. We further identified SV-cycling-dependent phosphorylation sites on syntaxin-1a (*Stx1a*-T21, T23), synaptobrevin (*Vamp2*-S75), and cannabinoid receptor-1 (*Cnr1*-T314, T322). Finally, we demonstrated that phosphorylation of these sites elicits a pronounced effect on exo- and endocytosis in cultured hippocampal neurons by expressing phosphomimetic and non-phosphorylatable variants of these proteins.

5.4 Experimental Procedures

5.4.1 Ethical statement

All experiments involving animals complied with the regulations as designated in the section 4 of the Animal Welfare Law of the Federal Republic of Germany (section 4 Tierschutzgesetz der Bundesrepublik Deutschland, TierSchG). All experiments were conducted in the animal facility at the Max-Planck-Institute for Biophysical Chemistry, Göttingen, Germany and registered accordingly to the section 11 Abs. 1 TierSchG as documented by 39 20 00_2a Si/rö, dated 11th Dec 2013 ("Erlaubnis, Wirbeltiere zu Versuchszwecken zu züchten und zu halten") by the Veterinär- und Verbraucherschutzamt für den Landkreis und die Stadt Göttingen and examined regularly by the supervisory veterinary authority of the Landkreis Göttingen. All procedures were supervised by the animal welfare officer and the animal welfare committee of the Max-Planck-Institute for Biophysical Chemistry, Göttingen, Germany established in accordance with the TierSchG and the regulation of animal experiments, dated on 31st Aug 2015 (Tierschutz-Versuchstier-Verordung, TierSchVersV).

5.4.2 Chemicals

LC/MS-grade water, methanol, and acetonitrile (ACN) were used in this study if not otherwise stated and were purchased together with chloroform, 25% (v/v) NH_4OH, $CaCl_2$, KCl, KH_2PO_4, $MgCl_2$, NaCl, $NaHCO_3$, $NaHPO_4$, sucrose, and glucose from Merck, Darmstadt, Germany. Trifluoroethanol (TFE), triethylammonium bicarbonate buffer (TEAB), formic acid (FA), EGTA, PM400-Ficoll (Ficoll), NADP, L-Glutamic dehydrogenase from bovine liver (GluDH), guanidine hydrochloride, tris(2-carboxyethyl)phosphine (TCEP), chloroacetamide (CAA), Triton-X100 and MS-grade trypsin were obtained from Sigma-Aldrich, Taufkirchen, Germany. HEPES was purchased from VWR Chemicals, Darmstadt, Germany. SDS was purchased from Serva Electrophoresis GmbH, Heidelberg, Germany. TFA was obtained from Roth, Karlsruhe, Germany. Peptide-N(4)-(N-acetyl-beta-glucosaminyl)asparagine amidase (PNGase F) was obtained from Roche, Mannheim, Germany. Rapigest was obtained from Waters, Milford, USA. Pierce 660 nm protein assay, Halt Protease and phosphatase inhibitor cocktail, and TMTsixplex isobaric labeling reagents (TMT6) were purchased from Thermo Fisher Scientific, Bleiswijk, Netherlands. *C. botulinum strain A-D* cell culture supernatants (BoNT A, B, C1, D) were obtained from Miprolab, Göttingen, Germany.

5.4.3 Isolated nerve terminals

Isolated nerve terminals were prepared from brains of 5-6 weeks old Wistar rats as described previously (362). Briefly, brains were quickly homogenized in ice-cold homogenization buffer (320 mM sucrose, 5 mM HEPES is water) using a Teflon/glass homogenizer. The homogenate was cleared by centrifugation for 2 min at 2988 × *g* in an SS-34 fixed angle rotor (Thermo Fisher Scientific, Waltham, USA). The supernatant was collected and re-centrifuged for 12 min at 14462× *g*. The synaptosomal pellet was resuspended in the homogenization buffer and loaded onto discontinuous Ficoll gradient (6%/9%/13% (wt/v) Ficoll in the homogenization buffer) and centrifuged for 35 min at 86575 × *g* in an SW-41 swinging bucket rotor (Beckman Coulter, Krefeld, Germany). The synaptosomal band at the interface between 9% and 13% Ficoll was collected and washed with the homogenization buffer. Synaptosomal protein concentration was estimated using Pierce 660 nm protein assay according to manufacturer's instructions. The viability of synaptosomes was confirmed by glutamate release assay (118).

5.4.4 BoNT-treatment and glutamate release assay

1-1.5 mL of synaptosomal suspension was centrifuged at 6900 × *g* for 3 min in a table-top centrifuge, and synaptosomal pellet was resuspended in the sodium-containing buffer (10 mM glucose, 5 mM KCl, 140 mM NaCl, 5 mM $NaHCO_3$, 1 mM $MgCl_2$, 1.2 mM $NaHPO_4$,

20 mM HEPES in water) to achieve a final concentration of 1 mg/mL of synaptosomal proteins. $CaCl_2$ was added to a final concentration of 1.3 mM and synaptosomes were incubated for 5 min at 37°C before adding BoNT. For Ca *vs.* EGTA experiments, synaptosomes were pre-incubated with 1.3 mM $CaCl_2$ or 0.5 mM EGTA for 15 min at 37 C before stimulation with KCl (50 mM). To block SNARE-assisted neurotransmitter release, 20 µL of each BoNT were added per 1 mg of estimated synaptosomal protein (the final BoNT concentration of 100–200 nM was estimated on the basis of the total protein content of the semi-purified BoNT, which amounted to approximately 10 µg/µL). The following combinations of *C. botulinum* cell culture supernatants were used: i) *C. botulinum* A and D or ii) *C. botulinum* C1 and B. Alternatively, synaptosomes were treated with the same amount of respective cell culture supernatants inactivated by heating at 95°C for 1 h (mock-control). BoNT- and mock-treated synaptosomes were incubated at 37°C for 90 min and then directly subjected to the glutamate release assay. In brief, synaptosomal suspension was transferred into a quartz glass cuvette (Hellma, Müllheim, Germany) and kept stirred at 37°C during the measurements. 1 mM NADP, and 50 U per 1 mg of synaptosomal protein of GluDH were stepwise added to the suspension. Synaptosomes were depolarized by adding KCl to a final concentration of 50 mM. NADPH-fluorescence at 440 nm was monitored at each step using Fluorolog-3 fluorimeter (Horiba Jobin Yvon, Bensheim, Germany). After 2 min of stimulation, the reaction was quenched with an equal volume of lysis buffer (6 M Guanidine hydrochloride, 200 mM HEPES, 20 mM TCEP, 80 mM CAA, 1 × Halt Protease and phosphatase inhibitor cocktail). The synaptosomal sample was incubated for 5 min at 95°C, chilled on ice and then sonicated for 10 min using 30 s on/30 s off – cycles at the maximum output of Bioruptor ultrasonication device (Diagenode, Seraing, Belgium). The sample was repeatedly incubated for 5 min at 95°C, and proteins were precipitated following methanol/chloroform protein precipitation method (363).

5.4.5 Phosphopeptide enrichment and TMT-Labeling

Precipitated synaptosomal proteins (1–2 mg per condition) were re-dissolved in a digestion buffer (100 mM TEAB, 10% TFE, 0.1% Rapigest) and sonicated in the Bioruptor for 10 min at maximum intensity using 30 s on/30 s off cycles. Trypsin was added at 1:40 trypsin-to-protein ratio (wt/wt) and proteins were digested overnight at 37°C. Next day, the sample was treated with 2.5 U of PNGase F per 1 mg of the initial protein amount for 1 h. Afterwards, ACN was added to a final concentration of 45% (v/v) and the sample was incubated with a second portion of trypsin (1:100 trypsin-to-protein ratio, wt/wt) for 1 h. The sample was centrifuged for 15 min at 17,000 × *g* in a table-top centrifuge, and the cleared supernatant was subjected to phosphopeptide enrichment as previously described with modifications (364). Briefly, equal input peptide amounts were assured by measuring

peptide concentration in Nanodrop-1000 (Thermo Fisher Scientific, Waltham, USA) using an A280 method. KCl, KH_2PO_4, and TFA were added to the peptide sample to reach final concentrations of 228 mM, 3.9 mM, and 38% (v/v), respectively. Peptides were incubated with TiO_2 –beads (GL Sciences, Tokyo, Japan) at 1:10 protein-to-beads ratio for 20 min at 40°C. Unbound peptide fraction (not-phosphorylated peptides) was collected, and TiO_2-beads were subjected to four washing steps using washing buffer (60% (v/v) ACN, 1% (v/v) TFA in water). Bound phosphopeptides were eluted using 3.75% (v/v) NH_4OH 40% (v/v) ACN in water, snap-frozen in liquid nitrogen and dried in a centrifugal Savant SpeedVac vacuum concentrator (Thermo Fisher Scientific, Waltham, USA). Dried phosphopeptides and peptides in the unbound fraction were subjected to desalting using pre-packed C18 spin-columns (Harvard Apparatus, Holliston, USA). Desalted and dried peptides were re-dissolved in 50 mM TEAB 50% (v/v) ACN in water, and TMT6-labeling reaction was conducted according to manufacturer's instructions. After the labelling, peptide samples were accordingly combined, cleaned using the pre-packed C18 spin columns, and concentrated in a SpeedVac.

5.4.6 Basic reversed-phase (bRP) chromatography

TMT6-labeled peptides were fractionated using Agilent 1100 series HPLC system (Agilent, Santa Clara, USA) equipped with a C18-X-Bridge column (3.5 µm particles, 1.0 mm inner diameter, 150 mm length; Waters, Milford, USA). The HPLC was operated at the flow rate of 60 µL/min under basic pH (buffer A: 10 mM NH_4OH in water, pH ~10; buffer B: 10 mM NH_4OH and 80% (v/v) ACN in water, pH ~10). The column was equilibrated with the 95% buffer A and 5% buffer B mixture. Peptides were resolved using a linear gradient ranging from 10% to 35% buffer B for 35 min followed by a linear increase to 60% over 5 min and a washing step at 90% buffer B for 5 min. One-minute fractions were collected and concatenated into 24 (for Mock/BoNT phosphorylated peptides) or 12 (for Mock/BoNT not phosphorylated peptides and Ca/EGTA phosphorylated peptides) final fractions as suggested elsewhere (284). BRP-Fractions were snap-frozen in liquid nitrogen and dried in the SpeedVac.

5.4.7 LC-MS/MS

Dried peptides were re-dissolved in 2% (v/v) ACN 0.1% (v/v) TFA in water. Each concatenated bRP-fraction was analyzed in triplicates (phosphorylated peptides) or as a single injection (non-phosphorylated peptides). Dissolved peptides were injected onto a C18 PepMap100-trapping column (0.3 x 5 mm, 5 µm, Thermo Fisher Scientific, Waltham, USA) connected to an in-house packed C18 analytical column (75 µm x 300 mm; Reprosil-Pur 120C18-AQ, 1.9 µm, Dr. Maisch GmbH, Ammerbuch, Germany). The columns were

pre-equilibrated using a mixture of 98% buffer A (0.1% (v/v) FA in water), 2% buffer B (80% (v/v) ACN, 0.1% (v/v) FA in water) or 95% buffer A, 5% buffer B (not-phosphorylated peptides). Liquid chromatography was operated on an UltiMate-3000 RSLC nanosystem (Thermo Fisher Scientific, Waltham, USA). Phosphopeptides were eluted using a 60 min-linear gradient ranging from 10% to 25% buffer B (80% (v/v) ACN, 0.1% (v/v) FA in water) followed by a linear increase to 45% buffer B over 10 min and a washing step at 90% of buffer B for 5 min. For not-phosphorylated peptides, a steeper gradient was applied ranging from 10% to 45% buffer B followed by an increase to 60% buffer B and a washing step at 90% buffer B. Eluting peptides were sprayed into a Q Exactive HF-X or Orbitrap Exploris 480 (Thermo Fisher Scientific, Bremen, Germany). For the analysis of phosphorylated peptides, MS1 scans (350 to 1,600 m/z) were acquired with a resolution of 120,000 at 200 m/z, 3e6 automatic gain control (AGC) target, and 50 ms maximum injection time. Precursor ions were isolated using a 0.8 m/z isolation window, and a normalized collision energy of 33% was applied to obtain fragment spectra. Only charge states from 2+ to 6+ were considered, and the dynamic exclusion was set to 25 s. The fragment spectra were acquired with a resolution of 30,000, 1e5 AGC target, and 130 ms maximum injection time. For the analysis of not-phosphorylated peptides, following parameters were set differently: MS1 scans were acquired with a resolution of 60,000 at 200 m/z, 300% normalized AGC target. Fragment spectra were acquired with the resolution of 15,000 at 200 m/z, 50% of the normalized AGC-target and 54 ms maximum injection time.

5.4.8 Data Analysis

Raw files were processed using MaxQuant version 1.6.10.2 (295, 365) under default settings with some exceptions. Specifically, cysteine carbamidomethylation was selected as a fixed modification, whereas methionine oxidation, acetylation of protein N-termini and phosphorylation of serine, threonine, and tyrosine (only for phosphorylated peptides) were set as variable modifications. Up to 5 variable modifications were allowed per peptide. Specific trypsin digestion was selected with up to two missed cleavage sites allowed per peptide. Maximal peptide mass was increased to 6000. Quantification using reporter ions in MS2 (TMT6plex) and minimal parent ion fraction of 0.75 were selected. MS1 and MS2 mass tolerances were kept at 4.5 ppm and 20 ppm, respectively. Canonical amino acid sequences of *Rattus norvegicus* proteins were retrieved from Uniprot (366) (February 2019, 29951 entries). Reference proteome of *C. botulinum* (strain Hall / ATCC 3502 / NCTC 13319 / Type A) containing canonical protein sequences (Uniprot, January 2020, 3590 entries) was supplemented with sequences of BoNT B-D (strain Okra / Type B1, *C. botulinum* C phage, *C. botulinum* D phage, respectively). Peptide-spectrum matches (PSM) and protein FDR threshold were kept at 0.01. Following steps in data analysis were

conducted in R statistical programming language using custom scripts. The scripts are available at github (https://github.com/IvanSilbern/2021_Silbern_etal_Synapt_BoNT_KCl). For each phosphorylation site, a leading protein was selected based on the list of potential candidate proteins for this site reported by MaxQuant. Proteins were ranked based on (listed from the most to the least significant) i) the number of the unique phosphorylation sites assigned to the protein in the data set; ii) the number of all phosphorylation sites per protein in the data set; iii) "reviewed" status and Uniprot-annotation score of the protein sequence; iv) isoform status of the protein sequence. The official gene name and Uniprot accession of the leading protein was used in the subsequent analyses. Impurity-corrected reporter ion intensities for each phosphorylation site identified at one of the three multiplicity levels were extracted from MaxQuant "Phospho(S, T, Y).txt" output table. Potential contaminants, reversed sequences and phosphorylation sites identified with localization probability < 0.75 as determined by MaxQuant (295, 365) were excluded from further analysis. Phosphorylation sites quantified at different multiplicity levels ("1" means that the phosphorylation site was quantified on singly, "2" on doubly, and "3" on multiply phosphorylated peptides) were considered as separate entities or phosphorylation events. If a phosphorylation event contained < 3 non-zero intensity values for a given labeling experiment, the event was considered as not quantified in this labeling experiment. Otherwise, missing values were imputed for each TMT-channel/experiment-pair individually by random sampling from a gauss distribution with a mean at the 5% quantile and a double standard deviation of the log-transformed intensities. Only a minor proportion of phosphorylation events required imputation (< 1% per channel). Log_2-transformed reporter ion intensities were then normalized using Tukey median polishing individually for each labeling experiment and subjected to statistical testing using limma package (311).

5.4.9 Experimental design and statistical rationale

In total, 216 .raw files were analyzed in order to quantify changes in phosphorylation site intensities in BoNT- or mock-treated synaptosomes or synaptosomes stimulated in the presence of calcium or EGTA. Out of the 216 .raw files, 144 .raw files were obtained from two TMT6-labeling sets of mock- *vs.* BoNT-treated synaptosomes. These files correspond to 24 concatenated bRP-fractions and three injection replicates per fraction. Remaining 72 .raw files were obtained from another two TMT6-labeling experiments of synaptosomes stimulated in the presence of Ca^{2+} or EGTA. The files correspond to 12 concatenated bRP-fractions and three injection replicates per fraction. Each set of TMT6-labeled samples contained three independent replicates for each of the two treatment conditions, resulting in six independent replicates for each treatment regime (Mock, BoNT, Ca, or EGTA). The choice for this number of replicates was dictated by the constraints of the TMT6-labeling

and the previous study (351). The phosphorylation site intensities resulting from the three technical replicates were summed in order to obtain a single value reported by MaxQuant (295). We used log_2-transformed and normalized reporter ion intensities to assess changes in the phosphorylation site intensities. Specifically, we used the limma package (311) to test the difference in phosphorylation site intensities between mock- and BoNT-treated synaptosomes and synaptosomes stimulated in the presence of calcium or EGTA. Linear models were specified to account for treatment differences (Mock, BoNT, Ca, EGTA) and batch effects between TMT6-sets. Differences in the peptide intensities between mock- and BoNT-treated synaptosomes and synaptosomes stimulated in the presence/absence of calcium were tested. Empirical-Bayes moderated p-values (311) were subjected to multiple testing correction using q-value approach (367). Phosphorylation events (phosphorylation site at a given multiplicity) were considered as significantly regulated when showing at least 1.2 intensity fold change (FC, corresponds to absolute log_2 FC > 0.263), and q-value < 0.01 (corresponds to false discovery rate (FDR) < 1%).

5.4.10 Defining primary Ca^{2+}-dependent and SV-cycling-dependent phosphorylation sites

Phosphorylation events were defined as “primary Ca^{2+}-dependent” if they show absolute log_2 (Ca/EGTA) > 0.263 and absolute log_2 (Mock/BoNT) < 0.263 or were not quantified in the Mock/BoNT experiment. Conversely, events showing absolute log_2 (Mock/BoNT) > 0.263 were termed as “SV-cycling-dependent”. Phosphorylation events that exhibited only small changes in both experiments (absolute log_2 (Ca/EGTA) < 0.263 and absolute log_2 (Mock/BoNT) < 0.263) were considered as being “not-affected”. In the following analyses, only phosphorylation events that surpassed an FDR-threshold of < 1% were considered. Specifically, “primary Ca^{2+}-dependent” phosphorylation events had to satisfy a q-value threshold of < 0.01 in the Ca/EGTA experiment, whereas “SV-cycling-dependent” sites had to meet a q-value threshold of < 0.01 in Mock/BoNT experiment or a q-value-threshold of < 0.01 and an absolute log_2 FC threshold of > 0.263 in Ca/EGTA experiment. Phosphorylation events that did not match these criteria were considered as being “not-affected” as well. If a phosphorylation site was quantified at different multiplicities (phosphorylation events), whereby one of which was classified as being “SV-cycling-dependent”, the site was considered as being “SV-cycling-dependent”. To define regulation groups at protein level, number of significantly regulated phosphorylation sites were counted per protein (gene). Proteins were distributed in the following groups i) “mostly primary Ca^{2+}-dependent” (> 60% of sites being categorized as “primary Ca^{2+}-dependent”); ii) “mostly SV-cycling-dependent” (> 60% of sites being categorized as “SV-cycling-dependent”); iii) “mixed” (none of the groups was dominating).

5.4.11 Bioinformatic analysis

Gene enrichment analyses were conducted using gene names of proteins carrying significantly regulated phosphorylation sites in Ca/EGTA or Mock/BoNT experiments. Gene ontology enrichment analysis was performed using David web interface and whole *Rattus norvegicus* proteome as a background (368). Direct GO term categories surpassing Benjamini-Hochberg-adjusted p-value threshold of 0.001 were considered for further analysis. For Reactome pathway analysis, only enriched (Benjamini-Hochberg-adjusted p-value < 0.1) “neuronal system” categories were selected (369). Synapse-specific SynGO database was used to retrieve significantly enriched (GSEA “gene cluster” FDR corrected p-value < 0.001) GO-biological function terms (324). Experimentally validated kinase-substrate interactions were derived from PhosphoSitePlus database (“Kinase_Substrate_Dataset.txt”, version of 10.04.2018) (325). In order to account for possible differences in phosphorylation site annotation, sequence windows of the phosphorylation sites in the data set were aligned against sequence windows reported in the PhosphoSitePlus database using BLAST+ software (version: 2.7.1, additional command line parameters: -max_target_seqs 20) (370). Only exact alignments of the phosphorylation sites showing the minimum bitscore of 20 were considered. The best match was selected from filtered alignments ranked based on the alignment bitscore, number of amino acid positions considered identical (nident), number of open sequence gaps, kinase and substrate species (rat > mouse > human > rabbit). Phosphorylation sites with no assignment were subjected to NetworKIN kinase-substrate prediction tool (144, 323). Specifically, rat protein sequences were aligned against the reference set of human protein sequences (STRING (322) database version 9.05) by using BLAST+ (additional command line parameters: -max_target_seqs 40 -word_size 6 -gapopen 12 -gapextend 1). The best alignment for each rat protein sequence was selected based on the rat protein sequence coverage, number of amino acid positions considered identical, alignment bitscore, number of open sequence gaps (listed with decreasing importance). Positions of phosphorylation sites in the best matching human protein sequences were subjected to NerworKIN tool. The kinase prediction with the highest NetworKIN score was selected for each phosphorylation site. Predicted kinases were organized in the kinase groups introduced by Netphorest classification (144). The second-level and top-level kinase groups in the kinase hierarchy were used for enrichment analyses and visualizations. The overrepresentation analysis of predicted kinase-substrate interactions for phosphorylation sites significantly regulated in Ca/EGTA or Mock/BoNT experiments was conducted in comparison to NetworKIN kinase-substrate predictions for human proteome. To assess the disbalance in the number of up/down regulated phosphorylation events, the number of up/down regulated

phosphorylation events controlled by each kinase group was compared to the total number of up/down phosphorylation events among significantly regulated phosphorylated sites. All tests of differential term or kinase enrichment between two groups were done using Fisher's exact test. Benjamini-Hochberg adjusted p-values are reported throughout the study if not specified otherwise. The anticipated phosphatase–substrate interactions rely upon described PP1 and Calcineurin docking motifs (371). To demonstrate possible phosphatase-substrate connections, interaction maps were extracted from protein–protein interactions annotated for *Rattus norvegicus* (STRING (322) database version 10.5). Shortest paths from phosphatase to target proteins (phosphoproteins involved in endo/exocytosis and containing PP1 or Calcineurin docking motif) were computed using *shortest_path* function from *igraph* package (372) (version 1.4.6). Only proteins previously identified in synaptosomes and interactions with experimental evidence or annotated in curated databases were included in the analysis. Phosphorylation site occupancy was calculated using a 3D model presented by *Hogrebe et al* (300). In brief, a linear model of the form $Ph = m_1 \cdot Prot - m_2 \cdot NPh$, where *Ph* is the normalized (by median polishing) intensity of the phosphorylated peptide; *Prot* is the normalized protein intensity and *NPh* is the normalized intensity of non-phosphorylated peptide. The model was fit by using intensity data from Mock/BoNT experiments. Phosphorylation occupancy was then calculated using the following formula: $Occupancy = a/(1+a)$, where $a = m_2 \cdot Ph/NPh$. "Illegal" stoichiometry values, *i.e.*, values outside the interval (0;1) were excluded from the analysis. Only m_2 values with a *p* value below 0.1 were considered.

5.4.12 *C. botulinum* cell culture supernatants profiling

For protein profiling, supernatants of *C. botulinum* cell culture were digested overnight using trypsin. Digested peptides were desalted using pre-packed C18 spin-columns. Samples were analyzed on Q Exactive HF-X and liquid chromatography setup as described above.

To test for unspecific phosphatase activity, *C. botulinum* cell culture supernatants were incubated with the nuclear extract of HeLa-cells. The nuclear extract was prepared as previously described (373) in Roeder D buffer (20 mM Hepes-KOH pH 7.9, 100 mM KCl, 1.5 mM $MgCl_2$, 10% (v/v) glycerol, 0.5 mM DTT, 0.5 mM PMSF, 0.2 mM EDTA) and was a generous gift of Prof. Dr. Lührmann laboratory. The extract was supplemented with 1.3 mM $CaCl_2$ and 20 µL of each *C. botulinum* cell culture supernatant (A and D or C1 and B), heat-inactivated cell culture supernatants, or 40 µL of the sodium buffer per 1 mg of nuclear proteins. Each treatment condition was performed in triplicate, resulting in a total of 9 samples. The samples were incubated for 1.5 h at 37°C. Afterwards, urea in 100 mM HEPES pH 8 was added to the final concentration of 1 M and proteins were digested overnight at 30°C using MS-grade trypsin at a trypsin-to-protein ration (wt/wt) of 1:50. Next

day, peptides were subjected to phosphopeptide enrichment as described above excluding the de-glycosylation and second endoproteinase digestion steps. Enriched phosphopeptides were cleaned using the pre-packed C18 spin columns, re-dissolved in 2% (v/v) ACN, 0.1% (v/v) TFA in water and analyzed on UltiMate 3000 RSLC nanosystem connected to Orbitrap Exploris 480 mass spectrometer. Raw phosphorylation site intensities as reported by MaxQuant were analyzed as described before using R scripts and the limma package for data normalization, visualization, and statistical testing.

5.4.13 Calcium influx in synaptosomes following BoNT-treatment and KCl-stimulation

Synaptosomes suspensions containing 1 mg of synaptosomal proteins were prepared as described for glutamate release assay. Suspensions were supplemented with 1.3 mM $CaCl_2$ and additional 40 µL of the sodium-containing buffer or 1.3 mM $CaCl_2$ and 20 µL of each *C. botulinum* cell culture supernatants in two combinations (A and D or C1 and B). Synaptosomes were then incubated for 1 h at 37°C under mild agitation. Afterward, synaptosome suspensions were supplemented with 5 µM of Fura-2AM dye (Molecular probes, Eugene, USA) and incubated for additional 30 min at 37°C. Following steps were conducted as previously described (101). Briefly, synaptosomes were resuspended in 1 mL of fresh sodium-containing buffer and loaded into the quartz glass cuvette. The synaptosomal suspension was stirred and kept at 37°C during the measurements. The fluorescence was continuously measured using Fluorolog-3 at excitation wavelengths of 340 and 380 nm and emission at 505 nm, for 2 s at each wavelength. 1.3 mM $CaCl_2$, 50 mM KCl, 0.4% (wt/v) SDS, 1 mM EGTA were added stepwise, and the signal was acquired for 3 min at each step. Fluorescence intensity at 340 nm excitation was divided by the intensity at 380 nm excitation and then by the maximum fluorescence ratio following SDS-lysis. Median fluorescence ratio before stimulation with KCl was subtracted to obtain proportional changes in fluorescence intensity relatively to its maximum.

5.4.14 Cell cultures and transfections

Primary hippocampal neuronal cultures were prepared from P2 rats as previously described (374). HEK293T cells were obtained by a commercial supplier (Sirion Biotech GmbH; Germany). HEK293T cells were grown in DMEM supplemented with 10% FBS, 4 mM L-glutamine and 600 U/ml penicillin-streptomycin (Lonza). For transfection Lipofectamine 2000 transfection reagent was used following the guidelines of the manufacturer (Thermo Fisher Scientific, Invitrogen, USA). All plasmids for transfection were produced in bacteria

and purified with the NucleoBond Xtra Midi endotoxin-free plasmid DNA kit (Macherey-Nagel, Germany).

5.4.15 DNA cloning of wild type proteins and respective phosphomimetic mutants

All the sequences (including mutants) were designed *in silico* based on rat genes with the appropriate restriction enzymes for viral cloning and ordered at GenScript (USA). The synaptobrevin (*Vamp2*) mutants were based on rat *Vamp2* (Uniprot: P63045) fused to the optimized version of superecliptic GFP (pHluorin) (375) by mean of a short peptide linker. We used AgeI and SdaI (SbfI) restriction sites for inserting *Vamp2*-pHluorin and the respective mutants (S75D pseudo-phosphorylated and S75A non-phosphorylatable) in the viral vector (previously described, (376)) allowing neuron-specific expression under the human synapsin-1 promoter. For all the following subcloning steps we relied on commercial chemically competent SURE bacteria from Agilent, to avoid the loss of ITR sequences. Positive clones were confirmed by sequencing, and before transfection in the packaging HEK293T cells, the presence of ITRs and the correct length of all plasmids were checked by restriction enzyme analysis. Syntaxin-1a (*Stx1a*; P32851) and cannabinoid receptor 1 (*Cnr1*; P20272) and their mutants (respectively T21E-T23E pseudo-phosphorylated *Stx1a*, T21A-T23A non-phosphorylatable *Stx1a*, T314E-T322E pseudo-phosphorylated *Cnr1* and T314A-T322A non-phosphorylatable *Cnr1*) were inserted in the WT *Vamp2*-pHluorin viral vector by cutting with the enzymes SgsI (AscI) and SbfI (SdaI). Their expression was driven by mean of a second human synapsin-1 promoter from the same viral plasmid to allow consistent coexpression. To distinguish these proteins from the endogenous, an ALFA-tag was added (377). Also in this case, positive clones were confirmed by sequencing, and before transfection in the packaging HEK293T cells, the presence of ITRs and the correct length of all plasmids were checked by restriction enzyme analysis. All synthetic plasmids and their respective sequences are available from the authors upon request.

5.4.16 Immuno staining with NbALFA

The expression of *Stx1a* and *Cnr1* in all viruses and mutants was confirmed by staining with the NbALFA (377). Briefly, neurons were fixed with 4% paraformaldehyde (PFA; w/v) for 30 min at room temperature (RT). Cells were quenched in 100 mM NH_4Cl and permeabilized in PBS containing 4% bovine serum albumin (BSA; wt/v) and 0.1% (v/v) Triton-X 100 for 15 min at RT. Fluorescently labeled NbALFA (FluoTag-X2 anti-ALFA AbberiorStar635P, NanoTag Biotechnologies #N1502-Ab635P-L, Germany) was diluted 1:200 in blocking solution for 1 h at RT and subsequently washed three times for 5 min with PBS. Coverslips were mounted on glass-slides using Mowiol solution, dried at and imaged.

Note that superecliptic GFP (pHluorin) keeps its fluorescence in Mowiol solution since its pH is ~7.5 and can thus be imaged with no additional staining.

5.4.17 Adeno associated virus preparation

Recombinant AAV particles were prepared as previously described (376). Briefly, vectors were packaged in HEK293T cells using the pDP6 helper plasmid (avoiding adenoviral contamination). Packaging cells were lysed in Tyrode's solution (124 mM NaCl, 5 mM KCl, 30 mM glucose, 25 mM HEPES, 2 mM $CaCl_2$, 1 mM $MgCl_2$, pH 7.4), passed through 0.22 µm syringe filters and viral titer was adjusted by serial dilution on primary hippocampal neurons monitoring pHluorin levels (always expressed under the neurospecific human synapsin-1 promoter).

5.4.18 Synaptic vesicle exo-/endocytosis measurements

SV exo/endocytosis assays were performed analogously to what previously described (374, 378). Briefly, neurons were field-stimulated with platinum electrodes in custom-made chambers housing 18 mm coverslips (8 mm distance between electrodes). We used a Stimulus Isolator combined with an A310 Accupulser Stimulator (both from World Precision Instruments, Sarasota, USA) with a nominal output of 100 mA for stimulation. In the case of *Stx1a* and *Cnr1*, co-expression was confirmed by imaging. Live experiments were performed in Tyrode's solution (124 mM NaCl, 5 mM KCl, 30 mM glucose, 25 mM HEPES, 2 mM $CaCl_2$, 1 mM $MgCl_2$, pH 7.4) supplemented with 10 µM 6-cyano-7-nitroquinoxaline-2,3-dione (CNQX; Tocris Bioscience, Cambridge, UK) and 50 µM 2-amino-5-phosphonopentanoic acid (D-AP5; Tocris Bioscience, Cambridge, UK) to avoid spontaneous network activation. At the end of the imaging, 50 mM NH_4Cl was applied to evaluate total SV content. Live imaging was performed with an inverted Nikon Ti epifluorescence microscope (Nikon, Tokyo, Japan) equipped with a Plan Apochromat 60x 1.4 NA oil-immersion objective, an HBO-100W Lamp, an IXON X3897 Andor camera (Northern Ireland, UK) and an OKOLab cage incubator system (OKOLab, Ottaviano, Italy) to maintain a constant temperature of 37°C. ND2 Images were imported using the Bio-Formats (OME) plug-in. For quantifications, the fluorescence intensity was measured with custom-made Matlab (USA) code that can be provided on an individual basis if requested. Briefly, multiple regions containing synaptic boutons were manually selected, in 5 to 8 independent experiments. Between 140 and 345 regions were selected for each condition, over all independent experiments. The *Vamp2*-pHluorin signal was then measured in the respective regions, and the background intensity (obtained in identically sized regions from the neuron-free adjoining regions) was subtracted. The *Vamp2*-pHluorin signal curves were then normalized to the maximum intensity obtained during the addition of NH_4Cl. To

compare easily different conditions and mutant variants, all curves were furthermore normalized to their initial (pre-stimulus) baselines. Statistical differences were tested in Matlab, relying on Kruskal-Wallis tests, followed by Tukey-Kramer post-hoc tests.

5.5 Results

We performed a quantitative in-depth analysis of changes in protein phosphorylation events in active synaptosomes. We first quantitatively compared the phosphorylation status of proteins in chemically stimulated synaptosomes under Ca^{2+}-deprived and free Ca^{2+} conditions; for the latter, depolarization of the plasma membrane of synaptosomes was induced by KCl in buffer containing EGTA or $CaCl_2$ (**Figure 5.1**). The viability of the synaptosomes was confirmed by monitoring release of the neurotransmitter (glutamate) (118) (**Figure 5.S1A**). We applied depolarization for 2 min; this duration was chosen in order (i) to achieve comparability with our previous studies (351) and (ii) to allow the capture of short- and medium-term changes in phosphorylation. Proteins from stimulated and non-stimulated synaptosomes were extracted, digested, and enriched for phosphopeptides in parallel; thereafter, the (phospho)peptides were labeled with unique isotopically labeled TMT6 reagents. Peptides were then pooled, pre-fractionated by basic reverse-phase chromatography and finally analyzed by LC-MS/MS (**Figure 5.1**). In the second approach, we inhibited SV cycling using BoNT and monitored quantitatively the changes in the phosphoproteome after K^+-mediated depolarization, comparing synaptosomes that were treated with active or, respectively, with inactive BoNT (**Figure 5.1**). Phosphopeptides were enriched and analyzed as described above. This second approach should differentiate phosphorylation events that are dependent on SV exo-endocytotic cycling.

Our analysis shows that phosphorylation is a prominent modification of synaptosomal proteins. Specifically, we identified and quantified phosphorylation under stimulated and non-stimulated conditions on 12021 sites belonging to more than 2600 proteins (unique gene names) with a localization probability of >75% as determined by MaxQuant (295, 365). This coverage greatly exceeds our earlier one (351) and is comparable to a recent study from another laboratory (352). When the phosphosites quantified from BoNT-treated synaptosomes are included, the number of sites quantified in this study increases to 18981 sites belonging to 3840 proteins (**Figure 5.2A**, left panel).

5.5.1 Synaptosome depolarization by KCl in the presence of Ca^{2+} results in substantial changes in protein phosphorylation.

When analyzing synaptosomes depolarized in the presence of calcium ions in comparison with those depolarized in the absence of calcium (EGTA control), we detected substantial

changes in protein phosphorylation. Specifically, there are 1363 phosphorylated sites mapped to approximately 470 proteins that show intensity changes of at least 20% at an FDR of 1% (**Figure 5.2B**). Using the PhosphoSitePlus database (325) to annotate known kinase-substrate relations and the NetworKIN tool (144, 323) to predict possible kinase-substrate pairs, we observed that certain kinase families were overrepresented including the CaMKII, MAPK and GSK3 kinase groups (**Table 5.S1**). Importantly, the distribution of up- or down-regulated sites between kinase groups is not random: CaMKII and PKC kinase groups are responsible for phosphorylation sites that appear upregulated, while the majority of sites controlled by MAPK, CDK and CK1 show reduced intensity in the presence of Ca^{2+} as compared with EGTA controls (**Figure 5.2E** and **Figure 5.S2**). The latter observation is in line with previous studies that demonstrated up-regulation of putative CaMKII substrates and down-regulation of predicted MAPK substrates following potassium-triggered depolarization of synaptosomes (351, 352).

We also observed changes of phosphorylated sites in response to KCl treatment that were similar to changes reported in earlier studies (352) for Bassoon (*Bsn*), Piccolo (*Pclo*), Synapsin 1 (*Syn1*), and Dynamin 1 (*Dnm1*), as well as the microtubule-associated protein Tau (*Mapt*) and the dihydropyrimidinase-related proteins 2 and 5 (*Dpysl2* and *Dpysl5*), and others (**Figure 5.2D**). Overall, the overlap of identified and quantified sites with the results of previous studies is approximately 60% as determined by the overlap in protein sequences flanking phosphorylation sites (sequence windows).

Enrichment analysis of the biological function of proteins carrying regulated phosphorylation sites (DAVID (368)) revealed gene ontology (GO) terms tightly connected with synaptic functioning, cytoskeleton organization, regulation of synaptic functions and neuronal projections development (**Figure 5.3A**). A similar picture (**Figure 5.3B**) was obtained when using the synapse-specific SynGO database in which a large set of synaptic proteins was annotated by experts (324). It shows that the significantly enriched terms describe biological functions connected with SV cycling, regulation of neurotransmitter release and synapse organization (for a complete list of enriched terms see **Table 5.S2**). Interestingly, regulation of some functions might be linked to the activity of certain kinase groups (**Figure 5.3A**). For example, the number of sites predicted to be substrates for GSK3 and CDK is proportionally higher among proteins involved into the GO term "*axonogenesis*" as compared with other GO terms. Similarly, many phosphorylated sites on proteins that are involved in the "*calcium-dependent regulation of synaptic functions*" were also predicted as CaMKII substrates. The proportion of putative MAPK-substrates is higher for proteins associated with "*synapse assembly*" and "*cytoskeleton organization*" as compared with other GO terms.

This analysis reflects, in accordance with recent studies (351, 352), the overall changes of phosphorylation in isolated nerve terminals upon stimulation – including the phosphosites that are important for exocytosis and endocytosis, *i.e.*, for SV cycling. However, the observed effects can be a result of both, Ca^{2+}-influx and active SV cycling.

5.5.2 Block of SV cycling with botulinum neurotoxins induces changes in protein phosphorylation.

As indicated above, our first quantitative analysis does not allow for differentiating phosphorylation changes that are directly dependent on active membrane trafficking in the synapse rather than being caused by the activation of calcium-dependent kinases and phosphatases such as CaMKII (337), calcineurin (379), *etc*. Of course, these processes are intertwined since these enzymes are known to regulate the phosphorylation status of proteins closely associated with the process of SV cycling (205, 380).

We suppressed SV cycling by incubating synaptosomes with BoNT that block exocytosis by cleaving SNARE proteins. Toxin-treated synaptosomes and (as controls) synaptosomes incubated with inactivated toxins were stimulated with the high-potassium buffer in the presence of Ca^{2+} ions (**Figure 5.1**). The toxin treatment greatly inhibited neurotransmitter release (**Figure 5.S1B**) but did not compromise Ca^{2+}-influx (**Figure 5.S1C**). It led to significant changes in the phosphoproteome of the synaptosomes: 1497 sites showed significant difference with a minimum of 20% intensity changes at 1% FDR that can be mapped to approximately 700 proteins. Strikingly, BoNT treatment reduced the intensity of many phosphorylation sites (**Figure 5.2C**). The phosphorylation status of these sites and their corresponding proteins is apparently dependent on the Ca^{2+}-induced SV cycling activity in the presynapse.

The enrichment analyses for GO terms did not show substantial differences when compared with proteins carrying regulated sites in Ca *vs*. EGTA experiments (not shown). The impact of BoNT treatment became apparent when we investigated possible substrate–kinase relationships. The enrichment analysis showed significant overrepresentation ($P < 0.01$) of phosphorylation sites that can be attributed to MAPK, PKC and GSK3 kinase groups (**Table 5.S3**). When comparing the quantitative Ca *vs*. EGTA phosphorylation data, significantly fewer ($P \cong 1.0 \times 10^{-5}$) regulated phosphorylation sites could be ascribed to being CaMKII substrates, whereas putative sites for MAPK (1), CLK (2), and PAK (3) were slightly over- (1, 2) or under- (3) represented, respectively (**Figure 5.2F**, **Table 5.S4**). Therefore, the crucial point in this analysis is the distribution of up- or downregulated phosphorylation sites for the different kinase groups. While depolarization of synaptosomes

by KCl in the presence of Ca^{2+} leads to significantly reduced intensities of phosphorylation sites presumably regulated by MAPK and CDK kinases, the intensities of the putative MAPK, CDK and GSK3 substrates appear higher when comparing mock-treated with BoNT-treated synaptosomes (compare **Figure 5.2E** and **Figure 5.2F**). The balance of up- and downregulated phosphorylation sites was also significantly altered ($P < 0.01$) for CLK, CK1 and PAK kinases.

5.5.3 Dissecting primary Ca^{2+}-driven phosphorylation events from events linked to SV cycling.

Assuming that the comparison of mock-treated synaptosomes with the BoNT-treated ones reveals the phosphorylation changes caused by Ca^{2+}-induced SV cycling, we were able to identify phosphorylation events that are primarily dependent on Ca^{2+}-influx and are not affected if SV cycling is inhibited (**Figure 5.4A** and **S3**, orange dots). In the following, we refer to these sites as "primary Ca^{2+}-dependent" sites. They are presumably directly (de)phosphorylated by Ca^{2+}-dependent protein kinases and phosphatases upon Ca^{2+} influx. Conversely, a large group of phosphorylation events has shown changes when comparing mock- and BoNT-treated synaptosomes. Hence, we termed these sites "SV-cycling-dependent". We noted with interest that the majority of "SV-cycling-dependent" sites did not show significant intensity changes in the Ca/EGTA-experiment. We also noted that many proteins tend to carry regulated phosphorylation sites of one of the two groups introduced above, *e.g.*, mostly "primary Ca^{2+}-dependent" or "SV-cycling-dependent" sites, while only a few contain sites of various categories (**Figure 5.4B**). Interestingly, the number of proteins that carry mostly "primarily Ca^{2+}-dependent" sites is lower than the number of proteins that carry mostly "SV-cycling-dependent" sites (**Figure 5.4B**). It indicates the tendency that "primary Ca^{2+}-dependent" phosphorylation sites appear clustered on a few proteins whereas "SV-cycling-dependent" sites are often found as the only significantly regulated phosphorylation site in a single protein. The site occupancy assessment (based on the model of *Hogrebe et al*. (300)) suggests high phosphorylation levels (>60%) for a number of phosphoproteins, including *Bsn*, *Pclo*, *Dnm1*, *Camk2a*, *Mapt*, and *Dplysl5*, underlining the importance of the observed phosphorylation events (**Figure 5.S4**). It should be noted that the estimated phosphorylation levels represent only a rough estimate, as the ratio compression, which is a known issue for the TMT-based quantification, might severely affect the occupancy calculation. In terms of probable kinase regulation (**Figure 5.4C**), sites predicted to be CaMKII-substrates include significantly more "primary Ca^{2+}-dependent" sites than sites classified as "SV-cycling-dependent". This harmonizes well with the strict Ca^{2+}-dependence of CaMKII-activity (381). Conversely, the MAPK group controls significantly more "SV-cycling-dependent" sites than "primary Ca^{2+}-dependent" sites.

Similarly, predicted PAK-substrates are overrepresented among “primary Ca^{2+}-dependent” sites, whereas predicted PKC, CDK, and CLK-substrates appear more often among “SV-cycling-dependent” sites (**Figure 5.4C**). The majority of phosphorylation sites on CAMKII, MAPK1, MAPK3, and PRKCB themselves show dependence on calcium ions. Increased phosphorylation of the regulatory sites of CaMKII, MAPK1, MAPK3, and PRKCB (*Camk2a*-T286, *Camk2b*-T287, *Camk2d*-T287, *Mapk1*-T183, Y185, *Mapk3*-T203, Y205, *Prkcb*-T640) points to the activation of those kinases following depolarization of synaptosomes by KCl (**Figure 5.S5, S6**).

We noticed that numerous phosphorylation events on phosphatases and phosphatase regulators were significantly regulated in our study (**Figure 5.S7A**). Particularly, Neurabin-1 (*Ppp1r9a*), a PP1 regulator, showed increased phosphorylation in the Mock/BoNT experiment, suggesting the involvement of PP1 in regulating SV cycling. Although phosphatase–substrate interactions are more difficult to analyze due to the degenerated nature of phosphatase docking motifs, previous studies led to the proposal of docking motifs of PP1 and the Ca^{2+}-calmodulin-dependent phosphatase calcineurin (371). We therefore examined possible interactions between exo- and endocytosis-related proteins containing PP1 or Calcineurin docking motifs and the respective phosphatase (**Figure 5.S7B-C**). Available interactome data suggest a partially overlapping set of proteins that can be regulated by the phosphatases (*e.g.*, *Rims2, Bsn, Bin1, Stxbp1*), which does not allow confident assignment of a phosphatase to a particular phosphorylation event. When considering all potential targets, our results show a minor increase in the percentage of “SV-cycling-dependent” sites over “primary Ca^{2+}-dependent” sites on proteins that can be regulated by PP1 (Fisher’s exact test, $P = 0.075$, **Figure 5.S7D**).

Because of the tendency of proteins to carry preferentially one of the two groups of significantly regulated phosphorylation sites, we set out to investigate the putative biological functions of these proteins in order to delineate processes that can be controlled by “primary Ca^{2+}-dependent” or “SV-cycling-dependent” phosphorylations. Reactome pathway analysis (369) sheds light on the putative different function of the involved phosphorylated proteins (**Figure 5.4D**). One obvious difference regarding the two groups are proteins connected to potassium channels (“*Voltage-gated potassium channels*”) which are more enriched in the “SV-cycling-dependent” group. Another striking difference is that phosphorylated proteins termed with “*Synaptic adhesion-like molecules*” and “*Neurexins and neuroligins*” are enriched in “SV-cycling-dependent” group. In contrast, terms associated with “*Neurotransmitter release cycle*”, *e.g.*, glutamate, acetylcholine, *etc*. release, are barely enriched in phosphorylated proteins that carry “SV-cycling-dependent” sites (**Figure 5.4D, top**). Reactome pathway annotation aligned well with the manual annotation of key-words

describing protein function or location according to information available in the literature (**Figure 5.S8**). On the basis of our annotation, we noted that 234 out of 301 phosphorylation sites on proteins directly involved in the processes of exo- and endocytosis belong to the "primary Ca^{2+}-dependent" group. For example, phosphorylation of RIM, RIM-binding protein, synapsin-1, and "dephosphins" such as dynamin-1 (*Dnm1*), amphiphysin (*Amph*) and AP180 (*Snap91*) showed a clear Ca^{2+}-dependent character (**Figure 5.S9, S10**). Importantly, phosphorylation sites on synapsin-1 followed the previously described pattern of phosphorylation changes when comparing Ca with the EGTA condition: increased phosphorylation of S9 and S603 and de-phosphorylation of S62, S67, S549, and S551 (153, 171, 348, 382-385) (**Figure 5.S11**). In contrast, the "SV-cycling-dependent" phosphorylation sites tended to be present on proteins that are described as being associated with cytoskeleton elements and channels, for example, spectrin beta (*Sptb, Sptan1, Sptbn1, Sptbn2, Sptbn4*) and spectrin-binding proteins adducin alpha (*Add1*) and beta (*Add2*), as well as potassium channel subunits that are known constituents or modulators of Kv1 (*Kcna2, Kcna4, Kcnab2),* Kv2 (*Kcnb1, Kcnb2*), Kv4.3 (*Kcnd2*), Kv7.2 (*Kcnq2*), K2p10.1 *(Kcnk10*), Hcn (*Hcn1, Hcn2, Kctd3*) potassium channels (29) (**Figure 5.S12-S15**). As mentioned above, the observed SV cycling effect on several potassium channels seems to be very specific for the particular proteins and results in increased phosphorylation of the majority of those proteins except *Add1* and *Kcnma2* (**Figure 5.S16**). Conversely, the Ca^{2+}-activated potassium channel subunit alpha-1 (*Kcnma1*) and several other potassium channel subunits and modulators (*Kcnc3, Kcnh1, Kcnip2, Kcnq5*) have shown the "primary Ca^{2+}-dependent" character of phosphorylation (**Figure 5.S17)**. We summarize changes in phosphorylation site intensities for protein sequences that contain phosphorylation sites significantly regulated in one of the experiments and provide them as graphics in **Suppl. Data 5 and 6** (log_2(Ca/EGTA) and log_2(Mock/BoNT), respectively). These can be also visualized using a shiny-app accessible at https://s1608-shiny.mpibpc.mpg.de. **Figure 5.5** summarizes our results according to the schematic representation of proteins at the pre-synapse (386). Importantly, the proteins of the core exocytotic machinery including VAMP2, SNAP25, syntaxin-1a, and Munc18 exhibit SV-cycling-dependent sites, while Munc13 reveals one SV-cycling-dependent site which is close to the significance cut-off.

5.5.4 Phosphomimetic sites on SNARE proteins and cannabinoid receptor-1 modulate neurotransmitter release.

Since protein phosphorylation can be an epiphenomenon of intracellular signaling, we selected a few of the changing phosphosites for determining directly whether they indeed have a modulatory effect on synaptic transmission.

We noted with interest that certain phosphorylation sites on SNARE proteins, including synaptobrevin (*Vamp2*) and syntaxin-1a (*Stx1a*), have a phenotype which belongs to the "SV-cycling-dependent" group (**Figure 5.S18**). More intriguing, some of those sites (such as *Vamp2*-S75) were previously described as being important for the interaction with Munc18-1, a protein that can exhibit a stimulatory effect on trans-SNARE zippering (356). Similarly, we noted that two sites on the cannabinoid receptor-1 (*Cnr1*), T314 and T322, belong to the "SV-cycling-dependent" group as well. In order to test the effects of phosphorylation at these sites, we expressed the respective wild type (WT) proteins, their phosphomimetic mutants and phosphorylation-null mutants in cultured hippocampal neurons (**Figure 5.6A**).

With this strategy, we addressed *Vamp2*-S75, *Stx1*-S21/S23, *Cnr1*-T314/T322, and their respective mutants (*Vamp2*-S75D; *Vamp2*-S75A; *Stx1*-S21E/S23E; *Stx1*-S21A/S23A; *Cnr1*-T314E/T322E and *Cnr1*-T314A/T322A). For these proteins, we created adeno-associated viruses (AAVs) that allowed us to mimic the effects of phosphorylation, and we expressed them in neurons together with *Vamp2*-pHluorin, as a sensor for exo-/endocytosis (**Figure 5.6B and 6C**).

Our stimulation experiments demonstrated that both phosphomimetic and non-phosphorylatable amino-acid substitutions, in both proteins, influence exo- and endocytosis in the cultured neurons. Specifically, we stimulated neurons with either 60 action potentials (AP) at 20 Hz (short stimulation) targeting the readily releasable pool of SVs and thus reflecting the immediate exocytotic response, or using 600 AP at 20 Hz (long stimulation) to mobilize the more inert recycling SV pools, reaching a state in which the entire vesicle cycle is fully activated (123). The expression of phosphomimetic *Vamp2*-S75D reduced exocytosis following short and long stimulation; it also reduced endocytosis in response to long stimulation. Expression of non-phosphorylatable *Vamp2*-S75A reduced exo- and endocytosis following both long and short stimulation (**Figure 5.6D and 6E**). Conversely, pseudo-phosphorylated *Stx1a*-T21E/T23E enhances exocytosis efficiency during short stimulation, while the non-phosphorylatable variant does the opposite (**Figure 5.6F**). The effects on exocytosis become negligible during long stimulation, but both mutant variants result in an enhancement of endocytosis under these conditions (**Figure 5.6G**).

The cannabinoid receptor-1 is known for modulation of the neurotransmitter release (359, 387, 388), and its activation can also be linked, through the activation of MAP kinases, to the phosphorylation of Munc18 (347). Our experiments show that the pseudo-phosphorylated variant *Cnr1*-T314E/T322E reduced exocytosis (most evident during short stimulation), while the non-phosphorylatable variant *Cnr1*-T314A/T322A increased exocytosis in response to long or short stimulation. The effect on endocytosis was observed

only for the pseudo-phosphorylatable *Cnr1* variant after long stimulation (**Figure 5.6H and 6I**).

These experiments tested only three of the synaptic phosphorylation sites that we found differentially phosphorylated in this work. Nevertheless, even if these experiments are based on overexpression in a background containing normal levels of wild type proteins, all tested candidates resulted in significant modulations of exo- or endocytosis. Although in the case of *Vamp2* both mutants led to a substantial reduction in exocytosis rates, its pseudo-phosphorylated form (*Vamp2*-S75D) showed a greater effect on exocytosis than the non-phosphorylatable form (*Vamp2*-S75A). Presumably, the absence of a charged residue did not fully compensate the steric effect caused by the amino acid substitution at position 75 of *Vamp2*, which has apparently a stronger impact on protein function than the double mutant at positions 21/23 of *Stx1a*. The S75 phosphorylation site is located within the R-SNARE motif required for forming a coiled-coil complex with *Stx1a* and SNAP-25 during exocytosis. In contrast, the T21/T23 positions of *Stx1a* are located in the regulatory N-terminal helical bundle, explaining why mutations show different effects on exocytosis. Overall, these findings support the concept that protein phosphorylation is a key regulatory mechanism in neurotransmitter release that modulates different steps in the SV cycle.

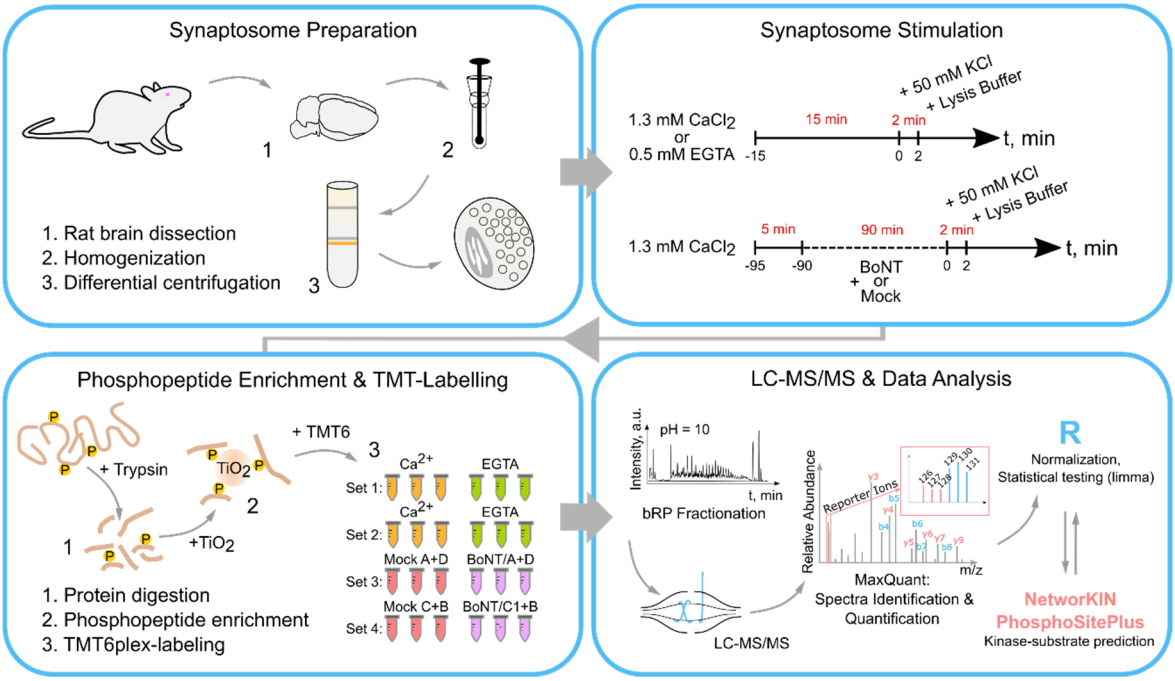

Figure 5.1: Workflow for the phosphoproteome analyses of synaptosomes under different stimuli. *Brains of 5-6 weeks old Wistar rats were homogenized and the synaptosomal fraction was enriched by differential centrifugation in discontinuous Ficoll gradient. Two sets of experiments were performed that compared a) stimulation of synaptosomes in the presence of Ca^{2+} (1.3 mM) or Ca^{2+}-chelator (EGTA, 0.5 mM), or b) stimulation of synaptosomes pre-treated with inactivated toxins (Mock) or a combination of two botulinum toxins (BoNT, A+D or C1+B). Synaptosomes were depolarized by 50 mM KCl for 2 min. Each experiment included three independent control stimulations (EGTA or Mock-treated) and three independent test stimulations (Ca or BoNT). Samples were processed in a conventional bottom-up proteomics workflow and phosphorylated peptides were enriched by metal-oxide chromatography (TiO_2). Replicates within one experiment were labeled with a set of TMT6 isobaric labeling reagents. A pooled peptide sample was fractionated by reversed-phased chromatography at basic pH and measured in a high-resolution quadrupole-orbitrap mass spectrometer. Reporter ion intensities were utilized to infer relative abundances of phosphorylated peptides.*

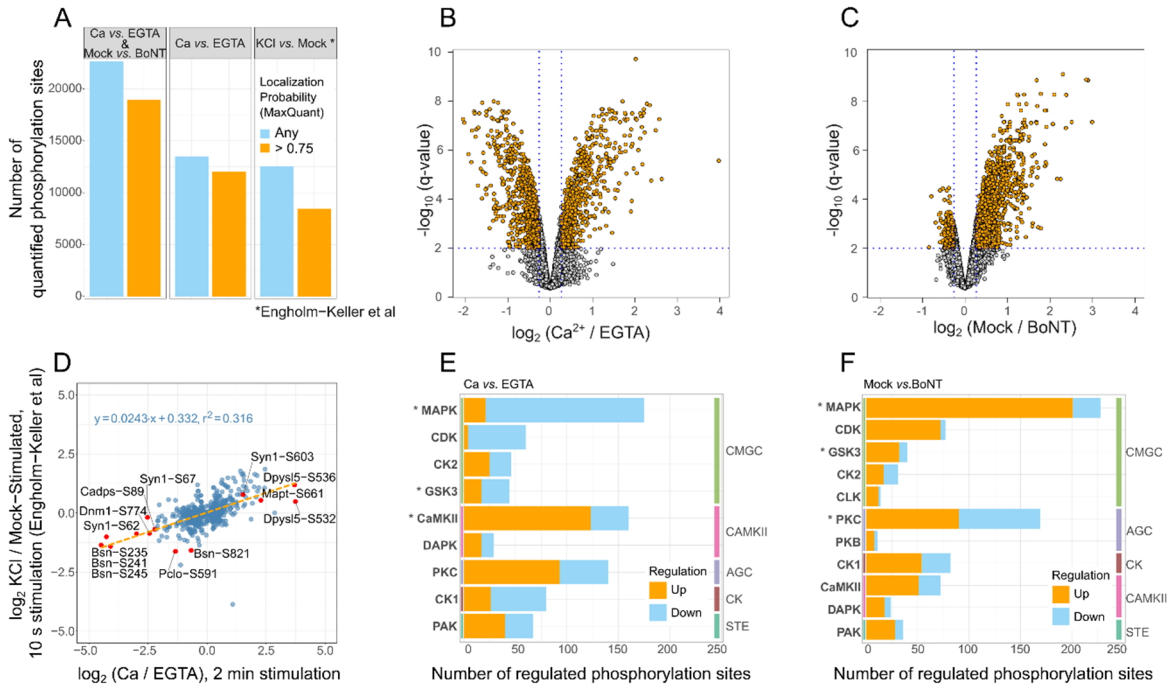

Figure 5.2: Substantial changes in synaptic phosphoproteome following depolarization and responsible kinase groups. *(**A**) Number of quantified phosphorylation sites in Ca vs. EGTA and Mock vs. BoNT experiments (panel 1), Ca vs. EGTA experiments only (panel 2) and recently published data set (Engholm-Keller (352), panel 3). (**B, C**) volcano plots depicting -log$_{10}$ (q-value) vs. log$_2$ (intensity fold change) of phosphorylation sites quantified within Ca vs. EGTA and Mock vs. BoNT experiments, respectively. (**D**) Comparison of log$_2$ fold changes between our and Engholm-Keller et al (352) data sets. Selected phosphorylation sites are marked as official gene symbol with phosphorylated amino acid and position. (**E, F**) the stacked bar graphs show the total number of significantly regulated phosphorylation events in Ca vs. EGTA (e) or Mock vs. BoNT (f) experiments that can be a result of known (PhosphoSitePlus database (325)) or predicted (NetworKIN (144, 323)) kinase-substrate interactions. Orange bars depict the number of phosphorylation events that show significant intensity increase in Ca^{2+} or Mock-treated synaptosomes versus respective control (EGTA or BoNT). Blue bars correspond to down-regulated events, respectively. The kinase classification (Netphorest Groups) follows one introduced by Netphorest (144) and uses its second-level group annotation. Colored vertical bars delineate the highest-level group in the kinase classification. Asterisks mark kinase groups which are predicted to control significantly more phosphorylation sites than expected as based on predicted kinase-substrate interactions in human proteome (Fisher's exact test Benjamini-Hochberg adjusted p-value < 0.01). Abbreviations: AGC ~ protein kinase A, G, C kinase group; CaMKII ~ calcium-calmodulin kinase 2; CDK ~ cyclin-dependent kinase; CK ~ casein kinase; CK1 ~ casein kinase 1; CK2 ~ casein kinase 2; CLK ~ SRPK1 and Clk/Sty protein kinase; CMGC ~ CDK, MAP, GSK, CDKL kinase group; DAPK ~ death associated protein kinase; MAPK ~ mitogen activated protein kinase; GSK3 ~ glycogen synthase kinase 3; PAK ~ p21 activated kinase; PKC ~ protein kinase C; STE ~ "sterile" serine/threonine protein kinases.*

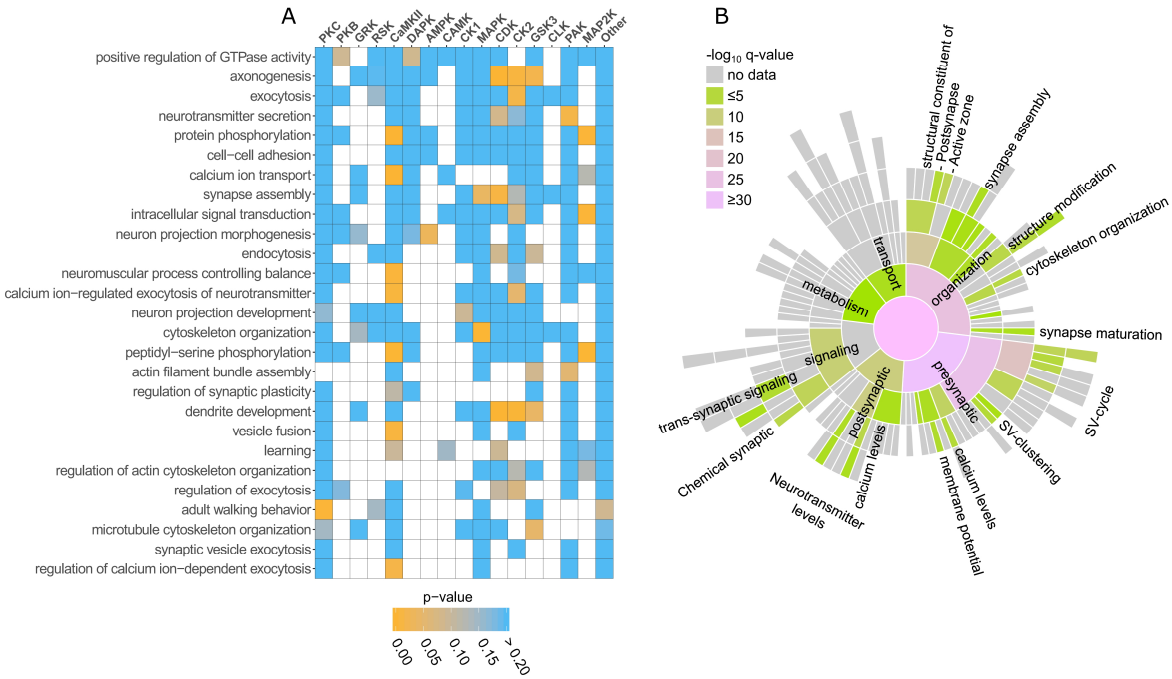

Figure 5.3: Functional annotation of proteins carrying regulated phosphorylation sites based on Ca vs. EGTA experiments. *(**A**) Association between significantly enriched GO terms and kinase groups. The enriched biological function-GO terms (background: Rattus norvegicus, Benjamini-Hochberg adjusted p-value < 0.001) were derived using DAVID web service (368) for proteins carrying regulated phosphorylation sites. Overrepresentation of putative kinase-substrates relationships was tested for proteins annotated by each GO term. Frequencies of putative kinase-substrate relationships across all regulated sites for Ca vs. EGTA experiments were taken as a background. The color encodes raw p-values (Fisher's exact test). (**B**) Sunburst diagram showing enriched biological function terms based on the synapse-specific SynGO database annotation (324). The color encodes the significance of the enrichment (-log$_{10}$ (q-value)). Full list of enriched biological functions can be found in Table 5.S2.*

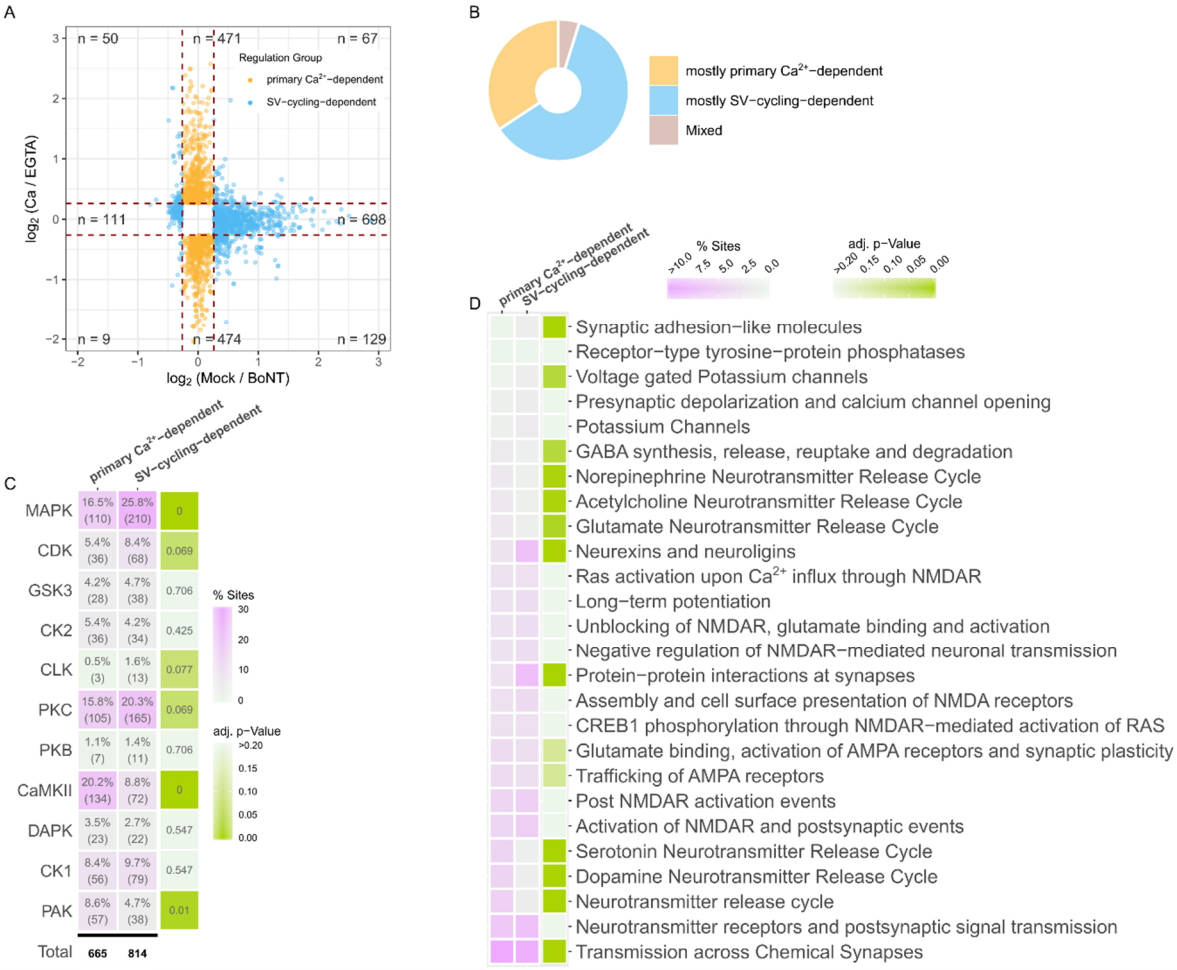

Figure 5.4: Dependence of regulated phosphorylation sites on calcium influx and SV cycling. *(**A**) Categorization of phosphorylation events based on the magnitude of the log_2 fold changes in Mock vs. BoNT experiment (x-axis) and log_2 fold changes in Ca vs. EGTA experiment (y-axis). Only events quantified in both experiments and satisfying a q-value threshold of < 0.01 are shown. The events are classified into two regulation groups: (i) "primary Ca^{2+}-dependent" (sites with no significant or not-quantified SV cycling effect, i.e., absolute log_2 (Mock/BoNT) < 0.263 and absolute log_2 (Ca/EGTA) > 0.263), shown as orange dots; and (ii) "SV-cycling-dependent" (absolute log_2 (Mock/BoNT) > 0.263). (**B**) Proportion of proteins that can be organized in one of the regulation groups based on the categorization of phosphorylation sites they carry. Only sites that surpassed the FDR-threshold of < 1% were considered. If > 60% of the significantly regulated sites on a protein belong to one of the two regulation groups ("primary Ca^{2+}-dependent" or "SV-cycling-dependent"), the protein is categorized in "mostly primary Ca^{2+}-dependent" or "mostly SV-cycling-dependent", respectively. (**C**) Enrichment of predicted kinase-substrate interactions for "primary Ca^{2+}-dependent" and "SV-cycling-dependent" regulation groups. The left panel shows the percentage and the absolute number of sites in each category (x-axis) that can be regulated by a particular kinase group (y-axis). The number under the black line provides the total number of sites with predicted kinase-substrate relationship in each category. The right panel shows Benjamini-Hochberg adjusted p-values after a Fisher's exact test. An equal distribution of kinase-substrates relationships between the "primary Ca^{2+}-dependent" and "SV-cycling-dependent" categories was set as a null hypothesis.*

Figure 5.4: Dependence of regulated phosphorylation sites on calcium influx and SV cycling (continued from previous page). *(**D**) Reactome pathway terms of neuronal origin (369). Reactome pathway terms of neuronal origin were selected based on their enrichment (Benjamini-Hochberg adjusted p-value < 0.1) for all proteins carrying significantly regulated phosphorylation sites. Proportion of "primary Ca^{2+}-dependent" and "SV-cycling-dependent" sites of all "primary Ca^{2+}-dependent" or "SV-cycling-dependent" sites per functional term is shown as color code (magenta). Fisher's exact test was applied to test equal distribution of "primary Ca^{2+}-dependent" and "SV-cycling-dependent" sites for each term. Benjamini-Hochberg adjusted p-values are represented as a color code (green). Abbreviations: AMPAR stays for α-amino-3-hydroxy-5-methyl-4-isoxazolepropionic acid receptor; CREB1 ~ CAMP responsive element binding protein 1; GABA ~ γ-amminobutyric acid; NMDAR ~ N-methyl-d-aspartate receptor; RAS ~ rat sarcoma gene.*

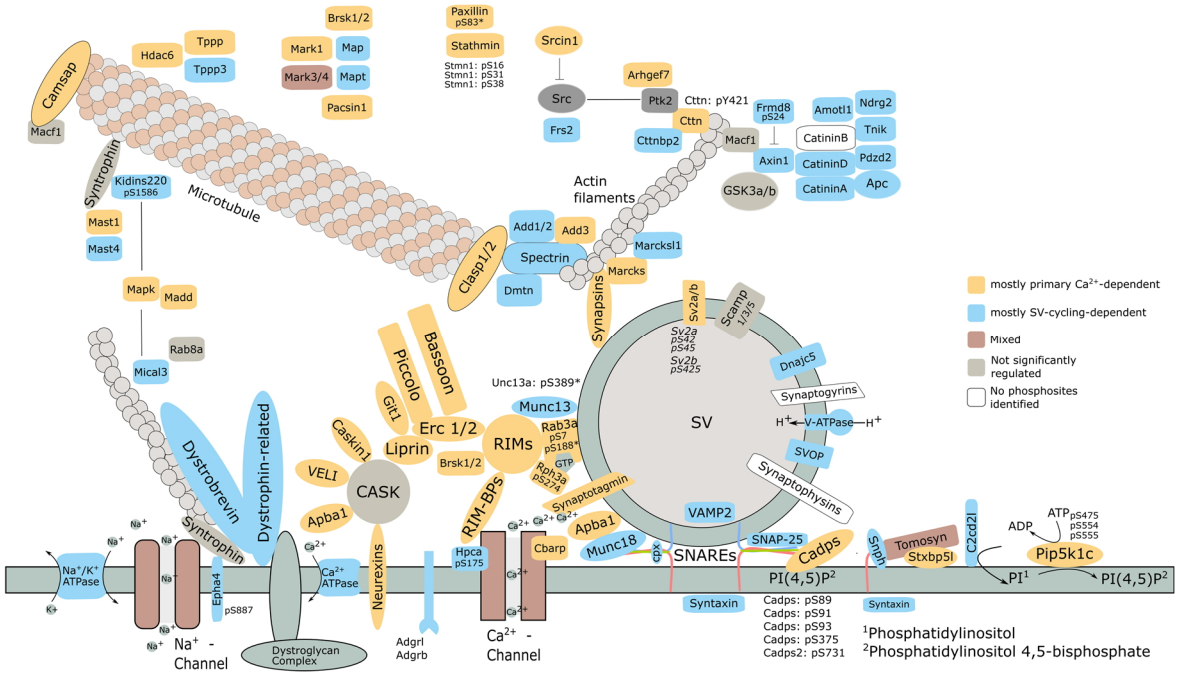

Figure 5.5: Schematic representation of presynaptic compartment with a single docked synaptic vesicle, plasma membrane and cytoskeleton elements, based on Chua et al (386). *The represented proteins are categorized in "mostly primary Ca^{2+}-dependent" (yellow), "mostly SV-cycling-dependent" (blue), "Mixed" (brown) based on the regulation type of the phosphorylation sites they carry. Proteins with no significantly regulated phosphorylation sites are represented in grey; proteins for which no first-class phosphorylation sites (MaxQuant localization probability < 0.75) were identified are represented in white. In most cases, an official gene symbol was used to name proteins, except: Bassoon stays for Bsn; Ca^{2+}-ATPase ~ Atp2b1, Atp2b2, Atp2b3; Camsap ~ Camsap1, Camsap3; CatininA ~ Cttna2; CatininD ~ Ctnnd1, Ctnnd2; Dystrobrevin ~ Dtnb; Dystrophin-related ~ Drp2; Liprin ~ Ppfia1, Ppfia2, Ppfia3, Ppfia4; Map ~ Map1a, Map1b, Map1s, Map2, Map4, Map6, Map7d1, Map7d2; Mapk ~ Mapk1, Mapk3; Na^+/K^+ ATPase ~ Atp1a1, Atp1a2, Atp1a3; Na^+-Channel ~ Scn1a, Scn1b, Scn2b, Scn3a; Neurexins ~ Nrxn1; Piccolo ~ Pcl; RIM-BPs ~ Rimbp1, Rimbp2; RIMs ~ Rim1, Rim2; Spectrin ~ Sptan1, Sptb, Sptbn1, Sptbn2, Sptbn4; Stathmin ~ Stmn1; Synaptotagmin ~ Syt1, Syt6, Syt9, Syt10, Syt17, Styl5, Esyt2; Syntaxin ~ Stx1a, Stx1b, Stx12; Syntrophin ~ Sntb2; Tomosyn ~ Stxbp5; VAMP ~ Vamp2; V-ATPase ~ Atp6v1d; VELI ~ Lin7a, Lin7b, Lin7c. Asterisks mark sites that do not meet significance criteria of q-value < 0.01: Unc13a-pS389 (q-value = 0.013), Rab3a-pS188 (q-value = 0.012).*

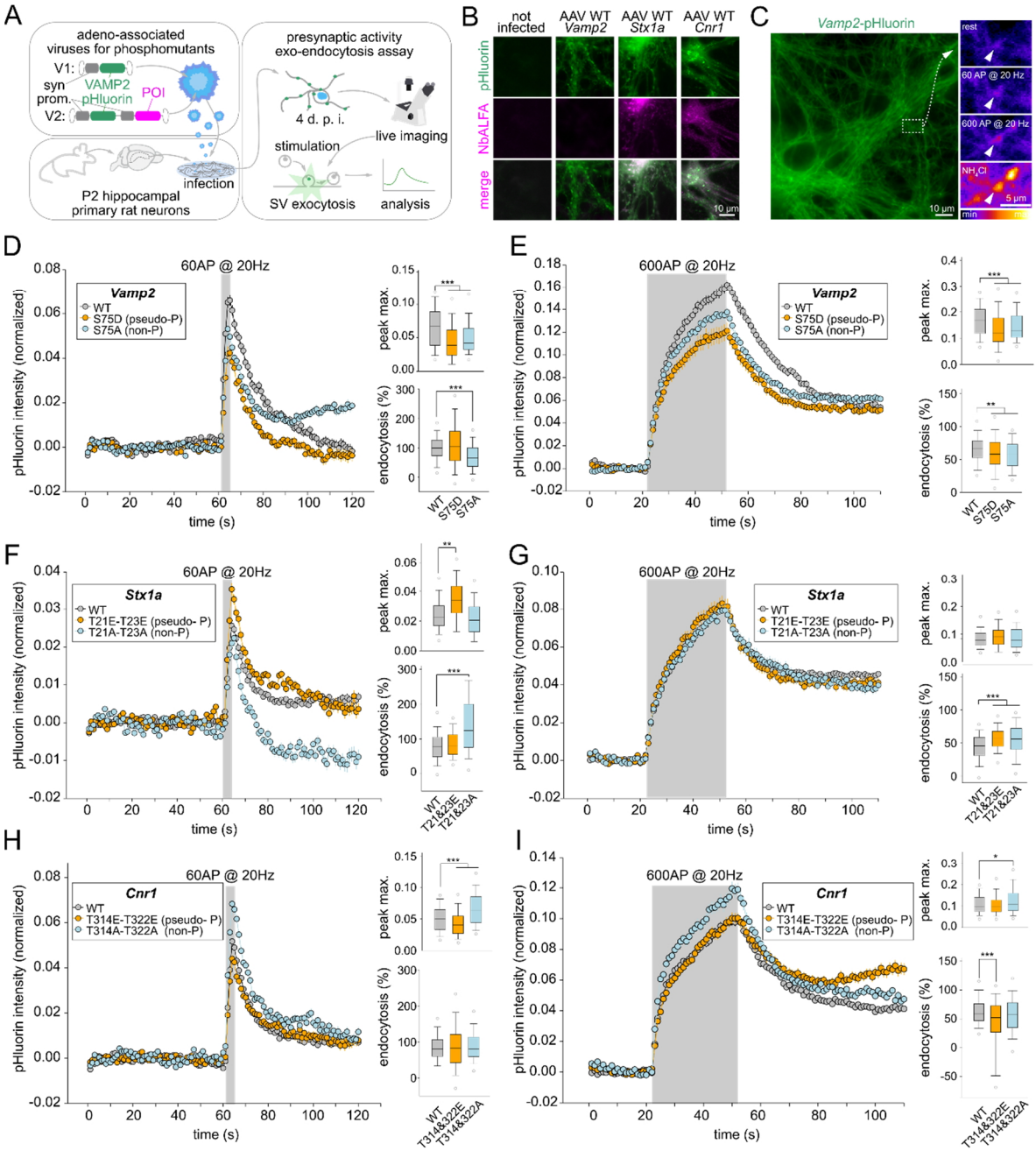

Figure 5.6: Phosphomimetic modulation of phosphorylation sites found differentially regulated in synaptobrevin (Vamp2), syntaxin-1 and cannabinoid receptor-1 affects SV recycling properties (s. next page for details).

Figure 5.6: Phosphomimetic modulation of phosphorylation sites found differentially regulated in synaptobrevin (Vamp2), syntaxin-1 and cannabinoid receptor-1 affects SV recycling properties (continued from previous page). *(**A**) Experimental scheme. Two versions of the adeno associated viral (AAV) constructs were prepared (V1 and V2). V1 contained Vamp2 wild-type or the respective Vamp2 mutants (Vamp2-S75D and Vamp2-S75A) fused to the superecliptic (pH-dependent) green fluorescence protein (pHluorin; (375)). The expression of recombinant proteins is driven by the neuron-specific synapsin promoter. In these experiments the Vamp2-pHluorin is used both as the test protein and as a sensor for exo- and endocytosis. V2 contained both WT Vamp2-pHluorin (used as an exo-/endocytosis sensor) and the proteins of interest (POI; respectively Stx1a-WT, Stx1a-T21E-T23E; Stx1a-T21A-T23A; Cnr1-WT; Cnr1-T314E-T322E and Cnr1-T314A-T322A); see methods for details. To distinguish these proteins from the endogenous versions, an ALFA-tag sequence has been added (377). Mutants were expressed in rat primary hippocampal neurons and exo-/endocytosis was measured 4 days post infection (d.p.i.). In order to evaluate exo-/endocytosis, neurons were field-stimulated and changes in fluorescence were measured (375). (**B**) Immunofluorescence of infected neurons. The high efficiency of infection and the co-expression of the POIs (Stx1a; Cnr1) is confirmed by immunofluorescence using a nanobody directed against the ALFA tag (NbALFA; (377)). Scale bar 10 µm (**C**) The basal fluorescence of Vamp2-pHluorin (left image) allows to identify single synaptic boutons (inset on the right). Following a defined number of action potentials (AP), SVs fuse with the plasma membrane (middle insets on the right). Upon fusion, the intravesicular pH increases, resulting in higher pHluorin fluorescence intensity. Ammonium chloride (NH_4Cl) is used at the end of each experiment to reveal the localization of SVs. Scale bars: 10 µm (left image) and 5 µm (right insets). (**D, E**) Both the phosphomimetic and the phosphorylation-null mutants of Vamp2 showed decreased exocytosis, for both short and long train of stimuli, respectively 60 and 600 action potentials (APs). The maximum peak intensity was significantly lower in both stimuli ($P < 0.001$). The fraction of endocytosed Vamp2 (measured at 30 seconds after the stimulation, as % of the exocytosed Vamp2) was also decreased, especially for the longer stimulus. (**F** and **G**) The phosphomimetic mutant of Stx1a (T21-T23) enhanced exocytosis for short stimuli, while the phosphorylation-null mutant left exocytosis unaffected, while enhancing endocytosis. Under long stimuli the enhancement of exocytosis was no longer significant, but the increase in endocytosis was, for both phosphomimetic and phosphorylation-null mutants. (**H** and **I**) The phosphomimetic mutants of Cnr1 (T314E-T322E) reduced exocytosis during short stimuli, while the non-phosphorylatable variant increased exocytosis. The latter effect was also observed during long stimuli. Neither of the Cnr1 variants had a substantial effect on endocytosis. In all panels statistical differences were tested relying on Kruskal-Wallis tests, followed by Tukey-Kramer post-hoc tests (* $P < 0.05$, ** $P < 0.01$ and *** $P < 0.001$).*

5.6 Discussion

In this study, we have used isolated nerve terminals as a model to differentiate phosphorylation changes that are induced by calcium influx alone from those that in addition require active endo-exocytotic SV cycling. Surprisingly, we found that inhibition of exocytosis by BoNT had a profound effect on the phosphoproteome despite unchanged calcium influx. These findings reveal complex signaling cascades during which regulatory changes in protein phosphorylation are not only dependent on the activation of kinase/phosphatase networks but also on the progression of vesicular trafficking.

By using isobaric tandem-mass tags for labeling of phosphorylated peptides, we were able to substantially increase the phosphoproteome coverage and to achieve reliable quantification for thousands of phosphorylation sites. Despite differences in the synaptosome preparation (Ficoll-purified synaptosomes *vs*. crude synaptosomal pellet) and stimulation (50 mM KCl for 2 min *vs.* 75 mM KCl for 10 s), many of the regulated phosphorylation sites observed by us are in excellent agreement with earlier results from another laboratory (**Figure 5.2D**) (352). Our data show higher magnitudes of changes, which are probably a consequence of the prolonged stimulation time used in our study. The most drastic changes were observed for pacsin (*Pacs1*-S517, $\log_2$ fold change of 3.98), thymosin beta (*Tmsb4x*-T23, 2.63), ADP-ribosylation factor GTPase activating protein 1 (*Arfgap1*-S247 2.57), calcium/calmodulin-dependent protein kinase type II subunit delta (*Camk2d*-S315/S319, 2.49), protein Bassoon (*Bsn*-S1354, –2.06), septin 5 (*Sept5*-S17, –1.93), and RIM-binding protein 2 (*Rimbp2*-S554, –1.86). We also confirm phosphorylation changes in response to stimulation that were reported earlier for synapsin-1, dynamin-1, Tau protein, as well as the multi-site phosphorylations of the giant active zone proteins Bassoon and Piccolo (242, 338, 341, 346).

It seems that several proteins known to function at the postsynapse respond to potassium chloride stimulation and BoNT treatment in synaptosomes (*e.g.*, *Shank1, 2, 3*; components of NMDAR, *Grin1, Grin2a, Grin2b*). It would be of interest to investigate whether these proteins are also present at measurable levels in the presynapse and whether they are affected by synaptic activity. Although synaptosomal preparations are known contain fragments of the postsynaptic membrane (97), they usually do not retain metabolic activity, in contrast to functionally active membrane-enclosed nerve terminals that can maintain the ATP levels needed for phosphorylation (98, 99, 115, 360).

Clearly, the primary trigger for the phosphorylation changes is calcium that enters synaptosomes following potassium-induced depolarization. Calcium directly regulates the activity of kinases and phosphatases, including CaMKII, PKC, calcineurin, PP1 *etc*. (243,

337, 379, 389). Accordingly, we observe increased phosphorylation of specific sites on CaMKII and MAP kinases that are known to result in activation of the kinases as well as enrichment of possible substrates for CaMKII, MAPK, and GSK3 kinases among regulated phosphorylation sites.

However, the fact that selective inhibition of calcium-activated SV cycling results in major changes of the phosphoproteome documents that the activation status of the kinase/phosphatase networks is directly dependent on the progression of the exo-endocytotic cycle. In most cases, BoNT treatment inhibited phosphorylation, and these results are in line with a very early study that used BoNT-treated synaptosomes from the electric organ of *Torpedo marmorata* and radioactive phosphate for protein labeling (390). Interestingly, phosphorylation events known to be directly regulated by some of the major calcium-dependent kinases and phosphatases such as those on synapsin-1 and dynamin-1, as well as on many of the predicted CaMKII-phosphorylation sites, were almost unaffected by the BoNT treatment. Conversely, predicted sites of MAPK, PKC, and CDK were affected more strongly by the BoNT-treatment. These observations support the view that the activity of MAPK is dependent on active SV cycling, resulting in the phosphorylation of delta catenin, metabotropic glutamate receptor and other proteins in the synapse (391-394). Indeed, we observe SV-cycling-dependent phosphorylation changes not only in catenin-delta (*Cttnd2*) but also in other proteins that might take part in the Wnt pathway such as *Apc, Amotl1*, and *Tnik*. Given the connection between the Wnt pathway and the regulation of cell–cell contacts and cytoskeletal elements, it is not surprising that many cytoskeleton- and cell-adhesion-related proteins contain BoNT-responsive phosphorylation sites (*e.g.*, spectrin beta, adducin alpha and beta, neurofascin, neuronal cell adhesion molecule). It is tempting to speculate that these phosphorylation changes represent the activation of pathways directed at increasing synaptic strength (most importantly LTP) by mechanisms such as size increase of the synaptic contact zone, enlargement of the presynaptic bouton and adaptations of the presynaptic cytoskeleton to increase the efficiency of SV cycling (395-398).

How can the wide-ranging neurotoxin effects be explained when considering the extraordinary specificity of the SNARE-proteases, which should have no direct effect on kinases or phosphatases? Given that toxin treatment causes dephosphorylation of many substrates, the observed effect can be explained either by activation of phosphatase or by suppression of kinase activities that are not caused directly by calcium but by changes in proteins that are themselves regulated by the activity of the SV cycle and in turn control kinases or phosphatases. Moreover, it is conceivable that the availability of phosphorylation sites on substrate proteins is coupled to its “activity cycle”. Trafficking steps such as SV

docking, priming, fusion, coat formation, fission, and SV movement are associated with numerous changes in protein conformation and the dynamic assembly and disassembly of multimolecular complexes. Thus, it is to be expected that phosphorylation site accessibility is dependent on these dynamic changes, many of which are likely to be arrested following inhibition of the SV cycle.

An interesting example is given by the protein phosphatase-1 (PP1) whose postsynaptic activation appears to be dependent on synaptic activity (237). Neurabin-1 (*Ppp1r9a*) can play a crucial role in this, by recruiting PP1 to the synapse by regulating its binding to actin filaments which impacts PP1 activity (399, 400). Our observations suggest that PP1 undergoes similar activity-dependent regulation also in the presynapse as we observe “SV-cycling-dependent” sites within the actin-binding region of Neurabin-1. It is tempting to speculate whether SV-cycling-dependent activity of PP1 or other phosphatases can be opposed by Ca^{2+}-activated kinases such as CaMKII, MAPK1, MAPK3. This would explain reduced intensities of predicted MAPK-substrates in Ca/EGTA experiments despite apparent activation of MAPK following K^{+}-induced depolarization and Ca^{2+}-influx. Furthermore, it would explain why many phosphosites appear significantly regulated when comparing mock- with BoNT-treated synaptosomes, but do not show significant changes in Ca/EGTA experiments, since comparison of Ca^{2+} with EGTA conditions reveals a composite effect of Ca^{2+} influx and SV cycling on protein phosphorylation.

Experiments involving botulinum neurotoxins also led us to the discovery of phosphorylation sites on the core SNARE proteins, sites that otherwise did not appear significant. We showed that these sites can affect exo- and endocytosis in hippocampal neurons under stimulation. One possible mechanism is the impaired interaction with Munc18-1, which can facilitate SNARE zippering and thereby promote SV fusion with the plasma membrane (356). The changes of endocytosis are possibly a consequence of altered exocytosis. In contrast to many other BoNT-responsive phosphorylation sites, the phosphorylation sites on *Vamp2* and *Stx1a* that we examined showed increased phosphorylation following toxin treatment, suggesting that the phosphorylation is due to adaptive changes in the synapse rather than a result of SNARE-cleavage by BoNT.

In contrast to the phosphomimetic and nonphosphorylatable variants of the SNARE proteins, the corresponding variants of cannabinoid recepor-1 (*Cnr1*) had an effect only on exocytosis in cultured hippocampal neurons. The effect can be also linked through the activation of MAPK to Munc18 phosphorylation and regulation of SNARE assembly (387). Similarly, the intensity of phosphorylation of T314/T321 sites was increased following toxin treatment. Although *Vamp*2-S75, *Stx1a*-S21/S23, *Cnr1*-T314/T321 phosphorylation sites were identified in previous studies (356, 357, 401, 402), it is the first time, to the best of our

knowledge, that phosphorylation of these sites has been shown to have an impact on the exo- and endocytosis in the context of stimulation experiments.

Interestingly, we also found phosphorylation sites on Munc18 that are regulated in SV-cycling-dependent manner, namely *Stxbp1*-S313 and *Stxbp1*-S506. Both sites were significantly downregulated in the BoNT-treated samples. Although not much known about S506, S313 site was previously described as a possible target of PKC and that its phosphorylation can negatively affect interaction of Munc18 with syntaxin-1 (187, 358).

A remarkable aspect of the synapse phosphoproteome regulation has recently been addressed by *F. Brüning et al*. (403). Their analysis shows that phosphorylation sites on many synaptic proteins undergo oscillations during the course of the day. Interestingly, a few of these sites are shown to be regulated upon depolarization by potassium chloride and treatment with botulinum neurotoxins, including phosphorylation sites on proteins previously discussed: *Cnr1, Vamp2, Stx1a, Cttnd2, Add1, Add2, Sptbn1, Sptbn4, Kcnb1, Kcnd2, Hcn2, Kcnma1, Tnik, Apc, Camk2a, etc*. This also suggests that, despite the caveat that potassium-induced depolarization is non-physiological (352), it allows for identifying regulated phosphorylation sites that are of high functional relevance for normal synapse physiology.

Despite major progress, many aspects of synapse regulation remain to be uncovered. Our study has added another layer of complexity by showing how intricately the phosphorylation-dephosphorylation cascade in the synapse is linked to SV cycling. We believe that the results presented here provide a firm basis for future investigations about how synaptic activity and synaptic plasticity is regulated at the molecular level.

5.7 Acknowledgments

We sincerely thank Thomas Gundlach and Sascha Krause for their assistance in animal experiments; Sofia Ainatzi and Dr. Momchil Ninov for help in synaptosome preparations; Monika Raabe, Uwe Plessmann, Dr. Sabine König, and Dr. Ralf Pflanz for technical support; Heiko Ludwig for launching of the shiny-server.

5.8 Funding

S.B., S.O.R., H.U., and R.J. are funded by the Deutsche Forschungsgemeinschaft through collaborative research center SFB1286, projects A08, A03, Z02 and Z03.

5.9 Author Contributions

R.J., H.U., and I.S. conceptualized the study; E.F. conceptualized and performed phosphomimetic studies in neurons; I.S. performed synaptosomal experiments under the

supervision of K.T.P., H.U., and R.J.; I.S. analyzed data; M.F. and S.B. contributed to the bioinformatics analysis; initial draft was written by I.S. and H.U., reviewed and edited by H.U, R.J., E.F., S.O.R., and K.T.P.

5.10 Conflict of interest

The authors declare that they have no conflicts of interest with the contents of this article.

5.11 Data availability

The mass spectrometry data have been deposited to the ProteomeXchange Consortium via the PRIDE(404) partner repository with the dataset identifier PXD020564.

R scripts used for data analysis are available at github: https://github.com/IvanSilbern/2021_Silbern_etal_Synapt_BoNT_KCl.

We also provide a visualization tool in a shiny-app format. The source data and code are available at github: https://github.com/IvanSilbern/2021_Silbern_etal_ShinyApp. The app is deployed and accessible at: https://s1608-shiny.mpibpc.mpg.de.

5.12 Overview of the supplementary material (supplementary tables, figures and datasets)

1. 20200901_SupplData_Notes_Figures_Tables.pdf
   Supplementary Information
2. “SupplData01_Phosphosite_Intensities.xlsx”
   Phosphorylation site intensities used for the assessment of differential protein phosphorylation in Ca *vs.* EGTA and Mock *vs.* BoNT experiments
3. “SupplData02_Proteingroups_Intensities_MockBoNT_AD.xlsx”
   Protein group intensities used for the assessment of the differential protein content in depolarized synaptosomes following Mock (A+D) or BoNT (A+D) treatment.
4. “SupplData03_Proteingroups_Intensities_MockBoNT_CB.xlsx”
   Protein group intensities used for the assessment of the differential protein content in depolarized synaptosomes following Mock (C1+B) or BoNT (C1+B) treatment.
5. “SupplData04_Protein_classification.xlsx”
   Classification of proteins based on the classification of the regulated phosphorylation sites they carry.
6. “SupplData05_Phosphoproteins_regulated_CaEGTA.pdf”
   Representation of $\log_2$ fold changes of the phosphorylation site intensities in depolarized synaptosomes following incubation with Ca^{2+} or EGTA per protein sequence. Only protein with significantly regulated phosphorylation sites are shown.

7. “SupplData06_Phosphoproteins_regulated_MockBoNT.pdf”
   Representation of log_2 fold changes of the phosphorylation site intensities in depolarized synaptosomes following incubation with Mock or BoNT per protein sequence. Only protein with significantly regulated phosphorylation sites are shown.

5.13 Supplemental Materials

5.13.1 Table of contents:

Supplementary Notes:

Supplementary Figures：

Figure 5.S17: Changes in phosphorylation site intensities for Calcium-activated potassium channel subunit alpha 1, Potassium voltage-gated channel subfamily H member 1, and Potassium voltage-gated channel subfamily Q member 5.

Figure 5.S18: Changes in phosphorylation site intensities for Syntaxin 1A, Vesicle-associated membrane protein 2, Syntaxin-binding protein 1, and Cannabinoid receptor 1.

Figure 5.S19: Proteomic profiling of *C. botulinum* cell culture supernatants.

Figure 5.S20: Phosphoproteome analysis of BoNT-treated HeLa nuclear extract.

Figure 5.S21: Proteomics analysis of Mock- or BoNT-treated synaptosomes.

Supplementary Tables:

Table 5.S1: Number of regulated phosphorylation events per predicted kinase group in Ca *vs.* EGTA experiment.

Table 5.S2: Enriched gene ontology biological function terms based on synapse-specific SynGO database

Table 5.S3 Number of regulated phosphorylation events per predicted kinase group in Mock *vs*. BoNT experiment.

Table 5.S4: Number of regulated phosphorylation events per predicted kinase group in Ca *vs.* EGTA and Mock *vs.* BoNT experiments.

Supplementary Data:

“SupplData01_Phosphosite_Intensities.xlsx”
Phosphorylation site intensities used for the assessment of differential protein phosphorylation in Ca *vs.* EGTA and Mock *vs.* BoNT experiments

“SupplData02_Proteingroups_Intensities_MockBoNT_AD.xlsx”
Protein group intensities used for the assessment of the differential protein content in depolarized synaptosomes following Mock (A+D) or BoNT (A+D) treatment.

“SupplData03_Proteingroups_Intensities_MockBoNT_CB.xlsx”
Protein group intensities used for the assessment of the differential protein content in depolarized synaptosomes following Mock (C1+B) or BoNT (C1+B) treatment.

“SupplData04_Protein_classification.xlsx”
Classification of proteins based on the classification of the regulated phosphorylation sites they carry.

“SupplData05_Phosphoproteins_regulated_CaEGTA.pdf”
Representation of $\log_2$ fold changes of the phosphorylation site intensities per protein

sequence in depolarized synaptosomes following incubation with Ca^{2+} or EGTA. Only proteins with significantly regulated phosphorylation sites are shown.

"SupplData06_Phosphoproteins_regulated_MockBoNT.pdf"
Representation of log_2 fold changes of the phosphorylation site intensities per protein sequence in depolarized synaptosomes following incubation with Mock or BoNT. Only proteins with significantly regulated phosphorylation sites are shown.

5.13.2 Supplementary Note

C. botulinum cell culture supernatant activity assessment

BoNT-treatment of synaptosomes negatively affected glutamate release and did not compromise the increase in cytoplasmatic Ca^{2+}-concentration following KCl-stimulation (**Figure 5.S1B, C**). Proteome profiling of the *C. botulinum* cell culture supernatants used in the study (**Figure 5.S19**) identified BoNTs among the most abundant proteins. However, we could detect presence of a putative protease and two putative phosphatases in the cell culture supernatants as well. To exclude unspecific phosphatase activity, we treated nuclear extract of HeLa cells with a combination of BoNT/A-D and subsequently performed a total quantitative phosphoproteome analysis. The analysis did not reveal significant phosphatase activity that could be attributed to the treatment with *C. botulinum* cell culture supernatants (**Figure 5.S20**). To exclude unspecific protease activity, we analyzed peptides in the unbound fraction following TiO_2.enrichment of phosphorylated peptides. The analysis did not show strong changes in protein intensities in synaptosomes following BoNT-treatment (**Figure 5.S21**). Although the intensities of some proteins seem to be slightly affected by BoNT/C1+ BoNT/B treatment, the observed mild effect is not at all comparable with the extreme effect that BoNT-treatment has on the phosphorylation of synaptic proteins. Neither have we seen a significant reduction in the level of SNARE proteins (**Figure 5.S4E, F**). We, therefore, hypothesized that only a minor pool of SNARE proteins is cleaved following BoNT-treatment. SNARE proteins that reside inside non-functional synaptosomes would be protected from cleavage and mask the reduction in SNARE-proteins. We also cannot exclude some non-proteolytic effects of BoNT since such effects were previously discussed (405). Important for this study, BoNT-treatment dampened glutamate release without compromising calcium influx, which allowed us to investigate calcium and SV cycling effects on protein phosphorylation in synaptosomes.

5.13.3 Supplementary Figures

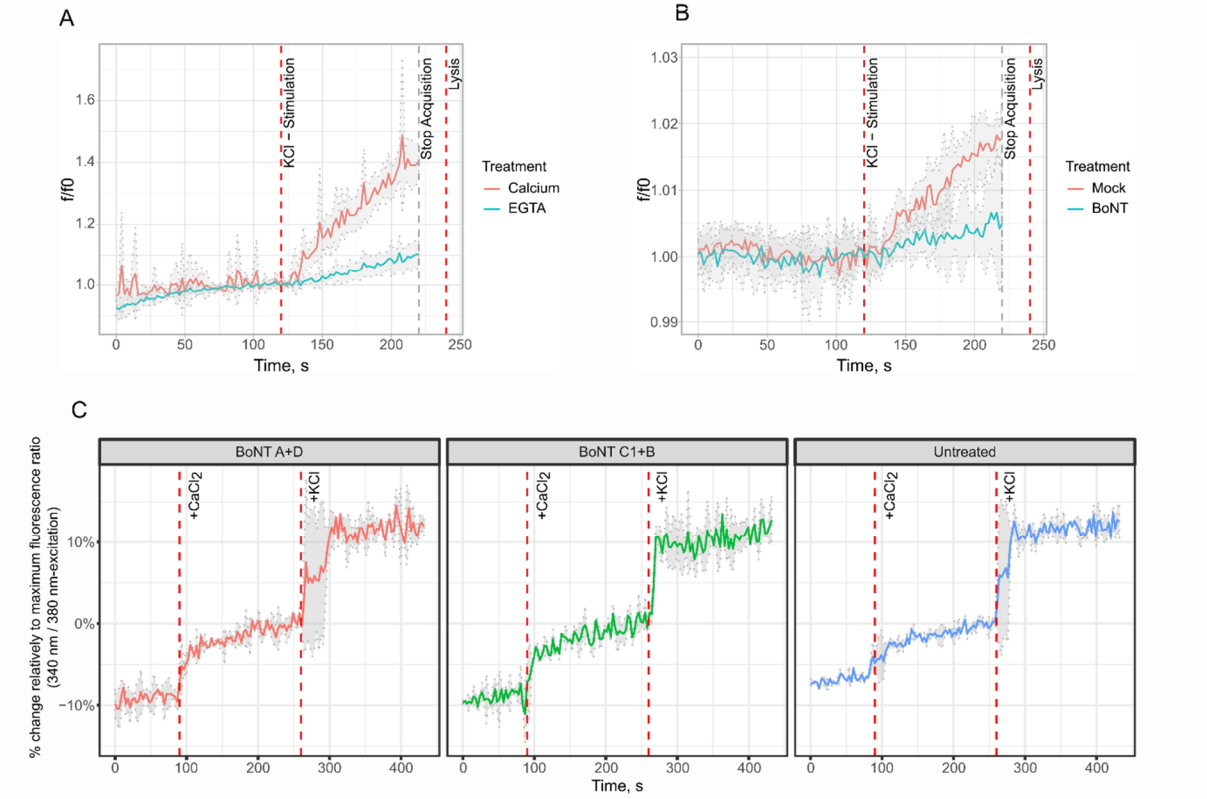

Figure 5.S1 Glutamate release assay and Ca^{2+}-levels in cytoplasm. *(**A**) Glutamate release following depolarization with potassium chloride in the presence of Ca^{2+} ions or EGTA. X-axis: time in seconds, Y-axis: normalized fluorescence intensity (f0 = fluorescence intensity before KCl-stimulation). Red line: synaptosomes stimulated in the presence of Ca^{2+} (average of 6 replicates). Green line: synaptosomes stimulated in the presence of EGTA (average of 6 replicates). Shaded grey area corresponds to the standard deviation at each time point. (**B**) Glutamate release of Mock- or BoNT- treated synaptosomes. X-axis: time in seconds, Y-axis: fluorescent intensity (f) normalized by fluorescence intensity before KCl-stimulation (f0). Red line: mock-treated synaptosomes (average of 6 replicates). Green line: BoNT-treated synaptosomes (average of 6 replicates). Shaded grey area corresponds to the standard deviation at each time point. Due to the presence of an interfering agent in the cell culture supernatants of C. botulinum, the magnitude of the fluorescence is reduced and experiences increased fluctuations. (C) Cytoplasmatic calcium levels in BoNT or untreated synaptosomes. Synaptosomes were pre-incubated with BoNT/A and BoNT/D, BoNT/C1 and BoNT/B or an equal volume of sodium-containing buffer (untreated). Changes in cytoplasmic calcium levels were monitored with Fura2-AM dye using an approach previously introduced elsewhere (118). Fluorescence ratios were calculated by dividing fluorescence signal at 340 nm excitation wavelength by the signal at 380 nm excitation. Fluorescence ratio was normalized by the maximum fluorescence ratio after synaptosomal lysis. The normalized fluorescence ratio before KCl stimulation was subtracted to reveal proportional changes in cytoplasmatic Ca^{2+}-levels.*

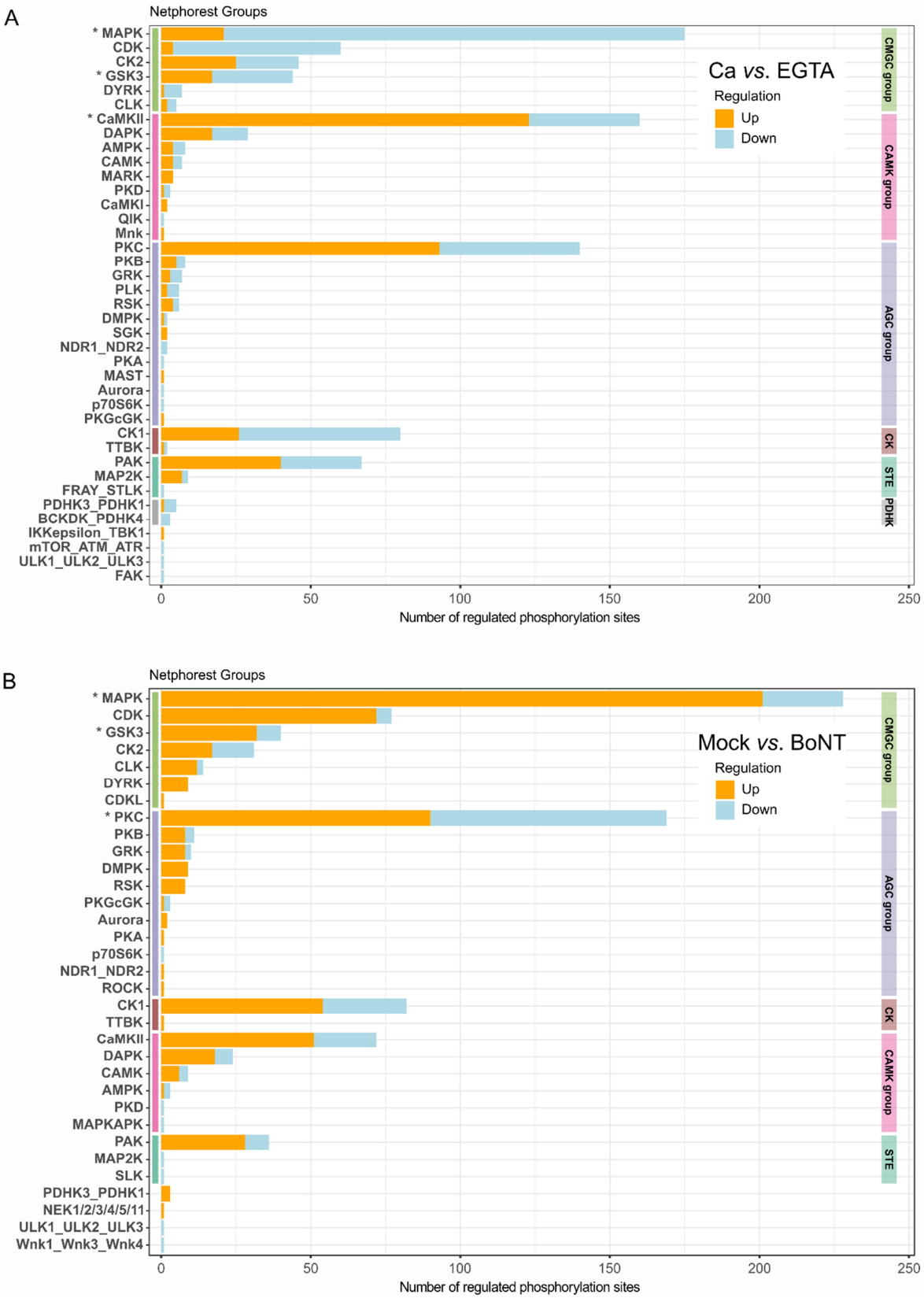

Figure 5.S2: Kinase groups that might be responsible for the observed phosphorylation changes (s. next page for details).

Figure 5.S2: Kinase groups that might be responsible for the observed phosphorylation changes. *(**A, B**) Extended versions of Figure 5.3E and F, respectively. The stacked bar graphs show the total number of significantly regulated phosphorylation events in Ca vs. EGTA (a) or Mock vs. BoNT (b) experiments that can be a result of known (PhosphoSitePlus database (325)) or predicted (NetworKIN (144, 323)) kinase-substrate interactions. Orange bars depict the number of phosphorylation events that show significant intensity increase in Ca^{2+} or Mock-treated synaptosomes versus respective control (EGTA or BoNT). Blue bars correspond to down-regulated sites, respectively. The kinase classification (Netphorest Groups) follows one introduced by Netphorest (144) and uses its second-level group annotation. Colored horizontal bars delineate the highest-level group in the kinase classification. Asterisks mark kinase groups which are predicted to control significantly more phosphorylation sites than expected as based on predicted kinase-substrate interactions in human proteome (Fisher's exact test Benjamini-Hochberg adjusted p-value < 0.01). Abbreviations: AMPK, AMP-activated protein kinase; BCKDK, branched chain ketoacid dehydrogenase kinase; CaMKII calcium-calmodulin kinase 2; CDK, cyclin-dependent kinase; CDKL, cyclin-dependent-like kinase; CK1, casein kinase 1; CK2, casein kinase 2; CLK, SRPK1 and Clk/Sty protein kinase; DAPK, death associated protein kinase; DMPK, DYRK, dual-specificity tyrosine (Y) phosphorylation-regulated kinase; FAK, focal adhesion kinase GRK, G protein coupled receptor kinase; GSK3, glycogen synthase kinase 3; MAPK, mitogen activated protein kinase; MAP2K, mitogen activated protein kinase kinase; MAPKAPK, MAP kinase activated protein kinase; MARK, microtubule associated kinases; Mnk, MAPK-interacting protein kinases; NDR, nuclear dbf2-related kinase; NEK, NIMA (never in mitosis A)-related kinase; PAK, p21 activated kinase; MAST, microtubule-associated serine/threonine-protein kinase; PKA, protein kinase A; PKB, protein kinase B; PKC, protein kinase C; PKD, protein kinase D; PDHK, pyruvate dehydrogenase kinase; PKGcGK, cGMP-dependent protein kinase; QIK, Qin-induced kinase; ROCK, Rho-associated protein kinase; RSK, ribosomal S6 kinase; SGK, serum and glucocorticoid regulated kinase; STLK, STE20-like serine/threonine-protein kinase; TBK, TANK-binding kinase; TTBK, tau-tubulin kinase; ULK, Unc-51 like autophagy activating kinase; Wnk, with-no-lysine (K) kinase.*

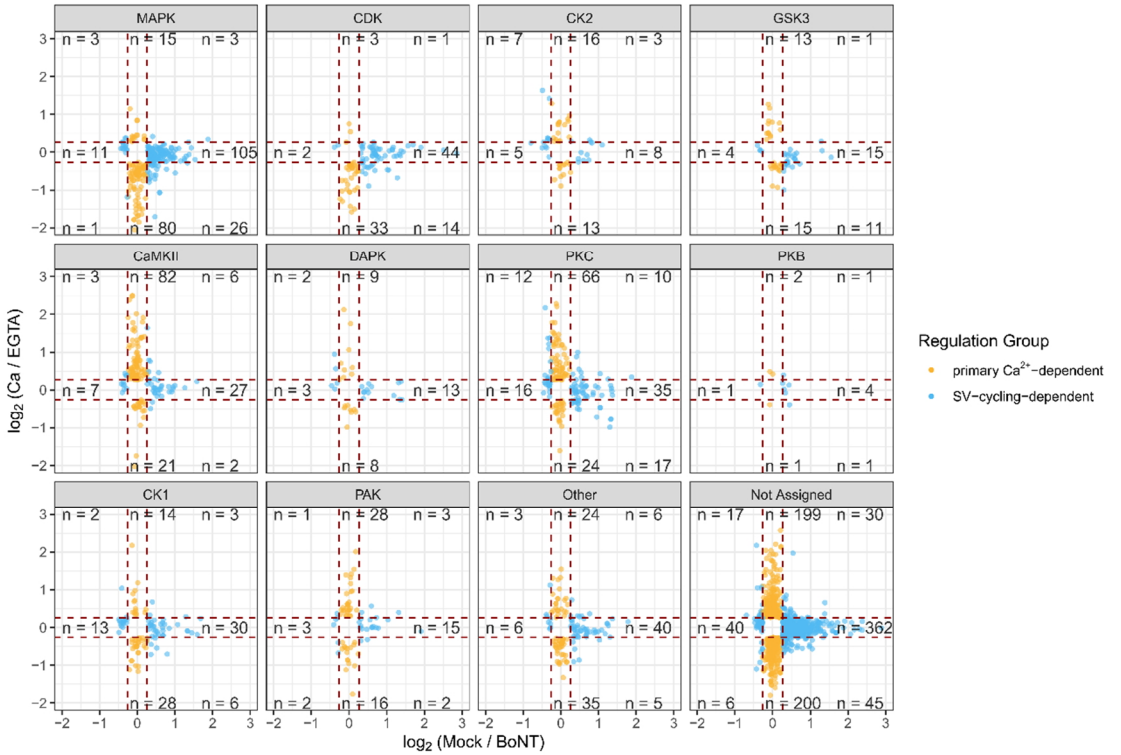

Figure 5.S3: Dependence of phosphorylation sites on calcium influx and SV cycling. *An extended version of Figure 5.4A: categorization of phosphorylation events based on the magnitude of the log2 fold changes in Mock vs. BoNT experiment (x-axis) and log2 fold changes in Ca vs. EGTA experiment (y-axis). Phosphorylation events were further segregated based on the known / predicted kinase class. The kinase classification (Netphorest Groups) follows one introduced by Netphorest (144) and uses its second-level group annotation. "Other" category contains phosphorylation evens attributed to smaller kinase classes. Only events quantified in both experiments are shown, and their q-values satisfy a q-value threshold of < 0.01. The events are classified into two regulation groups: (i) "primary Ca^{2+}-dependent" (sites with no significant or not-quantified SV cycling effect, i.e., absolute log2 (Mock/BoNT) < 0.263 and absolute log2 (Ca/EGTA) > 0.263), shown as orange dots; and (ii) "SV-cycling-dependent" (absolute log2 (Mock/BoNT) > 0.263).*

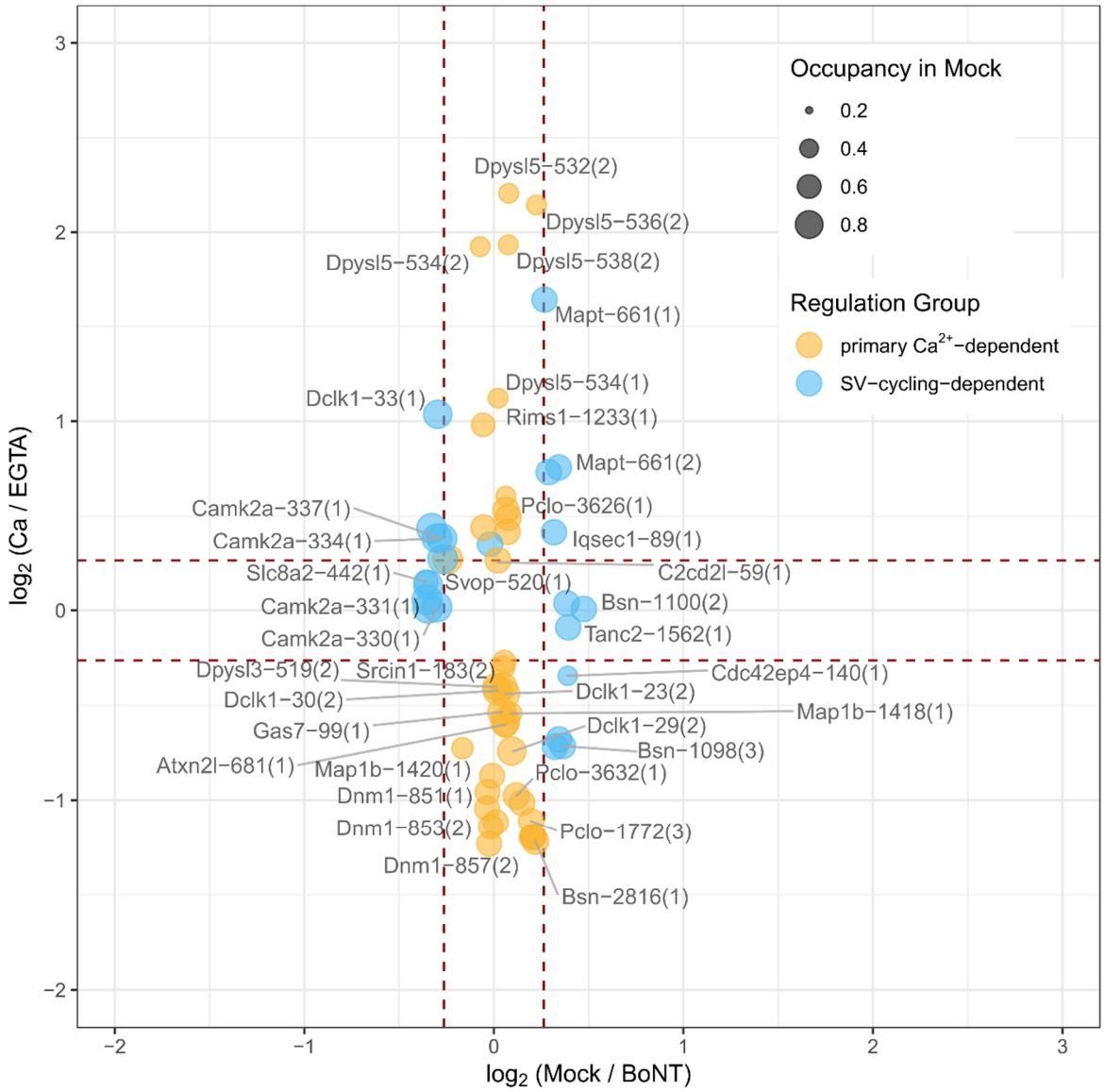

Figure 5.S4: Site occupancy assessment. *Site occupancies were calculated using the 3D linear model as suggested by Hogrebe et al (300) and are based on the observed intensity changes in phosphorylated peptide/non-phosphorylated peptide pairs and total protein intensity in Mock/BoNT experiments. Only occupancy estimations with a p value below 0.1 were considered.*

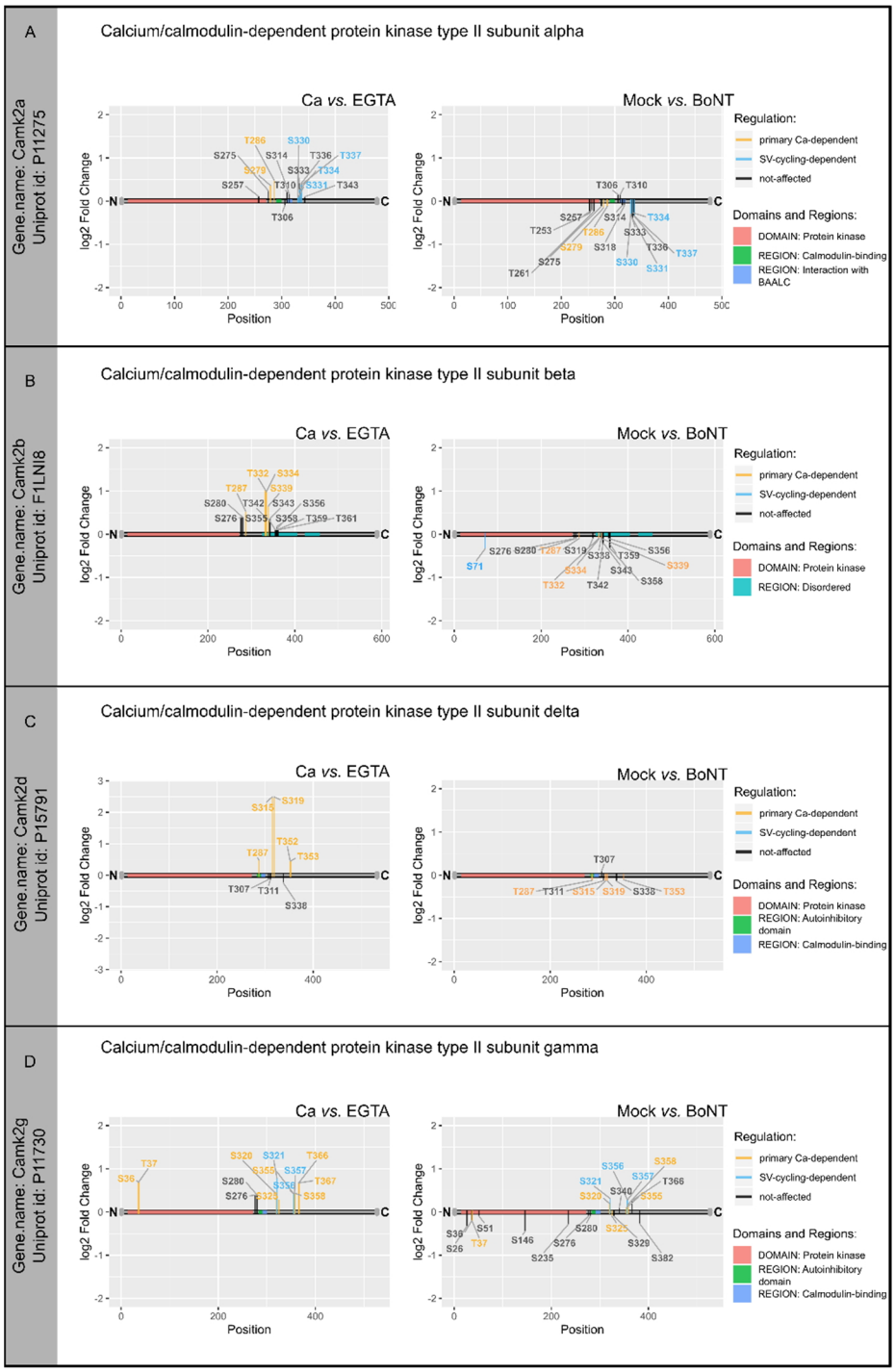

Figure 5.S5: Changes in phosphorylation site intensities for Calcium/calmodulin-dependent kinase 2 alpha, beta, gamma, and delta. *X-axis shows positions of modified amino acids. A grey horizontal bar represents a protein sequence with its N- and C termini denoted as "N" and "C". Colored segments mark positions of domains and regions on protein sequence as annotated in Uniprot (366). Changes in phosphorylation site intensities are expressed as log_2 fold changes (y-axis). Non-significant changes in phosphorylation site intensities are colored black. Significant changes are shown in orange or blue, depending on the classification of the site as "primarily Ca-dependent", or "SV-cycling-dependent", respectively. If a phosphorylation site was quantified on peptides that were singly, doubly or multiply phosphorylated (also known as "multiplicity"), the multiplicity with the highest magnitude of log2 fold change is depicted. Proteins are grouped by the gene name and Uniprot identifier.*

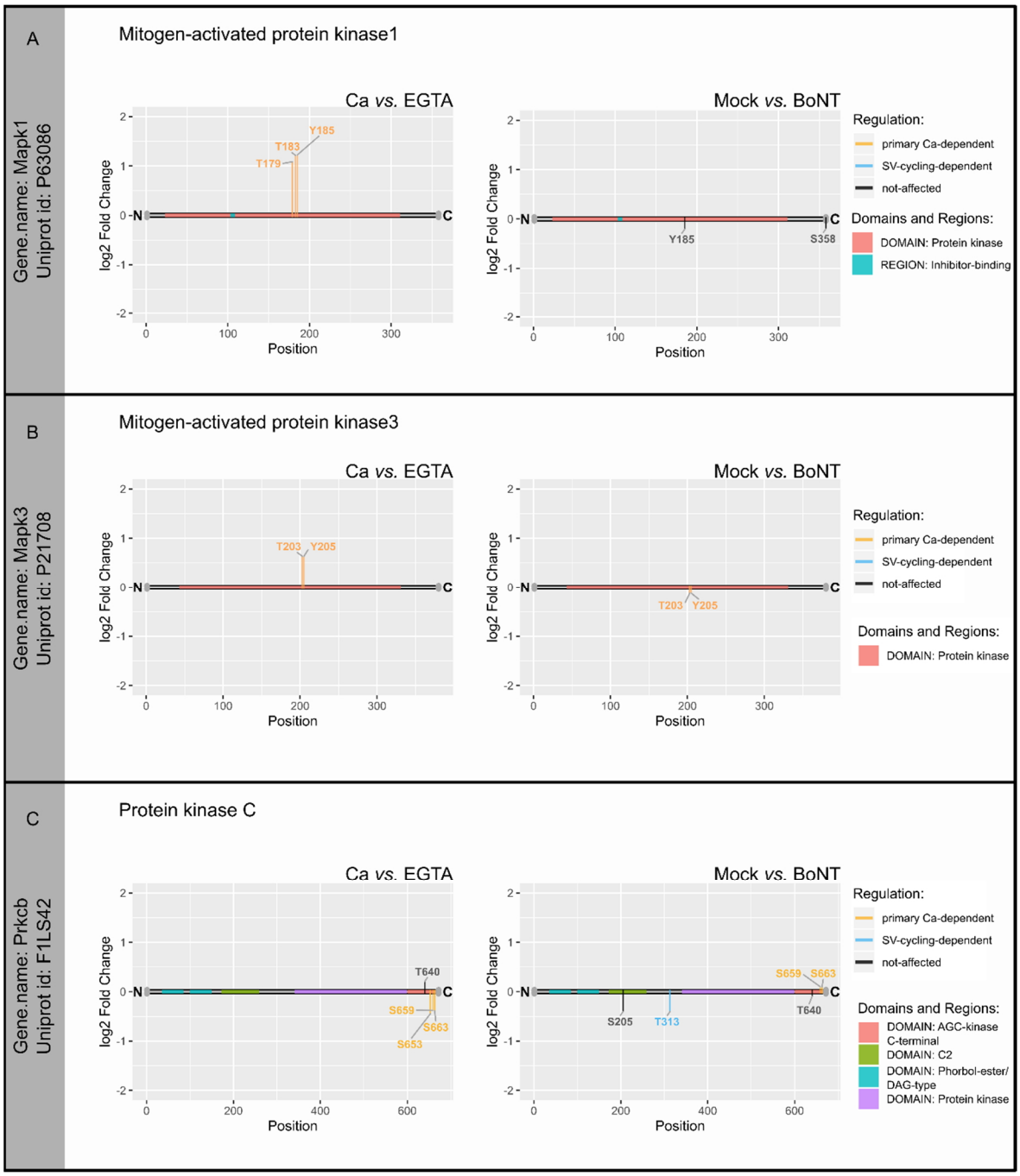

Figure 5.S6: Changes in phosphorylation site intensities for Mitogen-activated protein kinase 1, 3, and Protein kinase C beta. *X-axis shows positions of modified amino acids. A grey horizontal bar represents a protein sequence with its N- and C termini denoted as "N" and "C". Colored segments mark positions of domains and regions on protein sequence as annotated in Uniprot (366). Changes in phosphorylation site intensities are expressed as log2 fold changes (y-axis). Non-significant changes in phosphorylation site intensities are colored black. Significant changes are shown in orange or blue, depending on the classification of the site as "primarily Ca-dependent", or "SV-cycling-dependent", respectively. If a phosphorylation site was quantified on peptides that were singly, doubly or multiply phosphorylated (also known as "multiplicity"), the multiplicity with the highest magnitude of log2 fold change is depicted. Proteins are grouped by the gene name and Uniprot identifier.*

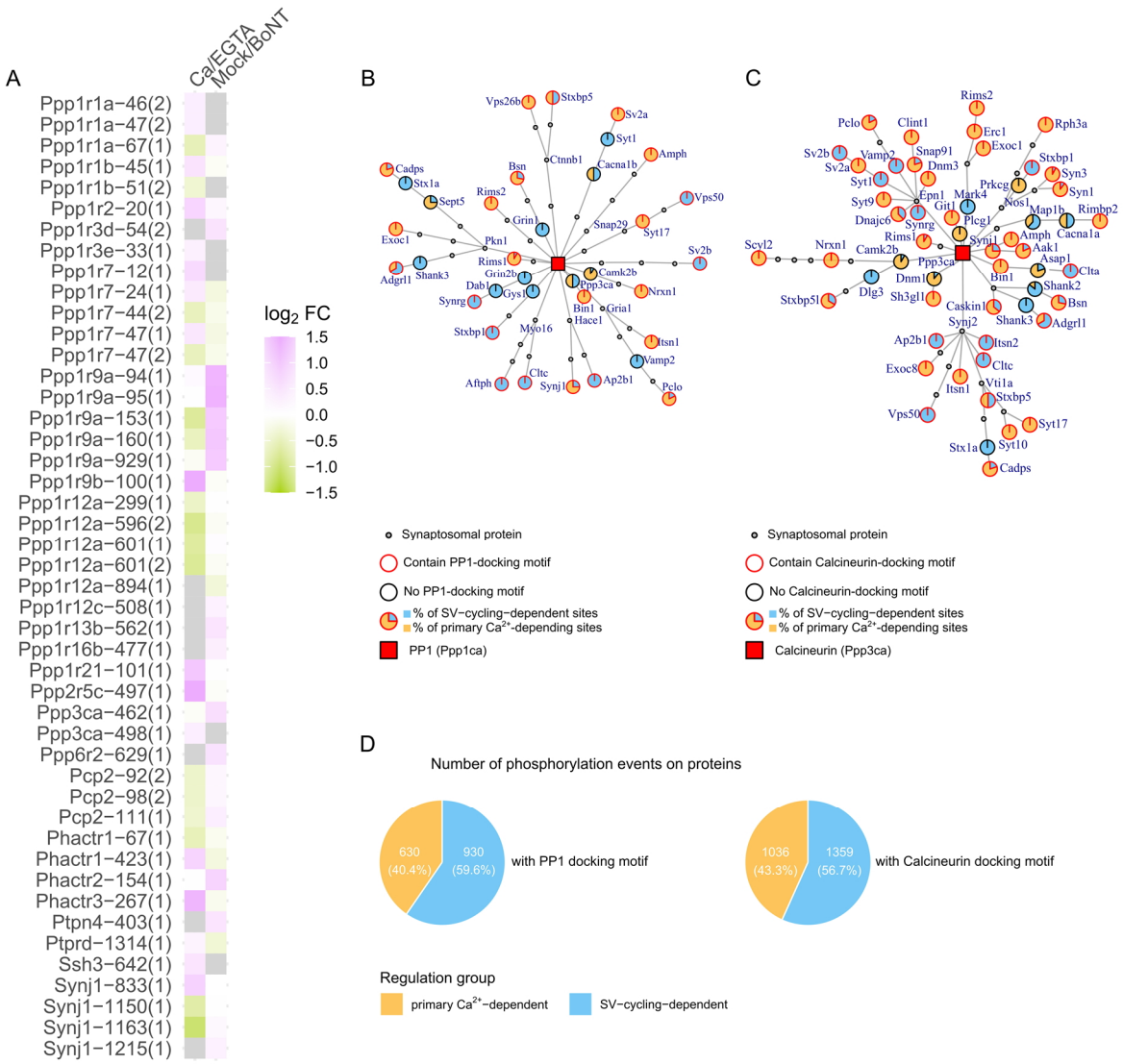

Figure 5.S7: Phosphatases and their putative substrates. (A) *Significantly regulated phosphorylation events on phosphatases and phosphatase-related proteins in Ca/EGTA or Mock/BoNT experiment. Phosphorylation events are designated as gene name followed by the amino acid position and phosphorylation multiplicity (in brackets).* ***(B and C)****. Protein-Protein Interaction map between phosphatase (PP1 in B and Calcineurin in C) and selected phosphoproteins involved in endo/exocytosis and containing PP1 (B) or Calcineurin (C) docking motif (shown as blue/orange-colored circles with red edges). Docking motifs described in (371) were used for the analysis. Phosphoproteins that did not contain docking motifs are shown as blue/orange-colored circles with black edges. The blue/orange area within a circle correspond to a percentage of sites classified as "primary Ca^{2+}-dependent" (orange) or "SV-cycling-dependent" (blue). Synaptosomal proteins not containing significantly regulated phosphorylation sites are shown as small grey circles. Phosphatases (PP1 or Calcineurin) are represented by red squares. Protein-protein interactions were extracted from String database (322) and included interactions between synaptosomal proteins which are experimentally supported or annotated in manually curated databases.* ***(D)*** *Number of "primary Ca^{2+}-dependent" (orange) and "SV-cycling-dependent" (blue) phosphorylation events on proteins containing a PP1 (E) or Calcineurin (F) docking motif (371).*

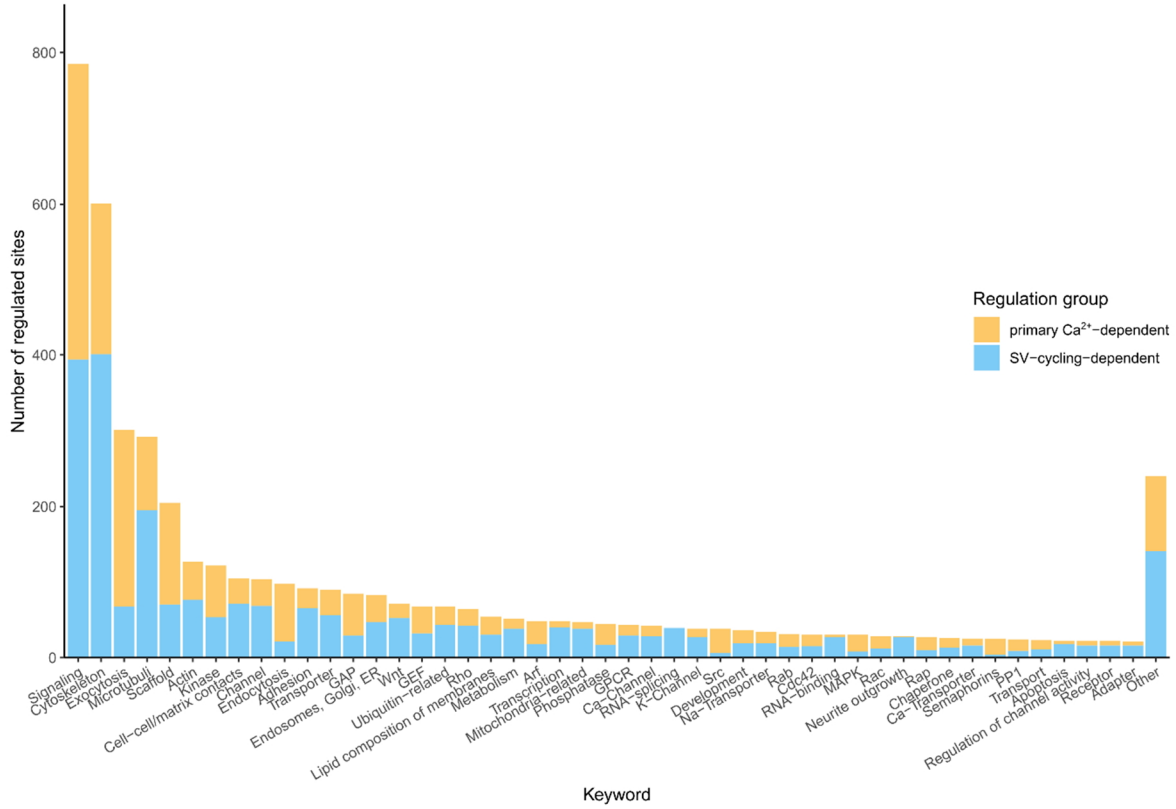

Figure 5.S8: Manual annotation of proteins carrying regulated phosphorylation sites. *Key-words were assigned to proteins carrying regulated phosphorylation sites that specify a function / localization the protein might be related to. One protein can have one or more terms assigned. Number of significantly regulated phosphorylation sites for each term is shown as stacked bars with colors representing regulation group of the phosphorylation sites. Arf stays for ADP-ribosylation factor small GTPase; ER ~ endoplasmatic reticulum; GAP ~ GTPase activating protein; GEF ~ GTP exchanging factor; GPCR ~ G-protein coupled receptor; PP1 ~ protein phosphatase-1*

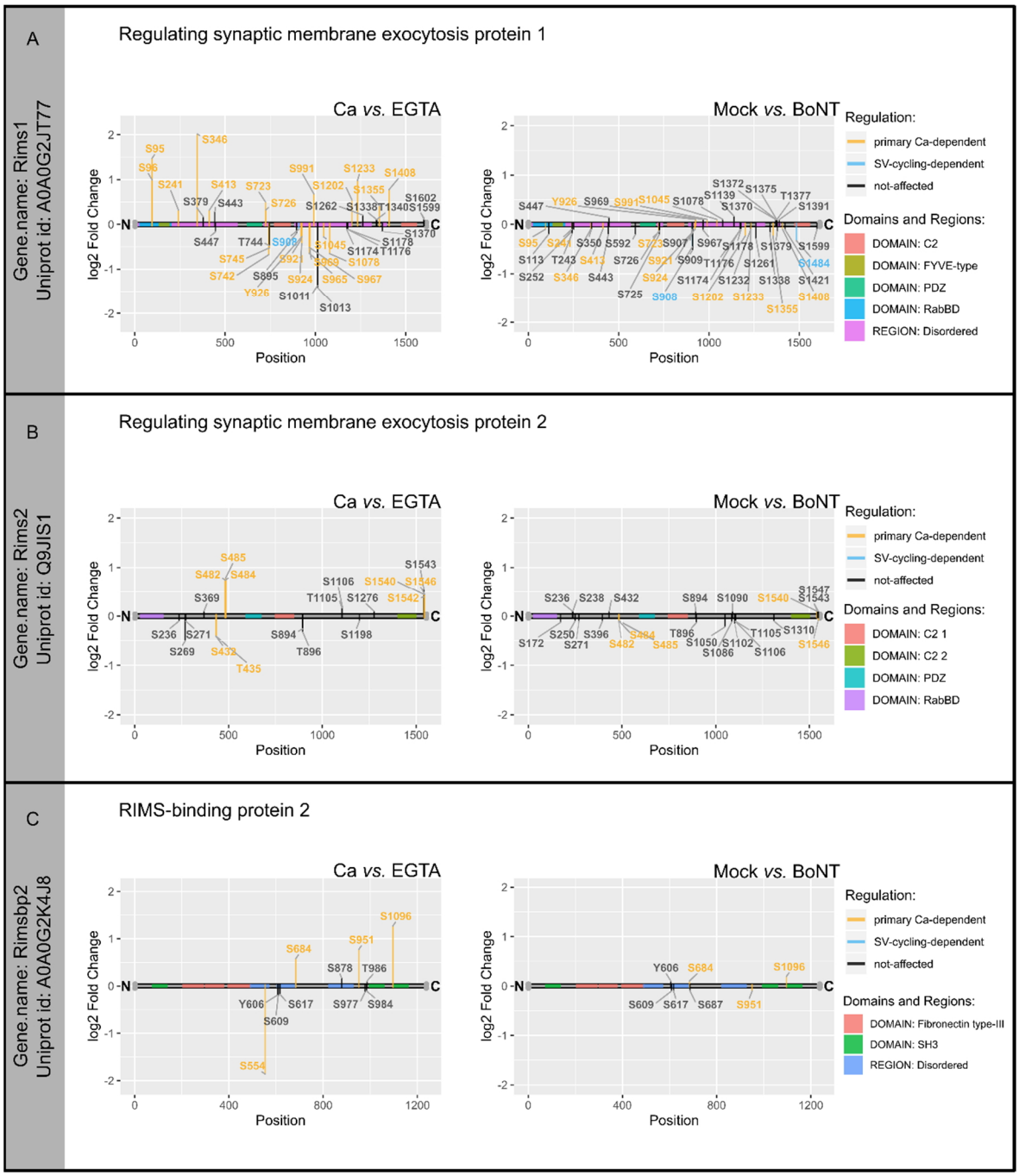

Figure 5.S9: Changes in phosphorylation site intensities for Regulating synaptic membrane exocytosis (RIM) protein 1, 2, and RIM-binding protein 2. X-axis shows positions of modified amino acids. *A grey horizontal bar represents a protein sequence with its N- and C termini denoted as "N" and "C". Colored segments mark positions of domains and regions on protein sequence as annotated in Uniprot (366). Changes in phosphorylation site intensities are expressed as log_2 fold changes (y-axis). Non-significant changes in phosphorylation site intensities are colored black. Significant changes are shown in orange or blue, depending on the classification of the site as "primarily Ca-dependent", or "SV-cycling-dependent", respectively. If a phosphorylation site was quantified on peptides that were singly, doubly or multiply phosphorylated (also known as "multiplicity"), the multiplicity with the highest magnitude of log2 fold change is depicted. Proteins are grouped by the gene name and Uniprot identifier.*

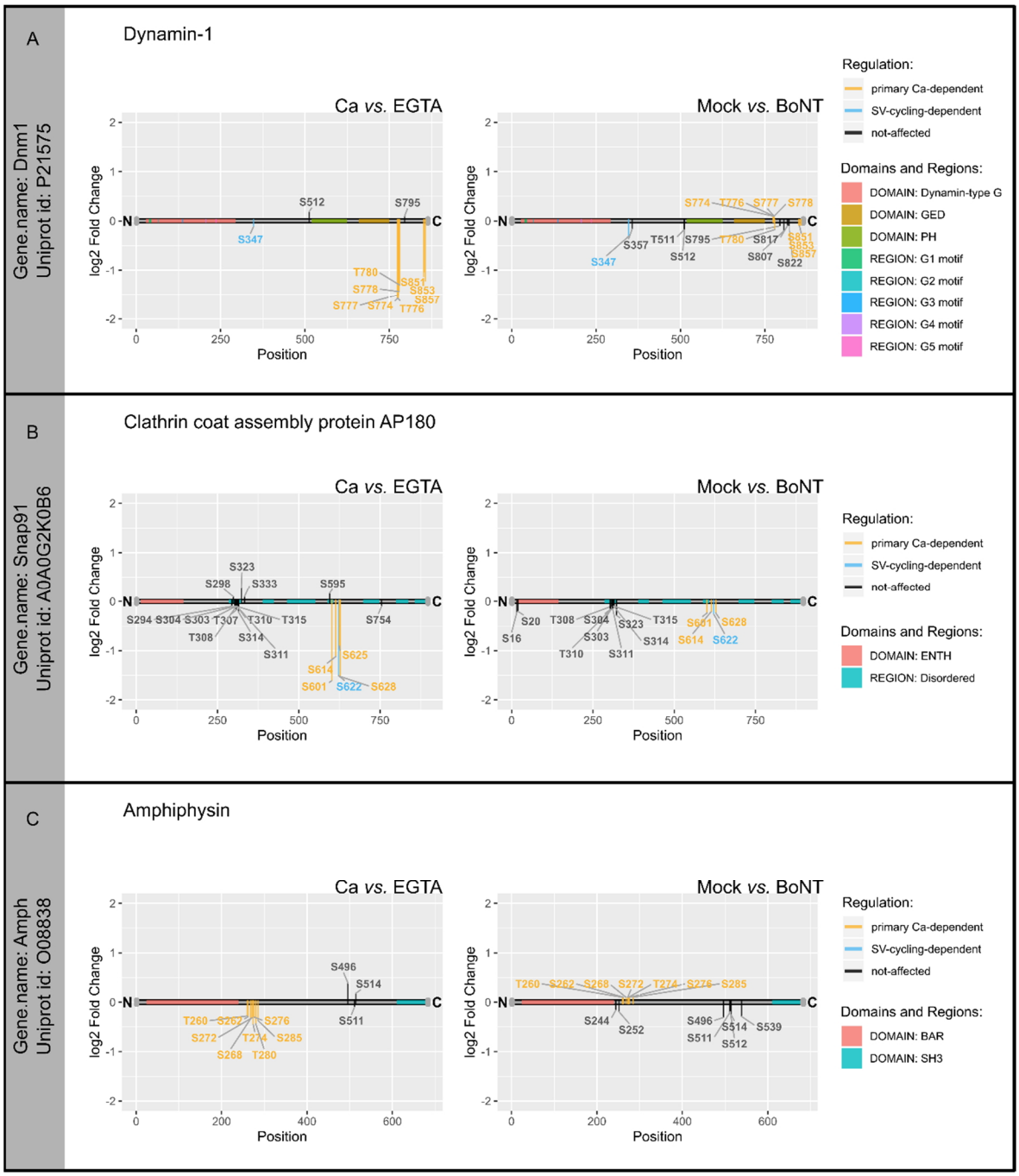

Figure 5.S10: Changes in phosphorylation site intensities for Dynamin-1, Clathrin coat assembly protein AP180, and Amphiphysin. *X-axis shows positions of modified amino acids. A grey horizontal bar represents a protein sequence with its N- and C termini denoted as "N" and "C". Colored segments mark positions of domains and regions on protein sequence as annotated in Uniprot (366). Changes in phosphorylation site intensities are expressed as log_2 fold changes (y-axis). Non-significant changes in phosphorylation site intensities are colored black. Significant changes are shown in orange or blue, depending on the classification of the site as "primarily Ca-dependent", or "SV-cycling-dependent", respectively. If a phosphorylation site was quantified on peptides that were singly, doubly or multiply phosphorylated (also known as "multiplicity"), the multiplicity with the highest magnitude of log2 fold change is depicted. Proteins are grouped by the gene name and Uniprot identifier.*

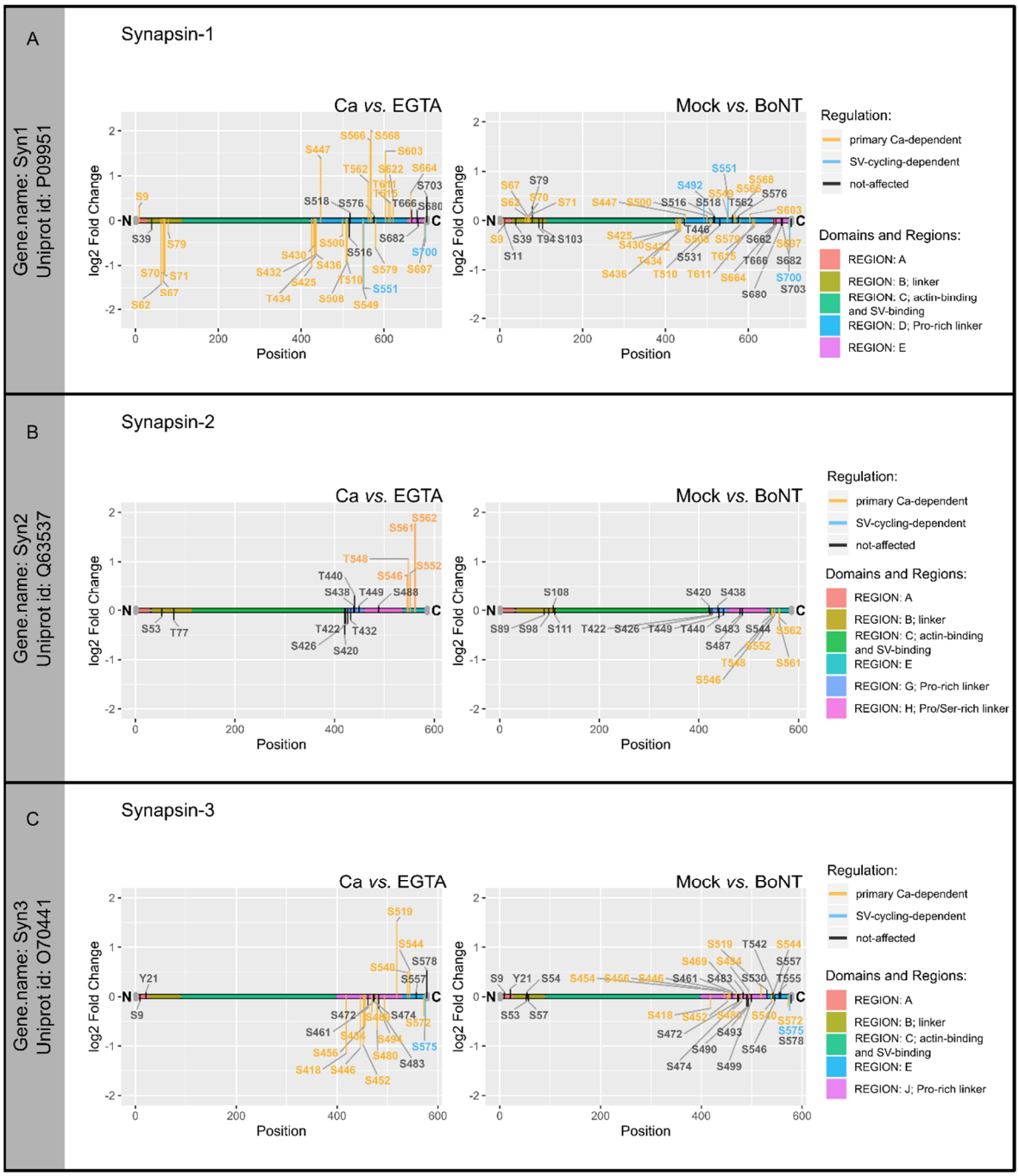

Figure 5.S11: Changes in phosphorylation site intensities for Synapsin-1, 2, and 3. X-axis shows positions of modified amino acids. *A grey horizontal bar represents a protein sequence with its N- and C termini denoted as "N" and "C". Colored segments mark positions of domains and regions on protein sequence as annotated in Uniprot (366). Changes in phosphorylation site intensities are expressed as log_2 fold changes (y-axis). Non-significant changes in phosphorylation site intensities are colored black. Significant changes are shown in orange or blue, depending on the classification of the site as "primarily Ca-dependent", or "SV-cycling-dependent", respectively. If a phosphorylation site was quantified on peptides that were singly, doubly or multiply phosphorylated (also known as "multiplicity"), the multiplicity with the highest magnitude of log_2 fold change is depicted. Proteins are grouped by the gene name and Uniprot identifier.*

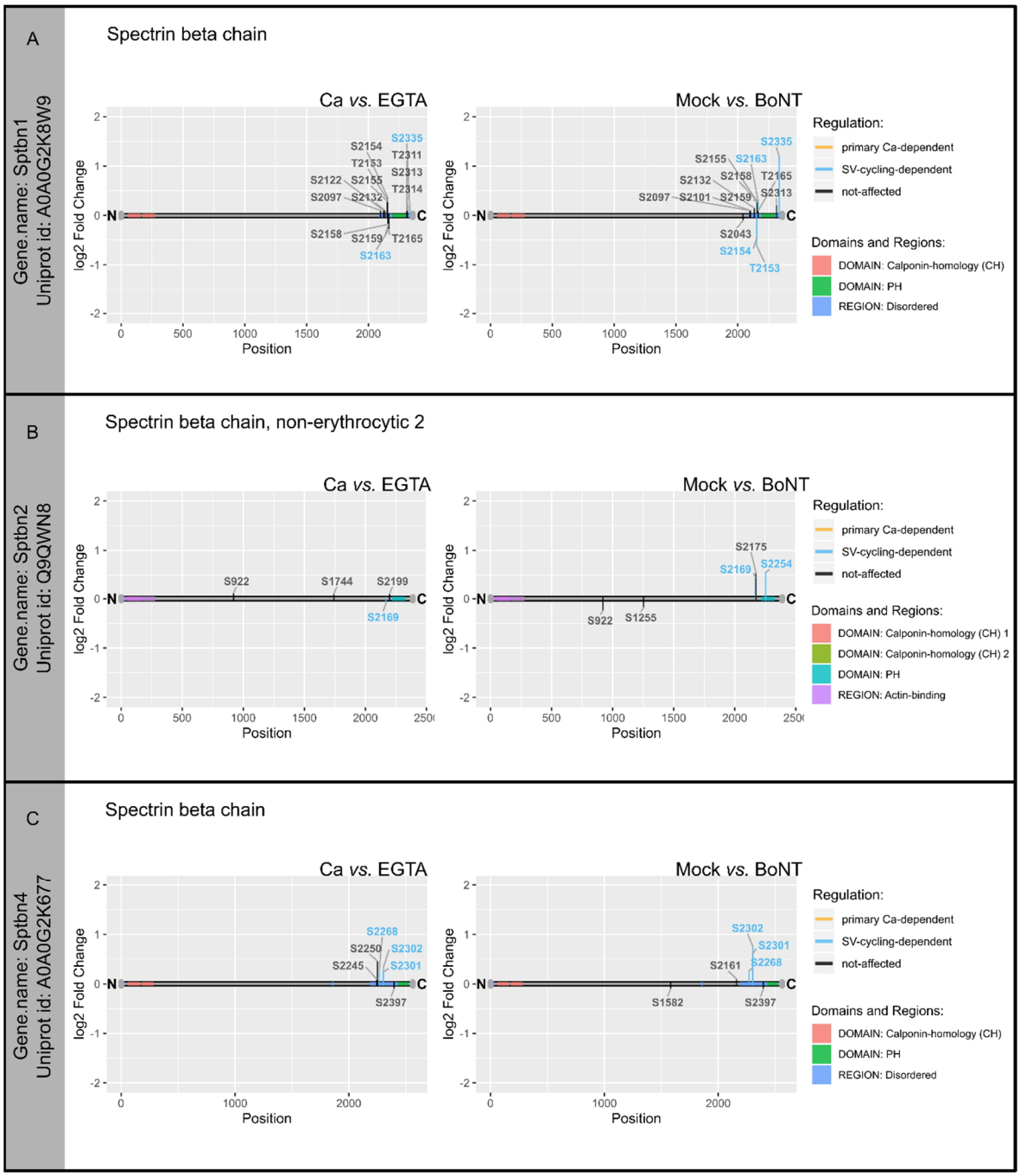

Figure 5.S12: Changes in phosphorylation site intensities for Spectrin beta chain. X-axis shows positions of modified amino acids. *A grey horizontal bar represents a protein sequence with its N- and C termini denoted as "N" and "C". Colored segments mark positions of domains and regions on protein sequence as annotated in Uniprot (366). Changes in phosphorylation site intensities are expressed as log_2 fold changes (y-axis). Non-significant changes in phosphorylation site intensities are colored black. Significant changes are shown in orange or blue, depending on the classification of the site as "primarily Ca-dependent", or "SV-cycling-dependent", respectively. If a phosphorylation site was quantified on peptides that were singly, doubly or multiply phosphorylated (also known as "multiplicity"), the multiplicity with the highest magnitude of log_2 fold change is depicted. Proteins are grouped by the gene name and Uniprot identifier.*

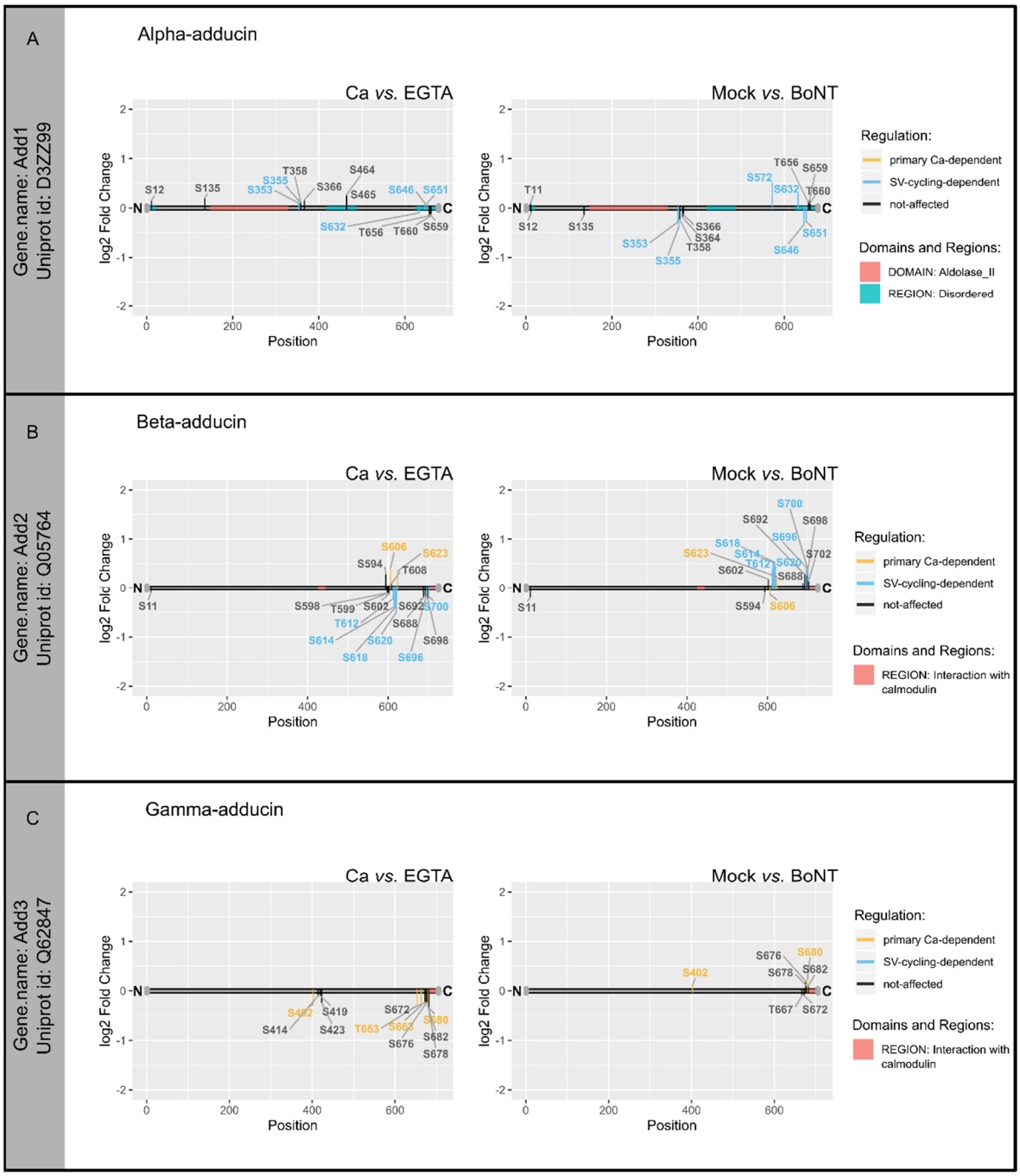

Figure 5.S13: Changes in phosphorylation site intensities for Adducin alpha, beta, and gamma. X-axis shows positions of modified amino acids. *A grey horizontal bar represents a protein sequence with its N- and C termini denoted as "N" and "C". Colored segments mark positions of domains and regions on protein sequence as annotated in Uniprot (366). Changes in phosphorylation site intensities are expressed as log_2 fold changes (y-axis). Non-significant changes in phosphorylation site intensities are colored black. Significant changes are shown in orange or blue, depending on the classification of the site as "primarily Ca-dependent", or "SV-cycling-dependent", respectively. If a phosphorylation site was quantified on peptides that were singly, doubly or multiply phosphorylated (also known as "multiplicity"), the multiplicity with the highest magnitude of log_2 fold change is depicted. Proteins are grouped by the gene name and Uniprot identifier.*

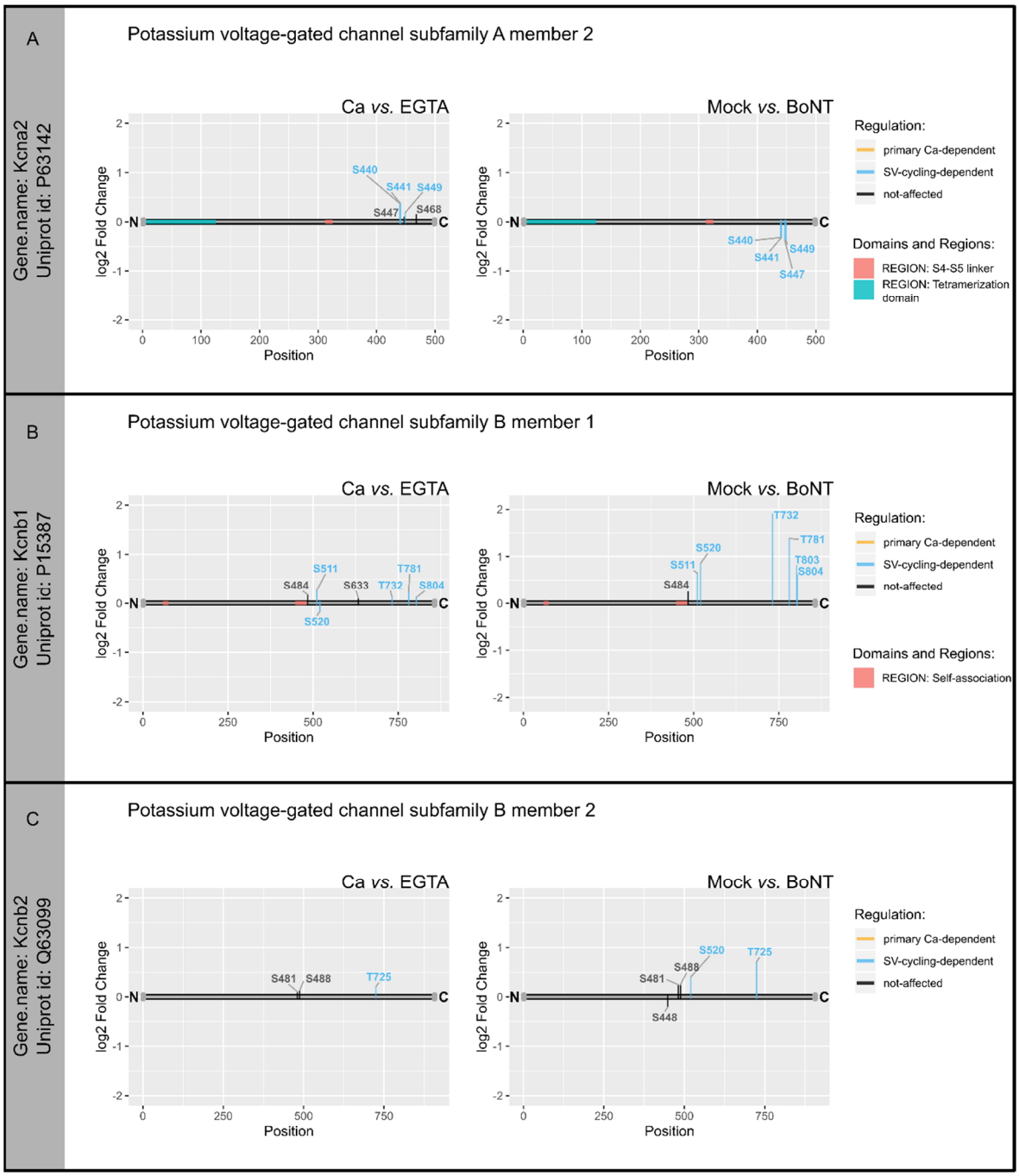

Figure 5.S14: Changes in phosphorylation site intensities for Potassium voltage-gated channel subfamily A member 2, and subfamily B member 1 and 2. *X-axis shows positions of modified amino acids. A grey horizontal bar represents a protein sequence with its N- and C termini denoted as "N" and "C". Colored segments mark positions of domains and regions on protein sequence as annotated in Uniprot (366). Changes in phosphorylation site intensities are expressed as log_2 fold changes (y-axis). Non-significant changes in phosphorylation site intensities are colored black. Significant changes are shown in orange or blue, depending on the classification of the site as "primarily Ca-dependent", or "SV-cycling-dependent", respectively. If a phosphorylation site was quantified on peptides that were singly, doubly or multiply phosphorylated (also known as "multiplicity"), the multiplicity with the highest magnitude of log_2 fold change is depicted. Proteins are grouped by the gene name and Uniprot identifier.*

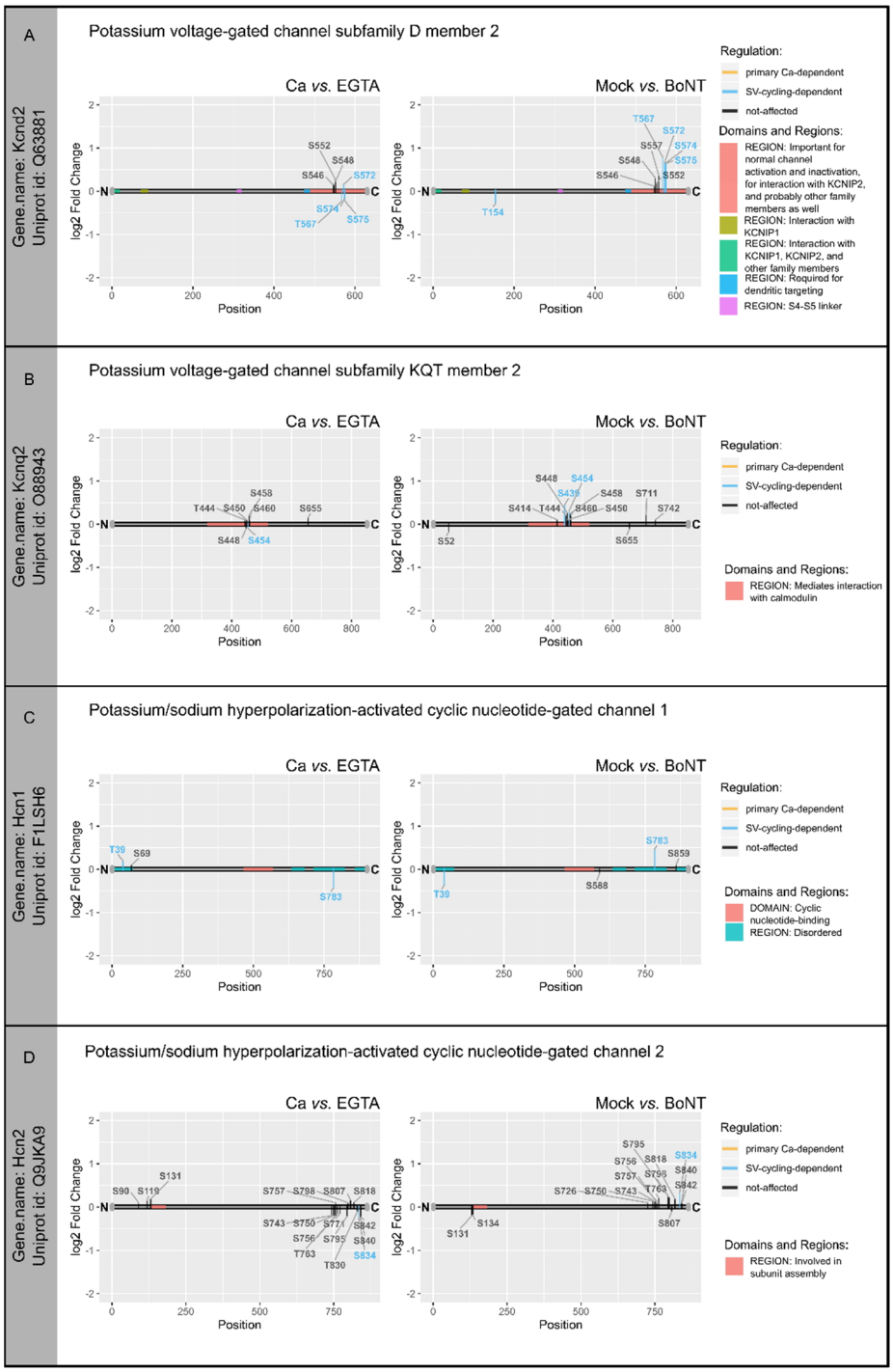

Figure 5.S15: Changes in phosphorylation site intensities for Potassium voltage-gated channel subfamily D member 2, subfamily KQT member 2, Potassium/sodium hyperpolarization-activated cyclic nucleotide-gated channel 1 and 2. *X-axis shows positions of modified amino acids. A grey horizontal bar represents a protein sequence with its N- and C termini denoted as "N" and "C". Colored segments mark positions of domains and regions on protein sequence as annotated in Uniprot (366). Changes in phosphorylation site intensities are expressed as log_2 fold changes (y-axis). Non-significant changes in phosphorylation site intensities are colored black. Significant changes are shown in orange or blue, depending on the classification of the site as "primarily Ca-dependent", or "SV-cycling-dependent", respectively. If a phosphorylation site was quantified on peptides that were singly, doubly or multiply phosphorylated (also known*

as “multiplicity”), the multiplicity with the highest magnitude of log_2 fold change is depicted. Proteins are grouped by the gene name and Uniprot identifier.

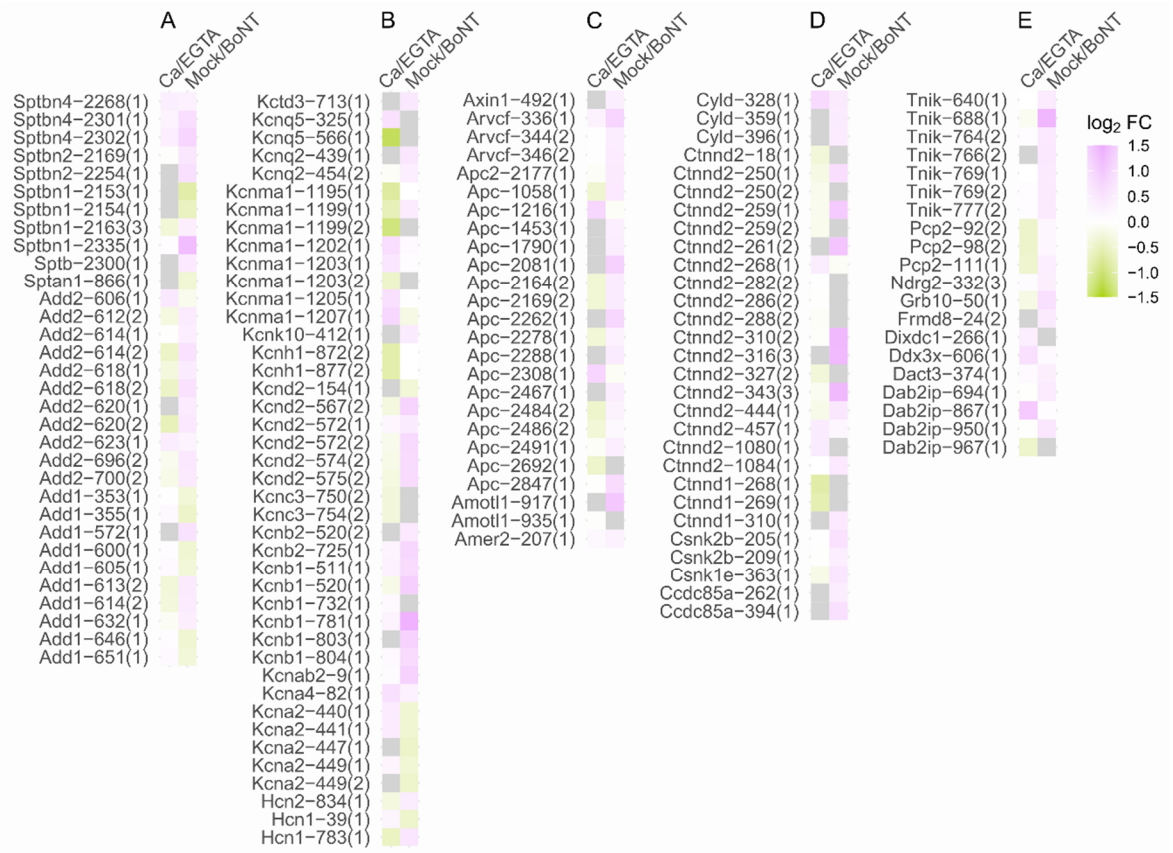

Figure 5.S16: Regulated phosphorylation sites on selected proteins. *(**A**) Regulated sites on cytoskeleton-related proteins spectrin and adducing. (**B**) Regulated sites on potassium-channel proteins. (**C-E**). Regulated sites on Wnt-pathway-related proteins. Phosphorylation events are designated as gene name followed by the amino acid position and phosphorylation multiplicity (in brackets).*

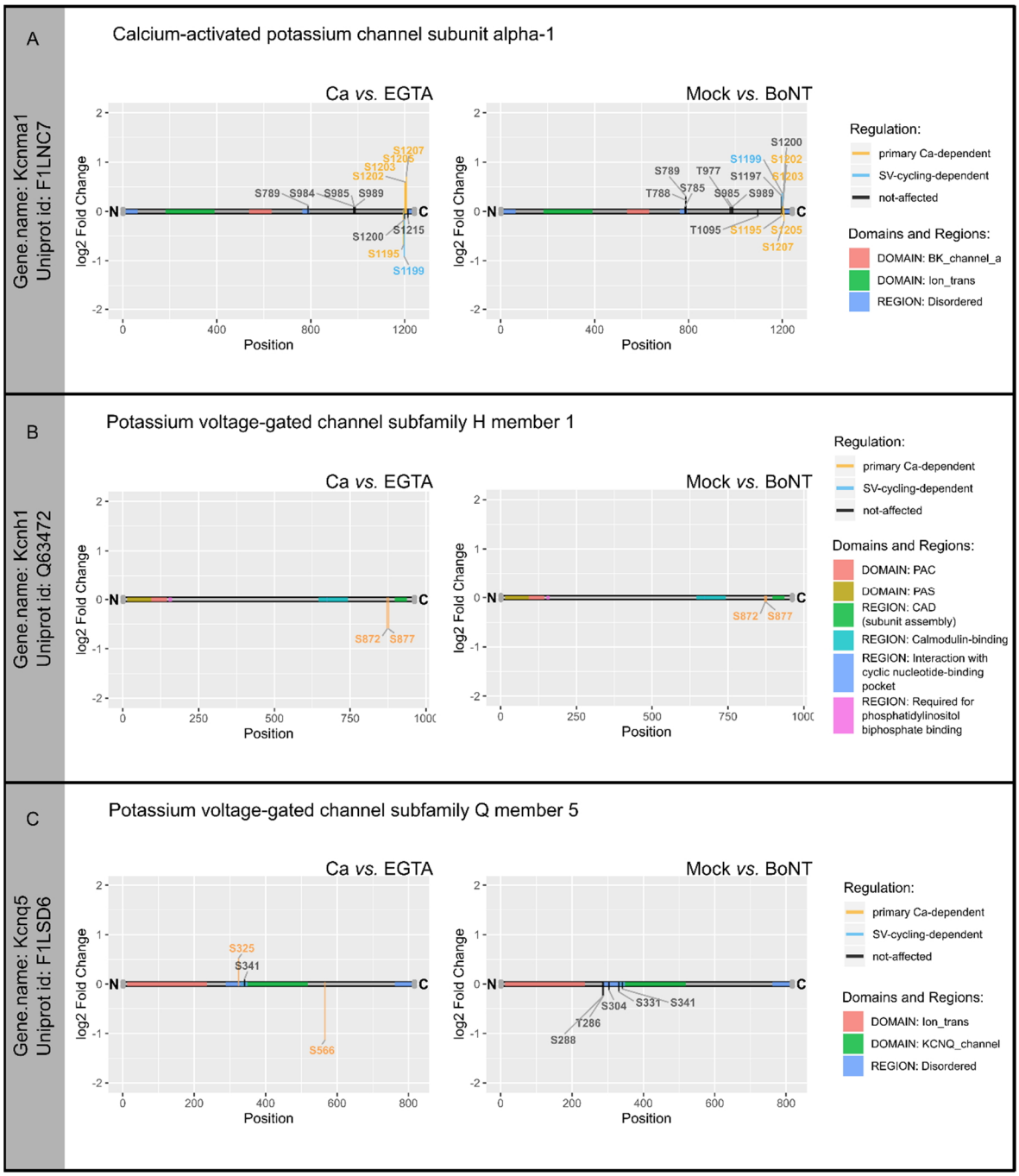

Figure 5.S17: Changes in phosphorylation site intensities for Calcium-activated potassium channel subunit alpha-1, Potassium voltage-gated channel subfamily H member 1, and Potassium voltage-gated channel subfamily Q member 5. *X-axis shows positions of modified amino acids. A grey horizontal bar represents a protein sequence with its N- and C termini denoted as "N" and "C". Colored segments mark positions of domains and regions on protein sequence as annotated in Uniprot (366). Changes in phosphorylation site intensities are expressed as log_2 fold changes (y-axis). Non-significant changes in phosphorylation site intensities are colored black. Significant changes are shown in orange or blue, depending on the classification of the site as "primarily Ca-dependent", or "SV-cycling-dependent", respectively. If a phosphorylation site was quantified on peptides that were singly, doubly or multiply phosphorylated (also known as "multiplicity"), the multiplicity with the highest magnitude of log_2 fold change is depicted. Proteins are grouped by the gene name and Uniprot identifier.*

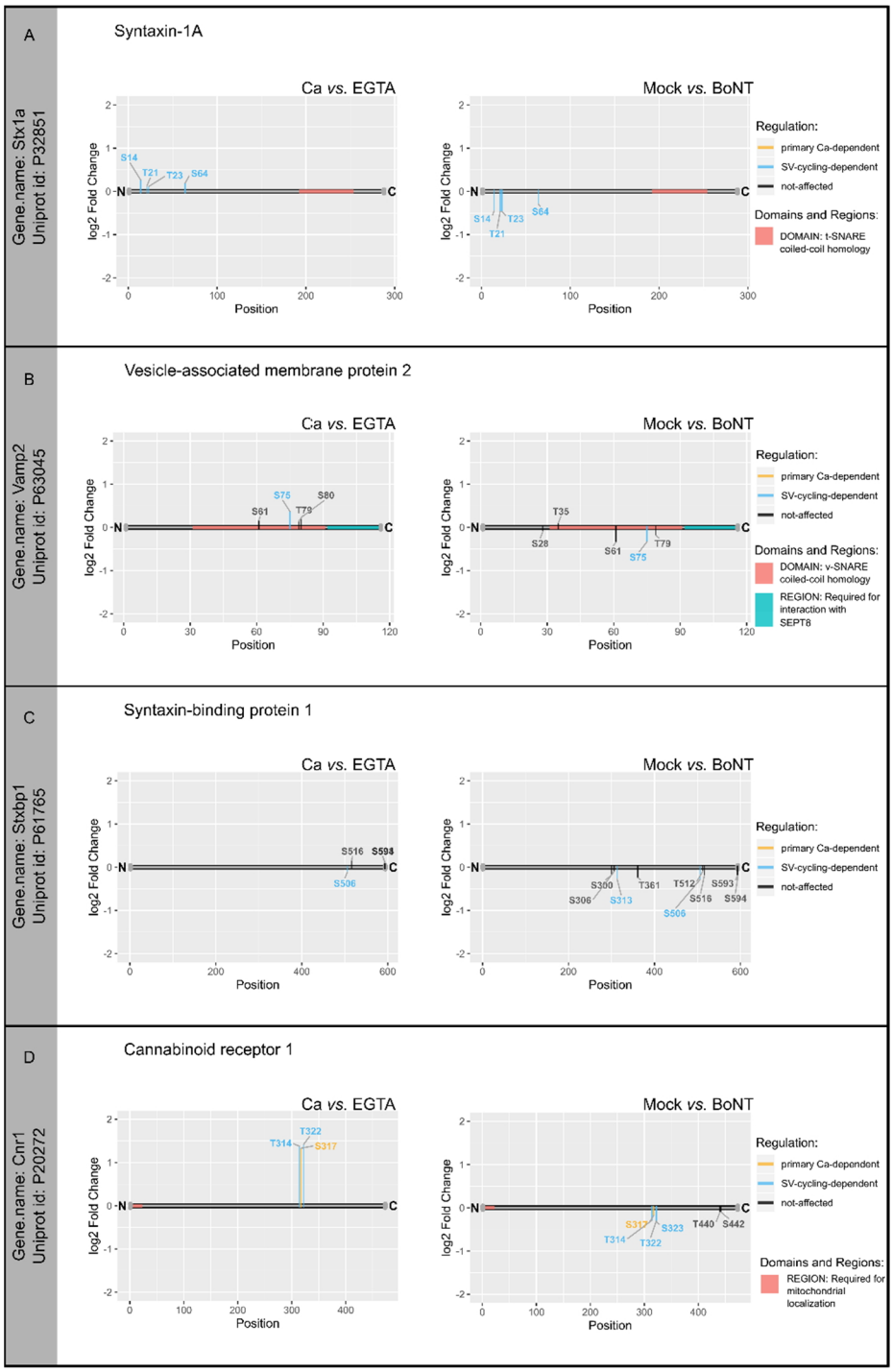

Figure 5.S18: Changes in phosphorylation site intensities for Syntaxin-1A, Vesicle-associated membrane protein 2, Syntaxin-binding protein 1, and Cannabinoid receptor 1. *X-axis shows positions of modified amino acids. A grey horizontal bar represents a protein sequence with its N- and C termini denoted as "N" and "C". Colored segments mark positions of domains and regions on protein sequence as annotated in Uniprot (366). Changes in phosphorylation site intensities are expressed as log_2 fold changes (y-axis). Non-significant changes in phosphorylation site intensities are colored black. Significant changes are shown in orange or blue, depending on the classification of the site as "primarily Ca-dependent", or "SV-cycling-dependent", respectively. If a phosphorylation site was quantified on peptides that were singly, doubly or multiply phosphorylated (also known as "multiplicity"), the multiplicity with the highest magnitude of log_2 fold change is depicted. Proteins are grouped by the gene name and Uniprot identifier.*

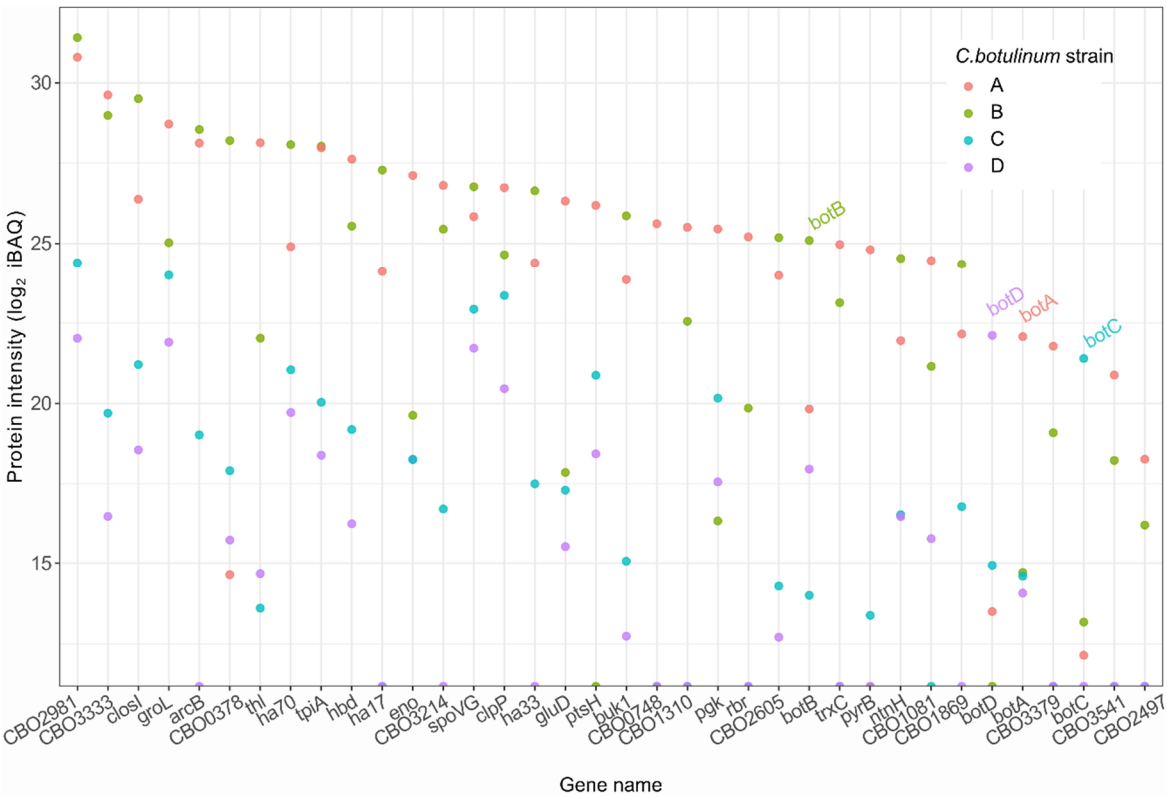

Figure 5.S19: Proteomic profiling of C. botulinum cell culture supernatants. *Protein content in C. botulinum cell culture supernatants was assessed using iBAQ values (406). Top 30 most intense proteins, botulinum toxins (botA, botB, botC, botD), as well as putative protease (CBO3541) and putative phosphatases (CBO3379, CBO2497) that were identified in the cell culture supernatants are ranked based on iBAQ intensity. Colors encode C.botulinum strains: A, red; B, green; C, blue; D, violet.*

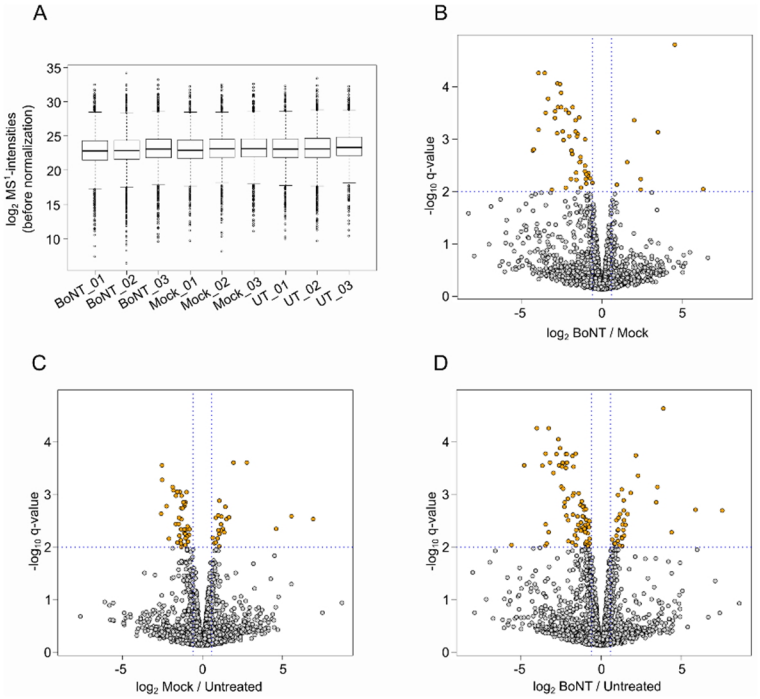

Figure 5.S20: Phosphoproteome analysis of BoNT-treated HeLa nuclear extract. *Unspecific activity of C. botulinum cell culture supernatants was tested in nuclear extract of HeLa cells. Nuclear extract was treated for 1.5 h with a combination of the four C. botulinum cell culture supernatants, BoNT A-D (BoNT); heat-inactivated BoNT A-D (Mock), or buffer (Untreated, UT). Afterwards, proteins were digested with trypsin and phosphorylated peptides were enriched using TiO2-beads. Precursor intensities in MS1 scans were used to assess intensities of phosphorylated sites. (A) Box-whisker plot of log_2 phosphorylation site intensities before normalization. Boxes indicate 25% and 75% quantiles (interquartile range, IQR), vertical lines indicate medians, and whiskers indicate data within 1.5 × IQR. (B-D) Differences in phosphorylation site intensities were assessed using limma package (311). Volcano plots of $–log_{10}$ q-values vs. log_2 fold change: BoNT vs. Mock (b), Mock vs. Untreated (c), BoNT vs. Untreated (d). Orange dots represent phosphorylation events with a q-value of < 0.01 and an absolute log_2 FC of at least 0.586.*

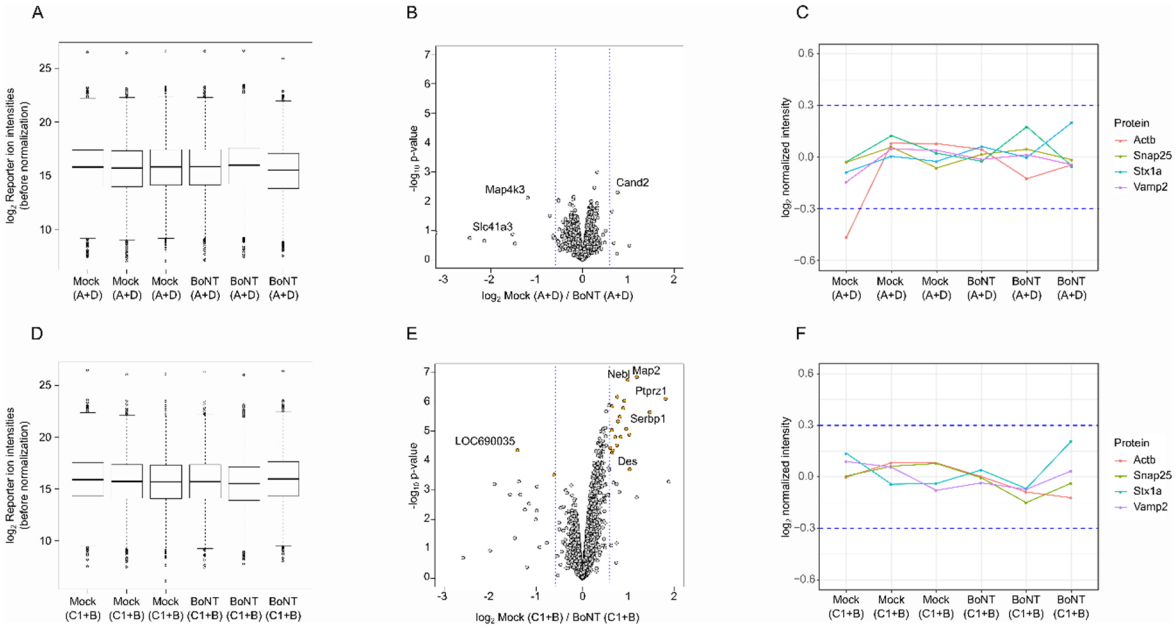

Figure 5.S21: Proteomics analysis of Mock- or BoNT-treated synaptosomes. *Protein content in Mock- or BoNT-treated synaptosomes was assessed using TMT6-labeled peptides in the unbound fraction (not-phosphorylated peptides) after phosphopeptide enrichment. Following C. botulinum cell culture supernatants were used: (**A-C**) C. botulinum A+D, (**D-E**) C. botulinum C1+B. (**A, D**) Box-whisker plot of log_2 reporter ion intensities before normalization. Boxes indicate 25% and 75% quantiles (interquartile range, IQR), vertical lines indicate medians, and whiskers indicate data within 1.5 × IQR. (**B, E**) Differential protein content was assessed using limma package (311). Volcano plots of –log10 p-values vs. log_2 Mock/BoNT. Orange dots: proteins with a Benjamini-Hochberg adjusted p-value of < 0.01 and an absolute log_2FC of at least 0.586. (**C, E**) log_2 normalized reporter ion intensities of selected proteins, actin-beta (Actb), Snap25, syntaxin-1a (Stx1a), Vamp2.*

5.13.4 Supplementary Tables

Table 5.S1: Number of regulated phosphorylation events per predicted kinase group in Ca vs. EGTA experiment. *"Sites in" show number of phosphorylation events that can be regulated by a respective kinase group as determined in the Ca vs. EGTA experiment. "Sites out" contains the number of phosphorylation events possibly regulated by other kinases. Similarly, "Sites in bcgr" and "Sites out bcgr" summarize the number of predicted substrate-kinase relations in the human proteome (used as background). Fisher's exact test was applied to test enrichment of substrate-kinase relationships as compared to predicted substrate-kinase relations in the human proteome. "p.val" and "p.adj" are raw and Benjamini-Hochberg adjusted p-values, respectively.*

Kinase group	Sites in	Sites out	Sites in bcgr	Sites out bcgr	p.val	p.adj
MAPK	175	728	6329	34101	0.003	0.009
CaMKII	160	743	2764	37666	0.000	0.000
PKC	141	762	5783	34647	0.269	0.377
CK1	80	823	4292	36138	0.100	0.201
PAK	67	836	3317	37113	0.425	0.518
CDK	60	843	3278	37152	0.122	0.221
CK2	46	857	2457	37973	0.258	0.371
GSK3	44	859	970	39460	0.000	0.000
DAPK	29	874	2043	38387	0.011	0.026
MAP2K	9	894	1967	38463	0.000	0.000
AMPK	8	895	196	40234	0.091	0.196
PKB	8	895	601	39829	0.162	0.283
CAMK	7	896	261	40169	0.531	0.627
GRK	7	896	798	39632	0.007	0.018
RSK	6	897	276	40154	1.000	1.000
PLK	6	897	929	39501	0.000	0.001
PDHK3_PDHK1	5	898	250	40180	1.000	1.000
CLK	5	898	771	39659	0.001	0.004
MARK	4	899	279	40151	0.537	0.627
SGK	3	900	69	40361	0.208	0.315
BCKDK_PDHK4	3	900	74	40356	0.237	0.349
PKD	3	900	193	40237	0.804	0.868
CaMKI	2	901	36	40394	0.201	0.314
DMPK	2	901	198	40232	0.335	0.446
p70S6K	1	902	49	40381	1.000	1.000
PKGcGK	1	902	414	40016	0.002	0.006
PKA	1	902	425	40005	0.002	0.006
mTOR_ATM_ATR	1	902	507	39923	0.000	0.001
Aurora	1	902	904	39526	0.000	0.000

Table 5.S2: Enriched gene ontology biological function terms based on synapse-specific SynGO database (324). *Proteins carrying regulated phosphorylation sites as determined in Ca vs. EGTA experiments were annotated using the synapse specific SynGO database. Significantly enriched (FDR < 0.001) GO biological function terms are presented together with the hierarchical structure. Note that only a part of proteins carrying regulated phosphorylation sites could be annotated using SynGO database (161 out of 463 unique genes).*

GO term ID	GO term name - hierarchical structure	FDR
SYNGO:synprocess	process in the synapse	5.58E-54
SYNGO:presynprocess	├─ process in the presynapse	9.91E-32
GO:0099509	│ ├─ regulation of presynaptic cytosolic calcium levels	8.86E-09
GO:0099626	│ │ └─ voltage-gated calcium channel activity involved in regulation of presynaptic cytosolic calcium levels	3.02E-05
GO:0099508	│ │ ├─ voltage-gated ion channel activity involved in regulation of presynaptic membrane potential	2.38E-04
GO:0099504	│ ├─ synaptic vesicle cycle	2.42E-27
GO:0097091	│ │ ├─ synaptic vesicle clustering	3.02E-05
GO:0016079	│ │ ├─ synaptic vesicle exocytosis	4.57E-17
GO:0099502	│ │ │ ├─ calcium-dependent activation of synaptic vesicle fusion	8.08E-08
GO:0150037	│ │ │ │ └─ regulation of calcium-dependent activation of synaptic vesicle fusion	7.22E-08
GO:2000300	│ │ │ ├─ regulation of synaptic vesicle exocytosis	1.13E-05
GO:0016081	│ │ │ ├─ synaptic vesicle docking	1.41E-06
GO:0016082	│ │ │ └─ synaptic vesicle priming	6.78E-09
GO:0048488	│ │ └─ synaptic vesicle endocytosis	8.40E-08
GO:0099525	│ ├─ presynaptic dense core vesicle exocytosis	7.59E-04
SYNGO:postsynprocess	├─ process in the postsynapse	7.05E-11
GO:0099072	│ ├─ regulation of postsynaptic membrane neurotransmitter receptor levels	2.16E-11
GO:0099645	│ │ ├─ neurotransmitter receptor localization to postsynaptic specialization membrane	1.38E-06
GO:0098884	│ │ └─ postsynaptic neurotransmitter receptor endocytosis	6.86E-04
GO:0099537	│ ├─ trans-synaptic signaling	3.84E-10
GO:0099542	│ │ │ └─ trans-synaptic signaling by endocannabinoid	1.27E-04
GO:0007268	│ │ └─ chemical synaptic transmission	7.22E-08
GO:0050804	│ │ ├─ modulation of chemical synaptic transmission	1.41E-06
GO:0050808	├─ synapse organization	1.53E-24
GO:0099173	│ ├─ postsynapse organization	7.98E-04
GO:0099175	│ │ ├─ regulation of postsynapse organization	7.69E-04
GO:0099010	│ │ └─ modification of postsynaptic structure	1.10E-06
GO:0098885	│ │ └─ modification of postsynaptic actin cytoskeleton	4.06E-06
GO:1905274	│ │ └─ regulation of modification of postsynaptic actin cytoskeleton	2.61E-04
GO:0098918	│ ├─ structural constituent of synapse	2.45E-13
GO:0098882	│ │ │ ├─ structural constituent of active zone	1.01E-07
GO:0099186	│ │ └─ structural constituent of postsynapse	1.80E-07
GO:0098919	│ │ └─ structural constituent of postsynaptic density	6.09E-05
GO:0007416	│ ├─ synapse assembly	2.38E-04
GO:0099188	│ └─ postsynaptic cytoskeleton organization	1.38E-06
GO:0098974	│ ├─ postsynaptic actin cytoskeleton organization	4.06E-06

Table 5.S3 Number of regulated phosphorylation events per predicted kinase group in Mock vs. BoNT experiment. *"Sites in" show number of phosphorylation events that can be regulated by a respective kinase group as determined in the Mock vs. BoNT experiment. "Sites out" contains the number of phosphorylation events possibly regulated by other kinases. Similarly, "Sites in bcgr" and "Sites out bcgr" summarize the number of predicted substrate-kinase relations in human proteome (used as background). Fisher's exact test was applied to test enrichment of substrate-kinase relationships as compared to predicted substrate-kinase relations in the human proteome. "p.val" and "p.adj" are raw and Benjamini-Hochberg adjusted p-values, respectively.*

Kinase group	Sites in	Sites out	Sites in bcgr	Sites out bcgr	p.val	p.adj
MAPK	229	628	6320	34052	0.000	0.000
PKC	169	688	5933	34439	0.000	0.000
CK1	82	775	4486	35886	0.169	0.287
CDK	78	779	3324	37048	0.347	0.452
CaMKII	72	785	2812	37560	0.104	0.201
GSK3	40	817	984	39388	0.000	0.001
PAK	36	821	3407	36965	0.000	0.000
CK2	32	825	2565	37807	0.001	0.004
DAPK	24	833	2076	38296	0.001	0.004
CLK	14	843	773	39599	0.704	0.804
PKB	11	846	603	39769	0.775	0.868
GRK	10	847	794	39578	0.104	0.201
DMPK	9	848	171	40201	0.013	0.031
RSK	9	848	245	40127	0.116	0.216
CAMK	9	848	273	40099	0.202	0.314
AMPK	3	854	208	40164	0.806	0.868
PDHK3_PDHK1	3	854	266	40106	0.387	0.493
PKGcGK	3	854	404	39968	0.054	0.120
Aurora	2	855	1078	39294	0.000	0.000
MAPKAPK	1	856	18	40354	0.329	0.446
SLK	1	856	23	40349	0.396	0.493
p70S6K	1	856	50	40322	1.000	1.000
PKD	1	856	191	40181	0.196	0.314
ROCK	1	856	355	40017	0.008	0.021
PKA	1	856	430	39942	0.002	0.006
NEK1_NEK5_NEK3_NEK4_NEK11_NEK2	1	856	601	39771	0.000	0.000
MAP2K	1	856	1982	38390	0.000	0.000

Table 5.S4: Number of regulated phosphorylation events per predicted kinase group in Ca vs. EGTA and Mock vs. BoNT experiments. *"CaEGTA" and "MockBoNT" show the number of the regulated phosphorylation events per kinase group in Ca^{2+} vs. EGTA and Mock vs. BoNT experiments, respectively. "Total CaEGTA" and "Total MockBoNT" show the total number of the regulated phosphorylation events with a predicted substrate-kinase relationship in respective experiment. Fisher's exact test was used to test the difference in the occurrence of predicted substrate-kinase relationships in Ca vs. EGTA and Mock vs. BoNT experiments. "p.val" is a p-value of the respective test. "p.adj.BH" is the p-value after Benjamini-Hochberg correction.*

Kinase group	CaEGTA	Total CaEGTA	MockBoTN	Total MockBoTN	p.val	p.adj
CaMKII	160	903	72	857	0.000	0.000
MAPK	175	903	229	857	0.004	0.039
PAK	67	903	36	857	0.008	0.051
MAP2K	9	903	1	857	0.022	0.101
PLK	6	903	0	857	0.031	0.101
DMPK	2	903	9	857	0.034	0.101
CLK	5	903	14	857	0.037	0.101
PKC	141	903	169	857	0.065	0.153
CDK	60	903	78	857	0.078	0.164
CK2	46	903	32	857	0.204	0.387
AMPK	8	903	3	857	0.227	0.393
RSK	6	903	9	857	0.443	0.669
GRK	7	903	10	857	0.470	0.669
PKB	8	903	11	857	0.493	0.669
DAPK	29	903	24	857	0.677	0.719
CAMK	7	903	9	857	0.620	0.719
DYRK	7	903	9	857	0.620	0.719
CK1	80	903	82	857	0.682	0.719
GSK3	44	903	40	857	0.911	0.911

6 Discussion

In this thesis, I applied an MS-based quantification workflow to study phosphoproteome changes in synaptosomes. Specifically, the investigations were focused on identifying phosphorylation sites that require active SV cycling and to distinguish them from phosphorylation events that are primarily triggered by the increase in the cytoplasmic Ca^{2+} concentration due to the depolarization of the plasma membrane. To achieve this, I utilized synaptosomes that were a) electrically stimulated or b) chemically stimulated using KCl. While the electrical stimulation remained ambiguous for the reasons discussed below, KCl-stimulation in combination with BoNT-treatment allowed for the differentiation of "SV-cycling-dependent" and "primarily Ca^{2+}-dependent" sites, respectively.

6.1 Electrical field-stimulation of synaptosomes

Synaptosomes represent pinched-off axonal terminals which plasma membrane re-seals during the homogenization process. While axolemma contains Na^{+}-channels that facilitate the propagation of the action potential, the diversity of Na^{+}-channels in the terminals is less pronounced (25). Therefore, it was hypothesized that the depolarization spreads passively at the nerve terminal and not in the form of an action potential. Considering this, the electrical field-stimulation would probably not be able to evoke an action potential in synaptosomes as it does in the whole cell cultures. Earlier studies utilized harsh stimulation regimes resulting in the release of neurotransmitters from synaptosomes, accumulation of lactate, and Ca^{2+}, but the underlying mechanisms of these changes were not further investigated (105-112). Here I applied a milder 10 Hz stimulation in order to achieve a Ca^{2+}-dependent glutamate release, since Ca^{2+} is considered as a trigger of SV exocytosis in nerve terminals. Although the release was significantly lower in EGTA, monitoring of the cytoplasmic Ca^{2+} concentration using Fura-2 did not show any Ca^{2+}-influx that could be attributed to the electrical stimulation. However, Fura-2 assay reflects Ca^{2+} concentration in the whole cytoplasm, but it would not capture local spikes of Ca^{2+} concentration at the active zone, which are already sufficient to trigger the neurotransmitter release (407). Earlier studies demonstrated Ca^{2+} accumulation in synaptosomes during the course of electrical stimulation (111, 112). The measurements were conducted using a ^{45}Ca isotope and showed a significant, although a relatively moderate increase (~4 nM increase *vs*. up to 200 nM when using KCl stimulation), which might not be captured by Fura-2 fluorimetry as applied in this study. However, application of Ca^{2+} channel blockers such as Cd^{2+} or ω-conotoxin MVCII was not able to abolish the release. The effect was rather controversial: while the release was slightly decreased using 20 µM Cd^{2+} or 1-2 µM of the ω-conotoxin after a repeated stimulation, the effect was paradoxically stronger when using 60 µM Cd^{2+}.

However, adding Cd^{2+} to the phosphate-containing buffer might cause a precipitation of a phosphate salt, which would reduce the net Cd^{2+} concentration and unpredictably affect the release. Another set of experiments utilized acridine orange to monitor the neurotransmitter release and SV recycling. Here, electrical stimulation did not cause an observable change in AO fluorescence. Nonetheless, the latter might be explained by that rapid recycling mechanisms efficiently dampen the increase in AO-fluorescence, since even in the case of a KCl-evoked release, the initial spike in the AO-fluorescence returns to the basal levels within 2-3 seconds. Strikingly, treatment with BoNT A/D did not suppress the release. This fact raises the question, whether the observed glutamate liberation occurs via SV exocytosis. Other routs of the release are possible, *e.g.*, leakage of the cytoplasmic glutamate via the glutamate transporter in the plasma membrane. However, the latter would not explain the significant suppression of the release in EGTA condition. Taken together, these observations do not favor the hypothesis that the electrical stimulation evokes glutamate release via exocytosis, though it is not possible to exclude that some glutamate (probably < 30%) is released exocytotically.

Although exact mechanisms of the neurotransmitter release caused by electrical stimulation need to be further elucidated, electrical stimulation is advantageous for kinetics studies since it is free of mixing effects (such in the case of adding KCl) and has, therefore, clearly defined start and end points. As a proof of principle, phosphoproteome changes in synaptosomes were measured at six time points, including a time point before stimulation and two time points after the stimulation. A selection of sites that showed a Pearson correlation of >0.6 between the two kinetic measurements and a minimum 50% intensity change at any time point has shown that changes affect proteins that are already known to regulate SV cycling, such as synapsin-1 or CaMKII, active zone proteins, SV proteins, proteins involved in endocytosis, *etc*. This implies that the changes might reflect adaptations of the synapse to the altered membrane potential and an increased energy demand due to the glutamate release caused by the electrical stimulation. In this regard, it is tempting to speculate, whether the electrical stimulation might appear useful in deciphering molecular mechanisms underlying the modulation of the neuronal excitability and short behavior effects such as those induced by transcranial direct current stimulation (408, 409).

6.2 BoNT treatment of synaptosomes

BoNTs are highly potent clostridial toxins that exert an exceptionally specific action in cleaving SNARE proteins. In this study, a combination of two BoNT types was applied, *i.e.*, A and D or C1 and B. Each pair of toxins cleaves plasma membrane-standing t-SNARE and vesicular v-SNARE, SNAP-25 and synaptobrevin-2 or syntaxin-1 and synaptobrevin-2, respectively. It has to be noted that the toxins are applied in their native form, which consists

of a heavy and light chain. The heavy chain facilitates the toxin uptake into the nerve terminal, while the light chain exerts its catalytic activity (410). The toxin entry relies on endocytosis and can occur, therefore, only in a functional synaptosome. The latter is the probable reason for an overall unaltered content of SNARE proteins in BoNT- and Mock-treated synaptosomes, as discussed in section 5.13.2. Of note, BoNT-treated synaptosomes were compared against synaptosomes treated with heat-inactivated (Mock) toxins. This experimental detail is important as it allows to compensate for prolonged incubation times and unforeseen effects of adding *C. botulinum* cell culture supernatants to synaptosomal suspensions. Furthermore, an application of the four different toxin types (A+D and C1+B) aimed to minimize unpredictable effects associated with a particular toxin type. As shown by previous studies (121, 122) and confirmed here (**Figure 5.S1**), glutamate liberation following KCl-evoked depolarization is significantly reduced in BoNT-treated synaptosomes, while the Ca^{2+}-influx is unaffected. This fact allowed identifying phosphorylation events that are responsive to BoNT-treatment, *i.e.*, dependent on active SV cycling, and separate phosphorylation events that are primarily triggered by Ca^{2+}-influx.

6.3 Categorization of phosphorylation events

This study categorizes phosphorylation events in two groups, namely, “SV-cycling-dependent” and “primarily Ca^{2+}-dependent”. The categorization is based on the responsiveness of protein phosphorylation to BoNT-treatment and changes following depolarization under Ca or EGTA condition (**Figure 5.4**). This categorization follows a simplified assumption that there are three basic triggers: a) Ca^{2+}-influx; b) membrane depolarization; and c) SV cycling. While *A* is a generally accepted cause of the synaptic phosphoproteome changes given the abundance of Ca^{2+}-regulated kinases and phosphatases such as CaMKII and calcineurin in the brain, *C* was a working hypothesis, and *B* could not be addressed in this study, since we lack means to control membrane potential in synaptosomes, apart from persistent depolarization using chemical agents. Accordingly, all conditions compared here are based on synaptosomes depolarized using 50 mM KCl. Comparison of KCl-stimulated synaptosomes under Ca or EGTA conditions shows, therefore, changes that are Ca^{2+} and/or SV-cycling-dependent, since EGTA prevents Ca^{2+}-influx and, consequently, an active SV cycling. BoNT-treatment hampers SV cycling, but not the Ca^{2+}-influx and thus allows to demarcate phosphorylation events that require SV cycling. Indeed, identification of BoNT-responsive phosphorylation sites supports the hypothesis that SV cycling is required for certain phosphorylation events to take place. A hypothesis is that SV cycling relies on multiple protein rearrangements, interaction with cytoskeleton elements and assembly/disassembly of multimeric protein complexes (3). These rearrangements might expose docking sites for kinases and

phosphatases that can then exert their actions (**Figure 6.1**). As already discussed in section 5.6, PP1 is a probable mediator of SV-cycling-dependent changes, as it can be targeted to cytoskeleton elements via regulatory subunits. Accordingly, differentially phosphorylated sites were observed on Neurabin-1 and other PP1 regulators (**Figure 5.S7**), which may influence the synaptic localization of PP1 (238).

The classification of phosphorylation events into “primarily Ca^{2+}-dependent” and “SV-cycling-dependent” is indirectly corroborated by the fact that predicted CaMKII phosphorylation sites are significantly enriched among “primarily Ca^{2+}-dependent” group. This observation is expected given the Ca^{2+}-dependence of CaMKII. Moreover, phosphorylation sites on “dephosphins” which are known targets for calcineurin, a Ca^{2+}/calmodulin-dependent phosphatase, fall into the same group. It has to be noted, however, that such dichotomic classification is likely an oversimplification, which, as any other model, does not consider the whole palette of relationships between kinases, phosphatases and their substrates in the synapse. Thus, it is reported that CaMKII may also act as a scaffold, therefore, it is likely that protein rearrangements during SV cycling influence this type of CaMKII activity (157, 158). Kinases/phosphosphatases can activate or inhibit each other via respective (de)phosphorylation reactions. For instance, calcineurin regulates PP1 activity via dephosphorylation of its regulatory subunits (259), while PP1 is known to dephosphorylate CaMKII, thus inhibiting its kinase activity (411). Nonetheless, this classification proved useful, as it is first to suggest that the synaptic phosphoproteome is affected by SV cycling. Moreover, it can be used for selection of candidate sites that might regulate SV cycling. Thus, SV-cycling-dependent sites on syntaxin-1, synaptobrevin-2 and cannabinoid receptor-1 have drawn our attention, and their modulatory effect on effect on exo- and endocytosis could be demonstrated in cultured hippocampal neurons.

6.4 Challenges and limitations of MS-based phosphoproteomics

Technical advances in the field of mass spectrometry allowed for identification and quantification of thousands of phosphorylation sites (288). Nonetheless, analysis of PTMs poses additional experimental and analytical challenges. When analyzing phosphorylated peptides, one needs to consider that phosphorylated peptides are generally underrepresented in the proteome. Current state of the enrichment techniques, such as TiO_2-based enrichment, allows to enrich phosphorylated peptides with high specificity (>90%). However, none of the available techniques would cover all phosphorylated peptides. Moreover, different enrichment techniques have varying affinities toward certain types of peptides. For example, IMAC-based enrichment outperforms TiO_2 in the enrichment of multiply phosphorylated peptides (412). Other analytical challenges arise during LC-MS/MS acquisition. Phosphorylation provides an additional negative charge to a

peptide, which decreases its “flyability” in the MS if analyzed in the positive ion mode. Moreover, phosphorylation is a labile chemical modification that is first to be eliminated during the fragmentation process, which creates an additional site localization problem. The latter is further complicated by existing phosphorylation isoforms – peptides that carry the same number of phosphorylation groups on different positions. Such peptides are poorly resolved by conventional LC systems and often produce mixed spectra of co-fragmented precursors. The subsequent analysis usually considers only phosphorylation sites identified with a high localization probability (>75%). Onethe one hand, this approach decreases the number of analyzed phosphorylation sites, on the other hand, it increases the confidence of the identifications, since phosphorylation sites with a high localization probability are usually identified based on high-score PSMs with a comprehensive fragmentation pattern (413).

In this study, it was possible to alleviate some of the problems by using TMT labeling approach and extensive pre-fractionation using bRP. This allowed us to significantly increase coverage of the identified and quantified phosphorylation sites as compared to other studies (**Figure 5.2**) (351, 352). Furthermore, TMT-labeling reduced the missing value problem, which arises due to the semi-stochastic nature of MS acquisition. The latter increased the number of sites that could be compared among different experiments and conditions. However, higher sensitivity and better comparability come at the cost of a reduced dynamic range. Due to the co-fragmentation of several precursors, TMT-based quantification does not accurately depict intensity changes and tends to underestimate them (300). The latter was taken into account when determining the candidate sites, since phosphorylation sites that showed an intensity fold change of 1.2 were considered as significant, if satisfying other criteria. For kinetics analysis, the quantification was achieved using an SPS-MS3 approach, which allows for an accurate ratio estimation though at the cost of reduced sensitivity (301).

6.5 Challenges and limitations of the functional analysis of phosphorylation sites

Another type of challenges associates with the functional analysis of the phosphorylation sites. Thus, in the case of a protein expression analysis, it is legitimate to assume that the decrease in the protein amount correlates with a decreased functional activity of the protein. This, however, does not hold true for protein phosphorylation: a reduced/increased phosphorylation might result in both, a gain or loss of a protein function, and the degree of a change does not necessarily reflect the degree of a functional change. Moreover, since the function of the most phosphorylation sites remains unknown, it is not always possible to

anticipate the functional consequences of a phosphorylation. Therefore, the functional analysis in phosphoproteomics is usually restricted to the analysis of general protein functions. A further complication is that a phosphorylation site might appear on a multiply phosphorylated peptide. It is common, therefore, to distinguish a single, double, or multiple phosphorylation states (multiplicity) and consider each multiplicity state of a site as a separate phosphorylation event. The differential analysis is often conducted at the level of phosphorylation events, because singly or multiply phosphorylated species of the same peptide might be regulated differently. However, when using global functional analysis of differentially phosphorylated proteins, it is currently not possible to account for these differences.

Here, the functional analysis was focused on identifying possible kinase-substrate relationships and the association of the identified regulating kinase groups with functional terms (**Figure 5.3**). For the kinase-substrate prediction, an experimental information available in PhosphoSitePlus database was utilized in the first place. For other sites, a kinase was predicted using an available NetworKIN algorithm, which utilizes the information about the consensus sequence motif known protein-protein interactions (323). Although a prediction in each particular case might be error-prone, however, it provides a global view on possible kinase-substrate interactions. In the following, application of different annotation sources such as general GO terms (317), as well as the neuron/synapse-specific annotations (Reactome pathways (319) and SynGO database (324), respectively), and manually assigned keywords (**Figure 5.S8**) demonstrated that a) pre-synaptic proteins are significantly enriched among differentially phosphorylated proteins; b) putative sites for CaMKII and MAPK are preferably enriched among “primary Ca^{2+}-dependent” and “SV-cycling-dependent” sites, respectively; c) while CaMKII preferentially regulates sites on proteins that are directly involved in Ca^{2+}-dependent neurotransmitter release or its regulation, putative MAPK targets are mostly involved in the synapse organization, *i.e.*, cytoskeleton protein, adhesion molecules, *etc*.

6.6 Regulation of the kinase and phosphatase activity via phosphorylation

Kinases and phosphatases control the phosphorylation status of their substrates. However, phosphorylation of the kinases, phosphatases or their direct regulators may further shed light on the activation status of these enzymes and hint at the intricate coordination of their activities.

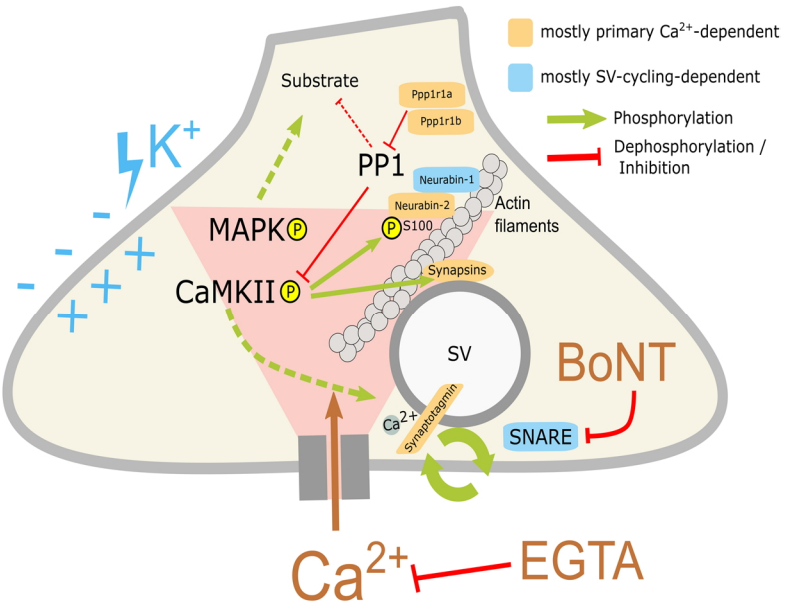

Figure 6.1: KCl stimulation of synaptosomes: proposed connection of protein phosphorylation and SV cycling activity. *The scheme shows effects of BoNT and EGTA on SV cycling, as well as proposed balanced activities of CaMKII, MAPK and PP1. Following depolarization by 50 mM KCl, Ca^{2+}-influx triggers SV cycling via interaction with Ca^{2+} sensor synaptotagmin. EGTA prevents Ca^{2+}-influx and subsequently, SV exocytosis. BoNTs blocks exocytosis via cleavage of SNARE proteins, but do not compromise Ca^{2+}-influx. EGTA prevents Ca^{2+}-influx and subsequently, SV exocytosis. BoNTs blocks exocytosis via cleavage of SNARE proteins, but do not compromise Ca^{2+}-influx. Increase in Ca^{2+} concentration activates CaMKII (via autophosphorylation) and MAPK (presumably via Ras activation). CaMKII is deactivated via dephosphorylation by PP1. Following Ca^{2+}-influx, PP1 cannot keep pace in dephosphorylating CaMKII, which results in the sustained CaMKII activity and phosphorylation of its substrates. Comparison of synaptosomes stimulated under Ca and EGTA conditions implies dephosphorylation of putative MAPK substrates and even stronger dephosphorylation in the case of stalled SV cycling due to BoNT-treatment, which contradicts apparent MAPK activation. A suggested hypothesis is that PP1 dephosphorylates MAPK substrates, which further sequesters PP1 activity and disinhibits CaMKII. PP1 is targeted to F-actin via its regulatory subunits, neurabin-1 and neurabin-2. CaMKII presumably attenuates this targeting and the PP1 activity towards MAPK substrates via phosphorylating neurabin-2 at S100. (De)phosphorylation of PP1 inhibitors Ppp1r1a and Ppp1r1b, e.g., via PKA, calcineurin, etc., may further modulate PP1 activity. Active SV cycling might attenuate the dephosphorylation of MAPK targets probably due to the protein complex rearrangements and due to the detachment of SVs from actin filaments during SV cycling. Synapsin-1 phosphorylation may affect SV association with actin filaments. Accordingly, block of SV cycling by BoNT causes even stronger dephosphorylation of MAPK targets, which appear as an increased phosphorylation when comparing Mock vs. BoNT treated synaptosomes. Green arrows represent kinase/substrate interaction (phosphorylation). Blunt-end arrows represent dephosphorylation and/or inhibition, see in text. Dashed lines represent hypothetical interactions. Protein names on blue/orange background denote the prevalent phosphorylation type, "SV-cycling-dependent", or "primary Ca^{2+}-dependent", respectively.*

6.6.1 CaMKII, MAPK, and PP1

Remarkably, the phosphorylation sites on CaMKII and MAPK themselves fall into the group of "primarily Ca^{2+}-dependent". Specifically, the phosphorylation of *Camk2a*-T286, *Camk2b*-T287, *Camk2d*-T287, *Mapk1*-T183, Y185, *Mapk3*-T203, Y205 points out activation of these kinases following depolarization and Ca^{2+}-entry. Despite the apparent activation of MAPK,

the majority of MAPK substrates appear dephosphorylated. The latter can be explained by the competing phosphatase activity that counterbalance MAPK activation at the time point of observation. It was previously hypothesized that CaMKII and PP1 form a switch-like system in the synapse (414), where PP1 controls the phosphorylation status of CaMKII and, therefore, its activity. However, the catalytic activity of PP1 is a limiting factor. Once the rate of CaMKII autophosphorylation increases dramatically due to the Ca^{2+}-influx, thedephosphorylation by PP1 cannot keep pace, which results in a burst of CaMKII activity. It is tempting to speculate whether this model can be further extended to incorporate MAPK. Thus, increased Ca^{2+} concentration might activate MAPK via Ras activation (167). On the other hand, we observe the dephosphorylation of MAPK-targets when comparing Ca and EGTA conditions. If we assume that PP1 is at least partially responsible for the dephosphorylation of MAPK targets, this might further sequester the activity of PP1 towards CaMKII, thus keeping CaMKII longer in an active state, which results in an increased phosphorylation of CaMKII substrates. Furthermore, it seems that inhibition of SV cycling via BoNT further increases phosphatase activity towards MAPK-substrates (**Figure 5.2F**). Following hypothesis provides a solution to this conundrum (**Figure 6.1**): PP1 is targeted to F-actin via its regulatory subunits, neurabin-1 and neurabin-2. Ca^{2+}-influx leads to auto-phosphorylation of CaMKII and MAPK activation. PP1 counteracts MAPK activity via dephosphorylation of its substrates, which further disinhibits CaMKII and results in the phosphorylation of CaMKII substrates. CaMKII presumably attenuates the PP1 activity towards MAPK substrates via phosphorylating neurabin-2 at S100 and thus reducing the PP1 interaction with F-actin. Note that cytoskeleton-associated proteins are enriched among MAPK targets (**Figure 5.3A**). Active SV cycling might further attenuate the dephosphorylation of MAPK targets probably due to the protein complex rearrangements and due to the detachment of SVs from actin filaments during SV cycling. Accordingly, block of SV cycling by BoNT causes even stronger dephosphorylation of MAPK targets, which appear as an increased phosphorylation when comparing Mock *vs.* BoNT treated synaptosomes (**Figure 5.2F**).

6.6.2 PKA, CDK5, and GSK3

The action of PP1 can be further fine-tuned by the activity of PKA. Thus, PP1 inhibitors *Ppp1r1a* and *Ppp1r1b* attenuate PP1 activity following phosphorylation by PKA (245-247). Accordingly, *Ppp1r1a*-S46, S47 and *Ppp1r1b*-S45 sites are significantly upregulated in Ca condition, which implies the activation of the PP1 inhibitors. The CDK5-mediated phosphorylation at *Ppp1r1a*-S67 was previously shown to inhibit PKA activity (246, 247). Since this site appear dephosphorylated, it implies PKA activation following KCl-depolarization. Furthermore, PKA activation may be an adaptation towards increased

energy demand because of depolarization, since the kinase is involved in the regulation of metabolic pathways. Remarkably, the catalytic subunit of PKA itself is differentially phosphorylated at *Prkaa1*-S486. A stretch of S and T residues at the C-terminus of PKA is a probable target of GSK3 (415), which attenuates PKA activity. The dephosphorylation of the *Prkaa1* at these residues implies disinhibition of PKA. Phosphorylation of CDK5 or GSK3 themselves does not allow to deduce the activity status of the kinases. However, of note is the “SV-cycling-dependent” phosphorylation of a CDK5 regulator p39 (*Cdk5r2*-T84). Phosphorylation at this site has been previously shown to affect localization of CDK5 (416). Given that predicted CDK targets, similarly to MAPK targets, appear strongly dephosphorylated following BoNT-treatment (**Figure 5.2F**), it is tempting to speculate, whether the inhibition of SV cycling influences the localization of CDK5 and thus modulates its activity.

6.6.3 CK1 and CK2

Based on the phosphorylation pattern of CK1 isoforms, it is not possible to infer the activity status of CK1. However, increased phosphorylation of ϵ-CK1 (*Csnk1e*) at S363 implies inhibition of CK1 activity following BoNT-treatment, since C-terminal phosphorylation of the δ isoform (*Csnk1d*) by PKC or autophosphorylation has been shown to attenuate kinase activity (417, 418). The phosphorylation of *Csnk1e*-S363 has been previously identified by other studies; however, its functional role has not been elucidated yet .(419, 420)

Not much can be said about the activity CK2 following KCl-depolarization. A regulatory beta subunit of CK2 appear dephosphorylated under BoNT-treatment (*Csnk2b*-S205, S209). The phosphorylation at S209 has been previously observed in mitotic cells, but its functional role remained unknown, though it was hypothesized that it can affect the localization of CK2 (421).

6.6.4 PAK1

In our data, *Pak1* appears significantly dephosphorylated at several sites (T167, S218, S219, S222) in stimulated synaptosomes in the presence of Ca^{2+}. As shown by *Shin et al,* phosphorylation at S222 by CK2 is required for a complete PAK1 activation (422). The dephosphorylation of PAK1 at the aforementioned residues implies Ca^{2+}-dependent deactivation of PAK1 following 2 min of KCl-depolarization. Moreover, absence of differentially regulated sites on a PAK1-substrate *Raf1* implies that the observed MAPK activation is not mediated via PAK1/*Raf1* activation.

6.6.5 PKC

Increased phosphorylation of PKC at *Prkcb*-T640 (T642) implies catalytically active state of the kinase following KCl-depolarization in the presence of Ca^{2+}. Dephosphorylation of further "primarily Ca^{2+}-dependent" sites at the C-terminus of an unconventional *Prkcb* sequence (Uniprot accession F1LS42, sites S659, S653, and S663) implies regulation of its intracellular localization. The dephosphorylation is presumably mediated by PP2 (184).

6.6.6 PP2

The activity of PP2 might be linked to the regulation of PP1 and PKA activity via dephosphorylation of PP1 inhibitor *Ppp1r1b (254)*. It was previously shown that PKA-mediated phosphorylation of B56δ subunit (*Ppp2r5d*) has an activating effect on PP2A. PP2A dephosphorylates T75 on PP1 inhibitory subunit *Ppp1r1b* leading to PP1 inhibition (254) Though the proposed phosphorylation of the regulatory subunit *Ppp2r5d* was not observed in this study, the phosphorylation of another regulatory subunit, *Ppp2r5c,* at S497 is strongly upregulated following KCl-depolarization in the presence of Ca^{2+}. It is tempting to speculate whether this phosphorylation has a similar activating function for PP2.

6.6.7 Calcineurin

The activity of calcineurin following KCl-depolarization is indirectly corroborated by the dephosphorylated state of the proteins involved in endocytosis, also known as dephosphins. Remarkably, the majority of the differentially phosphorylated sites on dephosphins belong to the "primary Ca^{2+}-dependent" group. The latter reflects the high affinity of calcineurin towards Ca^{2+}/calmodulin, which is required to adequately adjust the endocytosis rate in response to the depolarization by KCl (257). Calcineurin might further participate in the regulation of PP1 activity via dephosphorylating *Ppp1r1a* and *Ppp1r1b* (259). Two sites of an α catalytic subunit close to an autoinhibitory segment are differentially regulated (**Figure 5.S7**), *i.e.*, *Ppp3ca*-S498 ("primary Ca^{2+}-dependent") and *Ppp3ca*-S462 ("SV-cycling-dependent"). Although the functional role of these sites is unknown, it is tempting to speculate that these phosphorylation events may affect the catalytic activity and/or the localization of the enzyme.

6.8 Primary Ca^{2+}-dependent sites and SV-cycling-dependent phosphorylation

Functional analysis of differentially phosphorylated proteins revealed that certain functional groups carry phosphorylation sites that are categorized either as "primary Ca^{2+}-dependent" or "SV-cycling-dependent" (**Figure 5.5** and **Figure 5.S16**). Unfortunately, the functional role of the most phosphorylation events is unknown and can only be speculated. However, it

appears that certain functional groups tend to be phosphorylated following the one or another type. Some of the prominent functional groups are discussed below.

6.8.1 Active zone and exocytosis-related proteins

The categorization of phosphorylation sites into “primary Ca^{2+}-dependent” and “SV-cycling-dependent” demonstrated that “primary Ca^{2+}-dependent” sites are preferably clustered on proteins that are located near the active zone and, except a few cases discussed below, are directly involved in the process of exo- and endocytosis. Primary Ca^{2+}-dependent phosphorylation of these proteins may be explained by the fact that they are located in a vicinity of Ca^{2+}-channel and, consequently, represent the closest targets for Ca^{2+}-activated kinases and phosphatases.

Large proteins of the active zone such as bassoon, piccolo, and RIM-proteins are strongly phosphorylated. Since these proteins are known to organize the active zone, it is tempting to speculate, whether their (de)phosphorylation provides a necessary milieu for various protein-protein interactions near the plasma membrane or acts as a Ca^{2+}-buffer. A very recent study indicates that bassoon might regulate the SV distribution between the readily releasable and reserved pools of SVs (423). Furthermore, bassoon deletion alters CDK5/calcineurin and PKA signaling in the presynapse, which may further affect phosphorylation of other exocytosis-related proteins. The phosphorylation of active zone proteins may indeed affect SV pool distributions. Thus, phosphorylation of a close cooperating partner of bassoon, *Erc2*, at S45 has been previously shown to impede the reloading of the RRP (424). Interestingly, our data show a strong upregulation of S45 phosphorylation on a related protein, *Erc1*, and only a sub-threshold dephosphorylation of *Erc2*-S45. Moreover, an active-zone associated kinase, *Brsk1*, which is responsible for *Erc2* phosphorylation, is dephosphorylated at multiple sites following KCl-depolarization in the presence of Ca^{2+}. Although the functional role of *Brsk1* phosphorylation sites is not known, these observations imply that SV pools and the neurotransmitter release might be tightly controlled via phosphorylation of the active zone proteins.

6.8.2 K^+-channels

A substantial group of SV-cycling-dependent phosphorylation sites constitutes sites on K^+-channel proteins (**Figure 5.S14-16**) that are differentially affected by BoNT-treatment. Remarkable is the dephosphorylation of several C-terminal sites of *Kcnd2* following BoNT treatment. This region is important for channel activation and inactivation (425), and the amino acid phosphorylation in this region is governed by PKC and MAPK (426), which may change the activation voltage and conductivity of the channel (427). Furthermore, C-terminal phosphorylation of another subunit, *Kcna2*, has been associated with the trafficking

and cell surface expression of K_V1.2 channels (428). In contrast to *Kcnd2*, *Kcna2*-S440, S441, S447, S449 show increased phosphorylation following BoNT-treatment. It is tempting to speculate if the C-terminal phosphorylation of *Kcna2* represents a compensatory mechanism to alleviate clamp-depolarization via increasing the presence of K^+-channels at the plasma membrane. Intriguingly, several sites on *Kcnb1*, a K_V2.1 forming subunit, are dephosphorylated following BoNT treatment. Similarly to *Kcna2* and *Kcnd2*, its phosphorylation has been implicated in the regulation of channel trafficking and gating properties (429, 430). Moreover, *Kcnb1* phosphorylation and membrane insertion have been proposed as a step accompanying neuronal apoptosis (431). The study of *Pal et al* (432) reported reduced plasma membrane expression of K_V2.1 in neurons expressing BoNT of type C1 or E. Authors hypothesized that the reduced channel expression at the plasma membrane may be due to the reduced direct interaction of SNARE proteins, as this interaction has been demonstrated previously (433-435). However, our data imply that the link might be indirect. It is tempting to speculate that the channel trafficking is regulated via phosphorylation, similar to *Kcna2,* and this phosphorylation depends on active SV cycling. The SV cycling dependence of the phosphorylation is governed by SNARE: BoNT-exposure leads to a stalled SV cycling and/or distorted direct interaction with SNARE, which may change the availability of phosphorylation sites for kinase/phosphatase activity as discussed above and, consequently, results in an altered plasma membrane presentation of the channel.

6.8.3 Cytoskeleton-associated proteins

Cytoskeleton-associated proteins comprise a large group of proteins that interact with microtubuli and/or actin filaments or other structural proteins and play important roles in the synapse organization and membrane trafficking. Especially the role of actin filaments in the synapse was extensively investigated. It was proposed that SV interaction with actin via phosphoprotein synapsin-1 might regulate the release probability of SVs. Thus, synapsin-1 (de)phosphorylation, *e.g.*, phosphorylation at S603 following KCl-depolarization reduces SVs binding to actin and facilitates their mobility (385). Notably, proteins constituting actin-spectrin network such as spectrin β-chain and adducin α, β contain preferably SV-cycling-dependent phosphorylation sites (**Figure 5.S16**). Although the exact function of these phosphorylation events is not known, it hints at the re-organization of the synapse in response to the active SV cycling. Considering the aspect of the synapse remodeling, it is interesting to note, that several members of the Wnt pathway show SV-cycling-dependent phosphorylations, including Adenomatous polyposis coli protein (*Apc*), TRAF2 and NCK-interacting kinase (*Tnik*), δ-catenin (*Ctnnd1, Ctnnd2*) and others. Given that Wnt pathway is implicated in synapse development and maintenance (436), it is tempting to speculate

whether these phosphorylation events reflect remodeling processes associated with SV cycling. A previous study has identified CDK5 as a mediator of *Ctnnd2* phosphorylation that affects its subcellular localization and the neuronal activity. Accordingly, dephosphorylation of *Cttnd2* following BoNT-treatment implies its reduced membrane localization, which might affect the cadherin-cytoskeletal interactions (437) and the stability of synaptic junctions (438, 439).

Remarkable is the dephosphorylation of microtubule-associated proteins 1a, 1b, 2, and tau (*Map1a, Map1b, Map2,* and *Mapt,* respectively) following BoNT treatment. Given that the phosphorylation status of these proteins might affect the microtubule stability, it is reasonable to speculate that SV cycling activity might additionally influence the synapse stability via phosphorylation of microtubule-associated proteins. The latter hypothesis aligns well with the observed SV-cycling-dependent phosphorylation of other cytoskeleton- and Wnt-related proteins. PAK, CK1, GSK3, and CDK5 have been previously suggested as candidate kinases that are capable of phosphorylating *Map2* and *Mapt* (220, 440), while PP2A and PP1 have being shown to dephosphorylate them at distinct positions (441, 442).

6.8.4 Phosphorylation of SNARE and its implication for exocytosis

In contrast to other exocytosis-related proteins, phosphorylation sites on the three core SNARE proteins, syntaxin-1, synaptobrevin-2, and SNAP25, as well as the closely associated Munc18-1 were exclusively SV-cycling-dependent. This notice has further strengthened the hypothesis that active SV cycling is necessary to provide an access for kinases and phosphatases to their substrates, as it is likely that the pre-assembled SNARE complexes are less accessible for kinases and phosphatases. These proteins may become modified after the disassembly, *e.g.*, after the exocytosis was complete. Remarkably, in contrast to the majority of SV-cycling-dependent phosphorylation sites, BoNT-treatment led to an increased phosphorylation of the three SNARE proteins and Munc18. The latter implies an increased kinase activity that may affect the SNARE complex formation (229, 353-358). In this work, expression of non-phosphorylatable or pseudo-phosphorylated variants of syntaxin-1 and synaptobrevin-2, as well as on the cannabinoid receptor-1 – a receptor known for its regulatory role in the exocytosis – in the cultured hippocampal neurons have shown modulatory effects of these modifications on the SV cycling. Interestingly, a recent study has investigated a non-phosphorylatable *Stx1a*-D17A using a similar pHluorin-based approach (229). According to authors, *Stx1a*-D17A prevents *Stx1a* phosphorylation at S14 by CK2. The analysis of exocytosis has shown an increased exocytosis in *Stx1a*-D17A expressing mutants under long (900 AP) stimulation. In contrast, our analysis revealed that pseudo-phosphorylated *Stx1a*-T21E/T23E increases exocytosis following short (60 AP) stimulation (**Figure 5.6**). This discrepancy implies that despite close

localization, the phosphorylations at S14 and T21/T23 sites might have a different impact on the exocytosis rate and, therefore, represent a possible molecular mechanism for fine-tuning of the neurotransmitter release.

6.9 Conclusions and Outlook

In this work, an optimized MS-based phosphoproteomics was applied to deepen our knowledge about the synaptic phosphoproteome and its dynamics in response to stimulation. Electrical field-stimulation of synaptosomes has been characterized in respect to Ca^{2+}-dependent neurotransmitter release and its utility for kinetics studies has been demonstrated. Using BoNT-treated synaptosomes it was possible to demonstrate SV cycling dependence of phosphorylation events in the synapse and dissect primary Ca^{2+}-dependent and SV-cycling-dependent phosphorylation events, respectively. Based on this categorization, selected SV-cycling-dependent phosphorylation sites on syntaxin-1, synaptobrevin-2, and cannabinoid receptor-1 were tested for their modulatory effects on the SV cycling. The effects they exert on exo- and endocytosis in cultured hippocampal cells confirmed the utility of this categorization.

Several aspects can be proposed for the future work. Firstly, using super-resolution microscopy it would be important to confirm the hypothesis that stalled SV cycling affects localization of kinases and phosphatases such as PP1, leading to the observation of SV-cycling-dependent phosphorylation events. Secondly, use of selective inhibitors of kinases and phosphatases may further help to unravel the complex enzyme-substrate interactions. Thirdly, other PTMs such as ubiquitination and glycosylation are likely to play important role in the synapse physiology. Studying interplay of glycosylation and phosphorylation may further broaden our understanding of the molecular mechanisms governing neurotransmitter release and synaptic functioning.

7 References

1. Ryan, T. J., and Grant, S. G. (2009) The origin and evolution of synapses. *Nature Reviews Neuroscience* 10, 701-712
2. Guzman, R. E., Alekov, A. K., Filippov, M., Hegermann, J., and Fahlke, C. (2014) Involvement of ClC-3 chloride/proton exchangers in controlling glutamatergic synaptic strength in cultured hippocampal neurons. *Frontiers in cellular neuroscience* 8, 143
3. Jahn, R., and Fasshauer, D. (2012) Molecular machines governing exocytosis of synaptic vesicles. *Nature* 490, 201-207
4. Takamori, S., Holt, M., Stenius, K., Lemke, E. A., Grønborg, M., Riedel, D., Urlaub, H., Schenck, S., Brügger, B., and Ringler, P. (2006) Molecular anatomy of a trafficking organelle. *Cell* 127, 831-846
5. Couteaux, R., and Pecot-Dechavassine, M. (1970) Synaptic vesicles and pouches at the level of" active zones" of the neuromuscular junction. *Comptes rendus hebdomadaires des seances de l'Academie des sciences. Serie D: Sciences naturelles* 271, 2346-2349
6. Landis, D. M. (1988) Membrane and cytoplasmic structure at synaptic junctions in the mammalian central nervous system. *Journal of electron microscopy technique* 10, 129-151
7. Südhof, T. C. (2012) The presynaptic active zone. *Neuron* 75, 11-25
8. Bloom, F. E., and Aghajanian, G. K. (1966) Cytochemistry of synapses: selective staining for electron microscopy. *Science* 154, 1575-1577
9. Collins, M. O., Husi, H., Yu, L., Brandon, J. M., Anderson, C. N., Blackstock, W. P., Choudhary, J. S., and Grant, S. G. (2006) Molecular characterization and comparison of the components and multiprotein complexes in the postsynaptic proteome. *Journal of neurochemistry* 97, 16-23
10. Ding, J. D., Kennedy, M. B., and Weinberg, R. J. (2013) Subcellular organization of camkii in rat hippocampal pyramidal neurons. *Journal of Comparative Neurology* 521, 3570-3583
11. Graziane, N., and Dong, Y. (2016) *Electrophysiological analysis of synaptic transmission*, Springer
12. Feiner, A.-S., and McEvoy, A. (1994) The Nernst equation. *Journal of chemical education* 71, 493
13. Goldman, D. E. (1943) Potential, impedance, and rectification in membranes. *The Journal of general physiology* 27, 37-60
14. Hodgkin, A. L., and Katz, B. (1949) The effect of sodium ions on the electrical activity of the giant axon of the squid. *The Journal of physiology* 108, 37-77
15. Johnston, D., and Wu, S. M.-S. (1994) *Foundations of cellular neurophysiology*, MIT press
16. Kaplan, J. H. (2002) Biochemistry of Na, K-ATPase. *Annual review of biochemistry* 71, 511-535
17. Khananshvili, D. (2013) The SLC8 gene family of sodium–calcium exchangers (NCX)–Structure, function, and regulation in health and disease. *Molecular aspects of medicine* 34, 220-235
18. Dang, D., and Rao, R. (2016) Calcium-ATPases: gene disorders and dysregulation in cancer. *Biochimica et Biophysica Acta (BBA)-Molecular Cell Research* 1863, 1344-1350
19. Bonar, P. T., and Casey, J. R. (2008) Plasma membrane Cl^-/HCO3-exchangers: structure, mechanism and physiology. *Channels* 2, 337-345
20. Virtanen, M. A., Uvarov, P., Hübner, C. A., and Kaila, K. (2020) NKCC1, an elusive molecular target in brain development: making sense of the existing data. *Cells* 9, 2607
21. Kaila, K., Price, T. J., Payne, J. A., Puskarjov, M., and Voipio, J. (2014) Cation-chloride cotransporters in neuronal development, plasticity and disease. *Nature Reviews Neuroscience* 15, 637-654

22. Catterall, W. A. (2011) Voltage-gated calcium channels. *Cold Spring Harbor perspectives in biology* 3, a003947
23. Reid, C. A., Bekkers, J. M., and Clements, J. D. (2003) Presynaptic Ca^{2+} channels: a functional patchwork. *Trends in neurosciences* 26, 683-687
24. Campiglio, M., and Flucher, B. E. (2015) The role of auxiliary subunits for the functional diversity of voltage-gated calcium channels. *Journal of cellular physiology* 230, 2019-2031
25. Debanne, D., Campanac, E., Bialowas, A., Carlier, E., and Alcaraz, G. (2011) Axon physiology. *Physiological reviews* 91, 555-602
26. Leão, R. M., Kushmerick, C., Pinaud, R., Renden, R., Li, G.-L., Taschenberger, H., Spirou, G., Levinson, S. R., and Von Gersdorff, H. (2005) Presynaptic Na^+ channels: locus, development, and recovery from inactivation at a high-fidelity synapse. *Journal of Neuroscience* 25, 3724-3738
27. Engel, D., and Jonas, P. (2005) Presynaptic action potential amplification by voltage-gated Na^+ channels in hippocampal mossy fiber boutons. *Neuron* 45, 405-417
28. Kawaguchi, S.-y., and Sakaba, T. (2015) Control of inhibitory synaptic outputs by low excitability of axon terminals revealed by direct recording. *Neuron* 85, 1273-1288
29. González, C., Baez-Nieto, D., Valencia, I., Oyarzún, I., Rojas, P., Naranjo, D., and Latorre, R. (2012) K^+ channels: function-structural overview. *Comprehensive physiology* 2, 2087-2149
30. Wang, H., Kunkel, D., Schwartzkroin, P. A., and Tempel, B. L. (1994) Localization of Kv1.1 and Kv1.2, two K channel proteins, to synaptic terminals, somata, and dendrites in the mouse brain. *Journal of Neuroscience* 14, 4588-4599
31. Dodson, P. D., Billups, B., Rusznák, Z., Szûcs, G., Barker, M. C., and Forsythe, I. D. (2003) Presynaptic rat Kv1.2 channels suppress synaptic terminal hyperexcitability following action potential invasion. Wiley Online Library
32. Ishikawa, T., Nakamura, Y., Saitoh, N., Li, W.-B., Iwasaki, S., and Takahashi, T. (2003) Distinct roles of Kv1 and Kv3 potassium channels at the calyx of Held presynaptic terminal. *Journal of Neuroscience* 23, 10445-10453
33. Dodson, P. D., and Forsythe, I. D. (2004) Presynaptic K^+ channels: electrifying regulators of synaptic terminal excitability. *Trends in neurosciences* 27, 210-217
34. Katz, B., and Miledi, R. (1967) The release of acetylcholine from nerve endings by graded electric pulses. *Proceedings of the Royal Society of London. Series B. Biological Sciences* 167, 23-38
35. Schneggenburger, R., and Neher, E. (2005) Presynaptic calcium and control of vesicle fusion. *Current opinion in neurobiology* 15, 266-274
36. Söllner, T., Whiteheart, S. W., Brunner, M., Erdjument-Bromage, H., Geromanos, S., Tempst, P., and Rothman, J. E. (1993) SNAP receptors implicated in vesicle targeting and fusion. *Nature* 362, 318-324
37. Chapman, E. R., An, S., Barton, N., and Jahn, R. (1994) SNAP-25, a t-SNARE which binds to both syntaxin and synaptobrevin via domains that may form coiled coils. *Journal of Biological Chemistry* 269, 27427-27432
38. Geppert, M., Goda, Y., Hammer, R. E., Li, C., Rosahl, T. W., Stevens, C. F., and Südhof, T. C. (1994) Synaptotagmin I: a major Ca^{2+} sensor for transmitter release at a central synapse. *Cell* 79, 717-727
39. Toonen, R. F., and Verhage, M. (2007) Munc18-1 in secretion: lonely Munc joins SNARE team and takes control. *Trends in neurosciences* 30, 564-572
40. Brose, N. (2008) Altered complexin expression in psychiatric and neurological disorders: cause or consequence? *Molecules & Cells (Springer Science & Business Media BV)* 25
41. Fernández-Chacón, R., Shin, O.-H., Königstorfer, A., Matos, M. F., Meyer, A. C., Garcia, J., Gerber, S. H., Rizo, J., Südhof, T. C., and Rosenmund, C. (2002) Structure/function analysis of Ca^{2+} binding to the C2A domain of synaptotagmin 1. *Journal of Neuroscience* 22, 8438-8446
42. Südhof, T. C. (2004) The synaptic vesicle cycle. *Annu. Rev. Neurosci.* 27, 509-547

43. Fujita, Y., Shirataki, H., Sakisaka, T., Asakura, T., Ohya, T., Kotani, H., Yokoyama, S., Nishioka, H., Matsuura, Y., and Mizoguchi, A. (1998) Tomosyn: a syntaxin-1–binding protein that forms a novel complex in the neurotransmitter release process. *Neuron* 20, 905-915
44. Scales, S. J., Hesser, B. A., Masuda, E. S., and Scheller, R. H. (2002) Amisyn, a novel syntaxin-binding protein that may regulate SNARE complex assembly. *Journal of Biological Chemistry* 277, 28271-28279
45. Edelmann, L., Hanson, P., Chapman, E., and Jahn, R. (1995) Synaptobrevin binding to synaptophysin: a potential mechanism for controlling the exocytotic fusion machine. *The EMBO journal* 14, 224-231
46. Südhof, T. C., and Rizo, J. (2011) Synaptic vesicle exocytosis. *Cold Spring Harbor perspectives in biology* 3, a005637
47. Gandhi, S. P., and Stevens, C. F. (2003) Three modes of synaptic vesicular recycling revealed by single-vesicle imaging. *Nature* 423, 607-613
48. Chanaday, N. L., Cousin, M. A., Milosevic, I., Watanabe, S., and Morgan, J. R. (2019) The synaptic vesicle cycle revisited: new insights into the modes and mechanisms. *Journal of Neuroscience* 39, 8209-8216
49. Heuser, J., and Reese, T. (1973) Evidence for recycling of synaptic vesicle membrane during transmitter release at the frog neuromuscular junction. *The Journal of cell biology* 57, 315-344
50. Beck, K. A., and Keen, J. H. (1991) Interaction of phosphoinositide cycle intermediates with the plasma membrane-associated clathrin assembly protein AP-2. *Journal of Biological Chemistry* 266, 4442-4447
51. Ahle, S., and Ungewickell, E. (1986) Purification and properties of a new clathrin assembly protein. *The EMBO Journal* 5, 3143-3149
52. Chen, H., Fre, S., Slepnev, V. I., Capua, M. R., Takei, K., Butler, M. H., Di Fiore, P. P., and De Camilli, P. (1998) Epsin is an EH-domain-binding protein implicated in clathrin-mediated endocytosis. *Nature* 394, 793-797
53. Henne, W. M., Kent, H. M., Ford, M. G., Hegde, B. G., Daumke, O., Butler, P. J. G., Mittal, R., Langen, R., Evans, P. R., and McMahon, H. T. (2007) Structure and analysis of FCHo2 F-BAR domain: a dimerizing and membrane recruitment module that effects membrane curvature. *Structure* 15, 839-852
54. Shimada, A., Niwa, H., Tsujita, K., Suetsugu, S., Nitta, K., Hanawa-Suetsugu, K., Akasaka, R., Nishino, Y., Toyama, M., and Chen, L. (2007) Curved EFC/F-BAR-domain dimers are joined end to end into a filament for membrane invagination in endocytosis. *Cell* 129, 761-772
55. Edeling, M. A., Smith, C., and Owen, D. (2006) Life of a clathrin coat: insights from clathrin and AP structures. *Nature reviews Molecular cell biology* 7, 32-44
56. Sweitzer, S. M., and Hinshaw, J. E. (1998) Dynamin undergoes a GTP-dependent conformational change causing vesiculation. *Cell* 93, 1021-1029
57. Haffner, C., Takei, K., Chen, H., Ringstad, N., Hudson, A., Butler, M. H., Salcini, A. E., Di Fiore, P. P., and De Camilli, P. (1997) Synaptojanin 1: localization on coated endocytic intermediates in nerve terminals and interaction of its 170 kDa isoform with Eps15. *FEBS letters* 419, 175-180
58. Schuske, K. R., Richmond, J. E., Matthies, D. S., Davis, W. S., Runz, S., Rube, D. A., van der Bliek, A. M., and Jorgensen, E. M. (2003) Endophilin is required for synaptic vesicle endocytosis by localizing synaptojanin. *Neuron* 40, 749-762
59. Chappell, T. G., Welch, W. J., Schlossman, D. M., Palter, K. B., Schlesinger, M. J., and Rothman, J. E. (1986) Uncoating ATPase is a member of the 70 kilodalton family of stress proteins. *Cell* 45, 3-13
60. Prasad, K., Barouch, W., Greene, L., and Eisenberg, E. (1993) A protein cofactor is required for uncoating of clathrin baskets by uncoating ATPase. *Journal of Biological Chemistry* 268, 23758-23761

61. Wong, K. A., Wilson, J., Russo, A., Wang, L., Okur, M. N., Wang, X., Martin, N. P., Scappini, E., Carnegie, G. K., and O'Bryan, J. P. (2012) Intersectin (ITSN) family of scaffolds function as molecular hubs in protein interaction networks. *PLoS One* 7, e36023
62. Wang, L., Johnson, A., Hanna, M., and Audhya, A. (2016) Eps15 membrane-binding and-bending activity acts redundantly with Fcho1 during clathrin-mediated endocytosis. *Molecular biology of the cell* 27, 2675-2687
63. Salazar, M. A., Kwiatkowski, A. V., Pellegrini, L., Cestra, G., Butler, M. H., Rossman, K. L., Serna, D. M., Sondek, J., Gertler, F. B., and De Camilli, P. (2003) Tuba, a novel protein containing bin/amphiphysin/Rvs and Dbl homology domains, links dynamin to regulation of the actin cytoskeleton. *Journal of Biological Chemistry* 278, 49031-49043
64. Miki, H., Miura, K., and Takenawa, T. (1996) N-WASP, a novel actin-depolymerizing protein, regulates the cortical cytoskeletal rearrangement in a PIP2-dependent manner downstream of tyrosine kinases. *The EMBO journal* 15, 5326-5335
65. Saheki, Y., and De Camilli, P. (2012) Synaptic vesicle endocytosis. *Cold Spring Harbor perspectives in biology* 4, a005645
66. Peter, B. J., Kent, H. M., Mills, I. G., Vallis, Y., Butler, P. J. G., Evans, P. R., and McMahon, H. T. (2004) BAR domains as sensors of membrane curvature: the amphiphysin BAR structure. *Science* 303, 495-499
67. Wu, T., and Baumgart, T. (2014) BIN1 membrane curvature sensing and generation show autoinhibition regulated by downstream ligands and PI (4, 5) P2. *Biochemistry* 53, 7297-7309
68. Taylor, M. J., Perrais, D., and Merrifield, C. J. (2011) A high precision survey of the molecular dynamics of mammalian clathrin-mediated endocytosis. *PLoS biol* 9, e1000604
69. Ceccarelli, B., Hurlbut, W., and Mauro, A. (1973) Turnover of transmitter and synaptic vesicles at the frog neuromuscular junction. *The Journal of cell biology* 57, 499-524
70. Staal, R. G., Mosharov, E. V., and Sulzer, D. (2004) Dopamine neurons release transmitter via a flickering fusion pore. *Nature neuroscience* 7, 341-346
71. Qin, X., Tsien, R. W., and Park, H. (2019) Real-time three-dimensional tracking of single synaptic vesicles reveals that synaptic vesicles undergoing kiss-and-run fusion remain close to their original fusion site before reuse. *Biochemical and biophysical research communications* 514, 1004-1008
72. Watanabe, S., Rost, B. R., Camacho-Pérez, M., Davis, M. W., Söhl-Kielczynski, B., Rosenmund, C., and Jorgensen, E. M. (2013) Ultrafast endocytosis at mouse hippocampal synapses. *Nature* 504, 242-247
73. Delvendahl, I., Vyleta, N. P., von Gersdorff, H., and Hallermann, S. (2016) Fast, temperature-sensitive and clathrin-independent endocytosis at central synapses. *Neuron* 90, 492-498
74. Watanabe, S., Mamer, L. E., Raychaudhuri, S., Luvsanjav, D., Eisen, J., Trimbuch, T., Söhl-Kielczynski, B., Fenske, P., Milosevic, I., and Rosenmund, C. (2018) Synaptojanin and endophilin mediate neck formation during ultrafast endocytosis. *Neuron* 98, 1184-1197. e1186
75. Clayton, E. L., Evans, G. J., and Cousin, M. A. (2008) Bulk synaptic vesicle endocytosis is rapidly triggered during strong stimulation. *Journal of Neuroscience* 28, 6627-6632
76. Cousin, M. A. (2009) Activity-dependent bulk synaptic vesicle endocytosis—a fast, high capacity membrane retrieval mechanism. *Molecular neurobiology* 39, 185-189
77. Wu, W., Xu, J., Wu, X.-S., and Wu, L.-G. (2005) Activity-dependent acceleration of endocytosis at a central synapse. *Journal of Neuroscience* 25, 11676-11683
78. Clayton, E. L., Anggono, V., Smillie, K. J., Chau, N., Robinson, P. J., and Cousin, M. A. (2009) The phospho-dependent dynamin–syndapin interaction triggers activity-dependent bulk endocytosis of synaptic vesicles. *Journal of Neuroscience* 29, 7706-7717
79. Cheung, G., and Cousin, M. A. (2019) Synaptic vesicle generation from activity-dependent bulk endosomes requires a dephosphorylation-dependent dynamin–syndapin interaction. *Journal of neurochemistry* 151, 570-583

80. Kononenko, N. L., Puchkov, D., Classen, G. A., Walter, A. M., Pechstein, A., Sawade, L., Kaempf, N., Trimbuch, T., Lorenz, D., and Rosenmund, C. (2014) Clathrin/AP-2 mediate synaptic vesicle reformation from endosome-like vacuoles but are not essential for membrane retrieval at central synapses. *Neuron* 82, 981-988
81. Cheung, G., and Cousin, M. A. (2012) Adaptor protein complexes 1 and 3 are essential for generation of synaptic vesicles from activity-dependent bulk endosomes. *Journal of Neuroscience* 32, 6014-6023
82. Hoopmann, P., Punge, A., Barysch, S. V., Westphal, V., Bückers, J., Opazo, F., Bethani, I., Lauterbach, M. A., Hell, S. W., and Rizzoli, S. O. (2010) Endosomal sorting of readily releasable synaptic vesicles. *Proceedings of the National Academy of Sciences* 107, 19055-19060
83. Stadler, H., and Tsukita, S. (1984) Synaptic vesicles contain an ATP-dependent proton pump and show ‘knob-like’protrusions on their surface. *The EMBO journal* 3, 3333-3337
84. Maycox, P., Deckwerth, T., Hell, J. W., and Jahn, R. (1988) Glutamate uptake by brain synaptic vesicles. Energy dependence of transport and functional reconstitution in proteoliposomes. *Journal of Biological Chemistry* 263, 15423-15428
85. Strata, P., and Harvey, R. (1999) Dale's principle. *Brain research bulletin* 50, 349-350
86. Zeisel, A., Hochgerner, H., Lönnerberg, P., Johnsson, A., Memic, F., Van Der Zwan, J., Häring, M., Braun, E., Borm, L. E., and La Manno, G. (2018) Molecular architecture of the mouse nervous system. *Cell* 174, 999-1014. e1022
87. Upmanyu, N., Jin, J., Ganzella, M., Bösche, L., Malviya, V. N., Zhuleku, E., Politi, A., Ninov, M., Silbern, I., Urlaub, H., Riedel, D., Preobraschenski, J., Milosevic, I., Jahn, R., and Sambandan, S. (2021) Co-localization of different Neurotransmitter Transporters on the same Synaptic Vesicle is Bona-fide yet Sparse. *bioRxiv*
88. Fernández-Busnadiego, R., Asano, S., Oprisoreanu, A.-M., Sakata, E., Doengi, M., Kochovski, Z., Zürner, M., Stein, V., Schoch, S., and Baumeister, W. (2013) Cryo–electron tomography reveals a critical role of RIM1α in synaptic vesicle tethering. *Journal of Cell Biology* 201, 725-740
89. Imig, C., Min, S.-W., Krinner, S., Arancillo, M., Rosenmund, C., Südhof, T. C., Rhee, J., Brose, N., and Cooper, B. H. (2014) The morphological and molecular nature of synaptic vesicle priming at presynaptic active zones. *Neuron* 84, 416-431
90. Neher, E., and Brose, N. (2018) Dynamically primed synaptic vesicle states: key to understand synaptic short-term plasticity. *Neuron* 100, 1283-1291
91. Schrimpf, S. P., Meskenaite, V., Brunner, E., Rutishauser, D., Walther, P., Eng, J., Aebersold, R., and Sonderegger, P. (2005) Proteomic analysis of synaptosomes using isotope-coded affinity tags and mass spectrometry. *Proteomics* 5, 2531-2541
92. Hebb, C. O., and Whittaker, V. (1958) Intracellular distributions of acetylcholine and choline acetylase. *The journal of physiology* 142, 187-196
93. Gray, E., and Whittaker, V. (1962) The isolation of nerve endings from brain: an electron microscopic study of cell fragments derived by homogenization and centrifugation. *Journal of anatomy* 96, 79
94. Nicholls, D. G. (1989) Release of glutamate, aspartate, and γ-aminobutyric acid from isolated nerve terminals. *Journal of neurochemistry* 52, 331-341
95. Xue, J., Quan, A., and Robinson, P. J. (2018) Preparation of P2 or Percoll-Purified Synaptosomes from Mammalian Brain Tissue. *Synaptosomes*, pp. 85-105, Springer
96. Dunkley, P. R., and Robinson, P. J. (2018) Synaptosome Preparations: Which Procedure Should I Use? *Synaptosomes*, pp. 27-53, Springer
97. Dunkley, P. R., Heath, J. W., Harrison, S. M., Jarvie, P. E., Glenfield, P. J., and Rostas, J. A. (1988) A rapid Percoll gradient procedure for isolation of synaptosomes directly from an S1 fraction: homogeneity and morphology of subcellular fractions. *Brain research* 441, 59-71

98. Kauppinen, R. A., and Nicholls, D. G. (1986) Synaptosomal bioenergetics: the role of glycolysis, pyruvate oxidation and responses to hypoglycaemia. *European journal of biochemistry* 158, 159-165
99. Nicholls, D. G. (2003) Bioenergetics and transmitter release in the isolated nerve terminal. *Neurochemical research* 28, 1433-1441
100. McMahon, H. T., and Nicholls, D. G. (1991) Transmitter glutamate release from isolated nerve terminals: evidence for biphasic release and triggering by localized Ca^{2+}. *Journal of neurochemistry* 56, 86-94
101. Komulainen, H., and Bondy, S. (1987) The estimation of free calcium within synaptosomes and mitochondria with fura-2; comparison to quin-2. *Neurochemistry international* 10, 55-64
102. Barrie, A. P., Nicholls, D. G., Sanchez-Prieto, J., and Sihra, T. S. (1991) An ion channel locus for the protein kinase C potentiation of transmitter glutamate release from guinea pig cerebrocortical synaptosomes. *Journal of neurochemistry* 57, 1398-1404
103. Cousin, M. A., and Robinson, P. J. (2000) Two mechanisms of synaptic vesicle recycling in rat brain nerve terminals. *Journal of neurochemistry* 75, 1645-1653
104. Zoccarato, F., Cavallini, L., and Alexandre, A. (1999) The pH-Sensitive Dye Acridine Orange as a Tool to MonitorExocytosis/Endocytosis in Synaptosomes. *Journal of neurochemistry* 72, 625-633
105. Bradford, H. F. (1970) Metabolic response of synaptosomes to electrical stimulation: release of amino acids. *Brain Res* 19, 239-247
106. Hawthorne, J. N., and Bleasdale, J. E. (1975) Phosphatidic acid metabolism, calcium ions and transmitter release from electrically stimulated synaptosomes. *Mol Cell Biochem* 8, 83-87
107. Bleasdale, J. E., and Hawthorne, J. N. (1975) The effect of electrical stimulation on the turnover of phosphatidic acid in synaptosomes from guinea-pig brain. *J Neurochem* 24, 373-379
108. Osborne, R. H., Bradford, H. F., and Jones, D. G. (1973) Patterns of amino acid release from nerve-endings isolated from spinal cord and medulla. *J Neurochem* 21, 407-419
109. Bradford, H. F., Bennett, G. W., and Thomas, A. J. (1973) Depolarizing stimuli and the release of physiologically active amino acids from suspensions of mammalian synaptosomes. *J Neurochem* 21, 495-505
110. Lahdesmaki, P., Pasula, M., and Oja, S. S. (1975) Effect of electrical stimulation and chlorpromazine on the uptake and release of taurine, gamma-aminobutyric acid and glutamic acid in mouse brain synaptosomes. *J Neurochem* 25, 675-680
111. Swanson, P. D., Anderson, L., and Stahl, W. L. (1974) Uptake of calcium ions by synaptosomes from rat brain. *Biochim Biophys Acta* 356, 174-183
112. Goncalves, M. L., Pinto, F., and Ribeiro, J. A. (1991) Effect of adenosine on $^{45}Ca^{2+}$ uptake by electrically stimulated rat brain synaptosomes. *J Neurochem* 56, 1769-1773
113. Osborne, R. H., and Bradford, H. F. (1973) Tetanus toxin inhibits amino acid release from nerve endings in vitro. *Nat New Biol* 244, 157-158
114. Nicholls, D. G. (2018) Synaptosomal Bioenergetics and Glutamate Release. *Synaptosomes*, pp. 109-129, Springer
115. Scott, I., and Nicholls, D. (1980) Energy transduction in intact synaptosomes. Influence of plasma-membrane depolarization on the respiration and membrane potential of internal mitochondria determined in situ. *Biochemical Journal* 186, 21-33
116. Tibbs, G. R., Dolly, J. O., and Nicholls, D. G. (1989) Dendrotoxin, 4-aminopyridine, and β-bungarotoxin act at common loci but by two distinct mechanisms to induce Ca^{2+}-dependent release of glutamate from guinea-pig cerebrocortical synaptosomes. *Journal of neurochemistry* 52, 201-206
117. Tibbs, G., Barrie, A., Van Mieghem, F., McMahon, H. a., and Nicholls, D. (1989) Repetitive action potentials in isolated nerve terminals in the presence of 4-aminopyridine: effects on cytosolic free Ca^{2+} and glutamate release. *Journal of neurochemistry* 53, 1693-1699

118. Nicholls, D. G., Sihra, T. S., and Sanchez-Prieto, J. (1987) Calcium-dependent and-independent release of glutamate from synaptosomes monitored by continuous fluorometry. *Journal of neurochemistry* 49, 50-57
119. Turner, T. J., Lampe, R. A., and Dunlap, K. (1995) Characterization of presynaptic calcium channels with omega-conotoxin MVIIC and omega-grammotoxin SIA: role for a resistant calcium channel type in neurosecretion. *Mol Pharmacol* 47, 348-353
120. Montecucco, C., Schiavo, G., and Pantano, S. (2005) SNARE complexes and neuroexocytosis: how many, how close? *Trends Biochem Sci* 30, 367-372
121. Sanchez-Prieto, J., Sihra, T. S., Evans, D., Ashton, A., Dolly, J. O., and Nicholls, D. G. (1987) Botulinum toxin A blocks glutamate exocytosis from guinea-pig cerebral cortical synaptosomes. *Eur J Biochem* 165, 675-681
122. McMahon, H. T., Foran, P., Dolly, J. O., Verhage, M., Wiegant, V. M., and Nicholls, D. G. (1992) Tetanus toxin and botulinum toxins type A and B inhibit glutamate, gamma-aminobutyric acid, aspartate, and met-enkephalin release from synaptosomes. Clues to the locus of action. *J Biol Chem* 267, 21338-21343
123. Rizzoli, S. O., and Betz, W. J. (2005) Synaptic vesicle pools. *Nature Reviews Neuroscience* 6, 57-69
124. Elmqvist, D., and Quastel, D. (1965) A quantitative study of end-plate potentials in isolated human muscle. *The Journal of physiology* 178, 505-529
125. Waters, J., and Smith, S. J. (2002) Vesicle pool partitioning influences presynaptic diversity and weighting in rat hippocampal synapses. *The Journal of physiology* 541, 811-823
126. Hanse, E., and Gustafsson, B. (2001) Vesicle release probability and pre-primed pool at glutamatergic synapses in area CA1 of the rat neonatal hippocampus. *The Journal of Physiology* 531, 481-493
127. Neher, E., and Taschenberger, H. (2021) Non-negative matrix factorization as a tool to distinguish between synaptic vesicles in different functional states. *Neuroscience* 458, 182-202
128. Zhang, Q., Li, Y., and Tsien, R. W. (2009) The dynamic control of kiss-and-run and vesicular reuse probed with single nanoparticles. *Science* 323, 1448-1453
129. Granseth, B., Odermatt, B., Royle, S. J., and Lagnado, L. (2009) Comment on “The Dynamic Control of Kiss-and-Run and Vesicular Reuse Probed with Single Nanoparticles”. *Science* 325, 1499-1499
130. Kamin, D., Lauterbach, M. A., Westphal, V., Keller, J., Schönle, A., Hell, S. W., and Rizzoli, S. O. (2010) High-and low-mobility stages in the synaptic vesicle cycle. *Biophysical Journal* 99, 675-684
131. Denker, A., and Rizzoli, S. O. (2010) Synaptic vesicle pools: an update. *Frontiers in synaptic neuroscience* 2, 135
132. Hayashi, M., Raimondi, A., O'Toole, E., Paradise, S., Collesi, C., Cremona, O., Ferguson, S. M., and De Camilli, P. (2008) Cell-and stimulus-dependent heterogeneity of synaptic vesicle endocytic recycling mechanisms revealed by studies of dynamin 1-null neurons. *Proceedings of the National Academy of Sciences* 105, 2175-2180
133. Citri, A., and Malenka, R. C. (2008) Synaptic plasticity: multiple forms, functions, and mechanisms. *Neuropsychopharmacology* 33, 18-41
134. Bairoch, A., and Apweiler, R. (2000) The SWISS-PROT protein sequence database and its supplement TrEMBL in 2000. *Nucleic acids research* 28, 45-48
135. Khoury, G. A., Baliban, R. C., and Floudas, C. A. (2011) Proteome-wide post-translational modification statistics: frequency analysis and curation of the swiss-prot database. *Scientific reports* 1, 1-5
136. Cohen, P. (2002) The origins of protein phosphorylation. *Nature cell biology* 4, E127-E130
137. Burnett, G., and Kennedy, E. P. (1954) The enzymatic phosphorylation of proteins. *Journal of Biological Chemistry* 211, 969-980
138. Cieśla, J., Frączyk, T., and Rode, W. (2011) Phosphorylation of basic amino acid residues in proteins: important but easily missed. *Acta Biochimica Polonica* 58

139. Fuhs, S. R., and Hunter, T. (2017) pHisphorylation: the emergence of histidine phosphorylation as a reversible regulatory modification. *Current opinion in cell biology* 45, 8-16
140. Ohsako, S., Nakazawa, H., Sekihara, S.-i., Ikai, A., and Yamauchi, T. (1991) Role of threonine-286 as autophosphorylation site for appearance of Ca^{2+}-independent activity of calmodulin-dependent protein kinase II α subunit. *The Journal of Biochemistry* 109, 137-143
141. Rellos, P., Pike, A. C., Niesen, F. H., Salah, E., Lee, W. H., Von Delft, F., and Knapp, S. (2010) Structure of the CaMKIIδ/calmodulin complex reveals the molecular mechanism of CaMKII kinase activation. *PLoS biology* 8, e1000426
142. Yaffe, M. B., and Elia, A. E. (2001) Phosphoserine/threonine-binding domains. *Current opinion in cell biology* 13, 131-138
143. Kaneko, T., Joshi, R., Feller, S. M., and Li, S. S. (2012) Phosphotyrosine recognition domains: the typical, the atypical and the versatile. *Cell Communication and Signaling* 10, 1-20
144. Miller, M. L., Jensen, L. J., Diella, F., Jørgensen, C., Tinti, M., Li, L., Hsiung, M., Parker, S. A., Bordeaux, J., and Sicheritz-Ponten, T. (2008) Linear motif atlas for phosphorylation-dependent signaling. *Science signaling* 1, ra2-ra2
145. Manning, G., Whyte, D. B., Martinez, R., Hunter, T., and Sudarsanam, S. (2002) The protein kinase complement of the human genome. *Science* 298, 1912-1934
146. Soderling, T. R., and Derkach, V. A. (2000) Postsynaptic protein phosphorylation and LTP. *Trends in neurosciences* 23, 75-80
147. Myers, J. B., Zaegel, V., Coultrap, S. J., Miller, A. P., Bayer, K. U., and Reichow, S. L. (2017) The CaMKII holoenzyme structure in activation-competent conformations. *Nature communications* 8, 1-15
148. Kennedy, M. B. (2010) Calcium/calmodulin-dependent protein kinase II. *Handbook of Cell Signaling*, pp. 565-568, Elsevier
149. Patton, B. L., Miller, S. G., and Kennedy, M. B. (1990) Activation of type II calcium/calmodulin-dependent protein kinase by Ca^{2+}/calmodulin is inhibited by autophosphorylation of threonine within the calmodulin-binding domain. *Journal of Biological Chemistry* 265, 11204-11212
150. Barria, A., Muller, D., Derkach, V., Griffith, L. C., and Soderling, T. R. (1997) Regulatory phosphorylation of AMPA-type glutamate receptors by CaM-KII during long-term potentiation. *Science* 276, 2042-2045
151. Omkumar, R. V., Kiely, M. J., Rosenstein, A. J., Min, K.-T., and Kennedy, M. B. (1996) Identification of a phosphorylation site for calcium/calmodulindependent protein kinase II in the NR2B subunit of the N-methyl-D-aspartate receptor. *Journal of Biological Chemistry* 271, 31670-31678
152. Chen, H.-J., Rojas-Soto, M., Oguni, A., and Kennedy, M. B. (1998) A synaptic Ras-GTPase activating protein (p135 SynGAP) inhibited by CaM kinase II. *Neuron* 20, 895-904
153. Huttner, W., DeGennaro, L., and Greengard, P. (1981) Differential phosphorylation of multiple sites in purified protein I by cyclic AMP-dependent and calcium-dependent protein kinases. *Journal of Biological Chemistry* 256, 1482-1488
154. Greengard, P., Benfenati, F., and Valtorta, F. (1994) Synapsin I, an actin-binding protein regulating synaptic vesicle traffic in the nerve terminal. *Advances in second messenger and phosphoprotein research* 29, 31-45
155. Ceccaldi, P.-E., Grohovaz, F., Benfenati, F., Chieregatti, E., Greengard, P., and Valtorta, F. (1995) Dephosphorylated synapsin I anchors synaptic vesicles to actin cytoskeleton: an analysis by videomicroscopy. *The Journal of cell biology* 128, 905-912
156. Ninan, I., and Arancio, O. (2004) Presynaptic CaMKII is necessary for synaptic plasticity in cultured hippocampal neurons. *Neuron* 42, 129-141
157. Hojjati, M. R., Van Woerden, G. M., Tyler, W. J., Giese, K. P., Silva, A. J., Pozzo-Miller, L., and Elgersma, Y. (2007) Kinase activity is not required for αCaMKII-dependent presynaptic plasticity at CA3-CA1 synapses. *Nature neuroscience* 10, 1125-1127

158. Okamoto, K.-I., Narayanan, R., Lee, S. H., Murata, K., and Hayashi, Y. (2007) The role of CaMKII as an F-actin-bundling protein crucial for maintenance of dendritic spine structure. *Proceedings of the National Academy of Sciences* 104, 6418-6423
159. Wortzel, I., and Seger, R. (2011) The ERK cascade: distinct functions within various subcellular organelles. *Genes & cancer* 2, 195-209
160. Johnson, G. L., and Lapadat, R. (2002) Mitogen-activated protein kinase pathways mediated by ERK, JNK, and p38 protein kinases. *Science* 298, 1911-1912
161. Payne, D. M., Rossomando, A., Martino, P., Erickson, A., Her, J., Shabanowitz, J., Hunt, D., Weber, M., and Sturgill, T. (1991) Identification of the regulatory phosphorylation sites in pp42/mitogen-activated protein kinase (MAP kinase). *The EMBO journal* 10, 885-892
162. Gonzalez, F. A., Raden, D. L., and Davis, R. J. (1991) Identification of substrate recognition determinants for human ERK1 and ERK2 protein kinases. *Journal of Biological Chemistry* 266, 22159-22163
163. Boulton, T. G., Nye, S. H., Robbins, D. J., Ip, N. Y., Radzlejewska, E., Morgenbesser, S. D., DePinho, R. A., Panayotatos, N., Cobb, M. H., and Yancopoulos, G. D. (1991) ERKs: a family of protein-serine/threonine kinases that are activated and tyrosine phosphorylated in response to insulin and NGF. *Cell* 65, 663-675
164. Fiore, R., Murphy, T., Sanghera, J., Pelech, S., and Baraban, J. M. (1993) Activation of p42 mitogen-activated protein kinase by glutamate receptor stimulation in rat primary cortical cultures. *Journal of neurochemistry* 61, 1626-1633
165. Kurino, M., Fukunaga, K., Ushio, Y., and Miyamoto, E. (1995) Activation of mitogen-activated protein kinase in cultured rat hippocampal neurons by stimulation of glutamate receptors. *Journal of neurochemistry* 65, 1282-1289
166. Xia, Z., Dudek, H., Miranti, C. K., and Greenberg, M. E. (1996) Calcium influx via the NMDA receptor induces immediate early gene transcription by a MAP kinase/ERK-dependent mechanism. *Journal of Neuroscience* 16, 5425-5436
167. Rosen, L. B., Ginty, D. D., Weber, M. J., and Greenberg, M. E. (1994) Membrane depolarization and calcium influx stimulate MEK and MAP kinase via activation of Ras. *Neuron* 12, 1207-1221
168. Walker, S. A., Cullen, P. J., Taylor, J. A., and Lockyer, P. J. (2003) Control of Ras cycling by Ca^{2+}. *FEBS letters* 546, 6-10
169. Thomas, G. M., and Huganir, R. L. (2004) MAPK cascade signalling and synaptic plasticity. *Nature Reviews Neuroscience* 5, 173-183
170. Adams, J. P., Anderson, A. E., Varga, A. W., Dineley, K. T., Cook, R. G., Pfaffinger, P. J., and Sweatt, J. D. (2000) The A-type potassium channel Kv4. 2 is a substrate for the mitogen-activated protein kinase ERK. *Journal of neurochemistry* 75, 2277-2287
171. Matsubara, M., Kusubata, M., Ishiguro, K., Uchida, T., Titani, K., and Taniguchi, H. (1996) Site-specific phosphorylation of synapsin I by mitogen-activated protein kinase and Cdk5 and its effects on physiological functions. *Journal of Biological Chemistry* 271, 21108-21113
172. Patterson, S. L., Pittenger, C., Morozov, A., Martin, K. C., Scanlin, H., Drake, C., and Kandel, E. R. (2001) Some forms of cAMP-mediated long-lasting potentiation are associated with release of BDNF and nuclear translocation of phospho-MAP kinase. *Neuron* 32, 123-140
173. Davis, S., Vanhoutte, P., Pages, C., Caboche, J., and Laroche, S. (2000) The MAPK/ERK cascade targets both Elk-1 and cAMP response element-binding protein to control long-term potentiation-dependent gene expression in the dentate gyrus in vivo. *Journal of Neuroscience* 20, 4563-4572
174. Elkins, J. M., and Knapp, S. (2012) The Structure of the Full-Length Tetrameric PKA Regulatory RIIβ Complex Reveals the Mechanism of Allosteric PKA Activation. *Science signaling* 5, pe21-pe21
175. Smith, F. D., Esseltine, J. L., Nygren, P. J., Veesler, D., Byrne, D. P., Vonderach, M., Strashnov, I., Eyers, C. E., Eyers, P. A., and Langeberg, L. K. (2017) Local protein kinase A action proceeds through intact holoenzymes. *Science* 356, 1288-1293

176. Lonart, G., Schoch, S., Kaeser, P. S., Larkin, C. J., Südhof, T. C., and Linden, D. J. (2003) Phosphorylation of RIM1α by PKA triggers presynaptic long-term potentiation at cerebellar parallel fiber synapses. *Cell* 115, 49-60
177. Kaeser, P. S., Kwon, H.-B., Blundell, J., Chevaleyre, V., Morishita, W., Malenka, R. C., Powell, C. M., Castillo, P. E., and Südhof, T. C. (2008) RIM1α phosphorylation at serine-413 by protein kinase A is not required for presynaptic long-term plasticity or learning. *Proceedings of the National Academy of Sciences* 105, 14680-14685
178. Nagy, G., Reim, K., Matti, U., Brose, N., Binz, T., Rettig, J., Neher, E., and Sørensen, J. B. (2004) Regulation of releasable vesicle pool sizes by protein kinase A-dependent phosphorylation of SNAP-25. *Neuron* 41, 417-429
179. Cho, R. W., Buhl, L. K., Volfson, D., Tran, A., Li, F., Akbergenova, Y., and Littleton, J. T. (2015) Phosphorylation of complexin by PKA regulates activity-dependent spontaneous neurotransmitter release and structural synaptic plasticity. *Neuron* 88, 749-761
180. Park, A. J., Havekes, R., Choi, J. H., Luczak, V., Nie, T., Huang, T., and Abel, T. (2014) A presynaptic role for PKA in synaptic tagging and memory. *Neurobiology of learning and memory* 114, 101-112
181. Waltereit, R., and Weller, M. (2003) Signaling from cAMP/PKA to MAPK and synaptic plasticity. *Molecular neurobiology* 27, 99-106
182. Newton, A. C. (2018) Protein kinase C: perfectly balanced. *Critical reviews in biochemistry and molecular biology* 53, 208-230
183. Nakanishi, H., and Exton, J. H. (1992) Purification and characterization of the zeta isoform of protein kinase C from bovine kidney. *Journal of Biological Chemistry* 267, 16347-16354
184. Keranen, L. M., Dutil, E. M., and Newton, A. C. (1995) Protein kinase C is regulated in vivo by three functionally distinct phosphorylations. *Current Biology* 5, 1394-1403
185. Wierda, K. D., Toonen, R. F., de Wit, H., Brussaard, A. B., and Verhage, M. (2007) Interdependence of PKC-dependent and PKC-independent pathways for presynaptic plasticity. *Neuron* 54, 275-290
186. Shimazaki, Y., Nishiki, T.-i., Omori, A., Sekiguchi, M., Kamata, Y., Kozaki, S., and Takahashi, M. (1996) Phosphorylation of 25-kDa synaptosome-associated protein: possible involvement in protein kinase C-mediated regulation of neurotransmitter release. *Journal of Biological Chemistry* 271, 14548-14553
187. Barclay, J. W., Craig, T. J., Fisher, R. J., Ciufo, L. F., Evans, G. J., Morgan, A., and Burgoyne, R. D. (2003) Phosphorylation of Munc18 by protein kinase C regulates the kinetics of exocytosis. *Journal of Biological Chemistry* 278, 10538-10545
188. Hilfiker, S., Pieribone, V. A., Nordstedt, C., Greengard, P., and Czernik, A. J. (1999) Regulation of synaptotagmin I phosphorylation by multiple protein kinases. *Journal of neurochemistry* 73, 921-932
189. Cheng, K., and Ip, N. Y. (2003) Cdk5: a new player at synapses. *Neurosignals* 12, 180-190
190. Lew, J., Huang, Q.-Q., Qi, Z., Winkfein, R. J., Aebersold, R., Hunt, T., and Wang, J. H. (1994) A brain-specific activator of cyclin-dependent kinase 5. *Nature* 371, 423-426
191. Tsai, L.-H., Delalle, I., Caviness, V. S., Chae, T., and Harlow, E. (1994) p35 is a neural-specific regulatory subunit of cyclin-dependent kinase 5. *Nature* 371, 419-423
192. Tang, D., Yeung, J., Lee, K.-Y., Matsushita, M., Matsui, H., Tomizawa, K., Hatase, O., and Wang, J. H. (1995) An isoform of the neuronal cyclin-dependent kinase 5 (Cdk5) activator. *Journal of Biological Chemistry* 270, 26897-26903
193. Humbert, S., Dhavan, R., and Tsai, L. (2000) p39 activates cdk5 in neurons, and is associated with the actin cytoskeleton. *Journal of cell science* 113, 975-983
194. Wei, F. Y., Tomizawa, K., Ohshima, T., Asada, A., Saito, T., Nguyen, C., Bibb, J. A., Ishiguro, K., Kulkarni, A. B., and Pant, H. C. (2005) Control of cyclin-dependent kinase 5 (Cdk5) activity by glutamatergic regulation of p35 stability. *Journal of neurochemistry* 93, 502-512

195. Zukerberg, L. R., Patrick, G. N., Nikolic, M., Humbert, S., Wu, C.-L., Lanier, L. M., Gertler, F. B., Vidal, M., Van Etten, R. A., and Tsai, L.-H. (2000) Cables links Cdk5 and c-Abl and facilitates Cdk5 tyrosine phosphorylation, kinase upregulation, and neurite outgrowth. *Neuron* 26, 633-646
196. Sasaki, Y., Cheng, C., Uchida, Y., Nakajima, O., Ohshima, T., Yagi, T., Taniguchi, M., Nakayama, T., Kishida, R., and Kudo, Y. (2002) Fyn and Cdk5 mediate semaphorin-3A signaling, which is involved in regulation of dendrite orientation in cerebral cortex. *Neuron* 35, 907-920
197. Jovanovic, J. N., Sihra, T. S., Nairn, A. C., Hemmings, H. C., Greengard, P., and Czernik, A. J. (2001) Opposing changes in phosphorylation of specific sites in synapsin I during Ca^{2+}-dependent glutamate release in isolated nerve terminals. *Journal of Neuroscience* 21, 7944-7953
198. Shuang, R., Zhang, L., Fletcher, A., Groblewski, G. E., Pevsner, J., and Stuenkel, E. L. (1998) Regulation of Munc-18/syntaxin 1A interaction by cyclin-dependent kinase 5 in nerve endings. *Journal of Biological Chemistry* 273, 4957-4966
199. Fletcher, A. I., Shuang, R., Giovannucci, D. R., Zhang, L., Bittner, M. A., and Stuenkel, E. L. (1999) Regulation of exocytosis by cyclin-dependent kinase 5 via phosphorylation of Munc18. *Journal of Biological Chemistry* 274, 4027-4035
200. Tomizawa, K., Ohta, J., Matsushita, M., Moriwaki, A., Li, S.-T., Takei, K., and Matsui, H. (2002) Cdk5/p35 regulates neurotransmitter release through phosphorylation and downregulation of P/Q-type voltage-dependent calcium channel activity. *Journal of Neuroscience* 22, 2590-2597
201. Floyd, S. R., Porro, E. B., Slepnev, V. I., Ochoa, G.-C., Tsai, L.-H., and De Camilli, P. (2001) Amphiphysin 1 binds the cyclin-dependent kinase (cdk) 5 regulatory subunit p35 and is phosphorylated by cdk5 and cdc2. *Journal of Biological Chemistry* 276, 8104-8110
202. Liang, S., Wei, F. Y., Wu, Y. M., Tanabe, K., Abe, T., Oda, Y., Yoshida, Y., Yamada, H., Matsui, H., and Tomizawa, K. (2007) Major Cdk5-dependent phosphorylation sites of amphiphysin 1 are implicated in the regulation of the membrane binding and endocytosis. *Journal of neurochemistry* 102, 1466-1476
203. Clayton, E. L., Sue, N., Smillie, K. J., O'Leary, T., Bache, N., Cheung, G., Cole, A. R., Wyllie, D. J., Sutherland, C., and Robinson, P. J. (2010) Dynamin I phosphorylation by GSK3 controls activity-dependent bulk endocytosis of synaptic vesicles. *Nature neuroscience* 13, 845-851
204. Lee, S. Y., Wenk, M. R., Kim, Y., Nairn, A. C., and De Camilli, P. (2004) Regulation of synaptojanin 1 by cyclin-dependent kinase 5 at synapses. *Proceedings of the National Academy of Sciences* 101, 546-551
205. Cousin, M. A., and Robinson, P. J. (2001) The dephosphins: dephosphorylation by calcineurin triggers synaptic vesicle endocytosis. *Trends in neurosciences* 24, 659-665
206. Tan, T. C., Valova, V. A., Malladi, C. S., Graham, M. E., Berven, L. A., Jupp, O. J., Hansra, G., McClure, S. J., Sarcevic, B., and Boadle, R. A. (2003) Cdk5 is essential for synaptic vesicle endocytosis. *Nature cell biology* 5, 701-710
207. Beurel, E., Grieco, S. F., and Jope, R. S. (2015) Glycogen synthase kinase-3 (GSK3): regulation, actions, and diseases. *Pharmacology & therapeutics* 148, 114-131
208. ter Haar, E., Coll, J. T., Austen, D. A., Hsiao, H.-M., Swenson, L., and Jain, J. (2001) Structure of GSK3β reveals a primed phosphorylation mechanism. *Nature structural biology* 8, 593-596
209. Frame, S., Cohen, P., and Biondi, R. M. (2001) A common phosphate binding site explains the unique substrate specificity of GSK3 and its inactivation by phosphorylation. *Molecular cell* 7, 1321-1327
210. Song, B., Lai, B., Zheng, Z., Zhang, Y., Luo, J., Wang, C., Chen, Y., Woodgett, J. R., and Li, M. (2010) Inhibitory phosphorylation of GSK-3 by CaMKII couples depolarization to neuronal survival. *Journal of Biological Chemistry* 285, 41122-41134
211. Zhu, L.-Q., Liu, D., Hu, J., Cheng, J., Wang, S.-H., Wang, Q., Wang, F., Chen, J.-G., and Wang, J.-Z. (2010) GSK-3β inhibits presynaptic vesicle exocytosis by

phosphorylating P/Q-type calcium channel and interrupting snare complex formation. *Journal of Neuroscience* 30, 3624-3633
212. Hanger, D. P., Hughes, K., Woodgett, J. R., Brion, J. P., and Anderton, B. H. (1992) Glycogen synthase kinase-3 induces Alzheimer's disease-like phosphorylation of tau: generation of paired helical filament epitopes and neuronal localisation of the kinase. *Neurosci Lett* 147, 58-62
213. Cheong, J. K., and Virshup, D. M. (2011) Casein kinase 1: Complexity in the family. *Int J Biochem Cell Biol* 43, 465-469
214. Eide, E. J., and Virshup, D. M. (2001) Casein kinase I: another cog in the circadian clockworks. *Chronobiology international* 18, 389-398
215. Ebisawa, T. (2007) Circadian rhythms in the CNS and peripheral clock disorders: human sleep disorders and clock genes. *Journal of pharmacological sciences* 103, 150-154
216. Lampe, P. D., and Lau, A. F. (2004) The effects of connexin phosphorylation on gap junctional communication. *The international journal of biochemistry & cell biology* 36, 1171-1186
217. Salinas, P. C. (2007) Modulation of the microtubule cytoskeleton: a role for a divergent canonical Wnt pathway. *Trends in cell biology* 17, 333-342
218. Purro, S. A., Galli, S., and Salinas, P. C. (2014) Dysfunction of Wnt signaling and synaptic disassembly in neurodegenerative diseases. *Journal of molecular cell biology* 6, 75-80
219. Price, M. A. (2006) CKI, there's more than one: casein kinase I family members in Wnt and Hedgehog signaling. *Genes & development* 20, 399-410
220. Flaherty, D., Soria, J., Tomasiewicz, H., and Wood, J. (2000) Phosphorylation of human tau protein by microtubule-associated kinases: GSK3β and cdk5 are key participants. *Journal of neuroscience research* 62, 463-472
221. Perez, D. I., Gil, C., and Martinez, A. (2011) Protein kinases CK1 and CK2 as new targets for neurodegenerative diseases. *Medicinal research reviews* 31, 924-954
222. Filhol, O., and Cochet, C. (2009) Protein kinase CK2 in health and disease. *Cellular and Molecular Life Sciences* 66, 1830-1839
223. Sanz-Clemente, A., Gray, J. A., Ogilvie, K. A., Nicoll, R. A., and Roche, K. W. (2013) Activated CaMKII couples GluN2B and casein kinase 2 to control synaptic NMDA receptors. *Cell reports* 3, 607-614
224. Agostinis, P., Goris, J., Pinna, L., and Merlevede, W. (1987) Regulation of casein kinase 2 by phosphorylation/dephosphorylation. *Biochemical Journal* 248, 785-789
225. Donella-Deana, A., Cesaro, L., Sarno, S., Ruzzene, M., Brunati, A. M., Marin, O., Vilk, G., Doherty-Kirby, A., Lajoie, G., and Litchfield, D. W. (2003) Tyrosine phosphorylation of protein kinase CK2 by Src-related tyrosine kinases correlates with increased catalytic activity. *Biochemical Journal* 372, 841-849
226. Bulat, V., Rast, M., and Pielage, J. (2014) Presynaptic CK2 promotes synapse organization and stability by targeting Ankyrin2. *Journal of Cell Biology* 204, 77-94
227. Kimura, R., and Matsuki, N. (2008) Protein kinase CK2 modulates synaptic plasticity by modification of synaptic NMDA receptors in the hippocampus. *The Journal of physiology* 586, 3195-3206
228. Risinger, C., and Bennett, M. K. (1999) Differential phosphorylation of syntaxin and synaptosome-associated protein of 25 kDa (SNAP-25) isoforms. *Journal of neurochemistry* 72, 614-624
229. Shi, V., Craig, T. J., Bishop, P., Nakamura, Y., Rocca, D., Wilkinson, K. A., and Henley, J. M. (2021) Phosphorylation of Syntaxin-1a by casein kinase 2α regulates pre-synaptic vesicle exocytosis from the reserve pool. *Journal of Neurochemistry* 156, 614-623
230. Chung, H. J., Huang, Y. H., Lau, L.-F., and Huganir, R. L. (2004) Regulation of the NMDA receptor complex and trafficking by activity-dependent phosphorylation of the NR2B subunit PDZ ligand. *Journal of Neuroscience* 24, 10248-10259
231. Manser, E., Leung, T., Salihuddin, H., Zhao, Z.-s., and Lim, L. (1994) A brain serine/threonine protein kinase activated by Cdc42 and Rac1. *Nature* 367, 40-46

232. Manser, E., Huang, H.-Y., Loo, T.-H., Chen, X.-Q., Dong, J.-M., Leung, T., and Lim, L. (1997) Expression of constitutively active alpha-PAK reveals effects of the kinase on actin and focal complexes. *Molecular and cellular biology* 17, 1129-1143
233. Sells, M. A., Boyd, J. T., and Chernoff, J. (1999) p21-activated kinase 1 (Pak1) regulates cell motility in mammalian fibroblasts. *The Journal of cell biology* 145, 837-849
234. Chaudhary, A., King, W., Mattaliano, M., Frost, J., Diaz, B., Morrison, D., Cobb, M., Marshall, M., and Brugge, J. (2000) Phosphatidylinositol 3-kinase regulates Raf1 through Pak phosphorylation of serine 338. *Current Biology* 10, 551-554
235. Sacco, F., Perfetto, L., Castagnoli, L., and Cesareni, G. (2012) The human phosphatase interactome: An intricate family portrait. *FEBS Lett* 586, 2732-2739
236. Tiganis, T., and Bennett, A. M. (2007) Protein tyrosine phosphatase function: the substrate perspective. *Biochem J* 402, 1-15
237. Woolfrey, K. M., and Dell'Acqua, M. L. (2015) Coordination of Protein Phosphorylation and Dephosphorylation in Synaptic Plasticity. *J Biol Chem* 290, 28604-28612
238. Peti, W., Nairn, A. C., and Page, R. (2013) Structural basis for protein phosphatase 1 regulation and specificity. *FEBS J* 280, 596-611
239. Morishita, W., Connor, J. H., Xia, H., Quinlan, E. M., Shenolikar, S., and Malenka, R. C. (2001) Regulation of synaptic strength by protein phosphatase 1. *Neuron* 32, 1133-1148
240. Hu, X. D., Huang, Q., Roadcap, D. W., Shenolikar, S. S., and Xia, H. (2006) Actin-associated neurabin-protein phosphatase-1 complex regulates hippocampal plasticity. *J Neurochem* 98, 1841-1851
241. Hu, X. D., Huang, Q., Yang, X., and Xia, H. (2007) Differential regulation of AMPA receptor trafficking by neurabin-targeted synaptic protein phosphatase-1 in synaptic transmission and long-term depression in hippocampus. *J Neurosci* 27, 4674-4686
242. Hsieh-Wilson, L. C., Benfenati, F., Snyder, G. L., Allen, P. B., Nairn, A. C., and Greengard, P. (2003) Phosphorylation of spinophilin modulates its interaction with actin filaments. *J Biol Chem* 278, 1186-1194
243. Grossman, S. D., Futter, M., Snyder, G. L., Allen, P. B., Nairn, A. C., Greengard, P., and Hsieh-Wilson, L. C. (2004) Spinophilin is phosphorylated by Ca^{2+}/calmodulin-dependent protein kinase II resulting in regulation of its binding to F-actin. *J Neurochem* 90, 317-324
244. McAvoy, T., Allen, P. B., Obaishi, H., Nakanishi, H., Takai, Y., Greengard, P., Nairn, A. C., and Hemmings, H. C., Jr. (1999) Regulation of neurabin I interaction with protein phosphatase 1 by phosphorylation. *Biochemistry* 38, 12943-12949
245. Svenningsson, P., Nishi, A., Fisone, G., Girault, J. A., Nairn, A. C., and Greengard, P. (2004) DARPP-32: an integrator of neurotransmission. *Annu Rev Pharmacol Toxicol* 44, 269-296
246. Nguyen, C., Hosokawa, T., Kuroiwa, M., Ip, N. Y., Nishi, A., Hisanaga, S., and Bibb, J. A. (2007) Differential regulation of the Cdk5-dependent phosphorylation sites of inhibitor-1 and DARPP-32 by depolarization. *J Neurochem* 103, 1582-1593
247. Rodriguez, P., Mitton, B., Nicolaou, P., Chen, G., and Kranias, E. G. (2007) Phosphorylation of human inhibitor-1 at Ser67 and/or Thr75 attenuates stimulatory effects of protein kinase A signaling in cardiac myocytes. *Am J Physiol Heart Circ Physiol* 293, H762-769
248. Xu, Y., Xing, Y., Chen, Y., Chao, Y., Lin, Z., Fan, E., Yu, J. W., Strack, S., Jeffrey, P. D., and Shi, Y. (2006) Structure of the protein phosphatase 2A holoenzyme. *Cell* 127, 1239-1251
249. Wang, J., Xie, R., Kou, X., Liu, Y., Qi, C., Liu, R., You, W., Gao, J., and Gao, X. (2019) A protein phosphatase 2A deficit in the hippocampal CA1 area impairs memory extinction. *Mol Brain* 12, 51
250. Fukunaga, K., Muller, D., Ohmitsu, M., Bako, E., DePaoli-Roach, A. A., and Miyamoto, E. (2000) Decreased protein phosphatase 2A activity in hippocampal long-term potentiation. *J Neurochem* 74, 807-817

251. Drewes, G., Mandelkow, E. M., Baumann, K., Goris, J., Merlevede, W., and Mandelkow, E. (1993) Dephosphorylation of tau protein and Alzheimer paired helical filaments by calcineurin and phosphatase-2A. *FEBS Lett* 336, 425-432
252. Gong, C. X., Grundke-Iqbal, I., and Iqbal, K. (1994) Dephosphorylation of Alzheimer's disease abnormally phosphorylated tau by protein phosphatase-2A. *Neuroscience* 61, 765-772
253. Xu, Y., Chen, Y., Zhang, P., Jeffrey, P. D., and Shi, Y. (2008) Structure of a protein phosphatase 2A holoenzyme: insights into B55-mediated Tau dephosphorylation. *Mol Cell* 31, 873-885
254. Ahn, J. H., McAvoy, T., Rakhilin, S. V., Nishi, A., Greengard, P., and Nairn, A. C. (2007) Protein kinase A activates protein phosphatase 2A by phosphorylation of the B56delta subunit. *Proc Natl Acad Sci U S A* 104, 2979-2984
255. Stewart, A. A., Ingebritsen, T. S., Manalan, A., Klee, C. B., and Cohen, P. (1982) Discovery of a Ca^{2+}- and calmodulin-dependent protein phosphatase: probable identity with calcineurin (CaM-BP80). *FEBS Lett* 137, 80-84
256. Stemmer, P. M., and Klee, C. B. (1994) Dual calcium ion regulation of calcineurin by calmodulin and calcineurin B. *Biochemistry* 33, 6859-6866
257. Groth, R. D., Dunbar, R. L., and Mermelstein, P. G. (2003) Calcineurin regulation of neuronal plasticity. *Biochem Biophys Res Commun* 311, 1159-1171
258. Sun, T., Wu, X. S., Xu, J., McNeil, B. D., Pang, Z. P., Yang, W., Bai, L., Qadri, S., Molkentin, J. D., Yue, D. T., and Wu, L. G. (2010) The role of calcium/calmodulin-activated calcineurin in rapid and slow endocytosis at central synapses. *J Neurosci* 30, 11838-11847
259. King, M. M., Huang, C. Y., Chock, P. B., Nairn, A. C., Hemmings, H. C., Jr., Chan, K. F., and Greengard, P. (1984) Mammalian brain phosphoproteins as substrates for calcineurin. *J Biol Chem* 259, 8080-8083
260. Goto, S., Yamamoto, H., Fukunaga, K., Iwasa, T., Matsukado, Y., and Miyamoto, E. (1985) Dephosphorylation of microtubule-associated protein 2, tau factor, and tubulin by calcineurin. *J Neurochem* 45, 276-283
261. Mandelkow, E. M., Biernat, J., Drewes, G., Gustke, N., Trinczek, B., and Mandelkow, E. (1995) Tau domains, phosphorylation, and interactions with microtubules. *Neurobiol Aging* 16, 355-362; discussion 362-353
262. Seki, K., Chen, H. C., and Huang, K. P. (1995) Dephosphorylation of protein kinase C substrates, neurogranin, neuromodulin, and MARCKS, by calcineurin and protein phosphatases 1 and 2A. *Arch Biochem Biophys* 316, 673-679
263. Yamashita, M., and Fenn, J. B. (1984) Electrospray ion source. Another variation on the free-jet theme. *The Journal of Physical Chemistry* 88, 4451-4459
264. Karas, M., Bachmann, D., and Hillenkamp, F. (1985) Influence of the wavelength in high-irradiance ultraviolet laser desorption mass spectrometry of organic molecules. *Analytical chemistry* 57, 2935-2939
265. Tanaka, K., Waki, H., Ido, Y., Akita, S., Yoshida, Y., Yoshida, T., and Matsuo, T. (1988) Protein and polymer analyses up to m/z 100 000 by laser ionization time-of-flight mass spectrometry. *Rapid communications in mass spectrometry* 2, 151-153
266. Griffiths, J. (2008) A brief history of mass spectrometry. *Anal. Chem* 80, 5678-5683
267. Scheltema, R. A., Hauschild, J.-P., Lange, O., Hornburg, D., Denisov, E., Damoc, E., Kuehn, A., Makarov, A., and Mann, M. (2014) The Q Exactive HF, a Benchtop mass spectrometer with a pre-filter, high-performance quadrupole and an ultra-high-field Orbitrap analyzer. *Molecular & Cellular Proteomics* 13, 3698-3708
268. Domon, B., and Aebersold, R. (2006) Mass spectrometry and protein analysis. *science* 312, 212-217
269. Wilm, M. (2011) Principles of electrospray ionization. *Molecular & cellular proteomics* 10
270. Michalski, A., Damoc, E., Hauschild, J.-P., Lange, O., Wieghaus, A., Makarov, A., Nagaraj, N., Cox, J., Mann, M., and Horning, S. (2011) Mass spectrometry-based proteomics using Q Exactive, a high-performance benchtop quadrupole Orbitrap mass spectrometer. *Molecular & cellular proteomics* 10

271. De Hoffmann, E., and Stroobant, V. (2007) *Mass spectrometry: principles and applications*, John Wiley & Sons
272. Olsen, J. V., Macek, B., Lange, O., Makarov, A., Horning, S., and Mann, M. (2007) Higher-energy C-trap dissociation for peptide modification analysis. *Nature methods* 4, 709-712
273. Steen, H., and Mann, M. (2004) The ABC's (and XYZ's) of peptide sequencing. *Nature reviews Molecular cell biology* 5, 699-711
274. Biemann, K. (1988) Contributions of mass spectrometry to peptide and protein structure. *Biomedical & environmental mass spectrometry* 16, 99-111
275. Roepstorff, P. (1984) Proposal for a nomen clature for sequence ions in mass spectra of peptides. *Biomed. Mass Spec.* 11, 60
276. Zubarev, R. A., and Makarov, A. (2013) Orbitrap mass spectrometry. ACS Publications
277. Makarov, A. (2000) Electrostatic axially harmonic orbital trapping: a high-performance technique of mass analysis. *Analytical chemistry* 72, 1156-1162
278. Chait, B. T. (2006) Mass spectrometry: bottom-up or top-down? *Science* 314, 65-66
279. Andersson, L., and Porath, J. (1986) Isolation of phosphoproteins by immobilized metal (Fe^{3+}) affinity chromatography. *Analytical biochemistry* 154, 250-254
280. Larsen, M. R., Thingholm, T. E., Jensen, O. N., Roepstorff, P., and Jørgensen, T. J. (2005) Highly selective enrichment of phosphorylated peptides from peptide mixtures using titanium dioxide microcolumns. *Molecular & cellular proteomics* 4, 873-886
281. Humphrey, S. J., Karayel, O., James, D. E., and Mann, M. (2018) High-throughput and high-sensitivity phosphoproteomics with the EasyPhos platform. *Nature protocols* 13, 1897-1916
282. Lenz, C., and Urlaub, H. (2014) Separation methodology to improve proteome coverage depth. *Expert review of proteomics* 11, 409-414
283. Song, C., Ye, M., Han, G., Jiang, X., Wang, F., Yu, Z., Chen, R., and Zou, H. (2010) Reversed-phase-reversed-phase liquid chromatography approach with high orthogonality for multidimensional separation of phosphopeptides. *Analytical chemistry* 82, 53-56
284. Wang, Y., Yang, F., Gritsenko, M. A., Wang, Y., Clauss, T., Liu, T., Shen, Y., Monroe, M. E., Lopez-Ferrer, D., and Reno, T. (2011) Reversed-phase chromatography with multiple fraction concatenation strategy for proteome profiling of human MCF10A cells. *Proteomics* 11, 2019-2026
285. McLafferty, F. W. (1981) Tandem mass spectrometry. *Science* 214, 280-287
286. Michalski, A., Cox, J., and Mann, M. (2011) More than 100,000 detectable peptide species elute in single shotgun proteomics runs but the majority is inaccessible to data-dependent LC− MS/MS. *Journal of proteome research* 10, 1785-1793
287. Nesvizhskii, A. I. (2007) Protein identification by tandem mass spectrometry and sequence database searching. *Mass Spectrometry Data Analysis in Proteomics*, 87-119
288. Olsen, J. V., Blagoev, B., Gnad, F., Macek, B., Kumar, C., Mortensen, P., and Mann, M. (2006) Global, in vivo, and site-specific phosphorylation dynamics in signaling networks. *Cell* 127, 635-648
289. Elias, J. E., and Gygi, S. P. (2010) Target-decoy search strategy for mass spectrometry-based proteomics. *Proteome bioinformatics*, pp. 55-71, Springer
290. Nesvizhskii, A. I. (2010) A survey of computational methods and error rate estimation procedures for peptide and protein identification in shotgun proteomics. *Journal of proteomics* 73, 2092-2123
291. Nesvizhskii, A. I., and Aebersold, R. (2005) Interpretation of shotgun proteomic data. *Molecular & cellular proteomics* 4, 1419-1440
292. Rappsilber, J., and Mann, M. (2002) What does it mean to identify a protein in proteomics? *Trends in biochemical sciences* 27, 74-78
293. Nesvizhskii, A. I., Keller, A., Kolker, E., and Aebersold, R. (2003) A statistical model for identifying proteins by tandem mass spectrometry. *Analytical chemistry* 75, 4646-4658
294. Vaudel, M., Sickmann, A., and Martens, L. (2010) Peptide and protein quantification: a map of the minefield. *Proteomics* 10, 650-670

295. Tyanova, S., Temu, T., and Cox, J. (2016) The MaxQuant computational platform for mass spectrometry-based shotgun proteomics. *Nature protocols* 11, 2301-2319
296. Cox, J., Hein, M. Y., Luber, C. A., Paron, I., Nagaraj, N., and Mann, M. (2014) Accurate proteome-wide label-free quantification by delayed normalization and maximal peptide ratio extraction, termed MaxLFQ. *Molecular & cellular proteomics* 13, 2513-2526
297. Bondarenko, P. V., Chelius, D., and Shaler, T. A. (2002) Identification and relative quantitation of protein mixtures by enzymatic digestion followed by capillary reversed-phase liquid chromatography− tandem mass spectrometry. *Analytical chemistry* 74, 4741-4749
298. Thompson, A., Schäfer, J., Kuhn, K., Kienle, S., Schwarz, J., Schmidt, G., Neumann, T., and Hamon, C. (2003) Tandem mass tags: a novel quantification strategy for comparative analysis of complex protein mixtures by MS/MS. *Analytical chemistry* 75, 1895-1904
299. Biringer, R. G., Horner, J. A., Viner, R., Hühmer, A. F., and Specht, A. (2011) Quantitation of TMT-Labeled Peptides Using Higher-Energy Collisional Dissociation on the Velos Pro Ion Trap Mass Spectrometer.
300. Hogrebe, A., von Stechow, L., Bekker-Jensen, D. B., Weinert, B. T., Kelstrup, C. D., and Olsen, J. V. (2018) Benchmarking common quantification strategies for large-scale phosphoproteomics. *Nature communications* 9, 1-13
301. McAlister, G. C., Nusinow, D. P., Jedrychowski, M. P., Wühr, M., Huttlin, E. L., Erickson, B. K., Rad, R., Haas, W., and Gygi, S. P. (2014) MultiNotch MS3 enables accurate, sensitive, and multiplexed detection of differential expression across cancer cell line proteomes. *Analytical chemistry* 86, 7150-7158
302. Huang, T., Choi, M., Tzouros, M., Golling, S., Pandya, N. J., Banfai, B., Dunkley, T., and Vitek, O. (2020) MSstatsTMT: Statistical detection of differentially abundant proteins in experiments with isobaric labeling and multiple mixtures. *Molecular & Cellular Proteomics* 19, 1706-1723
303. Sticker, A., Goeminne, L., Martens, L., and Clement, L. (2020) Robust summarization and inference in proteome-wide label-free quantification. *Molecular & Cellular Proteomics* 19, 1209-1219
304. Goeminne, L. J., Argentini, A., Martens, L., and Clement, L. (2015) Summarization vs peptide-based models in label-free quantitative proteomics: performance, pitfalls, and data analysis guidelines. *Journal of proteome research* 14, 2457-2465
305. Brönstrup, M. (2004) Absolute quantification strategies in proteomics based on mass spectrometry. *Expert review of proteomics* 1, 503-512
306. Aguilan, J. T., Kulej, K., and Sidoli, S. (2020) Guide for protein fold change and p-value calculation for non-experts in proteomics. *Molecular Omics* 16, 573-582
307. Karpievitch, Y. V., Dabney, A. R., and Smith, R. D. (2012) Normalization and missing value imputation for label-free LC-MS analysis. *BMC bioinformatics* 13, 1-9
308. Herbrich, S. M., Cole, R. N., West Jr, K. P., Schulze, K., Yager, J. D., Groopman, J. D., Christian, P., Wu, L., O'Meally, R. N., and May, D. H. (2013) Statistical inference from multiple iTRAQ experiments without using common reference standards. *Journal of proteome research* 12, 594-604
309. Quackenbush, J. (2001) Computational analysis of microarray data. *Nature reviews genetics* 2, 418-427
310. Plubell, D. L., Wilmarth, P. A., Zhao, Y., Fenton, A. M., Minnier, J., Reddy, A. P., Klimek, J., Yang, X., David, L. L., and Pamir, N. (2017) Extended multiplexing of tandem mass tags (TMT) labeling reveals age and high fat diet specific proteome changes in mouse epididymal adipose tissue. *Molecular & Cellular Proteomics* 16, 873-890
311. Smyth, G. K. (2005) Limma: linear models for microarray data. *Bioinformatics and computational biology solutions using R and Bioconductor*, pp. 397-420, Springer
312. Kammers, K., Cole, R. N., Tiengwe, C., and Ruczinski, I. (2015) Detecting significant changes in protein abundance. *EuPA open proteomics* 7, 11-19
313. Benjamini, Y., and Hochberg, Y. (1995) Controlling the false discovery rate: a practical and powerful approach to multiple testing. *Journal of the Royal statistical society: series B (Methodological)* 57, 289-300

314. Storey, J. D. (2002) A direct approach to false discovery rates. *Journal of the Royal Statistical Society: Series B (Statistical Methodology)* 64, 479-498
315. JD, T. R. (2003) Statistical significance for genome-wide experiments. *Proc Natl Acad Sci USA* 100, 94409445
316. Munk, S., Refsgaard, J. C., and Olsen, J. V. (2016) Systems analysis for interpretation of phosphoproteomics data. *Phospho-Proteomics*, 341-360
317. Ashburner, M., Ball, C. A., Blake, J. A., Botstein, D., Butler, H., Cherry, J. M., Davis, A. P., Dolinski, K., Dwight, S. S., and Eppig, J. T. (2000) Gene ontology: tool for the unification of biology. *Nature genetics* 25, 25-29
318. Kanehisa, M., and Goto, S. (2000) KEGG: kyoto encyclopedia of genes and genomes. *Nucleic acids research* 28, 27-30
319. Fabregat, A., Jupe, S., Matthews, L., Sidiropoulos, K., Gillespie, M., Garapati, P., Haw, R., Jassal, B., Korninger, F., and May, B. (2018) The reactome pathway knowledgebase. *Nucleic acids research* 46, D649-D655
320. Finn, R. D., Attwood, T. K., Babbitt, P. C., Bateman, A., Bork, P., Bridge, A. J., Chang, H.-Y., Dosztányi, Z., El-Gebali, S., and Fraser, M. (2017) InterPro in 2017—beyond protein family and domain annotations. *Nucleic acids research* 45, D190-D199
321. Colaert, N., Helsens, K., Martens, L., Vandekerckhove, J., and Gevaert, K. (2009) Improved visualization of protein consensus sequences by iceLogo. *Nature methods* 6, 786-787
322. Szklarczyk, D., Gable, A. L., Lyon, D., Junge, A., Wyder, S., Huerta-Cepas, J., Simonovic, M., Doncheva, N. T., Morris, J. H., and Bork, P. (2019) STRING v11: protein–protein association networks with increased coverage, supporting functional discovery in genome-wide experimental datasets. *Nucleic acids research* 47, D607-D613
323. Horn, H., Schoof, E. M., Kim, J., Robin, X., Miller, M. L., Diella, F., Palma, A., Cesareni, G., Jensen, L. J., and Linding, R. (2014) KinomeXplorer: an integrated platform for kinome biology studies. *Nature methods* 11, 603-604
324. Koopmans, F., van Nierop, P., Andres-Alonso, M., Byrnes, A., Cijsouw, T., Coba, M. P., Cornelisse, L. N., Farrell, R. J., Goldschmidt, H. L., and Howrigan, D. P. (2019) SynGO: an evidence-based, expert-curated knowledge base for the synapse. *Neuron* 103, 217-234. e214
325. Hornbeck, P. V., Zhang, B., Murray, B., Kornhauser, J. M., Latham, V., and Skrzypek, E. (2015) PhosphoSitePlus, 2014: mutations, PTMs and recalibrations. *Nucleic acids research* 43, D512-D520
326. Silbern, I., Pan, K.-T., Fiosins, M., Bonn, S., Rizzoli, S. O., Fornasiero, E. F., Urlaub, H., and Jahn, R. (2021) Protein Phosphorylation in Depolarized Synaptosomes: Dissecting Primary Effects of Calcium from Synaptic Vesicle Cycling. *Molecular & Cellular Proteomics* 20
327. Del Castillo, J., and Katz, B. (1956) Biophysical aspects of neuro-muscular transmission. *Prog Biophys Biophys Chem* 6, 121-170
328. Chapman, E. R. (2002) Synaptotagmin: A Ca^{2+} sensor that triggers exocytosis? *Nature Reviews Molecular Cell Biology* 3, 498-508
329. Fesce, R., Grohovaz, F., Valtorta, F., and Meldolesi, J. (1994) Neurotransmitter release: fusion or 'kiss-and-run'? *Trends in cell biology* 4, 1-4
330. Von Gersdorff, H., and Mathews, G. (1994) Dynamics of synaptic vesicle fusion and membrane retrieval in synaptic terminals. *Nature* 367, 735-739
331. Boucrot, E., Ferreira, A. P., Almeida-Souza, L., Debard, S., Vallis, Y., Howard, G., Bertot, L., Sauvonnet, N., and McMahon, H. T. (2015) Endophilin marks and controls a clathrin-independent endocytic pathway. *Nature* 517, 460-465
332. Gan, Q., and Watanabe, S. (2018) Synaptic vesicle endocytosis in different model systems. *Frontiers in cellular neuroscience* 12, 171
333. Edwards, R. H. (2007) The neurotransmitter cycle and quantal size. *Neuron* 55, 835-858
334. Sihra, T. S. (1997) Protein phosphorylation and dephosphorylation in isolated nerve terminals (synaptosomes). *Regulatory Protein Modification*, pp. 67-119, Springer

335. Gorelick, F. S., Wang, J., Lai, Y., Nairn, A., and Greengard, P. (1988) Autophosphorylation and activation of Ca^{2+}/calmodulin-dependent protein kinase II in intact nerve terminals. *Journal of Biological Chemistry* 263, 17209-17212
336. Walaas, S. I., Gorelick, F. S., and Greengard, P. (1989) Presence of calcium/calmodulin-dependent protein Kinase II in Nerve terminals of rat brain. *Synapse* 3, 356-362
337. Lisman, J., Schulman, H., and Cline, H. (2002) The molecular basis of CaMKII function in synaptic and behavioural memory. *Nature Reviews Neuroscience* 3, 175-190
338. De Camilli, P., Benfenati, F., Valtorta, F., and Greengard, P. (1990) The synapsins. *Annual review of cell biology* 6, 433-460
339. Robinson, P. J. (1992) Differential stimulation of protein kinase C activity by phorbol ester or calcium/phosphatidylserine in vitro and in intact synaptosomes. *Journal of Biological Chemistry* 267, 21637-21644
340. Robinson, P. J., Sontag, J.-M., Liu, J.-P., Fykse, E. M., Slaughter, C., McMahontt, H., and Südhof, T. C. (1993) Dynamin GTPase regulated by protein kinase C phosphorylation in nerve terminals. *Nature* 365, 163-166
341. Sihra, T., Bogonez, E., and Nicholls, D. (1992) Localized Ca^{2+} entry preferentially effects protein dephosphorylation, phosphorylation, and glutamate release. *Journal of Biological Chemistry* 267, 1983-1989
342. Liu, J.-P., Sim, A., and Robinson, P. J. (1994) Calcineurin inhibition of dynamin I GTPase activity coupled to nerve terminal depolarization. *Science* 265, 970-973
343. Nichols, R. A., Suplick, G. R., and Brown, J. M. (1994) Calcineurin-mediated protein dephosphorylation in brain nerve terminals regulates the release of glutamate. *Journal of Biological Chemistry* 269, 23817-23823
344. Bauerfeind, R., Takei, K., and De Camilli, P. (1997) Amphiphysin I is associated with coated endocytic intermediates and undergoes stimulation-dependent dephosphorylation in nerve terminals. *Journal of Biological Chemistry* 272, 30984-30992
345. Marks, B., and McMahon, H. T. (1998) Calcium triggers calcineurin-dependent synaptic vesicle recycling in mammalian nerve terminals. *Current biology* 8, 740-749
346. Cousin, M. A., Tan, T. C., and Robinson, P. J. (2001) Protein phosphorylation is required for endocytosis in nerve terminals: potential role for the dephosphins dynamin I and synaptojanin, but not AP180 or amphiphysin. *Journal of neurochemistry* 76, 105-116
347. Schmitz, S. K., King, C., Kortleven, C., Huson, V., Kroon, T., Kevenaar, J. T., Schut, D., Saarloos, I., Hoetjes, J. P., and de Wit, H. (2016) Presynaptic inhibition upon CB 1 or mG lu2/3 receptor activation requires ERK/MAPK phosphorylation of Munc18-1. *The EMBO journal* 35, 1236-1250
348. Jovanovic, J. N., Benfenati, F., Siow, Y., Sihra, T. S., Sanghera, J. S., Pelech, S. L., Greengard, P., and Czernik, A. J. (1996) Neurotrophins stimulate phosphorylation of synapsin I by MAP kinase and regulate synapsin I-actin interactions. *Proceedings of the National Academy of Sciences* 93, 3679-3683
349. Impey, S., Obrietan, K., Wong, S. T., Poser, S., Yano, S., Wayman, G., Deloulme, J. C., Chan, G., and Storm, D. R. (1998) Cross talk between ERK and PKA is required for Ca^{2+} stimulation of CREB-dependent transcription and ERK nuclear translocation. *Neuron* 21, 869-883
350. Levenson, J. M., O'Riordan, K. J., Brown, K. D., Trinh, M. A., Molfese, D. L., and Sweatt, J. D. (2004) Regulation of histone acetylation during memory formation in the hippocampus. *Journal of Biological Chemistry* 279, 40545-40559
351. Kohansal-Nodehi, M., Chua, J. J., Urlaub, H., Jahn, R., and Czernik, D. (2016) Analysis of protein phosphorylation in nerve terminal reveals extensive changes in active zone proteins upon exocytosis. *Elife* 5, e14530
352. Engholm-Keller, K., Waardenberg, A. J., Müller, J. A., Wark, J. R., Fernando, R. N., Arthur, J. W., Robinson, P. J., Dietrich, D., Schoch, S., and Graham, M. E. (2019) The temporal profile of activity-dependent presynaptic phospho-signalling reveals long-lasting patterns of poststimulus regulation. *PLoS biology* 17, e3000170

353. Gao, J., Hirata, M., Mizokami, A., Zhao, J., Takahashi, I., Takeuchi, H., and Hirata, M. (2016) Differential role of SNAP-25 phosphorylation by protein kinases A and C in the regulation of SNARE complex formation and exocytosis in PC12 cells. *Cellular signalling* 28, 425-437
354. Tian, J.-H., Das, S., and Sheng, Z.-H. (2003) Ca^{2+}-dependent phosphorylation of syntaxin-1A by the death-associated protein (DAP) kinase regulates its interaction with Munc18. *Journal of Biological Chemistry* 278, 26265-26274
355. Rickman, C., and Duncan, R. R. (2010) Munc18/Syntaxin Interaction Kinetics Control Secretory Vesicle Dynamics 2. *Journal of Biological Chemistry* 285, 3965-3972
356. Shen, C., Rathore, S. S., Yu, H., Gulbranson, D. R., Hua, R., Zhang, C., Schoppa, N. E., and Shen, J. (2015) The trans-SNARE-regulating function of Munc18-1 is essential to synaptic exocytosis. *Nature communications* 6, 1-10
357. Li, J., Han, Y. R., Plummer, M. R., and Herrup, K. (2009) Cytoplasmic ATM in neurons modulates synaptic function. *Current Biology* 19, 2091-2096
358. Craig, T. J., Evans, G. J., and Morgan, A. (2003) Physiological regulation of Munc18/nSec1 phosphorylation on serine-313. *Journal of neurochemistry* 86, 1450-1457
359. Garcia, D., Brown, S., Hille, B., and Mackie, K. (1998) Protein kinase C disrupts cannabinoid actions by phosphorylation of the CB1 cannabinoid receptor. *Journal of Neuroscience* 18, 2834-2841
360. Choi, S. W., Gerencser, A. A., Lee, D. W., Rajagopalan, S., Nicholls, D. G., Andersen, J. K., and Brand, M. D. (2011) Intrinsic bioenergetic properties and stress sensitivity of dopaminergic synaptosomes. *Journal of Neuroscience* 31, 4524-4534
361. Blaustein, M. (1975) Effects of potassium, veratridine, and scorpion venom on calcium accumulation and transmitter release by nerve terminals in vitro. *The Journal of physiology* 247, 617-655
362. von Mollard, G. F., Südhof, T. C., and Jahn, R. (1991) A small GTP-binding protein dissociates from synaptic vesicles during exocytosis. *Nature* 349, 79-81
363. Wessel, D., and Flügge, U. (1984) A method for the quantitative recovery of protein in dilute solution in the presence of detergents and lipids. *Analytical biochemistry* 138, 141-143
364. Humphrey, S. J., Azimifar, S. B., and Mann, M. (2015) High-throughput phosphoproteomics reveals in vivo insulin signaling dynamics. *Nature biotechnology* 33, 990-995
365. Cox, J., Neuhauser, N., Michalski, A., Scheltema, R. A., Olsen, J. V., and Mann, M. (2011) Andromeda: a peptide search engine integrated into the MaxQuant environment. *Journal of proteome research* 10, 1794-1805
366. Consortium, U. (2019) UniProt: a worldwide hub of protein knowledge. *Nucleic acids research* 47, D506-D515
367. Storey, J. D., and Tibshirani, R. (2003) Statistical significance for genomewide studies. *Proceedings of the National Academy of Sciences* 100, 9440-9445
368. Jiao, X., Sherman, B. T., Huang, D. W., Stephens, R., Baseler, M. W., Lane, H. C., and Lempicki, R. A. (2012) DAVID-WS: a stateful web service to facilitate gene/protein list analysis. *Bioinformatics* 28, 1805-1806
369. Jassal, B., Matthews, L., Viteri, G., Gong, C., Lorente, P., Fabregat, A., Sidiropoulos, K., Cook, J., Gillespie, M., and Haw, R. (2020) The reactome pathway knowledgebase. *Nucleic acids research* 48, D498-D503
370. Altschul, S. F., Gish, W., Miller, W., Myers, E. W., and Lipman, D. J. (1990) Basic local alignment search tool. *Journal of molecular biology* 215, 403-410
371. Roy, J., and Cyert, M. S. (2009) Cracking the phosphatase code: docking interactions determine substrate specificity. *Science signaling* 2, re9-re9
372. Csardi, G., and Nepusz, T. (2006) The igraph software package for complex network research. *InterJournal, complex systems* 1695, 1-9
373. Dignam, J. D., Lebovitz, R. M., and Roeder, R. G. (1983) Accurate transcription initiation by RNA polymerase II in a soluble extract from isolated mammalian nuclei. *Nucleic acids research* 11, 1475-1489

374. Truckenbrodt, S., Viplav, A., Jähne, S., Vogts, A., Denker, A., Wildhagen, H., Fornasiero, E. F., and Rizzoli, S. O. (2018) Newly produced synaptic vesicle proteins are preferentially used in synaptic transmission. *The EMBO journal* 37, e98044
375. Sankaranarayanan, S., De Angelis, D., Rothman, J. E., and Ryan, T. A. (2000) The use of pHluorins for optical measurements of presynaptic activity. *Biophysical journal* 79, 2199-2208
376. Keihani, S., Kluever, V., Mandad, S., Bansal, V., Rahman, R., Fritsch, E., Gomes, L. C., Gärtner, A., Kügler, S., and Urlaub, H. (2019) The long noncoding RNA neuroLNC regulates presynaptic activity by interacting with the neurodegeneration-associated protein TDP-43. *Science advances* 5, eaay2670
377. Götzke, H., Kilisch, M., Martínez-Carranza, M., Sograte-Idrissi, S., Rajavel, A., Schlichthaerle, T., Engels, N., Jungmann, R., Stenmark, P., and Opazo, F. (2019) The ALFA-tag is a highly versatile tool for nanobody-based bioscience applications. *Nature communications* 10, 1-12
378. Fornasiero, E. F., Raimondi, A., Guarnieri, F. C., Orlando, M., Fesce, R., Benfenati, F., and Valtorta, F. (2012) Synapsins contribute to the dynamic spatial organization of synaptic vesicles in an activity-dependent manner. *Journal of Neuroscience* 32, 12214-12227
379. Klee, C., Crouch, T., and Krinks, M. (1979) Calcineurin: a calcium-and calmodulin-binding protein of the nervous system. *Proceedings of the National Academy of Sciences* 76, 6270-6273
380. Wang, Z.-W. (2008) Regulation of synaptic transmission by presynaptic CaMKII and BK channels. *Molecular neurobiology* 38, 153-166
381. Rosenberg, O. S., Deindl, S., Sung, R.-J., Nairn, A. C., and Kuriyan, J. (2005) Structure of the autoinhibited kinase domain of CaMKII and SAXS analysis of the holoenzyme. *Cell* 123, 849-860
382. Czernik, A. J., Pang, D. T., and Greengard, P. (1987) Amino acid sequences surrounding the cAMP-dependent and calcium/calmodulin-dependent phosphorylation sites in rat and bovine synapsin I. *Proceedings of the National Academy of Sciences* 84, 7518-7522
383. Wang, J., Walaas, S., and Greengard, P. (1988) Protein phosphorylation in nerve terminals: comparison of calcium/calmodulin-dependent and calcium/diacylglycerol-dependent systems. *Journal of Neuroscience* 8, 281-288
384. Menegon, A., Dunlap, D. D., Castano, F., Benfenati, F., Czernik, A. J., Greengard, P., and Valtorta, F. (2000) Use of phosphosynapsin I-specific antibodies for image analysis of signal transduction in single nerve terminals. *Journal of Cell Science* 113, 3573-3582
385. Cesca, F., Baldelli, P., Valtorta, F., and Benfenati, F. (2010) The synapsins: key actors of synapse function and plasticity. *Progress in neurobiology* 91, 313-348
386. Chua, J. J., Kindler, S., Boyken, J., and Jahn, R. (2010) The architecture of an excitatory synapse. *Journal of cell science* 123, 819-823
387. Marsicano, G., Goodenough, S., Monory, K., Hermann, H., Eder, M., Cannich, A., Azad, S. C., Cascio, M. G., Gutiérrez, S. O., and Van der Stelt, M. (2003) CB1 cannabinoid receptors and on-demand defense against excitotoxicity. *Science* 302, 84-88
388. Kellogg, R., Mackie, K., and Straiker, A. (2009) Cannabinoid CB1 receptor-dependent long-term depression in autaptic excitatory neurons. *Journal of neurophysiology* 102, 1160-1171
389. Turner, K. M., Burgoyne, R. D., and Morgan, A. (1999) Protein phosphorylation and the regulation of synaptic membrane traffic. *Trends in neurosciences* 22, 459-464
390. Guitart, X., Egea, G., Solsona, C., and Marsal, J. (1987) Botulinum neurotoxin inhibits depolarization-stimulated protein phosphorylation in pure cholinergic synaptosomes. *FEBS letters* 219, 219-223
391. Boggio, E. M., Putignano, E., Sassoe-Pognetto, M., Pizzorusso, T., and Giustetto, M. (2007) Visual stimulation activates ERK in synaptic and somatic compartments of rat cortical neurons with parallel kinetics. *PLoS One* 2, e604

392. Edbauer, D., Cheng, D., Batterton, M. N., Wang, C.-F., Duong, D. M., Yaffe, M. B., Peng, J., and Sheng, M. (2009) Identification and Characterization of Neuronal Mitogen-activated Protein Kinase Substrates Using a Specific Phosphomotif Antibody* S. *Molecular & Cellular Proteomics* 8, 681-695
393. Park, J. M., Hu, J.-H., Milshteyn, A., Zhang, P.-W., Moore, C. G., Park, S., Datko, M. C., Domingo, R. D., Reyes, C. M., and Wang, X. J. (2013) A prolyl-isomerase mediates dopamine-dependent plasticity and cocaine motor sensitization. *Cell* 154, 637-650
394. Mao, L.-M., and Wang, J. Q. (2016) Synaptically localized mitogen-activated protein kinases: local substrates and regulation. *Molecular neurobiology* 53, 6309-6315
395. Ataman, B., Ashley, J., Gorczyca, M., Ramachandran, P., Fouquet, W., Sigrist, S. J., and Budnik, V. (2008) Rapid activity-dependent modifications in synaptic structure and function require bidirectional Wnt signaling. *Neuron* 57, 705-718
396. Cerpa, W., Godoy, J. A., Alfaro, I., Farías, G. G., Metcalfe, M. J., Fuentealba, R., Bonansco, C., and Inestrosa, N. C. (2008) Wnt-7a modulates the synaptic vesicle cycle and synaptic transmission in hippocampal neurons. *Journal of Biological Chemistry* 283, 5918-5927
397. Budnik, V., and Salinas, P. C. (2011) Wnt signaling during synaptic development and plasticity. *Current opinion in neurobiology* 21, 151-159
398. Ciani, L., Marzo, A., Boyle, K., Stamatakou, E., Lopes, D. M., Anane, D., McLeod, F., Rosso, S. B., Gibb, A., and Salinas, P. C. (2015) Wnt signalling tunes neurotransmitter release by directly targeting Synaptotagmin-1. *Nature communications* 6, 1-13
399. Allen, P. B., Greenfield, A. T., Svenningsson, P., Haspeslagh, D. C., and Greengard, P. (2004) Phactrs 1–4: A family of protein phosphatase 1 and actin regulatory proteins. *Proceedings of the National Academy of Sciences* 101, 7187-7192
400. Oliver, C. J., Terry-Lorenzo, R. T., Elliott, E., Bloomer, W. A. C., Li, S., Brautigan, D. L., Colbran, R. J., and Shenolikar, S. (2002) Targeting protein phosphatase 1 (PP1) to the actin cytoskeleton: the neurabin I/PP1 complex regulates cell morphology. *Molecular and cellular biology* 22, 4690-4701
401. Dubois, T., Kerai, P., Learmonth, M., Cronshaw, A., and Aitken, A. (2002) Identification of syntaxin-1A sites of phosphorylation by casein kinase I and casein kinase II. *European journal of biochemistry* 269, 909-914
402. Trinidad, J. C., Barkan, D. T., Gulledge, B. F., Thalhammer, A., Sali, A., Schoepfer, R., and Burlingame, A. L. (2012) Global identification and characterization of both O-GlcNAcylation and phosphorylation at the murine synapse. *Molecular & Cellular Proteomics* 11, 215-229
403. Brüning, F., Noya, S. B., Bange, T., Koutsouli, S., Rudolph, J. D., Tyagarajan, S. K., Cox, J., Mann, M., Brown, S. A., and Robles, M. S. (2019) Sleep-wake cycles drive daily dynamics of synaptic phosphorylation. *Science* 366
404. Perez-Riverol, Y., Csordas, A., Bai, J., Bernal-Llinares, M., Hewapathirana, S., Kundu, D. J., Inuganti, A., Griss, J., Mayer, G., and Eisenacher, M. (2019) The PRIDE database and related tools and resources in 2019: improving support for quantification data. *Nucleic acids research* 47, D442-D450
405. Popoff, M. R., and Poulain, B. (2010) Bacterial toxins and the nervous system: neurotoxins and multipotential toxins interacting with neuronal cells. *Toxins* 2, 683-737
406. Schwanhäusser, B., Busse, D., Li, N., Dittmar, G., Schuchhardt, J., Wolf, J., Chen, W., and Selbach, M. (2011) Global quantification of mammalian gene expression control. *Nature* 473, 337-342
407. Heidelberger, R., Heinemann, C., Neher, E., and Matthews, G. (1994) Calcium dependence of the rate of exocytosis in a synaptic terminal. *Nature* 371, 513-515
408. Stafford, J., Brownlow, M. L., Qualley, A., and Jankord, R. (2018) AMPA receptor translocation and phosphorylation are induced by transcranial direct current stimulation in rats. *Neurobiology of learning and memory* 150, 36-41
409. Stagg, C. J., and Nitsche, M. A. (2011) Physiological basis of transcranial direct current stimulation. *The Neuroscientist* 17, 37-53

410. Montecucco, C., and Schiavo, G. (1994) Mechanism of action of tetanus and botulinum neurotoxins. *Molecular microbiology* 13, 1-8
411. Shields, S. M., Ingebritsen, T. S., and Kelly, P. T. (1985) Identification of protein phosphatase 1 in synaptic junctions: dephosphorylation of endogenous calmodulin-dependent kinase II and synapse-enriched phosphoproteins. *Journal of Neuroscience* 5, 3414-3422
412. Yue, X., Schunter, A., and Hummon, A. B. (2015) Comparing multistep immobilized metal affinity chromatography and multistep TiO2 methods for phosphopeptide enrichment. *Anal Chem* 87, 8837-8844
413. Refsgaard, J. C., Munk, S., and Jensen, L. J. (2016) Search databases and statistics: pitfalls and best practices in phosphoproteomics. *Phospho-Proteomics*, 323-339
414. Lisman, J. E., and Zhabotinsky, A. M. (2001) A model of synaptic memory: a CaMKII/PP1 switch that potentiates transmission by organizing an AMPA receptor anchoring assembly. *Neuron* 31, 191-201
415. Suzuki, T., Bridges, D., Nakada, D., Skiniotis, G., Morrison, S. J., Lin, J. D., Saltiel, A. R., and Inoki, K. (2013) Inhibition of AMPK catabolic action by GSK3. *Molecular cell* 50, 407-419
416. Asada, A., Saito, T., and Hisanaga, S.-i. (2012) Phosphorylation of p35 and p39 by Cdk5 determines the subcellular location of the holokinase in a phosphorylation-site-specific manner. *Journal of cell science* 125, 3421-3429
417. Rivers, A., Gietzen, K. F., Vielhaber, E., and Virshup, D. M. (1998) Regulation of Casein Kinase I ε and Casein Kinase I δ by anin Vivo Futile Phosphorylation Cycle. *Journal of Biological Chemistry* 273, 15980-15984
418. Meng, Z., Bischof, J., Ianes, C., Henne-Bruns, D., Xu, P., and Knippschild, U. (2016) CK1δ kinase activity is modulated by protein kinase C α (PKCα)-mediated site-specific phosphorylation. *Amino Acids* 48, 1185-1197
419. Robles, M. S., Humphrey, S. J., and Mann, M. (2017) Phosphorylation is a central mechanism for circadian control of metabolism and physiology. *Cell metabolism* 25, 118-127
420. Sacco, F., Humphrey, S. J., Cox, J., Mischnik, M., Schulte, A., Klabunde, T., Schäfer, M., and Mann, M. (2016) Glucose-regulated and drug-perturbed phosphoproteome reveals molecular mechanisms controlling insulin secretion. *Nature communications* 7, 1-13
421. Litchfield, D., Lüscher, B., Lozeman, F., Eisenman, R., and Krebs, E. (1992) Phosphorylation of casein kinase II by p34cdc2 in vitro and at mitosis. *Journal of Biological Chemistry* 267, 13943-13951
422. Shin, Y. J., Kim, Y.-B., and Kim, J.-H. (2013) Protein kinase CK2 phosphorylates and activates p21-activated kinase 1. *Molecular biology of the cell* 24, 2990-2999
423. Montenegro-Venegas, C., Guhathakurta, D., Pina-Fernandez, E., Andres-Alonso, M., Plattner, F., Lazarevic, V., Gundelfinger, E. D., and Fejtova, A. (2021) Bassoon controls synaptic vesicle pools via regulation of presynaptic phosphorylation and cAMP homeostasis. *bioRxiv*
424. Mochida, S., Hida, Y., Tanifuji, S., Hagiwara, A., Hamada, S., Abe, M., Ma, H., Yasumura, M., Kitajima, I., and Sakimura, K. (2016) SAD-B phosphorylation of CAST controls active zone vesicle recycling for synaptic depression. *Cell reports* 16, 2901-2913
425. Han, W., Nattel, S., Noguchi, T., and Shrier, A. (2006) C-terminal domain of Kv4. 2 and associated KChIP2 interactions regulate functional expression and gating of Kv4. 2. *Journal of Biological Chemistry* 281, 27134-27144
426. Schrader, L. A., Ren, Y., Cheng, F., Bui, D., Sweatt, J. D., and Anderson, A. E. (2009) Kv4. 2 is a locus for PKC and ERK/MAPK cross-talk. *Biochemical Journal* 417, 705-715
427. Schrader, L. A., Birnbaum, S. G., Nadin, B. M., Ren, Y., Bui, D., Anderson, A. E., and Sweatt, J. D. (2006) ERK/MAPK regulates the Kv4. 2 potassium channel by direct phosphorylation of the pore-forming subunit. *American Journal of Physiology-Cell Physiology*

428. Yang, J.-W., Vacher, H., Park, K.-S., Clark, E., and Trimmer, J. S. (2007) Trafficking-dependent phosphorylation of Kv1. 2 regulates voltage-gated potassium channel cell surface expression. *Proceedings of the National Academy of Sciences* 104, 20055-20060
429. Park, K.-S., Mohapatra, D. P., and Trimmer, J. S. (2007) Proteomic analyses of Kv2. 1 channel phosphorylation sites determining cell background-specific differences in function. *Channels* 1, 59-61
430. Redman, P. T., He, K., Hartnett, K. A., Jefferson, B. S., Hu, L., Rosenberg, P. A., Levitan, E. S., and Aizenman, E. (2007) Apoptotic surge of potassium currents is mediated by p38 phosphorylation of Kv2. 1. *Proceedings of the National Academy of Sciences* 104, 3568-3573
431. Pal, S., Hartnett, K. A., Nerbonne, J. M., Levitan, E. S., and Aizenman, E. (2003) Mediation of neuronal apoptosis by Kv2. 1-encoded potassium channels. *Journal of Neuroscience* 23, 4798-4802
432. Pal, S., Takimoto, K., Aizenman, E., and Levitan, E. S. (2006) Apoptotic surface delivery of K^+ channels. *Cell Death & Differentiation* 13, 661-667
433. MacDonald, P. E., Wang, G., Tsuk, S., Dodo, C., Kang, Y., Tang, L., Wheeler, M. B., Cattral, M. S., Lakey, J. R., and Salapatek, A. M. F. (2002) Synaptosome-associated protein of 25 kilodaltons modulates Kv2. 1 voltage-dependent K^+ channels in neuroendocrine islet β-cells through an interaction with the channel N terminus. *Molecular endocrinology* 16, 2452-2461
434. Leung, Y. M., Kang, Y., Gao, X., Xia, F., Xie, H., Sheu, L., Tsuk, S., Lotan, I., Tsushima, R. G., and Gaisano, H. Y. (2003) Syntaxin 1A binds to the cytoplasmic C terminus of Kv2. 1 to regulate channel gating and trafficking. *Journal of Biological Chemistry* 278, 17532-17538
435. Kang, Y., Linial, M., Gaisano, H. Y., Michaelevski, I., Chikvashvili, D., Tsuk, S., Singer-Lahat, D., Fili, O., and Lotan, I. (2003) Direct interaction of target SNAREs with the Kv2. 1 channel: modal regulation of channel activation and inactivation gating. *Journal of Biological Chemistry* 278, 34320-34330
436. Teo, S., and Salinas, P. C. (2021) Wnt-Frizzled signaling regulates activity-mediated synapse formation. *Frontiers in Molecular Neuroscience* 14
437. Lu, Q., Paredes, M., Medina, M., Zhou, J., Cavallo, R., Peifer, M., Orecchio, L., and Kosik, K. S. (1999) δ-Catenin, an adhesive junction–associated protein which promotes cell scattering. *The Journal of cell biology* 144, 519-532
438. Kosik, K. S., Donahue, C. P., Israely, I., Liu, X., and Ochiishi, T. (2005) δ-Catenin at the synaptic–adherens junction. *Trends in cell biology* 15, 172-178
439. Ide, N., Hata, Y., Deguchi, M., Hirao, K., Yao, I., and Takai, Y. (1999) Interaction of S-SCAM with Neural Plakophilin-RelatedArmadillo-Repeat Protein/δ-Catenin. *Biochemical and biophysical research communications* 256, 456-461
440. Sánchez, C., Pérez, M., and Avila, J. (2000) GSK3β-mediated phosphorylation of the microtubule-associated protein 2C (MAP2C) prevents microtubule bundling. *European journal of cell biology* 79, 252-260
441. Sanchez, C., Díaz-Nido, J., and Avila, J. (1998) Regulation of a site-specific phosphorylation of the microtubule-associated protein 2 during the development of cultured neurons. *Neuroscience* 87, 861-870
442. Taymans, J.-M., and Baekelandt, V. (2014) Phosphatases of α-synuclein, LRRK2, and tau: important players in the phosphorylation-dependent pathology of Parkinsonism. *Frontiers in genetics* 5, 382

8 Appendix

Table 8.1: primary Ca^{2+}-dependent sites, selection from Suppl. Data 01. *UP.Accession ~ Uniprot accession; Gene.name ~ official gene symbol; AA ~ modified amino acid; Pos ~ position in the protein sequence; Mult ~ multiplicity of phosphorylation (1 – singly phosphorylated, 2 – doubly phosphorylated, 3 – multiply phosphorylated); Seq.window ~ ±7 amino acids flanking phosphorylated residue; CaEGTA ~ log_2 intensity fold change in Ca vs. EGTA experiment, MockBoNT ~ log_2 intensity fold change in Mock vs. BoNT experiment*

UP.Accession	Gene.name	AA	Pos	Mult	Seq.window	CaEGTA	MockBoNT
P0C1X8	Aak1	S	638	1	AGHRRILSDVTHSAV	-0.7362	0.1272
P0C1X8	Aak1	S	638	2	AGHRRILSDVTHSAV	-1.3276	0.0638
P0C1X8	Aak1	S	653	1	FGVPASKSTQLLHAA	-1.2734	0.0707
P0C1X8	Aak1	S	653	2	FGVPASKSTQLLHAA	-1.3278	
P0C1X8	Aak1	S	671	1	ASLSKSKSATTTPSG	-0.7759	0.0095
P0C1X8	Aak1	S	671	2	ASLSKSKSATTTPSG	-1.4722	0.0747
P0C1X8	Aak1	S	671	3	ASLSKSKSATTTPSG	-1.2298	-0.0267
P0C1X8	Aak1	T	675	3	KSKSATTTPSGSPRT	-1.2337	-0.0378
P0C1X8	Aak1	S	677	2	KSATTTPSGSPRTSQ	-0.7228	0.0769
P0C1X8	Aak1	S	679	1	ATTTPSGSPRTSQQN	0.3564	0.0833
P0C1X8	Aak1	S	679	3	ATTTPSGSPRTSQQN	-1.2337	-0.0340
P0C1X8	Aak1	S	732	1	LPEKLGGSAESLIPG	-0.3218	0.0157
P0C1X8	Aak1	S	732	2	LPEKLGGSAESLIPG	-0.8128	
P0C1X8	Aak1	T	743	2	LIPGFQATQGDAFAT	-0.8286	
P0C1X8	Aak1	S	847	1	PVAQRLPSHTESVTS	-0.6066	-0.0092
Q9QZM5	Abi1	S	217	1	TSPARLGSQHSPGRT	0.3935	-0.1388
Q9QZM5	Abi1	S	226	1	HSPGRTASLNQRPRT	0.6219	-0.1397
F1M0N1	Abl2	S	629	1	PRKQRDKSPSSLLED	-0.6648	
F1M0N1	Abl2	S	631	1	KQRDKSPSSLLEDAK	-0.7520	
F1M0N1	Abl2	S	799	1	LQLERTVSTSSQPEE	0.8680	
F1M8U2	Ablim3	S	393	1	MSPTFSRSPHHYYRS	-0.3155	
F1M8U2	Ablim3	S	408	2	GPESGRSSPYHSQLD	-0.5498	-0.0424
F1M8U2	Ablim3	S	412	2	GRSSPYHSQLDVRSS	-0.5587	-0.0495
A0A0G2K4T3	Acap2	S	612	2	ESLPSTVSANSLYEP	-0.4995	-0.0115
A0A0G2K4T3	Acap2	S	615	2	PSTVSANSLYEPEGE	-0.4995	-0.0115
M0R5P8	Adam22	S	726	3	RFRPRSNSTETLSPA	-0.3061	
M0R5P8	Adam22	T	729	3	PRSNSTETLSPAKSP	-0.2873	0.0317
M0R5P8	Adam22	S	731	3	SNSTETLSPAKSPSS	-0.2813	0.0340
M0R5P8	Adam22	S	735	1	ETLSPAKSPSSSTGS	-0.3635	0.0610
M0R5P8	Adam22	S	735	2	ETLSPAKSPSSSTGS	-0.2898	0.0877
M0R5P8	Adam22	S	735	3	ETLSPAKSPSSSTGS	-0.2655	0.0113
M0R5P8	Adam22	S	739	1	PAKSPSSSTGSIASS	0.2935	0.2130
M0R5P8	Adam22	S	742	1	SPSSSTGSIASSRKY	0.4259	0.0526
M0R5P8	Adam22	S	767	1	EKTVNRQSARLWETS	-0.7870	-0.1530
Q04400	Adcy5	T	62	1	KRSGGAVTPQQQQRL	-0.3139	0.0146
M0R5U4	Adcy9	S	1274	2	VDGSIGRSPTDEITN	-0.4237	

M0R5U4	Adcy9	T	1276	2	GSIGRSPTDEITNLV	-0.3969	
Q05764	Add2	S	606	1	TPASPVQSPTRAGTK	0.4197	-0.1341
Q05764	Add2	S	623	1	AVSPSKASEDAKKTE	0.3441	0.2358
Q62847	Add3	S	402	2	REKPRHKSDVEIPAT	-0.2680	0.1066
Q62847	Add3	T	653	3	SRLTTSTTIENIEIT	-0.3005	
Q62847	Add3	S	663	2	NIEITIKSPDRTEEV	-0.2971	
Q62847	Add3	S	680	1	PDGSPSKSPSKKKKK	-0.3335	0.2343
Q62847	Add3	S	680	2	PDGSPSKSPSKKKKK	-0.3241	0.1066
O88917	Adgrl1	S	1128	1	PPGGAHGSLKTSAMR	0.4962	-0.1920
Q9Z173	Adgrl3	S	1239	1	RYSTGSQSRIRRMWN	0.5008	-0.0398
O35889	Afdn	S	181	1	KEALRQASDKEERPS	0.6297	
A0A0G2K847	Agap1	S	345	1	GLESRADSIGSGRAI	1.5076	
Q8CGU4	Agap2	S	1172	1	PSPRRRSSAASLGRV	0.3920	0.1942
A0A0G2JZ83	Agap3	S	478	1	PSTAPGTSPRGANGL	-0.3562	0.1023
Q4KLH5	Agfg1	T	179	2	HLNKGTPTQSPVVGR	-0.3567	
Q4KLH5	Agfg1	S	298	1	SSSADFGSFSTSQSH	-0.5385	
Q5QD51	Akap12	S	304	1	KKTSFKKSKEDDLET	0.6604	-0.1102
P09117	Aldoc	S	39	1	AADESVGSMAKRLSQ	0.3393	-0.1296
P0C5Y8	Als2	S	477	2	EGGSRRLSLPGLLSQ	-0.3327	0.0436
P0C5Y8	Als2	S	486	2	PGLLSQVSPRLLRKA	-0.3327	0.0436
Q02356	Ampd2	S	21	1	YPFKKRASLQASAAA	1.0988	-0.1266
Q02356	Ampd2	S	113	1	QRLERQISQDVKLEP	1.6248	0.0362
O08838	Amph	T	260	3	GPLRIAKTPSPPEEA	-0.2793	0.0712
O08838	Amph	S	262	3	LRIAKTPSPPEEASP	-0.2958	0.0399
O08838	Amph	S	268	3	PSPPEEASPLPSPTA	-0.3349	0.0120
O08838	Amph	S	272	3	EEASPLPSPTASPNH	-0.3122	0.0231
O08838	Amph	T	274	3	ASPLPSPTASPNHTL	-0.4534	0.0175
O08838	Amph	S	276	3	PLPSPTASPNHTLAP	-0.3025	0.0945
O08838	Amph	T	280	3	PTASPNHTLAPASPA	-0.4395	
O08838	Amph	S	285	3	NHTLAPASPAPVRPR	-0.3690	0.0108
A0A0G2JZ56	Ank2	S	1800	1	KIIRRYVSSDGTEKE	0.3369	0.0694
F1M9N9	Ank2	S	1726	1	LPTAKATSPLIEETP	-0.7095	
F1M9N9	Ank2	S	1797	1	SKMERHSSLTSSAKT	0.5266	0.1878
F1M9N9	Ank2	S	1813	2	RHSPVSPSSKNEKHS	-0.3515	
F1M9N9	Ank2	T	3054	2	PDTTPARTPTEEGTP	-0.5207	
Q5BJT1	Ankrd34a	T	315	1	GPLSRRNTAPEAQES	0.3036	-0.0611
Q5BJT1	Ankrd34a	S	448	2	QPGGRAPSLPAPPHS	0.2872	-0.0622
Q5BJT1	Ankrd34a	S	460	2	PHSGAPGSPRTKRKL	0.2872	-0.0622
Q5BJT1	Ankrd34a	S	472	1	RKLVRRHSMQTEQIR	0.4943	-0.0365
D3ZKP1	Ankrd34b	S	496	1	KMLLRRQSLQTEQIK	0.5918	-0.0012
F1LWB9	Ankrd50	S	1137	1	SLTIRSNSSGGTGGG	0.4376	
D4A0V6	Anln	S	633	1	DSSLSAPSPKPGKFQ	-0.3938	-0.1464
O35430	Apba1	S	286	1	KQSMSSQSLDKAAED	0.4552	
A0A0G2K8G0	Apc	T	1216	1	PSFSFSKTPSVQGTK	0.7146	-0.0676

A0A0G2K8G0	Apc	S	2278	1	LKTPASKSPSEGPVA	-0.2873	0.2612
A0A0G2K8G0	Apc	S	2308	1	SPITRQTSHISGSNK	0.7546	-0.0802
A0A0G2K8G0	Apc	S	2484	2	SASFESLSPSSRPDS	-0.3699	0.2488
A0A0G2K8G0	Apc	S	2486	2	SFESLSPSSRPDSPT	-0.2808	0.1414
A0A0G2K8G0	Apc	S	2692	1	NNPRSGRSPTGNTPP	-0.3685	
Q3S4A4	Arfgap1	S	247	1	FWGYKQQSEPASELG	2.5740	0.2088
Q3S4A4	Arfgap1	S	251	1	KQQSEPASELGHSLN	2.3481	
D4A631	Arfgef1	S	1076	1	TVRGREGSLTGTKDQ	0.7003	0.2252
D4A631	Arfgef1	S	1566	1	LDAISQKSVDIHDSA	0.7857	0.0497
Q6AY65	Arfip2	S	72	1	TGSGRHPSHSTSPSG	-0.7034	
Q6AY65	Arfip2	S	72	2	TGSGRHPSHSTSPSG	-0.6915	
Q6AY65	Arfip2	S	74	2	SGRHPSHSTSPSGPG	-0.4811	
Q6AY65	Arfip2	T	75	2	GRHPSHSTSPSGPGD	-0.4554	
Q6AY65	Arfip2	S	76	1	RHPSHSTSPSGPGDE	-0.3954	0.1709
Q6AY65	Arfip2	S	76	2	RHPSHSTSPSGPGDE	-0.5794	
D4A6C5	Arhgap1	S	27	1	LNQLKLASIDEKNWP	2.3853	-0.2110
A0A0G2K1Z2	Arhgap12	S	163	1	KFNSDSHSPKVSSQN	-0.4312	-0.0212
D4A9G6	Arhgap33	S	588	1	TTPKTPASPVERRKR	0.2905	0.0048
F1LR18	Arhgap39	S	294	1	LIQPRKPSSDSQPSS	0.4982	0.2614
F1LR18	Arhgap39	S	294	2	LIQPRKPSSDSQPSS	0.4835	0.1154
F1LR18	Arhgap39	S	297	1	PRKPSSDSQPSSPRY	0.4798	0.2303
F1LR18	Arhgap39	S	599	1	GPVVRAFSEDEALAQ	0.3240	-0.1117
F1LQX4	Arhgap44	S	598	1	VSKSKELSPGSGQKG	-0.4125	0.0799
F1LQX4	Arhgap44	S	798	1	LEHARRHSVTDKRDS	-0.6337	-0.0634
Q5XI73	Arhgdia	S	34	1	YKPPAQKSIQEIQEL	1.3931	-0.0808
F1LQS9	Arhgef11	S	563	1	RYIGKPKSSSQSIKP	1.4143	0.0625
F1LQS9	Arhgef11	S	1463	2	KSLGGESSGGTTPVG	-0.3669	-0.0500
F1LQS9	Arhgef11	T	1467	2	GESSGGTTPVGSFHT	-0.3503	
Q6P720	Arhgef25	S	491	1	IEYQRRESQTNSLGR	0.2863	0.2039
A0A0G2QC21	Arhgef7	S	135	1	HRIKSFDSLGSQSSH	0.4436	-0.0644
A0A0G2QC21	Arhgef7	S	673	1	RKPERKPSDEEFAVR	0.7728	0.1342
A0A0G2JVX9	Arpp21	S	32	1	NGILKSESLDEEEKL	1.2358	0.0077
A0A0G2JZQ0	Asap1	T	789	2	VALRKTETSHHLSLD	1.9411	0.0180
A0A0G2JZQ0	Asap1	S	794	2	TETSHHLSLDRANIP	1.7549	0.0134
A0A0G2JZQ0	Asap1	S	911	1	RSHTGDLSPNVQSRD	-0.4919	-0.1062
Q1AAU6	Asap1	S	855	2	RTLSDPPSPLPHGPP	-0.4220	0.0734
A0A0G2K9U6	Atg16l1	S	303	1	SDAARRRSVSSIPVP	-0.3397	-0.0117
D3ZFK6	Atg16l1	S	287	1	TNIFGRRSVSSIPVP	-0.3397	-0.0105
F1MAF8	Atg2b	S	280	1	RYYLRKDSLSLGVSS	0.7071	-0.0099
D4A8B3	Atp2b2	S	1152	1	NTFKSGASFQGALRR	0.5471	0.2346
D4A8B3	Atp2b2	S	1162	1	GALRRQSSVTSQSQD	0.2646	0.1806
D4A8B3	Atp2b2	S	1165	2	RRQSSVTSQSQDVAS	0.3672	0.0333
P11506	Atp2b2	S	1150	1	VVKAFRSSLYEGLEK	0.6029	-0.1874
A0A0G2K9Q6	Atp2b3	S	1124	1	VVSTFKRSGSFQGAV	0.6882	0.0592

A0A0G2K9Q6	Atp2b3	S	1126	1	STFKRSGSFQGAVRR	0.6155	0.0678
A0A0G2JYE0	Atxn2l	S	681	1	KSTSTPTSPGPRTHS	-0.6020	0.0597
Q6GMN2	Baiap2	S	455	1	LQQGKSSSTGNLLDK	-0.5024	-0.1230
A0A0G2K1L8	Basp1	S	214	1	PVASSEQSVAVKE__	0.4246	
Q05175	Basp1	S	130	1	AGEASAESTGAADGA	0.2954	
O08839	Bin1	S	321	2	NHEPEPASGASPGAT	-1.0804	-0.2199
O08839	Bin1	S	324	2	PEPASGASPGATIPK	-0.9200	-0.1813
O08839	Bin1	T	328	1	SGASPGATIPKSPSQ	-1.0314	0.0324
O08839	Bin1	T	328	2	SGASPGATIPKSPSQ	-0.9516	
O08839	Bin1	S	332	1	PGATIPKSPSQLRKG	-1.2854	-0.0424
O08839	Bin1	S	332	2	PGATIPKSPSQLRKG	-1.0277	-0.2360
O08839	Bin1	S	334	1	ATIPKSPSQLRKGPP	-0.9335	-0.0554
O08839	Bin1	S	334	2	ATIPKSPSQLRKGPP	-0.6960	
O08839	Bin1	T	349	1	VPPPPKHTPSKEMKQ	-0.7219	0.0673
Q5HZA7	Bin1	S	255	1	FTVKAQPSDSAPEKG	0.5255	0.0424
Q5HZA7	Bin1	S	257	1	VKAQPSDSAPEKGNK	0.4363	-0.0039
B2DD29	Brsk1	S	442	3	GASTGLSSSPLSSPR	-0.3172	
B2DD29	Brsk1	S	443	3	ASTGLSSSPLSSPRS	-0.3207	
B2DD29	Brsk1	S	446	3	GLSSSPLSSPRSPVF	-0.2889	
B2DD29	Brsk1	S	447	3	LSSSPLSSPRSPVFS	-0.2889	
D3ZML2	Brsk2	S	415	1	GQRSRSISGASSGLS	0.4132	0.0046
G3V984	Bsn	S	135	2	VDSRTQRSGRSPSVS	-1.3293	
G3V984	Bsn	S	138	2	RTQRSGRSPSVSPDR	-1.2617	
G3V984	Bsn	S	140	2	QRSGRSPSVSPDRGS	-1.3274	
G3V984	Bsn	S	142	1	SGRSPSVSPDRGSTP	0.8377	-0.0085
G3V984	Bsn	S	233	1	DMTTAPRSKSQQQLH	-0.9557	-0.0035
G3V984	Bsn	S	233	2	DMTTAPRSKSQQQLH	-1.4701	
G3V984	Bsn	S	235	1	TTAPRSKSQQQLHSP	-0.4854	-0.0400
G3V984	Bsn	S	235	2	TTAPRSKSQQQLHSP	-1.7446	-0.0285
G3V984	Bsn	S	235	3	TTAPRSKSQQQLHSP	-2.0305	-0.0749
G3V984	Bsn	S	241	1	KSQQQLHSPALSPAH	-0.9993	0.0631
G3V984	Bsn	S	241	2	KSQQQLHSPALSPAH	-1.6988	-0.0045
G3V984	Bsn	S	241	3	KSQQQLHSPALSPAH	-1.7851	-0.0857
G3V984	Bsn	S	249	2	PALSPAHSPAKQPLG	-1.6418	0.1175
G3V984	Bsn	S	249	3	PALSPAHSPAKQPLG	-0.9583	-0.0888
G3V984	Bsn	S	263	1	GKPEQERSRSPGATQ	-1.6065	-0.0269
G3V984	Bsn	S	265	1	PEQERSRSPGATQSG	-1.2681	-0.0251
G3V984	Bsn	S	283	1	AEAARATSVPGPTQA	0.3857	0.0342
G3V984	Bsn	S	821	1	DSSEGGLSPLPPQPP	-0.6741	-0.1626
G3V984	Bsn	S	1084	2	AQRRRERSKTPPSNL	-0.3376	
G3V984	Bsn	S	1084	3	AQRRRERSKTPPSNL	-0.9354	0.0842
G3V984	Bsn	S	1089	3	ERSKTPPSNLSPIED	-1.0130	0.1486
G3V984	Bsn	S	1220	1	TGPRSQGSFEYQDTQ	1.4265	
G3V984	Bsn	Y	1223	1	RSQGSFEYQDTQDHD	0.4604	

G3V984	Bsn	T	1226	1	GSFEYQDTQDHDYGG	2.2291	
G3V984	Bsn	S	1353	2	QEPLKLHSSPASPSL	-1.7652	0.0942
G3V984	Bsn	S	1354	2	EPLKLHSSPASPSLA	-2.0586	-0.0702
G3V984	Bsn	S	1357	2	KLHSSPASPSLASKE	-1.8484	0.0441
G3V984	Bsn	S	1484	3	PSESPTFSPSKLGPR	-0.5046	
G3V984	Bsn	S	1512	1	PSSDIPRSPGTPSPM	-1.1175	0.0101
G3V984	Bsn	S	2630	1	RSRLSRHSDSGSDSK	-0.4549	0.1325
G3V984	Bsn	S	2632	1	RLSRHSDSGSDSKHE	0.4575	0.2069
G3V984	Bsn	S	2636	1	HSDSGSDSKHEASAS	0.3991	0.2241
G3V984	Bsn	S	2783	2	VSRQPPKSPQVLYSP	-0.4416	0.0561
G3V984	Bsn	S	2783	3	VSRQPPKSPQVLYSP	-1.2145	
G3V984	Bsn	Y	2788	2	PKSPQVLYSPVSPLS	-0.4829	
G3V984	Bsn	Y	2788	3	PKSPQVLYSPVSPLS	-1.2421	
G3V984	Bsn	S	2789	2	KSPQVLYSPVSPLSP	-0.5423	
G3V984	Bsn	S	2789	3	KSPQVLYSPVSPLSP	-1.2370	
G3V984	Bsn	S	2792	2	QVLYSPVSPLSPHRL	-0.6353	
G3V984	Bsn	S	2792	3	QVLYSPVSPLSPHRL	-1.1586	
G3V984	Bsn	S	2795	2	YSPVSPLSPHRLLDT	-0.3497	0.0153
G3V984	Bsn	S	2795	3	YSPVSPLSPHRLLDT	-1.2543	
G3V984	Bsn	S	2816	1	RLNKAHVSPQKQFIA	-1.2191	0.2195
G3V984	Bsn	S	2842	1	PMKTLQRSLSDPKPL	0.3755	-0.0443
G3V984	Bsn	S	2842	2	PMKTLQRSLSDPKPL	-0.5480	0.1939
G3V984	Bsn	S	2842	3	PMKTLQRSLSDPKPL	0.4822	
G3V984	Bsn	S	2844	1	KTLQRSLSDPKPLSP	0.3129	0.0211
G3V984	Bsn	S	2844	2	KTLQRSLSDPKPLSP	-0.6985	0.2481
G3V984	Bsn	S	2844	3	KTLQRSLSDPKPLSP	0.4822	
G3V984	Bsn	T	2852	2	DPKPLSPTAEESAKE	-0.5246	0.1391
G3V984	Bsn	T	2852	3	DPKPLSPTAEESAKE	0.4447	
G3V984	Bsn	S	3006	1	GEHRDYLSDSELNQL	-0.5627	-0.1202
G3V984	Bsn	S	3445	1	SRVASAYSGEKLSSH	-0.5073	-0.0163
G3V984	Bsn	S	3494	2	RARPPMRSQASEEES	0.6707	-0.0001
G3V984	Bsn	S	3497	1	PPMRSQASEEESPVS	0.8959	-0.1090
G3V984	Bsn	S	3497	2	PPMRSQASEEESPVS	0.4470	-0.0378
G3V984	Bsn	S	3497	3	PPMRSQASEEESPVS	0.4998	
G3V984	Bsn	S	3501	3	SQASEEESPVSPLGR	0.4998	
G3V984	Bsn	S	3504	1	SEEESPVSPLGRPRP	-0.5009	0.2177
G3V984	Bsn	S	3504	3	SEEESPVSPLGRPRP	0.4998	
G3V984	Bsn	S	3680	1	TRPHPQASPAPAMQK	-0.3838	0.2030
G3V984	Bsn	S	3713	1	PSAYHHASDSKKGSR	0.8589	-0.2329
G3V984	Bsn	S	3715	1	AYHHASDSKKGSRQA	0.7428	-0.2368
G3V984	Bsn	S	3853	1	PRAEQAGSSKPAAKA	0.3747	0.0188
Q5U2P5	C2cd2l	S	59	1	SAAEPGGSLRELGVW	0.2643	0.0216
D3ZLU0	C2cd4c	S	156	2	GFATLAESPHTRRKE	-0.2947	
D3ZLU0	C2cd4c	S	168	2	RKESLFHSEHGALAQ	-0.8254	0.0302

D3ZLU0	C2cd4c	S	178	2	GALAQVGSPGASRRR	-0.6879	0.0314
D3ZLU0	C2cd4c	S	206	1	EVGGGLMSPSRYFSG	-0.5540	
D3ZLU0	C2cd4c	S	262	1	QSVGRHGSLSADDST	1.5349	-0.1817
D3ZLU0	C2cd4c	S	264	1	VGRHGSLSADDSTPD	0.7152	-0.1063
D3ZLU0	C2cd4c	S	273	1	DDSTPDTSPGVRRRL	-0.4055	-0.0212
D3ZLU0	C2cd4c	T	285	1	RRLTRRATPEPGPES	0.4295	-0.0938
A0A0G2K543	C2cd5	T	339	1	KALLRQQTQSALEQR	0.6985	-0.0514
A0A0G2JXK1	Cacna1a	S	431	1	RRATLKKSKTDLLNP	-0.4349	
A0A0G2JXK1	Cacna1a	S	1051	2	GHSGLPPSPAKIGNS	-0.3845	0.2385
A0A0G2JXK1	Cacna1a	S	2078	1	SPMKRSASVLGPKAR	0.3270	-0.2575
A0A0G2JXK1	Cacna1a	S	2214	1	HATHRQGSSSVSGSP	0.4048	0.0451
F1LQ87	Cacna1b	S	2128	1	SQERRQPSSSSSEKQ	1.3201	0.0436
F1LQ87	Cacna1b	S	2243	1	GRLSRGLSEHNALLQ	0.7221	0.0316
F1LMS1	Cacna1e	T	846	1	KGDIGGLTSVLDNQR	0.4889	
G3V6K8	Cacnb1	S	495	2	AGTLRALSRQDTFDA	0.4415	
G3V6K8	Cacnb1	T	499	2	RALSRQDTFDADTPG	0.4734	
G3V6K8	Cacnb1	T	504	2	QDTFDADTPGSRNSA	0.4240	
D4A055	Cacnb4	S	443	1	RMRHSNHSTENSPIE	0.3170	
Q8VHW5	Cacng8	S	314	2	YTLSRDPSKGSVAAG	-0.2903	
Q8VHW5	Cacng8	S	317	2	SRDPSKGSVAAGLAS	-0.2903	
F1LLX6	Cadps	S	36	2	SGARLSPSRTSEGSA	-0.3829	0.0236
F1LLX6	Cadps	S	91	2	GGRPSSPSPSVVSEK	-1.3491	
F1LLX6	Cadps	S	93	2	RPSSPSPSVVSEKEK	-1.2748	
F1LLX6	Cadps	S	375	1	LKRSHNASIIDMGEE	0.6236	-0.0708
F1LWT1	Cadps2	T	731	1	TETMNQATPARKLEE	0.3195	
F1LZG4	Camk2a	T	331	1	VKESSESTNTTIEDE	0.2713	-0.2447
P11275	Camk2a	S	279	1	SHRSTVASCMHRQET	0.3630	-0.1545
P11275	Camk2a	T	286	1	SCMHRQETVDCLKKF	0.4834	-0.1216
F1LNI8	Camk2b	T	287	1	SMMHRQETVECLKKF	0.5280	-0.0882
F1LNI8	Camk2b	T	332	1	ADGVKPQTNSTKNSS	1.0229	-0.0367
F1LNI8	Camk2b	S	334	1	GVKPQTNSTKNSSAI	0.9768	-0.0232
F1LNI8	Camk2b	S	339	1	TNSTKNSSAITSPKG	0.6501	-0.0160
F1LUE2	Camk2b	S	363	1	TNSTKNSSAITSPKG	0.6501	-0.0160
F1LUE2	Camk2b	S	371	2	AITSPKGSLPPAALE	0.8827	0.0229
F1LUE2	Camk2b	T	381	1	PAALEPQTTVIHNPV	0.7402	-0.0170
F1LUE2	Camk2b	T	381	2	PAALEPQTTVIHNPV	0.6928	
F1LUE2	Camk2b	T	382	1	AALEPQTTVIHNPVD	0.6101	-0.0094
F1LUE2	Camk2b	T	382	2	AALEPQTTVIHNPVD	1.1483	0.0175
F1LUE2	Camk2b	T	400	1	ESSDSTNTTIEDEDA	0.4735	
F1LUE2	Camk2b	T	401	1	SSDSTNTTIEDEDAK	0.6492	
P08413	Camk2b	T	400	1	ESSDSTNTTIEDEDA	0.3922	-0.1303
P15791	Camk2d	T	287	1	SMMHRQETVDCLKKF	0.4834	-0.1216
P15791	Camk2d	S	315	2	MLATRNFSAAKSLLK	2.4892	-0.1281
P15791	Camk2d	S	319	2	RNFSAAKSLLKKPDG	2.4892	-0.1281

P15791	Camk2d	T	352	1	TPALEPQTTVIHNPD	0.4576	
P15791	Camk2d	T	353	1	PALEPQTTVIHNPDG	0.4516	-0.1081
P11730	Camk2g	S	36	2	RRCVKKTSTQEYAAK	0.6906	
P11730	Camk2g	T	37	1	RCVKKTSTQEYAAKI	0.7043	-0.2138
P11730	Camk2g	S	320	1	NFSVGRQSSAPASPA	0.4161	0.1941
P11730	Camk2g	S	325	2	RQSSAPASPAASAAG	0.2855	-0.0143
P11730	Camk2g	S	355	3	GGVKKRKSSSSVHLM	0.4245	0.0900
P11730	Camk2g	S	358	2	KKRKSSSSVHLMEPQ	0.2650	0.1792
P11730	Camk2g	S	358	3	KKRKSSSSVHLMEPQ	0.4319	0.1192
P11730	Camk2g	T	366	3	VHLMEPQTTVVHNAT	0.6735	
P11730	Camk2g	T	367	2	HLMEPQTTVVHNATD	0.3787	
P11730	Camk2g	T	367	3	HLMEPQTTVVHNATD	0.6735	
P97756	Camkk1	S	74	1	SLSARKFSLQERPAG	1.5338	-0.2187
A0A0G2K5T1	Camsap1	S	619	1	TIMAKRPSEGSQPLV	0.5449	-0.0251
D3ZXQ2	Camsap3	S	572	1	SPKAVASSPAANNSE	-0.4486	-0.1590
D3ZXQ2	Camsap3	S	829	1	LPHLRKFSPSQVPVQ	-0.4597	0.0060
P35565	Canx	S	582	1	EDEILNRSPRNRKPR	0.2647	-0.0729
Q9WU49	Carhsp1	S	30	1	TPRARDRSPSPLRGN	-0.2699	
Q9WU49	Carhsp1	S	30	2	TPRARDRSPSPLRGN	-0.9148	0.1550
Q9WU49	Carhsp1	S	32	2	RARDRSPSPLRGNVV	-0.9148	0.1550
D3ZC15	Carmil2	S	1314	1	RPLRLQRSPVLKRRP	-1.0093	-0.1249
Q8VHK2	Caskin1	S	388	1	PFAGGDRSGSLSNVA	0.3151	
Q8VHK2	Caskin1	S	392	1	GDRSGSLSNVAGGRS	0.3390	-0.0119
Q8VHK2	Caskin1	S	423	1	ATVLSQKSVSESSPG	1.6786	0.0597
Q8VHK2	Caskin1	S	698	1	TTSRQESSLSGRARH	0.8719	
Q8VHK2	Caskin1	S	727	1	PGSPMSRSQEYLLDE	-0.8690	
Q8VHK2	Caskin1	S	753	1	RSSRHGHSVKRASVP	1.4594	-0.2100
Q8VHK2	Caskin1	S	827	1	SPRSLPQSPTHRGFA	-0.2758	0.1248
Q8VHK2	Caskin1	S	883	1	RPKKRAHSLNRYAAS	-1.2060	0.0203
Q8VHK2	Caskin1	S	988	1	RAQRRRASDLAGSVD	-0.3619	-0.0535
F1MAS1	Cbarp	S	46	1	ESSQRASSLDTRGSP	0.5411	0.0656
F1MAS1	Cbarp	S	245	2	RGAGDEVSELPAPAR	-0.3577	0.0579
F1MAS1	Cbarp	S	253	2	ELPAPARSPPRSPRA	-0.5350	0.2359
F1MAS1	Cbarp	S	257	2	PARSPPRSPRAWPRR	-0.5267	0.1857
D4A8V2	Ccdc177	S	299	2	PLTARSFSLGDLSHS	-0.2851	
D4A8V2	Ccdc177	S	306	2	SLGDLSHSPQTAQHV	-0.2821	
Q498D0	Ccdc28a	S	34	1	NTIPASKSTGFSNPA	-0.5972	-0.1475
Q5BK07	Ccdc43	S	186	1	RDSLRDESQRKKEQD	0.5968	
D4AEK9	Ccdc6	S	233	2	EKLDQPVSAPPSPRD	-0.3070	0.0611
D4AEK9	Ccdc6	S	237	2	QPVSAPPSPRDISME	-0.3070	0.0611
Q9JK72	Ccs	S	267	1	AGQGRKDSAQPPAHL	0.3818	0.1564
O35832	Cdk18	S	51	1	RDEPGQLSPGVQYQQ	-0.3465	-0.1181
Q91XU8	Cds2	S	59	1	EVLNRALSNLSSRWK	0.3561	-0.1886
Q5FVI4	Cend1	T	59	1	PAAPGPATTKKTPAK	0.3375	-0.1480

Q5FVI4	Cend1	T	60	1	AAPGPATTKKTPAKA	0.3068	-0.1635
D4A1G8	Cep170b	S	337	2	GPGDDRHSTKSDLPV	-0.3546	0.0277
D4A1G8	Cep170b	S	340	2	DDRHSTKSDLPVHTR	-0.3547	0.0332
D4A1G8	Cep170b	S	371	1	DPLAKTASVSGAPTE	0.2877	0.0019
D4A1G8	Cep170b	S	843	1	IQLRSGRSPEPDPAP	-0.3516	
D4A1G8	Cep170b	S	1101	1	QVLTRSNSLSTPRPT	0.2985	-0.0153
D4A1G8	Cep170b	S	1103	1	LTRSNSLSTPRPTRA	0.5202	-0.0230
D4A1G8	Cep170b	S	1166	1	MPRKRAGSFTGPSDS	0.3079	0.0975
D4A1G8	Cep170b	T	1168	1	RKRAGSFTGPSDSET	0.2993	-0.0049
O35314	Chgb	S	93	1	LRDPSDASVGRWASS	0.4304	
E9PSL7	Cit	S	1999	1	TELRRDKSPGRPLER	-0.7265	0.1714
A0A0G2JUI5	Clasp1	S	689	1	ANPAGAGSRSSSPGK	0.5121	-0.1134
A0A0G2JZM8	Clasp2	S	549	1	KSSGSVASLPQSDRS	0.3011	-0.1364
A0A0G2JZM8	Clasp2	S	637	2	AGALNPGSYASLEDT	0.3416	0.0175
A0A0G2JZM8	Clasp2	S	640	2	LNPGSYASLEDTSDK	0.3993	0.0343
A0A0G2JZM8	Clasp2	S	770	2	REASRESSRDTSPVR	0.8892	
A0A0G2JZM8	Clasp2	S	1492	1	IKRAQTGSAGADPTT	0.7901	-0.1096
A0A0G2JW94	Clint1	S	340	1	LGLPMSRSQNADMVQ	-0.7637	0.0095
A0A0G2JZF2	Clip2	S	50	1	SPLHKQASGPSSAGA	0.7926	-0.0099
P20272	Cnr1	S	317	1	IQRGTQKSIIIHTSE	1.1460	-0.1828
P20272	Cnr1	S	317	2	IQRGTQKSIIIHTSE	1.3301	-0.1186
Q91ZN1	Coro1a	S	426	1	PEPSSTLSSDTVSRL	0.5743	
P80432	Cox7c	S	17	1	TTSVVRRSHYEEGPG	0.4540	-0.1365
Q62950	Crmp1	S	518	2	KHAAPAPSAKSSPSK	-0.3473	0.0923
Q62950	Crmp1	S	522	2	PAPSAKSSPSKHQPP	-0.4149	0.0851
Q62950	Crmp1	S	540	1	NLHQSNFSLSGAQID	0.7557	-0.1175
Q62950	Crmp1	S	540	2	NLHQSNFSLSGAQID	0.8291	-0.1026
Q62950	Crmp1	S	542	1	HQSNFSLSGAQIDDN	1.2058	-0.1888
Q62950	Crmp1	S	542	2	HQSNFSLSGAQIDDN	0.9129	-0.0936
Q157S1	Crtc1	S	151	1	TSWRRTNSDSALHQS	-0.7189	0.0269
D3ZZZ9	Ctnnd1	S	268	1	PQVRVGGSSVDLHRF	-0.6217	
D3ZZZ9	Ctnnd1	S	269	1	QVRVGGSSVDLHRFH	-0.5609	
F1M787	Ctnnd2	S	18	1	SEKNSSLSPGLNTSN	-0.2771	
F1M787	Ctnnd2	S	268	1	TKLQRGGSAPEGAAY	0.3413	-0.0802
F1M787	Ctnnd2	S	327	2	VQSTISSSPIHQLSS	-0.2682	
F1M787	Ctnnd2	S	457	1	VPLQRTGSQHGPQNA	0.3550	0.1573
F1M787	Ctnnd2	S	1080	1	SPNNRSASAPASPRE	0.3608	
D3ZGE6	Cttn	T	401	3	QARAKKQTPPASPSP	-0.9357	-0.0188
D3ZGE6	Cttn	S	405	3	KKQTPPASPSPQPAE	-0.9635	0.0272
D3ZGE6	Cttn	S	407	3	QTPPASPSPQPAEDR	-0.8973	-0.0033
D3ZGE6	Cttn	S	417	3	PAEDRPPSSPIYEDA	-0.9579	0.0485
D3ZGE6	Cttn	Y	421	3	RPPSSPIYEDAAPLK	-0.8682	0.0985
A0A0G2JTF2	Dab2ip	S	867	1	ELARRQMSLTEKGGQ	0.9533	0.0521
A0A0G2JTF2	Dab2ip	S	967	1	KQGPSPVSPNALDRT	-0.3708	

A0A0H2UHL9	Dbn1	S	241	1	EHRRKQQSLEAEEAK	0.5914	0.0879
A0A0H2UHL9	Dbn1	S	383	1	PTPIPTRSPSDSSTA	-0.2675	0.0271
A0A0H2UHL9	Dbn1	S	383	2	PTPIPTRSPSDSSTA	-0.4051	
A0A0H2UHL9	Dbn1	S	388	2	TRSPSDSSTASTPIT	-0.4484	
A0A0H2UHL9	Dbn1	T	392	2	SDSSTASTPITEQIE	-0.4365	
Q9JHL4	Dbnl	S	277	1	KQKERAMSTTSVSSS	1.7864	-0.0446
A0A1W2Q6Q2	Dclk1	S	347	2	SLRKQRISQHGGSST	-0.3659	0.0488
Q9WVP7	Dclk1	S	23	2	STPRSGKSPSPSPTS	-0.4388	0.0613
Q9WVP7	Dclk1	T	29	2	KSPSPSPTSPGSLRK	-0.7406	0.0943
Q9WVP7	Dclk1	S	30	2	SPSPSPTSPGSLRKQ	-0.4227	0.0183
Q3ZAU5	Ddhd1	S	11	1	PGRGAPRSPERNGRG	-0.5791	0.2083
A0A0G2K719	Ddx3x	S	606	1	ARDYRQSSGASSSSF	0.5524	0.1227
A0A0G2JY22	Dip2b	S	177	1	AESWINRSIQGSSTS	0.3971	
D3ZBZ6	Disp2	S	6	1	__MAPEASPERSCSL	0.2660	
Q2VUH7	Dixdc1	S	266	1	NRTDETGSPLSRDWR	0.3216	
P31016	Dlg4	S	142	1	EALKEAGSIVRLYVM	0.4889	-0.1967
P97837	Dlgap2	S	983	1	NDWKIMESPERKEER	0.3887	-0.2288
F1M3D2	Dmwd	S	487	1	RSLSRSNSLPHPAGG	0.2725	-0.0063
D4AA13	Dmxl1	S	2375	1	QTTSKALSVEGEKQN	1.0821	
F1M3W5	Dmxl2	S	451	2	MKLDHELSLDRESEA	0.2673	
F1M3W5	Dmxl2	S	931	1	AKAAEGISSDSLLSV	-0.9400	
F1M3W5	Dmxl2	S	931	2	AKAAEGISSDSLLSV	-0.8829	-0.1497
F1M3W5	Dmxl2	S	932	2	KAAEGISSDSLLSVP	-0.7190	
F1M3W5	Dmxl2	S	934	2	AEGISSDSLLSVPGQ	-0.8811	-0.1497
F1M3W5	Dmxl2	S	962	1	SSMPHSSSIANLQTA	-1.1219	-0.0819
F1M3W5	Dmxl2	T	1399	2	TKRHLSRTISVSGST	1.1677	0.0437
F1M3W5	Dmxl2	S	1401	1	RHLSRTISVSGSTAK	1.1837	-0.2097
F1M3W5	Dmxl2	S	1401	2	RHLSRTISVSGSTAK	1.0069	-0.0031
F1M3W5	Dmxl2	S	1403	1	LSRTISVSGSTAKDT	1.1500	-0.1927
F1M3W5	Dmxl2	S	1405	2	RTISVSGSTAKDTVT	1.1854	0.0241
F1M3W5	Dmxl2	T	1406	2	TISVSGSTAKDTVTI	1.1876	
F1M3W5	Dmxl2	T	1410	2	SGSTAKDTVTIGKDG	1.1331	
F1M3W5	Dmxl2	S	2397	1	VVKPRRQSESIAAPP	0.4485	-0.1464
D3ZUU5	Dnajb1	S	16	1	LGLARGASDDEIKRA	0.2897	-0.1746
A0A0G2JY26	Dnajc6	S	591	2	TPRRATTSASASPTL	-0.5501	0.0367
A0A0G2JY26	Dnajc6	S	595	2	ATTSASASPTLRVGE	-0.5348	0.0227
A0A0G2JY26	Dnajc6	S	679	3	GFGMGSKSAATSPTG	-0.9546	
A0A0G2JY26	Dnajc6	T	682	2	MGSKSAATSPTGSTH	-0.9566	0.1294
A0A0G2JY26	Dnajc6	T	682	3	MGSKSAATSPTGSTH	-0.9652	
A0A0G2JY26	Dnajc6	S	683	3	GSKSAATSPTGSTHG	-0.9684	
P21575	Dnm1	S	774	1	SVPAGRRSPTSSPTP	-0.8548	-0.0382
P21575	Dnm1	S	774	2	SVPAGRRSPTSSPTP	-1.5821	0.0683
P21575	Dnm1	T	776	2	PAGRRSPTSSPTPQR	-1.5917	0.0676
P21575	Dnm1	S	777	1	AGRRSPTSSPTPQRR	0.8453	0.0008

P21575	Dnm1	S	777	2	AGRRSPTSSPTPQRR	-1.5037	0.0691
P21575	Dnm1	S	778	1	GRRSPTSSPTPQRRA	0.7520	0.0013
P21575	Dnm1	S	778	2	GRRSPTSSPTPQRRA	-1.4327	0.0340
P21575	Dnm1	T	780	2	RSPTSSPTPQRRAPA	-1.3000	-0.1746
P21575	Dnm1	S	851	1	PSRSGQASPSRPESP	-0.9563	-0.0336
P21575	Dnm1	S	851	2	PSRSGQASPSRPESP	-1.1410	-0.0158
P21575	Dnm1	S	853	2	RSGQASPSRPESPRP	-1.0425	-0.0360
P21575	Dnm1	S	857	1	ASPSRPESPRPPFDL	-0.8711	-0.0096
P21575	Dnm1	S	857	2	ASPSRPESPRPPFDL	-1.2327	-0.0245
Q08877	Dnm3	S	769	1	WLQHSRRSPPPSPTT	0.3444	-0.0584
Q08877	Dnm3	S	769	2	WLQHSRRSPPPSPTT	-0.4608	-0.0372
Q08877	Dnm3	S	773	2	SRRSPPPSPTTQRRL	-0.4533	-0.0451
P47942	Dpysl2	T	514	3	SVTPKTVTPASSAKT	-0.4724	0.1720
P47942	Dpysl2	S	517	3	PKTVTPASSAKTSPA	-0.5390	0.2232
P47942	Dpysl2	S	518	3	KTVTPASSAKTSPAK	-0.4917	0.1921
P47942	Dpysl2	S	540	1	NLHQSGFSLSGAQID	1.2689	-0.1140
P47942	Dpysl2	S	540	2	NLHQSGFSLSGAQID	1.1650	-0.0784
P47942	Dpysl2	S	542	1	HQSGFSLSGAQIDDN	1.1028	0.0921
P47942	Dpysl2	S	542	2	HQSGFSLSGAQIDDN	1.3511	-0.0789
Q62952	Dpysl3	S	518	2	KGGTPAGSTRGSPTR	-0.4003	0.0504
Q62952	Dpysl3	T	519	2	GGTPAGSTRGSPTRP	-0.4037	0.0113
Q62952	Dpysl3	S	522	2	PAGSTRGSPTRPNPP	-0.4384	0.0831
Q62952	Dpysl3	S	539	1	NLHQSGFSLSGTQVD	0.9523	-0.0892
Q62952	Dpysl3	S	539	2	NLHQSGFSLSGTQVD	0.8274	0.0047
Q62952	Dpysl3	S	541	2	HQSGFSLSGTQVDEG	0.8577	0.0308
Q62951	Dpysl4	S	532	2	NLHQSGFSLSGSQAD	0.3386	-0.1611
Q62951	Dpysl4	S	534	1	HQSGFSLSGSQADDH	0.4708	0.0449
Q62951	Dpysl4	S	536	1	SGFSLSGSQADDHIA	0.2995	-0.0264
Q62951	Dpysl4	S	536	2	SGFSLSGSQADDHIA	0.3386	-0.1276
Q9JHU0	Dpysl5	S	532	1	MRDLHESSFSLSGSQ	0.6056	0.0632
Q9JHU0	Dpysl5	S	532	2	MRDLHESSFSLSGSQ	2.2061	0.0784
Q9JHU0	Dpysl5	S	532	3	MRDLHESSFSLSGSQ	0.9265	
Q9JHU0	Dpysl5	S	534	1	DLHESSFSLSGSQID	1.1216	0.0222
Q9JHU0	Dpysl5	S	534	2	DLHESSFSLSGSQID	1.9246	-0.0721
Q9JHU0	Dpysl5	S	534	3	DLHESSFSLSGSQID	0.9265	
Q9JHU0	Dpysl5	S	536	2	HESSFSLSGSQIDDH	2.1442	0.2249
Q9JHU0	Dpysl5	S	536	3	HESSFSLSGSQIDDH	1.2867	
Q9JHU0	Dpysl5	S	538	2	SSFSLSGSQIDDHVP	1.9344	0.0760
Q9JHU0	Dpysl5	S	538	3	SSFSLSGSQIDDHVP	0.9265	
B0K014	Dtd1	S	196	1	RKEDRSASSGAEGDV	0.2855	
Q9QXU8	Dync1li1	T	512	2	KPASVSPTTPPSPTE	-0.3507	0.1281
G3V7D4	Efnb3	S	268	1	SRHPGPGSFGRGGSL	0.2958	-0.0672
F1LVX2	Ehbp1	S	310	1	TFVMIKDSPPQSTRR	1.1739	
F1LVX2	Ehbp1	S	1009	1	PEMKRQRSIQEDTER	0.7812	0.0782

Q6AYK8	Eif3d	S	161	1	SQKPRDSSVEVRSDW	0.4008	
Q5RKG9	Eif4b	S	340	1	KLNLKPRSTPKEDDS	2.1244	0.2214
Q5RKG9	Eif4b	S	495	2	SSNPPARSQSSDTEQ	0.6665	0.0021
Q5RKG9	Eif4b	T	500	2	ARSQSSDTEQPSPTS	0.4319	0.0922
Q5RKG9	Eif4b	S	504	1	SSDTEQPSPTSGGGK	-0.4848	0.1802
A0A0G2JY73	Eif4g3	S	1186	1	NTFLRGSSKDLLDNQ	0.9698	0.2274
P60841	Ensa	S	2	1	_____MSQKQEEEN	0.7105	
P60841	Ensa	S	67	1	KGQKYFDSGDYNMAK	0.6643	
A0A0G2K0F3	Epb41l1	S	540	1	ERERRLPSSPASPSP	-0.4341	-0.0865
A0A0G2K0F3	Epb41l1	S	540	2	ERERRLPSSPASPSP	-0.4486	0.0618
A0A0G2K0F3	Epb41l1	S	541	2	RERRLPSSPASPSPK	-0.3278	0.2383
A0A0G2K0F3	Epb41l1	T	1252	1	PRAPESDTGDEDQDQ	0.4163	-0.1111
A0A0G2K0F3	Epb41l1	S	1311	2	AFEDFSRSLPELDRD	-0.3508	0.1155
A0A0G2K0F3	Epb41l1	T	1394	1	MLQSRVSTADSTQVD	0.3181	
Q9WTP0	Epb41l1	S	540	1	ERERRLPSSPASPSP	-0.4341	-0.0865
Q9WTP0	Epb41l1	S	540	2	ERERRLPSSPASPSP	-0.4486	0.0618
Q9WTP0	Epb41l1	S	541	2	RERRLPSSPASPSPK	-0.3278	0.2256
D3ZM69	Epb41l2	S	543	2	RASSKRVSRSLDGAP	-0.3329	
D3ZM69	Epb41l2	S	545	2	SSKRVSRSLDGAPIG	-0.3821	
G3V874	Epb41l3	S	463	1	YATTKVISQTNLITT	-0.3907	-0.0745
G3V874	Epb41l3	T	465	1	TTKVISQTNLITTVT	-0.3476	-0.0238
A0A0G2JYT1	Erc1	S	17	1	KVEPSSQSPGRSPRL	0.3483	0.1966
A0A0G2JYT1	Erc1	S	17	2	KVEPSSQSPGRSPRL	-0.5493	
A0A0G2JYT1	Erc1	S	21	2	SSQSPGRSPRLPRSP	-0.5493	
A0A0G2JYT1	Erc1	S	37	1	LGHRRTNSTGGSSGN	0.6165	-0.1003
A0A0G2JYT1	Erc1	S	45	2	TGGSSGNSVGGGSGK	1.3096	-0.0558
Q8K3M6	Erc2	S	14	1	TISNPEGSPSRSPRL	0.3488	-0.0778
Q8K3M6	Erc2	S	18	1	PEGSPSRSPRLPRSP	-0.7571	-0.0054
Q8K3M6	Erc2	S	321	1	SKGLPSKSLEDDNER	0.7321	0.0318
M0R5H1	Etl4	T	59	1	RNIPRRHTLGGPRSS	0.4638	-0.2082
M0R5H1	Etl4	S	1088	1	SGLTTTRSGDVIYTG	0.5970	
M0R5H1	Etl4	S	1775	1	TSKNRPGSLDKASKP	1.9110	0.1575
O08719	Evl	S	335	1	KPWERSNSVEKPVSS	0.9272	0.2171
O08719	Evl	T	347	2	VSSLLSRTPSVAKSP	0.6636	
O08719	Evl	S	353	2	RTPSVAKSPEAKSPL	0.8704	
A0A0G2JYT4	Exoc1	S	470	2	KLTGSTSSLNKLSVQ	-0.4472	0.0102
O54924	Exoc8	S	28	1	RLYVKQLSQQSDGDR	0.3452	
Q4V7D4	Fam126b	S	321	1	RTAITTASIRRHRWR	0.5262	-0.1123
Q4V7D4	Fam126b	S	402	1	SNESPRDSVVGKQFL	0.9025	
F8WFH6	Fam131b	S	75	1	LPKLKRNSNAYGIGA	0.3855	-0.1059
F8WFH6	Fam131b	S	130	1	PAIQPQHSHEAVRRD	0.3407	0.0422
F8WFH6	Fam131b	T	344	1	SRKVSDVTSSGVQSF	-0.3788	
F1LZ91	Fam135b	S	539	1	DVDICRRSPGPEEGH	-0.2999	
D3ZTG3	Fam171b	S	346	2	TTHINHISSVKVALK	0.3446	-0.0647

A0A0G2JTS9	Fbxo42	S	365	2	PSGRAPLSPSLNSRP	-0.5242	0.0402
A0A0G2JTS9	Fbxo42	S	373	2	PSLNSRPSPISATPP	-0.5242	
A0A0G2JTS9	Fbxo42	S	488	1	SLVPRRGSLPDQKDL	0.3052	0.0323
D3ZYR1	Fcho2	S	403	1	VQMNRNSSNEELTKS	-0.4226	
F1LQJ2	Fhod3	S	367	1	RRRSRRHSIQNIKSP	0.6106	-0.0418
Q5RKI5	Flii	S	436	1	RLRRRKDSAQDVQAK	0.4074	0.1476
A0A0G2K749	Fry	S	1876	1	EERQLSRSTPSLNKM	-0.4531	0.0293
P18088	Gad1	S	55	1	GFLQRTNSLEEKSRL	1.5949	-0.1172
P07936	Gap43	S	103	1	SPKAEEPSKAGDAPS	0.6367	-0.1604
P07936	Gap43	S	122	1	GEGDAAPSEEKAGSA	0.4135	-0.2050
P07936	Gap43	S	209	1	DEAKPKESARQDEGK	0.7132	
A0A0G2JT50	Gas7	S	99	1	AHMSLRKSTGDSQNL	-0.5348	0.0439
Q9Z254	Gipc1	S	225	1	FDMISQRSSGGHPGS	0.3188	-0.0482
Q9Z272	Git1	S	419	2	TRNNRARSMDSSDLS	0.5820	0.0628
Q9Z272	Git1	S	422	2	NRARSMDSSDLSDGA	0.6005	
Q9Z272	Git1	S	507	1	TLMGPGGSTHRRDRQ	0.2789	0.0946
Q9Z272	Git1	S	601	1	SKLSRHGSGAESDYE	0.6731	-0.1728
Q9Z272	Git1	S	601	2	SKLSRHGSGAESDYE	0.2999	-0.0849
Q9Z272	Git1	S	605	1	RHGSGAESDYENTQS	0.6262	-0.1830
P08050	Gja1	S	325	2	NRMGQAGSTISNSHA	-0.3637	
P08050	Gja1	S	368	2	QRPSSRASSRASSRP	-0.4713	
P08050	Gja1	S	369	2	RPSSRASSRASSRPR	-0.4873	
G3V8K2	Gng3	T	10	1	GETPVNSTMSIGQAR	0.3304	-0.1404
G3V8K2	Gng3	S	12	1	TPVNSTMSIGQARKM	0.4048	-0.1214
Q6MG06	Gnl1	S	68	1	RRLNQQPSQGLGPRG	0.4925	0.0814
Q03555	Gphn	S	337	1	NILRASHSAVDITKV	-0.3981	0.1505
A0A0A0MY13	Gpr158	S	881	2	PLVCKSASAHNLSSE	-0.4135	-0.1182
A0A0A0MY13	Gpr158	S	886	2	SASAHNLSSEKKPGH	-0.5357	-0.0611
A0A0A0MY13	Gpr158	S	887	2	ASAHNLSSEKKPGHP	-0.4445	-0.2382
A0A0A0MY13	Gpr158	S	902	1	RTSMLQKSLSVIASA	0.5217	-0.2165
D3ZF21	Gprin3	S	570	2	GSEGPEVSPAPSPGR	-1.0652	
D3ZF21	Gprin3	S	574	2	PEVSPAPSPGRKSTV	-1.0652	
P97879	Grip1	S	937	1	SQLGRQASFQERSNS	0.9979	0.1220
P97879	Grip1	T	956	1	SQTTRSNTLPSDVGR	0.2678	-0.0551
P26817	Grk2	S	487	1	ADAFDIGSFDEEDTK	0.6897	-0.1126
P26817	Grk2	S	670	1	KMKNKPRSPVVELSK	-0.4126	-0.0658
A0A0G2JV93	Grm3	S	875	1	QPTPQHHSTKRQGIC	0.4652	
A0A0G2QC41	Hdac6	S	909	1	ALLAQGQSSEQAAKG	1.5552	0.0445
D4ADD3	Hecw2	S	1046	1	QHLTRQRSHSAGEVG	2.0798	
D4ADD3	Hecw2	S	1048	1	LTRQRSHSAGEVGED	-0.5176	
D4ADD3	Hecw2	S	1181	1	PVSSPQNSPGTQRAN	-0.4713	0.0664
P82995	Hsp90aa1	S	454	1	KLGIHEDSQNRKKLS	0.2657	-0.1694
Q9WVR1	Inpp5e	S	235	1	NRLVRAHSNLGPSRP	0.6923	
D3ZKG7	Inpp5f	S	905	2	APRLGSRSQSASSTD	-0.7695	

D3ZKG7	Inpp5f	S	935	2	ELGKGLESPLKKSPS	-0.8745	0.1800
D3ZKG7	Inpp5f	S	935	3	ELGKGLESPLKKSPS	-0.4006	
D3ZKG7	Inpp5f	S	940	2	LESPLKKSPSADNIH	-0.8348	0.1672
D3ZKG7	Inpp5f	S	940	3	LESPLKKSPSADNIH	-0.3992	
D3ZKG7	Inpp5f	S	942	3	SPLKKSPSADNIHTL	-0.3983	
D3ZKG7	Inpp5f	T	948	2	PSADNIHTLTGFAKP	-0.8675	0.1806
D3ZKG7	Inpp5f	T	948	3	PSADNIHTLTGFAKP	-0.4285	
Q9JMC1	Inpp5j	S	69	1	VGPRAAVSPPSERPR	-0.2664	
Q9JMC1	Inpp5j	S	320	2	LPESGTRSPGLLSPT	-0.4294	-0.0052
Q9JMC1	Inpp5j	S	325	2	TRSPGLLSPTFRPGI	-0.4152	
Q9JMC1	Inpp5j	S	881	2	GKSKRHRSRSPGLAR	-1.5195	-0.0308
Q9JMC1	Inpp5j	S	883	2	SKRHRSRSPGLARFP	-1.5195	-0.0308
Q9JMC1	Inpp5j	S	909	1	RGGSRSPSPQSRQLP	1.3746	0.1394
A0A0G2JUG7	Iqsec1	S	87	2	RRPRLQHSTSVLRKQ	0.5414	
A0A0G2JUG7	Iqsec1	T	88	1	RPRLQHSTSVLRKQA	0.4184	0.0725
A0A0G2JUG7	Iqsec1	T	88	2	RPRLQHSTSVLRKQA	0.5414	
A0A0G2JUG7	Iqsec1	S	103	2	EEEAIKRSRSLSESY	0.4101	-0.0594
A0A0G2JUG7	Iqsec1	S	105	1	EAIKRSRSLSESYEL	0.5338	-0.1523
A0A0G2JUG7	Iqsec1	S	105	2	EAIKRSRSLSESYEL	0.3977	-0.0289
A0A0G2JUG7	Iqsec1	S	109	2	RSRSLSESYELSSDL	0.4203	0.0033
A0A0G2JUG7	Iqsec1	Y	110	2	SRSLSESYELSSDLQ	0.3559	
A0A0G2JUG7	Iqsec1	S	180	1	SNMRMQFSFEGPEKV	0.4728	-0.1761
A0A0G2JUG7	Iqsec1	S	363	1	TSCRSTPSLERPEPR	0.4156	0.1319
A0A0G2JUG7	Iqsec1	S	404	1	RSSLKRQSAYERSLG	-0.6598	-0.0497
A0A0G2JZX5	Iqsec2	S	168	1	NFERLRSSASESRMS	0.4132	-0.0383
A0A0G2JZW3	Itfg2	S	219	1	TWNKDTGSPPASEEA	0.3066	
P17105	Itpka	S	135	2	SSSLLEDSEDDLLSD	-0.3497	
P17105	Itpka	S	141	2	DSEDDLLSDSESRSR	-0.4039	
F1LNT1	Itpr1	S	1613	1	RNAARRDSVLAASRD	0.3309	-0.0059
Q9WVE9	Itsn1	S	623	1	QQLQKQRSIEAERLK	0.4858	
Q9WVE9	Itsn1	S	896	1	TATGSSPSPVLGQGE	-0.3371	
Q9WVE9	Itsn1	S	970	1	GPVRKSTSIDTGPTE	0.5956	-0.0420
Q9WVE9	Itsn1	S	1129	2	ANYVKLLSPGTSKIT	-0.4416	-0.0088
Q9WVE9	Itsn1	T	1132	2	VKLLSPGTSKITPTE	-0.4362	-0.0202
Q9WVE9	Itsn1	T	1136	2	SPGTSKITPTELPKT	-0.4624	-0.0130
Q6AXU6	JPT1	S	17	1	VDPNSRNSSRVLRPP	0.4275	0.1108
Q6AXU6	JPT1	S	65	1	NPPSWAKSAGGREDS	0.9287	
Q6AXU6	JPT1	S	72	1	SAGGREDSESPGTQR	1.0504	
Q811T3	Kcnc3	T	750	2	LRLAPLATPPGSPRA	-0.2634	
Q811T3	Kcnc3	S	754	2	PLATPPGSPRATRRA	-0.2634	
Q63472	Kcnh1	S	872	2	DNVGEARSPQDRSPI	-0.5987	-0.0099
Q63472	Kcnh1	S	877	2	ARSPQDRSPILAEVK	-0.5987	-0.0099
F1LNC7	Kcnma1	S	1195	1	NAGQSRASLSHSSHS	-0.6826	-0.0030
F1LNC7	Kcnma1	S	1202	1	SLSHSSHSSQSSSKK	0.5978	0.1187

F1LNC7	Kcnma1	S	1203	1	LSHSSHSSQSSSKKS	0.4688	0.0637
F1LNC7	Kcnma1	S	1203	2	LSHSSHSSQSSSKKS	-0.3771	
F1LNC7	Kcnma1	S	1205	1	HSSHSSQSSSKKSSS	0.5777	-0.0135
F1LNC7	Kcnma1	S	1207	1	SHSSQSSSKKSSSVH	0.7169	-0.2007
F1LSD6	Kcnq5	S	325	1	SIKSRQASVGDRRSP	0.5278	
F1LSD6	Kcnq5	S	566	1	GCLSRSASANISRGL	-1.1393	
D4A0X3	Kiaa1107	S	218	1	ERLASTGSVDETKEN	0.4579	0.2013
D4A0X3	Kiaa1107	S	218	2	ERLASTGSVDETKEN	0.5732	
D4A0X3	Kiaa1107	T	222	2	STGSVDETKENGSVE	0.5796	
D4A0X3	Kiaa1107	S	336	1	TLAQTQGSQGESPHS	0.4046	0.2514
F1M4A4	Kif1a	S	425	2	ALSSRAASVSSLHER	0.2692	
F1M4A4	Kif1a	S	427	2	SSRAASVSSLHERIL	0.2833	
F1M4A4	Kif1a	S	428	2	SRAASVSSLHERILF	0.2754	
D3ZCG2	Kif21a	S	1227	1	EKKVPEPSPVTRRKA	-0.5134	-0.0754
G3V6L4	Kif5c	S	918	1	NMARRAHSAQIAKPI	0.9338	-0.1909
B2GV74	Klc2	S	582	2	SRMKRASSLNFLNKS	0.7248	0.1003
Q5PQM2	Klc4	S	565	1	IRDVLRRSSELLVRK	-0.4273	0.0318
F1LY04	Ksr2	S	313	1	TALHRSKSHEFQLGN	-0.5562	-0.0298
D3ZGM3	LOC100909750	S	909	1	KAGKPAQSPSQDVAG	-0.4034	0.0039
D3ZGM3	LOC100909750	S	911	1	GKPAQSPSQDVAGEA	-0.4092	0.0325
Q9Z252	Lin7b	S	201	1	RQQHHSYSSLESRG_	0.6229	-0.0449
D3ZBH5	Lmtk2	S	576	2	AEDSHAASIPGSPFN	-0.4634	
D3ZBH5	Lmtk2	S	580	2	HAASIPGSPFNIFSD	-0.4634	
F1LT49	Lrrc47	S	429	1	RKQKKRQSVSGLHRY	0.2906	-0.1208
Q4V7E8	Lrrfip2	S	125	1	ASATTPLSGNSSRRG	0.4261	0.1845
Q5HZA4	Lysmd1	S	194	1	DTGLYPSSPRMQQRA	-0.4872	-0.1054
O08873	Madd	S	708	1	SSTTASSSPSTIVHG	-0.3223	-0.0596
O08873	Madd	S	812	1	QKLLRPNSLKLASDS	0.7722	-0.0574
O08873	Madd	S	900	1	KSSVIKHSPTVKREP	-0.4991	-0.1397
O08873	Madd	S	1224	2	KPKEKPASSPVRSSE	-0.3080	
O08873	Madd	S	1225	2	PKEKPASSPVRSSED	-0.3132	-0.2056
O08873	Madd	S	1229	2	PASSPVRSSEDVSQR	-0.3586	-0.2083
M0R8T1	Magi1	S	644	1	QPLERKDSQNSSQHS	1.2018	0.1383
P34926	Map1a	S	2204	2	SSLPQLPSPSSPGGP	-0.6192	0.0517
P34926	Map1a	S	2206	2	LPQLPSPSSPGGPLL	-0.6310	0.0409
P34926	Map1a	S	2207	2	PQLPSPSSPGGPLLS	-0.4927	
P15205	Map1b	S	601	1	GKVESKPSVTEKEVP	1.0930	-0.2449
P15205	Map1b	T	1262	2	PPSPIEKTPLGERSV	-1.5088	
P15205	Map1b	T	1262	3	PPSPIEKTPLGERSV	-0.9297	0.1316
P15205	Map1b	S	1371	2	ENERSSISPMDEPVP	-0.2671	0.1807
P15205	Map1b	S	1380	2	MDEPVPDSESPIEKV	-0.3210	0.1043
P15205	Map1b	S	1382	2	EPVPDSESPIEKVLS	-0.2677	0.1361
P15205	Map1b	S	1389	2	SPIEKVLSPLRSPPL	-0.4273	0.0860
P15205	Map1b	S	1389	3	SPIEKVLSPLRSPPL	-0.8947	

P15205	Map1b	S	1393	2	KVLSPLRSPPLIGSE	-0.3423	0.0284
P15205	Map1b	S	1393	3	KVLSPLRSPPLIGSE	-0.9990	
P15205	Map1b	S	1401	3	PPLIGSESAYEDFLS	-1.0091	
P15205	Map1b	Y	1403	2	LIGSESAYEDFLSAD	-0.4042	0.0187
P15205	Map1b	S	1408	2	SAYEDFLSADDKALG	-0.4335	
P15205	Map1b	S	1418	1	DKALGRRSESPFEGK	-0.5421	0.0910
P15205	Map1b	S	1420	1	ALGRRSESPFEGKNG	-0.7258	-0.1655
P15205	Map1b	S	1494	2	RKLGGDGSPTQVDVS	-0.3031	0.2281
P15205	Map1b	S	1505	2	VDVSQFGSFKEDTKM	-0.3130	0.2266
P15205	Map1b	T	1626	1	PKTAKSRTPVQDHRS	-0.9447	0.2229
P15205	Map1b	S	1908	1	KTERTIKSPCDSGYS	-0.3411	0.0121
P0C5W1	Map1s	S	683	1	RKPPPPASPGSSDSS	-0.5918	0.1209
F1MAQ5	Map2	S	685	1	DDLTLSRSLGLGGRS	-0.3638	
F1MAQ5	Map2	T	749	3	DDYLPPTTPAVEKIP	-0.5705	
F1MAQ5	Map2	S	892	2	SENLSGESGSFYEGT	-0.3513	
F1MAQ5	Map2	S	1740	1	KAQAKVGSLDNAHHV	0.6089	0.1765
F1LP57	Map2k4	T	51	1	PHIERLRTHSIESSG	1.5600	-0.0711
F1LP57	Map2k4	S	53	1	IERLRTHSIESSGKL	1.5446	0.0113
Q4KSH7	Map2k7	S	61	1	RSPSSESSPQHPTPP	0.6976	0.2135
D3ZG83	Map3k10	S	714	1	GRFPRGLSPTGRPGG	-0.4770	
D3ZZH6	Map3k5	S	1035	2	DENFEDHSAPPSPEE	-0.7522	
D3ZZH6	Map3k5	S	1039	2	EDHSAPPSPEEKDSG	-0.7522	
A0A0G2JW88	Map4	S	2123	1	KAQAKVGSLDNVGHL	0.8840	-0.2160
P63086	Mapk1	T	179	2	ADPDHDHTGFLTEYV	1.0856	
P63086	Mapk1	T	183	2	HDHTGFLTEYVATRW	1.2139	
P63086	Mapk1	Y	185	2	HTGFLTEYVATRWYR	1.2236	
P21708	Mapk3	T	203	2	HDHTGFLTEYVATRW	0.6364	-0.1289
P21708	Mapk3	Y	205	2	HTGFLTEYVATRWYR	0.6364	-0.1289
E9PSK7	Mapk8ip3	T	287	2	SVPSAAVTPLNESLQ	-0.3905	
E9PSK7	Mapk8ip3	S	544	1	WTEMIRASREHPSVQ	1.0121	
E9PSK7	Mapk8ip3	S	740	1	EPKSTHPSPEKKKAK	0.3152	-0.1555
D4A1Q2	Mapt	T	421	2	TRIPAKTTPSPKTPP	-0.3117	0.2430
D4A1Q2	Mapt	S	423	2	IPAKTTPSPKTPPGS	-0.3336	0.2398
D4A1Q2	Mapt	S	430	2	SPKTPPGSGEPPKSG	-0.3070	0.1898
D4A1Q2	Mapt	S	550	1	KHVPGGGSVQIVYKP	0.5125	-0.1126
D4A1Q2	Mapt	S	597	2	DFKDRVQSKIGSLDN	1.4973	-0.1821
D4A1Q2	Mapt	T	631	2	RENAKAKTDHGAEIV	0.2979	-0.0877
D4A1Q2	Mapt	T	648	1	SPVVSGDTSPRHLSN	0.3757	0.1656
Q5XI50	7-Mar	S	302	1	TFFSRRSSQDSLNTR	0.4258	-0.0198
P30009	Marcks	S	138	2	AEDGAAPSPSSETPK	0.3653	-0.0819
P30009	Marcks	S	140	2	DGAAPSPSSETPKKK	0.3519	-0.0778
P30009	Marcks	T	143	2	APSPSSETPKKKKKR	0.3548	-0.0858
P30009	Marcks	S	156	2	KRFSFKKSFKLSGFS	2.2814	-0.1232
P30009	Marcks	S	156	3	KRFSFKKSFKLSGFS	2.1628	

P30009	Marcks	S	160	2	FKKSFKLSGFSFKKS	2.2087	-0.1044
P30009	Marcks	S	160	3	FKKSFKLSGFSFKKS	2.1628	
Q9EPH2	Marcksl1	T	85	1	GEVAPKETPKKKKKF	0.2748	-0.0953
O08678	Mark1	S	463	2	DTARRLGSTTVGSKS	-0.3653	-0.0135
O08678	Mark1	S	468	2	LGSTTVGSKSEVTAS	-0.3414	
O08678	Mark1	S	666	1	KFVRRDPSEGEASGR	1.7072	
A0A1B0GWN5	Mark3	S	416	1	PRGTASRSTFHGQPR	0.2891	-0.0964
Q810W7	Mast1	S	1254	2	IVRPRPKSAEPPRSP	-0.9991	
Q810W7	Mast1	S	1260	2	KSAEPPRSPLLKRVQ	-0.9991	
Q63406	Mcf2l	S	966	2	RALEQSHSLPLPTPA	0.2633	
A0A0G2KAL9	Mff	T	112	2	DLERPPPTPQSEEIR	-0.7970	
A0A0G2KAL9	Mff	S	115	2	RPPPTPQSEEIRAVG	-0.6719	
A0A0G2KAL9	Mff	S	146	1	GQLVRNDSIVTPSPP	0.4463	-0.0720
A0A0G2KAL9	Mff	T	149	2	VRNDSIVTPSPPQAR	-0.3660	-0.2130
A0A0G2KAL9	Mff	S	151	2	NDSIVTPSPPQARVC	-0.3522	-0.1127
A0A0G2K6P5	Mfsd4a	S	273	1	AEKEDTSSLAHKFQP	0.4445	
D3ZGN7	Mical3	S	976	1	HALLKGRSEEELEAS	0.3058	
D3ZGN7	Mical3	T	1404	2	GDQPPLLTPKSPSDK	-1.3259	
D3ZGN7	Mical3	S	1407	1	PPLLTPKSPSDKELR	-0.7991	0.0322
D3ZGN7	Mical3	S	1407	2	PPLLTPKSPSDKELR	-1.2930	
Q5XIS8	Mief1	S	59	1	RAISAPTSPTRLSHS	0.3628	
Q63327	Mobp	S	13	1	AKEGPRLSKNQKFSE	0.3604	-0.2624
P62775	Mtpn	T	31	1	KGEDVNRTLEGGRKP	0.4133	
D4A3S6	Mtss1l	S	419	1	MVLTRGLSLEHQKSS	1.3906	0.1037
Q9JLT0	Myh10	S	1939	1	GPISFSSSRSGRRQL	1.2267	-0.1313
Q9JLT0	Myh10	S	1952	2	QLHIEGASLELSDDD	0.8169	0.1984
Q9JLT0	Myh10	S	1956	2	EGASLELSDDDTESK	0.8770	0.1922
Q9JLT0	Myh10	T	1960	2	LELSDDDTESKTSDV	0.7400	
Q9QYF3	Myo5a	S	1624	2	TGLRKRTSSIADEGT	0.6037	-0.0037
Q9QYF3	Myo5a	S	1625	2	GLRKRTSSIADEGTY	0.4837	-0.0717
Q9QYF3	Myo5a	T	1631	2	SSIADEGTYTLDSIL	0.5006	0.0168
D4A5I4	Nav1	S	787	1	WRRERPESCDDSSKG	0.8499	
D4A5I4	Nav1	S	952	1	RSNIQYRSLPRPAKS	-0.3649	-0.2530
D4A5I4	Nav1	S	1085	2	ANLDKVNSNSLDLPS	0.8901	
D4A5I4	Nav1	S	1087	1	LDKVNSNSLDLPSSS	0.5835	0.0615
D4A5I4	Nav1	S	1087	2	LDKVNSNSLDLPSSS	0.9337	
D4A5I4	Nav1	S	1229	1	GLRYQLQSQEETKER	0.7471	-0.0383
D4A5I4	Nav1	S	1532	1	SPKLQHGSTETASPS	0.3691	0.0837
A0A0G2K0M8	Ncam1	T	846	2	ATSKPSPTPTPTPAG	-0.4029	0.1376
A0A0G2K0M8	Ncam1	S	856	2	PTPAGAASPLAAVAA	-0.4102	0.1460
F1LWN1	Ncoa7	S	184	2	ATVSPSSSDAEYDKL	-0.3126	-0.0293
A0A0G2JXP3	Nedd4l	S	434	2	IRRPRSLSSPTVTLS	-0.3085	
P97526	Nf1	S	2524	1	KLLGTRKSFDHLISD	0.3829	-0.0194
Q5BKC9	Ngef	S	687	1	KMEDPQRSQNKDRRK	0.8370	0.1487

A0A0G2JZL4	Nhsl1	S	1352	1	KVLGRKDSEDDHTRN	1.9045	
Q6AY81	Npdc1	S	235	1	ATAKGPTSPTTPRIS	0.4154	-0.2588
Q6AY81	Npdc1	S	242	1	SPTTPRISPGDERLA	0.3279	
O35764	Nptxr	S	251	1	EKERAALSHGSHQQR	0.3072	
A0A0G2JT23	Nrbp2	T	407	2	EEAQKAKTPTPEPFD	-0.4976	-0.1189
A0A0G2JT23	Nrbp2	T	409	2	AQKAKTPTPEPFDSE	-0.4918	-0.1210
P47245	Nrdc	S	85	1	ARLGADESEEEGRSL	0.3507	
Q63372	Nrxn1	S	1485	1	YRNRDEGSYHVDESR	0.2736	
O35987	Nsfl1c	S	176	1	AGERRRHSGQDVHVV	-0.3928	-0.0222
Q2LC84	Numb	T	437	1	FQAGHRRTPSEADRW	0.8087	
Q2LC84	Numb	S	635	1	PKQRTNPSPTNPFSS	-0.3916	0.0844
Q2LC84	Numb	T	637	1	QRTNPSPTNPFSSDA	-0.3634	
A1L1I3	Numbl	S	411	1	PGHKRTPSEAERWLE	0.9620	
P33535	Oprm1	T	370	1	STRVRQNTREHPSTA	0.3778	-0.0487
Q9ERC5	Otof	S	237	2	GLDPDSVSLASVTAL	-0.4323	
Q9ERC5	Otof	S	240	2	PDSVSLASVTALTSN	-0.4323	
A0A0G2K7Y2	Oxr1	S	15	1	WLKKKSQSVDITAPG	1.8243	-0.1610
A0A0G2K7Y2	Oxr1	S	90	1	KKDGRRMSFQKPKGT	0.3349	-0.0441
A0A0G2K7Y2	Oxr1	T	203	1	PARVVSSTSEEEEAF	0.4467	
A0A0G2K7Y2	Oxr1	S	204	1	ARVVSSTSEEEEAFT	0.5749	-0.1767
A0A0G2K7Y2	Oxr1	S	510	1	RKLWKTHSMQQAKQQ	0.9990	-0.0228
A0A0G2K7Y2	Oxr1	S	529	1	QQVAQRESKHRGAPA	0.5968	0.0356
D3ZUC9	Oxsr1	S	359	1	AAISQLRSPRVKDSL	-0.8200	-0.0337
O88588	Pacs1	S	408	1	FEGMSQSSSQTEIGS	-0.6444	0.0015
O88588	Pacs1	S	409	1	EGMSQSSSQTEIGSL	-0.5958	0.0706
O88588	Pacs1	S	449	1	WIKNQDDSLTETDTL	0.7954	-0.0387
O88588	Pacs1	S	495	2	LQGSASPSKVEGTHT	-0.3152	
O88588	Pacs1	S	517	1	PLKERQLSKPLSERT	3.9793	
D3ZJG4	Pacs2	S	328	1	RSHREPPSPADVPEK	-0.3468	-0.1059
Q9Z0W5	Pacsin1	T	335	2	ATGAVESTSQAGDRG	-0.5315	0.0397
Q9Z0W5	Pacsin1	T	335	3	ATGAVESTSQAGDRG	-0.4324	-0.1086
Q9Z0W5	Pacsin1	S	336	1	TGAVESTSQAGDRGS	-0.6145	-0.0869
Q9Z0W5	Pacsin1	S	336	2	TGAVESTSQAGDRGS	-0.5315	-0.0329
Q9Z0W5	Pacsin1	S	336	3	TGAVESTSQAGDRGS	-0.5510	-0.1060
Q9Z0W5	Pacsin1	S	343	3	SQAGDRGSVSSYDRG	-0.5359	-0.1000
Q9Z0W5	Pacsin1	S	346	3	GDRGSVSSYDRGQAY	-0.5783	-0.0912
P35465	Pak1	T	167	2	NVKTVSETPAVPPVS	-0.4176	
P35465	Pak1	T	218	2	TPTRDVATSPISPTE	-0.6000	-0.0892
P35465	Pak1	S	219	2	PTRDVATSPISPTEN	-0.4502	-0.0329
P35465	Pak1	S	222	2	DVATSPISPTENNTT	-0.4202	-0.0316
Q62829	Pak3	S	2	1	_____MSDSLDNEE	0.7232	-0.0747
Q62829	Pak3	S	4	1	____MSDSLDNEEKP	0.7206	-0.0785
D4A1J3	Palm3	S	524	1	QEKDGEGSLDRESKT	0.3757	
G3V7T3	Pank4	S	15	1	GGGSGGDSLDKSITL	0.4974	-0.0493

A1A5Q1	Parp9	S	342	3	LDKIKLSSDYQVVQV	-0.5958	
A1A5Q1	Parp9	Y	344	3	KIKLSSDYQVVQVTK	-0.5958	
A1A5Q1	Parp9	T	350	3	DYQVVQVTKGFKLSC	-0.5958	
A0A0G2K6T9	Pcdh1	S	923	2	GRHYRSNSPLPSIQL	-0.6286	
D3ZE55	Pcdh8	S	802	1	GGASAPGSPDETARG	0.2784	-0.1365
F1LS01	Pcdh9	T	954	2	AFHLKPDTPVSVKKH	-0.5631	0.1087
F1LS01	Pcdh9	S	957	2	LKPDTPVSVKKHHVI	-0.6447	
F1M7V4	Pclo	S	1458	2	YKLPSPTSPLSPHSN	0.5874	0.1347
F1M7V4	Pclo	S	1461	1	PSPTSPLSPHSNKSS	1.3287	0.1011
F1M7V4	Pclo	S	1461	2	PSPTSPLSPHSNKSS	0.5376	
F1M7V4	Pclo	S	1889	1	GGMKPSMSDTNLAEA	-0.4294	-0.0304
Q9JKS6	Pclo	T	111	1	PGLSKSRTTDTFRSE	-0.6717	0.1376
Q9JKS6	Pclo	S	125	2	EQKLPGRSPSTISLK	-0.9418	-0.0526
Q9JKS6	Pclo	S	130	2	GRSPSTISLKESKSR	-0.9429	-0.0431
Q9JKS6	Pclo	S	136	1	ISLKESKSRTDFKEE	-1.7957	-0.0628
Q9JKS6	Pclo	S	321	1	AGLEKTSSSQQPGPK	1.0283	-0.0291
Q9JKS6	Pclo	S	329	1	SQQPGPKSLAQTPGH	0.4233	
Q9JKS6	Pclo	S	591	1	LAAAIPSSPQPTPKA	-1.3396	0.0671
Q9JKS6	Pclo	S	857	3	QEQSRRFSLNLGGIT	-0.8680	0.0650
Q9JKS6	Pclo	S	869	2	GITDAPKSQPTTPQE	-1.1603	0.0867
Q9JKS6	Pclo	T	872	2	DAPKSQPTTPQETVT	-1.0963	0.0963
Q9JKS6	Pclo	T	872	3	DAPKSQPTTPQETVT	-0.8893	0.0650
Q9JKS6	Pclo	T	873	1	APKSQPTTPQETVTG	-0.2956	0.0188
Q9JKS6	Pclo	T	873	2	APKSQPTTPQETVTG	-1.1926	0.0854
Q9JKS6	Pclo	T	873	3	APKSQPTTPQETVTG	-0.8812	0.0650
Q9JKS6	Pclo	S	922	1	SKQAPTPSQSPAAQG	-0.7166	0.2026
Q9JKS6	Pclo	S	1162	1	ALPEKKPSEEEKAIS	0.4600	-0.0914
Q9JKS6	Pclo	S	1274	1	AQPQAEGSSKDGQGE	0.8448	0.1120
Q9JKS6	Pclo	S	1344	1	LKGLKKDSFSQESSP	0.9949	0.0444
Q9JKS6	Pclo	S	1344	2	LKGLKKDSFSQESSP	0.7988	0.0834
Q9JKS6	Pclo	S	1344	3	LKGLKKDSFSQESSP	0.6065	
Q9JKS6	Pclo	S	1346	1	GLKKDSFSQESSPSS	1.2388	0.0368
Q9JKS6	Pclo	S	1346	2	GLKKDSFSQESSPSS	0.7737	0.0833
Q9JKS6	Pclo	S	1349	2	KDSFSQESSPSSPSD	0.5097	-0.0632
Q9JKS6	Pclo	S	1451	1	PELVDDLSPRRASYD	-0.4573	0.1366
Q9JKS6	Pclo	S	1562	2	HRRLTRKSSTSFDDD	-0.3512	
Q9JKS6	Pclo	S	1563	1	RRLTRKSSTSFDDDA	0.7005	-0.1513
Q9JKS6	Pclo	S	1563	2	RRLTRKSSTSFDDDA	1.2929	
Q9JKS6	Pclo	T	1564	2	RLTRKSSTSFDDDAG	0.8613	-0.0266
Q9JKS6	Pclo	S	1565	2	LTRKSSTSFDDDAGR	1.7622	-0.0168
Q9JKS6	Pclo	S	1597	1	LKFRETKSQESEELV	0.8230	
Q9JKS6	Pclo	S	1597	2	LKFRETKSQESEELV	0.6233	-0.1401
Q9JKS6	Pclo	S	1600	2	RETKSQESEELVVAG	0.6233	-0.1351
Q9JKS6	Pclo	T	1772	3	RRRERPKTPPSNLSP	-1.1106	0.1970

Q9JKS6	Pclo	S	1775	3	ERPKTPPSNLSPIED	-1.1967	0.2002
Q9JKS6	Pclo	S	1778	3	KTPPSNLSPIEDASP	-1.1974	0.2073
Q9JKS6	Pclo	S	1784	1	LSPIEDASPTEELRQ	0.4405	-0.0546
Q9JKS6	Pclo	S	1784	3	LSPIEDASPTEELRQ	-1.1929	0.2073
Q9JKS6	Pclo	S	2326	1	TYRLPSGSLPVSTHP	0.8145	-0.0113
Q9JKS6	Pclo	S	3561	1	PTVQLAPSPPKSPKV	-0.6130	0.0390
Q9JKS6	Pclo	S	3561	2	PTVQLAPSPPKSPKV	-1.4290	-0.0484
Q9JKS6	Pclo	S	3565	2	LAPSPPKSPKVLYSP	-1.4290	-0.0484
Q9JKS6	Pclo	S	3624	1	TAKMMQRSMSDPKPL	0.5316	0.0640
Q9JKS6	Pclo	S	3626	1	KMMQRSMSDPKPLSP	0.4941	0.0753
Q9JKS6	Pclo	S	3632	1	MSDPKPLSPTADESS	-0.9768	0.1186
Q9JKS6	Pclo	S	3795	1	TRPSRVESQHGVERP	0.8349	-0.1093
Q9JKS6	Pclo	S	4034	1	RTTETRRSQEVTDFL	0.4750	-0.1052
Q9JKS6	Pclo	S	4155	1	KFSPIQESRDLEPDY	1.1757	-0.0865
Q9JKS6	Pclo	S	4235	3	PYSSGSRSRPSSRPS	-1.1264	-0.2367
Q9JKS6	Pclo	S	4242	3	SRPSSRPSSVYGLDL	-1.1308	
Q9JKS6	Pclo	S	4243	3	RPSSRPSSVYGLDLS	-1.0949	-0.2024
Q9JKS6	Pclo	S	4293	1	TSLPISQSRGRIPIV	-0.8673	-0.2072
Q9JKS6	Pclo	S	4341	2	TRDQFGSSHSLPEVQ	-0.3079	-0.0599
Q9JKS6	Pclo	S	4343	2	DQFGSSHSLPEVQQH	-0.2837	-0.0610
Q9JKS6	Pclo	S	4561	1	PKVDKAKSPGVDPKQ	-1.2484	-0.0666
Q9JKS6	Pclo	S	4801	1	PSVIKSRSHGIFPDP	-0.7649	-0.0786
Q9JKS6	Pclo	S	4831	2	PGSSKSSSEGHLRSH	-0.5241	
Q9JKS6	Pclo	S	4837	2	SSEGHLRSHGPSRSQ	-0.8698	-0.1027
Q9JKS6	Pclo	S	4841	2	HLRSHGPSRSQSKTS	-0.7898	-0.0213
A0A0G2K0X1	Pcm1	S	68	1	TNDISPESSPGVGRR	0.5319	
D3ZXP8	Pcp2	S	92	2	QKRPGTLSPQPLLSP	-0.3779	0.1603
D3ZXP8	Pcp2	S	98	2	LSPQPLLSPQDPAAL	-0.3779	0.1603
Q01066	Pde1b	S	465	1	SFQWRQPSLDVDVGD	0.4867	-0.0336
A0A0G2K876	Pde2a	S	885	1	FTIRGLPSNNSLDFL	-0.4167	0.0330
A0A0G2K876	Pde2a	S	888	1	RGLPSNNSLDFLDEE	0.6885	-0.0814
P54748	Pde4a	S	333	1	KKLVHTGSLNTNVPR	0.8807	-0.0738
P14646	Pde4b	S	197	1	HGAPNKRSPAASQAP	-0.7462	-0.1836
P14646	Pde4b	S	319	1	KKLMHSSSLNNTSIS	0.3080	0.0930
P14270	Pde4d	S	192	1	SFLYRSDSDYDLSPK	0.5242	-0.1299
P26284	Pdha1	S	293	1	TYRYHGHSMSDPGVS	-0.2879	-0.1225
P26284	Pdha1	S	293	2	TYRYHGHSMSDPGVS	-0.4282	-0.0391
P26284	Pdha1	S	295	1	RYHGHSMSDPGVSYR	-0.3564	-0.0983
P26284	Pdha1	S	295	2	RYHGHSMSDPGVSYR	-0.5864	0.0487
P26284	Pdha1	S	300	2	SMSDPGVSYRTREEI	-0.5043	0.0011
O55173	Pdpk1	T	33	1	PSMVRSQTEPSSSPG	0.5675	
D3ZC81	Pex10	S	259	1	NLSHRRSSLEDRAVC	0.2727	
P30835	Pfkl	S	775	1	HVTRRTLSIDKGF__	0.7158	0.0210
P47860	Pfkp	T	313	1	GHVQRGGTPSAFDRI	0.2776	-0.2613

P62024	Phactr1	S	67	1	IRRVRSKSDTPYLAE	-0.4952	-0.1166
P62024	Phactr1	S	423	1	MKVCRKDSLAIKLSN	0.7915	-0.2379
Q6RFY2	Phactr3	S	267	1	ATKHRQDSFQGRECR	1.3140	-0.1256
A0A0G2K9C8	Phkb	S	693	1	SKVKRQSSTADAPEL	0.3004	-0.0851
D3ZNS1	Phldb1	S	325	1	GGHERPPSPGLRGLL	-0.4931	0.0793
D3ZNS1	Phldb1	S	534	1	SLAPRKGSFSGRLSP	0.7066	-0.1720
D3ZNS1	Phldb1	S	579	2	IPRERKNSITEISDN	-0.2877	
D3ZNS1	Phldb1	S	584	2	KNSITEISDNEDDLL	-0.2877	
D3ZYT8	Pikfyve	S	487	2	KDIKFDDSDTEQIAE	-0.2938	
D3ZYT8	Pikfyve	S	505	2	DNLANSASPSKRTSV	-0.2938	
F1M8H6	Pip5k1c	S	475	1	LGPTAAFSASQIPSE	-0.4642	
F1M8H6	Pip5k1c	S	554	1	RYRRRTQSSGQDGRP	-0.3895	0.0441
F1M8H6	Pip5k1c	S	555	1	YRRRTQSSGQDGRPQ	-0.4020	-0.0083
F1LXD6	Pitpnm2	S	630	1	SSRHLSRSNIDIPRS	-0.4303	-0.0319
F1M2K6	Pkp4	S	213	1	RAMRRVSSVPSRAQS	0.4495	0.0223
F1M2K6	Pkp4	S	289	1	TAVRRVGSVTSRQTS	0.4468	0.0744
F1M2K6	Pkp4	S	405	2	QDLRSAVSPDLHITP	-0.8731	
F1M2K6	Pkp4	T	411	2	VSPDLHITPIYEGRT	-0.8731	
P10687	Plcb1	S	1199	2	KVNLKSPSSEEVQGE	-0.3128	0.1559
P10686	Plcg1	S	1248	1	HVRAREGSFEARYQQ	0.6989	0.1438
D4AAX6	Plch2	S	575	1	SKIKKVASVEEGDES	0.4315	-0.2224
Q91Z79	Ppfia3	S	507	2	RPPSYSRSLPGSALE	-0.8654	-0.0379
Q91Z79	Ppfia3	S	511	2	YSRSLPGSALELRYS	-0.8654	-0.0379
F1M863	Ppfia4	S	657	1	TPKLTSRSAAQDLDR	-0.4810	
F1M863	Ppfia4	S	721	1	KLGHPTLSQEEGKSA	0.7515	0.0906
Q6DGG0	Ppid	S	198	1	GIFPKDGSGDSHPDF	0.3916	
Q5M821	Ppm1h	S	118	1	TSTPNRNSKRRSSLP	0.3829	-0.1996
Q5M821	Ppm1h	S	123	1	RNSKRRSSLPNGEGL	0.3477	-0.2264
Q10728	Ppp1r12a	S	299	1	SEKRDKKSPLIESTA	-0.4110	0.0283
Q10728	Ppp1r12a	T	596	2	STSTTAKTPPGSSPA	-0.8074	-0.0874
Q10728	Ppp1r12a	S	601	1	AKTPPGSSPAGTQSS	-0.6787	0.0661
Q10728	Ppp1r12a	S	601	2	AKTPPGSSPAGTQSS	-0.7456	-0.0911
P19103	Ppp1r1a	S	46	2	LVLTSDQSSPEVDED	0.3068	
P19103	Ppp1r1a	S	47	2	VLTSDQSSPEVDEDR	0.3068	
P19103	Ppp1r1a	S	67	1	LKSTLSMSPRQRKKM	-0.5112	0.2069
Q6J4I0	Ppp1r1b	S	45	1	LFRVSEHSSPEEESS	0.5083	-0.0750
Q6J4I0	Ppp1r1b	S	51	2	HSSPEEESSPHQRTS	-0.3223	
P50411	Ppp1r2	S	20	1	GILKNKTSTTSSVVA	0.7712	0.1819
F1LYZ8	Ppp1r21	S	101	1	GESSSQLSQEQKSVF	0.9893	0.0334
P0C7L8	Ppp1r3e	S	33	1	YYRSQRPSLEEESEE	0.2933	
Q5HZV9	Ppp1r7	S	12	1	RGAGQQQSQEMMEVD	0.6518	
Q5HZV9	Ppp1r7	S	24	1	EVDRRVESEESGDEE	0.4007	-0.2439
Q5HZV9	Ppp1r7	S	44	2	GGIVADLSQQSLKDG	-0.4705	-0.1460
Q5HZV9	Ppp1r7	S	47	1	VADLSQQSLKDGVER	0.4434	-0.2049

Q5HZV9	Ppp1r7	S	47	2	VADLSQQSLKDGVER	-0.4705	-0.1460
O35274	Ppp1r9b	S	100	1	LSLPRASSLNENVDH	1.6476	-0.0739
D4A1A5	Ppp2r5c	S	497	1	RPLVRRKSELPQDPH	1.4669	-0.0572
P63329	Ppp3ca	S	498	1	PSDANLNSINKALAS	0.3204	
P80386	Prkab1	S	108	1	SKLPLTRSQNNFVAI	-0.3738	-0.1349
F1LS42	Prkcb	S	653	2	VIRNIDQSEFEGFSF	-0.4484	
F1LS42	Prkcb	S	659	2	QSEFEGFSFVNSEFL	-0.3817	0.0756
F1LS42	Prkcb	S	663	2	EGFSFVNSEFLKPEV	-0.3900	0.0785
P63319	Prkcg	T	689	2	HPDARSPTSPVPVPV	-0.2726	
D3ZFB6	Prrt2	T	74	2	LAPETTETPVETPET	-0.2690	0.1713
D3ZFB6	Prrt2	T	78	2	TTETPVETPETVQAT	-0.2690	0.1718
D3ZFB6	Prrt2	S	242	1	AHGGHPGSPRGSLSR	0.3057	-0.0474
D3ZWQ0	Prrt3	S	794	3	GSVGPAPSLSELDLR	-0.3372	0.0663
D3ZWQ0	Prrt3	S	796	3	VGPAPSLSELDLRPP	-0.3372	0.0694
D3ZWQ0	Prrt3	S	804	3	ELDLRPPSPINLSRS	-0.3372	0.0663
Q4FZT9	Psmd2	S	363	1	NRFGGSGSQVDSARM	0.4927	-0.1119
A0A0G2JZ88	RGD1306556	T	1677	1	EPPRVERTPVGHPQR	-0.7101	-0.1514
A0A0G2JZ88	RGD1306556	T	1721	2	SWTPQPKTPKSPFQP	-1.5606	
A0A0G2JZ88	RGD1306556	S	1724	2	PQPKTPKSPFQPGVL	-1.5606	
D4A3X1	RGD1308601	S	67	1	MELRRDSSESQLAST	-0.5254	-0.1338
D3ZBU7	RGD1310819	S	204	2	IKILVSSSRPQSPDH	-0.4348	-0.0988
D3ZBU7	RGD1310819	S	208	2	VSSSRPQSPDHMSDA	-0.3989	
D3ZBU7	RGD1310819	S	968	1	PAAGPDTSPGESERL	-0.4527	-0.0561
D4A5F4	RGD1311575	S	1129	1	PMLQSRHSLDGSKLT	2.0431	-0.1827
A0A0G2K1W1	Rab11fip5	S	251	1	RGSHGTSSLEAVPGQ	0.3793	
Q6NYB7	Rab1A	T	195	1	SNVKIQSTPVKQSGG	0.3121	-0.2403
B0BN19	Rab22a	S	187	1	FKLRRQPSEPKRSCC	0.3382	-0.1721
P63012	Rab3a	S	7	1	_MASATDSRYGQKES	0.5243	-0.1631
A0A0G2K1B4	Rab3ip	T	249	2	LVLSSSPTSPTQEPL	-0.2803	
G3V631	Rabgef1	S	143	1	PSINRQTSIETDRVT	0.4360	0.1663
Q5FVT1	Ralbp1	S	29	3	SGLTRTPSSEEISPT	-0.2654	
Q5FVT1	Ralbp1	S	34	3	TPSSEEISPTKFPGL	-0.3125	
O55007	Ralgapa1	S	796	1	QPLPRSSSTSDILEP	-0.3373	0.0302
O55007	Ralgapa1	S	860	2	TMTRRGSSPGSLEIP	-0.3146	0.1805
P86410	Ralgapb	T	416	2	VQHQASSTSPLSSPN	-0.4095	-0.0371
F1LV89	Rap1gap	S	524	1	NTVSTSHSGSFTPNN	-0.4142	0.1456
F1LV89	Rap1gap	S	557	2	SRFGRRGSALGIGAV	-0.9825	-0.0490
F1LV89	Rap1gap	S	574	2	SLIVPGKSPTRKKSG	-0.9825	-0.0577
F1LV89	Rap1gap	S	605	2	EVQEKRESPPAGQKT	-0.5546	0.0315
F1LV89	Rap1gap	T	612	2	SPPAGQKTPDSGHVS	-0.5390	
F1LV89	Rap1gap	S	615	1	AGQKTPDSGHVSQEP	-0.4297	0.0044
F1LV89	Rap1gap	S	615	2	AGQKTPDSGHVSQEP	-0.5004	0.0325
F1LV89	Rap1gap	S	721	1	SSPGLTRSPHPDAVK	-0.9933	
A0A0G2K0S7	Rap1gap2	S	558	1	TVKNQSRSPIKRRSG	-0.7596	0.1606

A0A0G2K0S7	Rap1gap2	S	572	1	GLFPRLHSGSEGQGD	1.0875	
A0A0G2K0S7	Rap1gap2	S	574	1	FPRLHSGSEGQGDSR	1.2779	
A0A0G2K0S7	Rap1gap2	S	727	1	DKLSHASSSAGH___	0.6419	-0.0360
A0A0G2K0S7	Rap1gap2	S	728	1	KLSHASSSAGH____	0.9734	0.0219
A0A0A0MP77	Rapgef2	S	1113	1	RQNQSRESLEQAQSR	1.1977	0.0371
D3ZHK4	Rb1cc1	S	257	2	TNTSLLTSFHKSVEH	-0.5214	
D3ZHK4	Rb1cc1	S	261	2	LLTSFHKSVEHVAPD	-0.5214	
D3ZL11	Rbsn	S	635	2	FDEEDLSSPIEGAVS	-0.4426	
D3ZL11	Rbsn	S	642	2	SPIEGAVSPAAVEAF	-0.4426	
A0A0G2JZY3	Reps1	S	93	1	QVKKAPGSHDAAQPR	0.9242	0.0417
A0A0G2JZY3	Reps1	S	430	1	GDHTNPTSPLLVKPS	-0.3629	
A0A0G2JZY3	Reps1	S	430	2	GDHTNPTSPLLVKPS	-0.4985	
A0A0G2JZY3	Reps1	T	492	2	SGASPDNTAPPPPPP	-0.3711	0.0837
A0A0G2K1L4	Reps2	S	407	1	KTHSRASSLDLNKVF	0.5464	0.1208
A0A0G2K326	Rgs12	S	477	1	GAPVKQSSAVNSSPR	1.7546	0.0396
A0A0G2K4J8	Rimbp2	S	554	1	STGPGRRSPSPSRIL	-1.8636	
A0A0G2K4J8	Rimbp2	S	684	1	DGGRRRPSGTSHNAL	0.5820	0.0562
A0A0G2K4J8	Rimbp2	S	951	1	EHVSRRYSHSGGGPQ	0.7729	-0.1000
A0A0G2K4J8	Rimbp2	S	1096	1	RRSGRGHSVPTRRMV	1.2722	0.1918
A0A0G2JT77	Rims1	S	95	1	VCVPRKPSSEEGGPE	1.4727	-0.0646
A0A0G2JT77	Rims1	S	96	1	CVPRKPSSEEGGPER	0.9897	
A0A0G2JT77	Rims1	S	241	2	RLQERSRSQTPLSTA	0.3231	-0.0551
A0A0G2JT77	Rims1	S	346	1	RRLEKGRSQDYSDRP	2.0172	-0.0242
A0A0G2JT77	Rims1	S	413	1	ARHERRHSDVALPHT	0.3195	-0.0491
A0A0G2JT77	Rims1	S	723	1	SSHPPLESSSSSFES	0.5020	-0.1555
A0A0G2JT77	Rims1	S	723	2	SSHPPLESSSSSFES	0.2918	
A0A0G2JT77	Rims1	S	726	2	PPLESSSSSFESQKM	0.3260	
A0A0G2JT77	Rims1	S	742	2	RPSISVISPTSPGAL	-0.6754	
A0A0G2JT77	Rims1	S	745	2	ISVISPTSPGALKDA	-0.5236	
A0A0G2JT77	Rims1	S	921	2	RSQRISDSDISDYEV	-0.3378	-0.0353
A0A0G2JT77	Rims1	S	921	3	RSQRISDSDISDYEV	-0.2802	
A0A0G2JT77	Rims1	S	924	2	RISDSDISDYEVDDG	-0.4309	-0.0358
A0A0G2JT77	Rims1	S	924	3	RISDSDISDYEVDDG	-0.2802	
A0A0G2JT77	Rims1	Y	926	2	SDSDISDYEVDDGIG	-0.2682	0.0200
A0A0G2JT77	Rims1	Y	926	3	SDSDISDYEVDDGIG	-0.2717	
A0A0G2JT77	Rims1	S	965	2	QRTTHHRSRSVSPHR	-0.6436	
A0A0G2JT77	Rims1	S	967	2	TTHHRSRSVSPHRGD	-0.5165	
A0A0G2JT77	Rims1	S	969	2	HHRSRSVSPHRGDDQ	-0.5674	
A0A0G2JT77	Rims1	S	991	1	PNVPLQRSLDEIHPT	0.6805	0.0579
A0A0G2JT77	Rims1	S	1045	1	PRAKRGRSAESLHMT	-0.2783	0.0225
A0A0G2JT77	Rims1	S	1078	2	RPDTSLHSPERERHS	-0.6512	
A0A0G2JT77	Rims1	S	1202	1	QVPVRSGSIEQASLV	0.5469	-0.2321
A0A0G2JT77	Rims1	S	1233	1	QTTGSGSSQELDHEQ	0.9811	-0.0565
A0A0G2JT77	Rims1	S	1355	1	GGKKRRSSLSAKVVA	0.4156	-0.2329

A0A0G2JT77	Rims1	S	1408	2	RKMVRQPSRESTDGS	0.7779	-0.0024
Q9JIS1	Rims2	S	432	2	PQRTTNHSPPTPRRS	-0.4042	
Q9JIS1	Rims2	T	435	2	TTNHSPPTPRRSPIP	-0.4138	
Q9JIS1	Rims2	S	482	2	ETMLRNDSLSSDQSE	0.7483	-0.0822
Q9JIS1	Rims2	S	484	2	MLRNDSLSSDQSESV	0.7508	-0.0708
Q9JIS1	Rims2	S	485	2	LRNDSLSSDQSESVR	0.7912	-0.0439
Q9JIS1	Rims2	S	1540	2	APLTRRASQSSLESS	0.4463	0.0158
Q9JIS1	Rims2	S	1542	2	LTRRASQSSLESSTG	0.3900	
Q9JIS1	Rims2	S	1546	2	ASQSSLESSTGPSYS	0.4419	-0.0556
P47709	Rph3a	S	274	1	QGLRRANSVQASRPA	0.7613	-0.0214
Q9JK11	Rtn4	S	425	1	EGRNEDASFPSTPEP	0.2691	0.1528
Q9JK11	Rtn4	S	425	2	EGRNEDASFPSTPEP	-0.8392	-0.0996
Q9JK11	Rtn4	S	428	2	NEDASFPSTPEPVKD	-0.7237	-0.1071
Q9JK11	Rtn4	T	429	1	EDASFPSTPEPVKDS	-0.2717	
Q9JK11	Rtn4	T	429	2	EDASFPSTPEPVKDS	-0.8198	-0.0852
F1LRZ9	Rundc3a	S	374	2	SKLFRRHSFMSTEPL	-0.3006	-0.1246
F1LRZ9	Rundc3a	S	377	2	FRRHSFMSTEPLSAE	-0.3006	-0.1464
Q5BJU3	Samd14	S	151	1	SAPSSDSSPSFVRRY	-0.3363	
P04774	Scn1a	S	620	1	RHGERRNSNLSQTSR	0.3643	0.0989
F1M9G9	Scn2a	S	531	1	RKSASEDSIRKKGFR	0.6118	-0.0418
F1M9G9	Scn2a	S	553	3	LTYEKRFSSPHQSLL	-0.3738	
F1M9G9	Scn2a	S	554	3	TYEKRFSSPHQSLLS	-0.4317	
F1M9G9	Scn2a	S	558	3	RFSSPHQSLLSIRGS	-0.5601	
F1M9G9	Scn2a	S	561	3	SPHQSLLSIRGSLFS	-0.4317	
F1M9G9	Scn2a	S	623	1	RHGERRPSNVSQASR	0.2891	-0.0487
F1M9G9	Scn2a	S	629	1	PSNVSQASRASRGIP	0.5120	-0.1655
F1M9G9	Scn2a	Y	689	2	RKRRSSSYHVSMDLL	-0.5081	
F1M9G9	Scn2a	S	692	2	RSSSYHVSMDLLEDP	-0.6492	-0.1148
A0A0G2JVC2	Scyl2	S	681	1	QGKQKRGSLTLEEKQ	0.2911	0.0096
A0A096MJN4	4-Sep	S	413	1	RNKLTRESGTDFPIP	-0.3381	-0.0250
D3ZDH8	5-Sep	S	17	1	RLVEQLLSPRTQAQR	-1.9315	
D3ZDH8	5-Sep	S	336	2	TQDSRMESPIPILPL	-0.6566	
D3ZDH8	5-Sep	T	345	1	IPILPLPTPDSETEK	-0.4997	
D3ZDH8	5-Sep	T	345	2	IPILPLPTPDSETEK	-0.6524	
A0A0U1RRT8	6-Sep	S	411	1	ELLQSQGSQAGGSQT	0.3933	-0.0665
Q9WVC0	7-Sep	S	422	1	RILEQQNSSRTLEKN	0.4303	-0.1912
P0DJJ3	Sgip1	S	142	2	TVDELKASIGNIALS	-0.6045	-0.1055
P0DJJ3	Sgip1	S	149	2	SIGNIALSPSPVRKS	-1.1080	-0.0493
P0DJJ3	Sgip1	S	151	2	GNIALSPSPVRKSPR	-1.1335	
P0DJJ3	Sgip1	S	160	1	VRKSPRRSPGAIKRN	-0.6349	-0.1676
P0DJJ3	Sgip1	S	289	2	IEKLPSISDLDSIFG	-0.2668	0.0222
P0DJJ3	Sgip1	S	371	1	PGPRHVPSPLNLEEV	-0.4934	-0.0077
D3ZAS2	Sgsm1	S	229	3	LCIQKRHSSGSMDDR	0.8637	
D3ZAS2	Sgsm1	S	230	3	CIQKRHSSGSMDDRP	0.8637	

D3ZAS2	Sgsm1	S	232	1	QKRHSSGSMDDRPSI	0.8959	-0.0640
D3ZAS2	Sgsm1	S	232	3	QKRHSSGSMDDRPSI	0.8637	
D3ZAS2	Sgsm1	S	406	2	QGSSESTSSDKEDDE	0.6522	
D3ZAS2	Sgsm1	S	407	2	GSSESTSSDKEDDEA	0.6508	
O70593	Sgta	S	302	1	IRSQVVRSRTPSASH	-0.5427	
Q80W98	Sgtb	S	299	1	RSRSFSSSTEEHS__	0.3234	
Q80W98	Sgtb	T	300	1	SRSFSSSTEEHS___	0.3110	
Q80W98	Sgtb	S	304	2	SSSTEEHS_____	0.5086	
O35964	Sh3gl1	S	288	1	PKITASSSFRSGDKP	-0.6301	-0.0967
Q925Q9	Sh3kbp1	S	274	1	PIKLRPRSIEVENDF	0.3344	0.0139
A0A0G2JX92	Sh3pxd2a	S	1014	1	RLAERAASQGSESPL	0.3855	-0.0660
Q9QX74	Shank2	T	903	1	GPLRRQETENKYETD	0.8834	0.1716
Q7TP36	Shroom2	S	918	1	STMETSRSPSPQFAP	-0.3903	0.1520
Q7TP36	Shroom2	S	920	1	METSRSPSPQFAPQK	-0.3751	0.0945
Q7TP36	Shroom2	S	996	1	IKIVHSESQPEKESR	1.3409	0.0149
A0A0G2KAW2	Sipa1l1	S	288	1	PLKRRSKSETGDSSI	0.4454	
A0A0G2KAW2	Sipa1l1	T	1190	1	ASIDRQNTQSDIGGS	0.9166	0.0176
A0A0G2KAW2	Sipa1l1	S	1192	1	IDRQNTQSDIGGSGK	0.9247	
A0A0G2KAW2	Sipa1l1	S	1384	1	SKSQGGSSPLTRENS	-0.5853	0.0600
E9PTX9	Slc12a2	S	73	1	KPLGPTPSQSRFQVD	-0.6815	0.0464
O54701	Slc24a2	S	334	1	PRLQRGGSSASLHNS	0.2874	-0.1903
O54701	Slc24a2	S	337	2	QRGGSSASLHNSLMR	0.6074	0.0371
O54701	Slc24a2	S	341	2	SSASLHNSLMRNSIF	0.5503	0.0358
Q921A2	Slc2a13	S	6	1	__MSRKASEDVEYTL	0.3491	-0.1206
Q921A2	Slc2a13	S	624	3	EYIRVKGSNYHLSDN	-0.9079	
Q921A2	Slc2a13	S	629	3	KGSNYHLSDNDASDV	-0.9308	
Q921A2	Slc2a13	S	634	3	HLSDNDASDVE____	-0.9308	
Q6QIX3	Slc30a3	T	35	2	LRLKSLFTEPSEPLP	2.1253	-0.1362
Q6QIX3	Slc30a3	S	38	2	KSLFTEPSEPLPEGP	2.1744	-0.1389
D4A517	Slc39a10	T	538	1	KWFMKQSTEESTIGR	0.2640	
A0A0H2UHB7	Slc4a4	S	261	1	THRNLTSSSLNDISD	-0.7861	0.1430
A0A0H2UHB7	Slc4a4	S	261	2	THRNLTSSSLNDISD	-0.8475	-0.1600
A0A0H2UHB7	Slc4a4	S	262	2	HRNLTSSSLNDISDK	-0.7890	-0.2629
Q9R1N3	Slc4a7	S	238	1	SRIPLVRSFADIGKK	-0.8533	-0.0336
P31662	Slc6a17	S	13	2	KVTQREHSNEHVTES	0.3012	-0.0643
P31662	Slc6a17	S	20	2	SNEHVTESVADLLAL	0.3383	-0.0506
P31662	Slc6a17	S	665	1	GRMMKDISNLEENDE	-0.7038	0.0260
P31662	Slc6a17	S	682	2	FILSKVPSEAPSPMP	-0.5428	0.0727
P31662	Slc6a17	S	686	2	KVPSEAPSPMPTHRS	-0.5428	0.0847
P31662	Slc6a17	S	715	2	HPNGRYGSGYLLAST	-1.2328	
P31662	Slc6a17	T	722	2	SGYLLASTPESEL__	-1.0214	-0.0431
P31662	Slc6a17	S	725	2	LLASTPESEL_____	-0.6762	-0.0715
P26431	Slc9a1	S	606	2	GKIPSAVSTVSMQNI	-0.9830	
P26431	Slc9a1	T	607	2	KIPSAVSTVSMQNIH	-0.9009	-0.0935

P26431	Slc9a1	S	609	2	PSAVSTVSMQNIHPK	-0.9693	-0.0406
P26431	Slc9a1	T	784	2	PGTDDVFTPGPSDSP	-0.8272	
P26431	Slc9a1	S	790	2	FTPGPSDSPGSQRIQ	-0.7406	-0.0930
D3ZJR6	Smcr8	S	488	1	SVLSKSDSQASLTVP	0.4111	-0.1000
D3ZJR6	Smcr8	S	488	3	SVLSKSDSQASLTVP	-0.3019	
D3ZJR6	Smcr8	S	491	3	SKSDSQASLTVPLSP	-0.3019	
D3ZJR6	Smcr8	S	497	3	ASLTVPLSPHVVRSK	-0.3019	
A0A0G2K0B6	Snap91	S	601	1	SSPPRGASPVPESSL	-0.7133	0.0110
A0A0G2K0B6	Snap91	S	601	2	SSPPRGASPVPESSL	-1.6128	-0.0318
A0A0G2K0B6	Snap91	S	601	3	SSPPRGASPVPESSL	-1.1729	-0.2366
A0A0G2K0B6	Snap91	S	614	1	SLTADLLSVDAFAAP	-0.6628	0.0201
A0A0G2K0B6	Snap91	S	614	2	SLTADLLSVDAFAAP	-1.0138	-0.0410
A0A0G2K0B6	Snap91	S	614	3	SLTADLLSVDAFAAP	-1.1190	-0.2085
A0A0G2K0B6	Snap91	S	625	2	FAAPSPASTASPAKA	-0.9133	
A0A0G2K0B6	Snap91	S	628	2	PSPASTASPAKAESS	-1.5278	
A0A0G2K0B6	Snap91	S	628	3	PSPASTASPAKAESS	-1.2359	-0.2366
A0A0G2JXH9	Snx11	S	197	1	WAQEERQSTSHLAKG	0.2744	-0.1758
P57769	Snx16	S	29	1	NRNQRSSSFGSVSTS	0.2668	-0.0638
B2RYP4	Snx2	S	117	1	APRIESKSISAPVIF	-0.8319	
D4A0A1	Soga3	S	748	1	IRGSPRDSDAESDAG	0.3034	
F1M820	Sorbs1	S	54	3	SYRETPSSSPVSPQE	-0.3778	0.2501
F1M820	Sorbs1	S	250	2	DDDSDLHSPRYSFSE	-0.3521	0.0407
F1M820	Sorbs1	S	254	1	DLHSPRYSFSEDTKS	0.7750	
F1M820	Sorbs1	S	254	2	DLHSPRYSFSEDTKS	-0.3350	0.0246
F1M820	Sorbs1	S	256	1	HSPRYSFSEDTKSPL	0.8683	
F1M820	Sorbs1	S	256	2	HSPRYSFSEDTKSPL	-0.3374	
F1M820	Sorbs1	S	670	1	LGASQEGSEHIPKHT	0.2737	
F1M820	Sorbs1	S	1209	1	PSRSATVSPQQPQAQ	-0.6414	0.1675
B2RYN7	Spast	S	222	1	KTVMKSGSTGLSGHH	1.1860	0.0135
D3ZEX7	Spire1	S	458	2	QPPQRRHSIEKETPT	0.7841	0.0221
Q3C2P9	Spred1	S	239	1	LKSIRHVSFQDEDEI	0.5939	
Q5HZA2	Spry2	S	111	1	AALSRSVSTVSSGSR	0.6266	
Q9QXY2	Srcin1	T	64	1	EYPREYRTLGGGGSG	-0.4775	-0.1177
Q9QXY2	Srcin1	S	79	1	GSGGRRFSNVGLVHT	0.3116	-0.0698
Q9QXY2	Srcin1	S	175	3	AAKLSYASAESLETM	-0.3806	
Q9QXY2	Srcin1	S	178	2	LSYASAESLETMSEA	-0.2710	0.0553
Q9QXY2	Srcin1	S	183	2	AESLETMSEAELPLG	-0.3012	0.0481
Q9QXY2	Srcin1	S	366	3	SPSRSRLSYAGGRPP	-0.4813	-0.1158
Q9QXY2	Srcin1	S	374	3	YAGGRPPSYAGSPVH	-0.4858	-0.0681
Q9QXY2	Srcin1	S	378	3	RPPSYAGSPVHHAAE	-0.4413	-0.0479
Q9QXY2	Srcin1	S	393	2	RLGGAPTSQGVSPSP	-0.8241	-0.1394
Q9QXY2	Srcin1	S	397	1	APTSQGVSPSPSAIL	-0.5616	-0.1322
Q9QXY2	Srcin1	S	397	2	APTSQGVSPSPSAIL	-0.6345	-0.1736
Q9QXY2	Srcin1	S	399	2	TSQGVSPSPSAILER	-0.5259	

Q9QXY2	Srcin1	S	401	2	QGVSPSPSAILERRD	-0.6874	-0.0950
Q9QXY2	Srcin1	S	469	3	YKRGSVRSLSTYSAA	-0.7115	
Q9QXY2	Srcin1	S	471	2	RGSVRSLSTYSAAAL	-1.3351	
Q9QXY2	Srcin1	S	471	3	RGSVRSLSTYSAAAL	-0.7664	
Q9QXY2	Srcin1	T	472	2	GSVRSLSTYSAAALQ	-1.3950	
Q9QXY2	Srcin1	T	472	3	GSVRSLSTYSAAALQ	-0.7925	
Q9QXY2	Srcin1	S	474	2	VRSLSTYSAAALQSD	-1.3818	
Q9QXY2	Srcin1	S	474	3	VRSLSTYSAAALQSD	-0.9562	
Q9QXY2	Srcin1	S	480	2	YSAAALQSDLEDSLY	-0.8938	0.0015
Q9QXY2	Srcin1	S	519	1	LADVSAPSGGPPPPH	-0.3956	-0.0253
Q9QXY2	Srcin1	S	527	1	GGPPPPHSPYSGPPS	-0.4985	-0.0086
Q9QXY2	Srcin1	S	527	3	GGPPPPHSPYSGPPS	-0.5016	
Q9QXY2	Srcin1	Y	529	3	PPPPHSPYSGPPSRG	-0.4765	
Q9QXY2	Srcin1	S	530	3	PPPHSPYSGPPSRGS	-0.5306	
Q9QXY2	Srcin1	S	534	3	SPYSGPPSRGSPVRQ	-0.5080	
Q9QXY2	Srcin1	S	537	3	SGPPSRGSPVRQSFR	-0.5645	
Q9QXY2	Srcin1	S	547	1	RQSFRKDSGSSSVFA	0.2939	0.1041
Q9QXY2	Srcin1	S	549	1	SFRKDSGSSSVFAES	0.4027	0.2027
Q9QXY2	Srcin1	S	551	2	RKDSGSSSVFAESPG	-0.3149	-0.1370
Q9QXY2	Srcin1	S	654	2	VCGSGSRSSGATPVS	-0.3337	
Q9QXY2	Srcin1	T	915	2	LSGPAEGTPLTPKSG	-0.4000	0.2483
Q9QXY2	Srcin1	T	918	2	PAEGTPLTPKSGNPT	-0.5858	
Q9QXY2	Srcin1	S	941	1	RNMDKAVSVEAAERD	1.8802	
Q9QXY2	Srcin1	S	1077	1	VFIKKAESEELEIQK	1.2660	-0.0746
Q9QXY2	Srcin1	S	1094	1	VKLRRAVSEVVRPAS	1.1119	-0.2221
D4A208	Srgap2	T	989	2	TSPVVAPTSEPSSPL	-0.5533	0.1469
D4A208	Srgap2	S	990	2	SPVVAPTSEPSSPLH	-0.5762	0.1763
D4A208	Srgap2	S	994	2	APTSEPSSPLHTQLL	-0.5865	0.1820
F1M5M9	Srgap3	S	948	2	CGSTRHSSLGDHKSL	1.3223	-0.0092
F1M5M9	Srgap3	S	954	2	SSLGDHKSLEAEALA	1.3223	-0.0092
F1M5M9	Srgap3	S	1078	2	SSSSGVGSPAVTPTE	-0.9918	
F1M5M9	Srgap3	T	1082	2	GVGSPAVTPTEKMFP	-0.9918	
Q5XIS1	Ssh3	S	642	1	RKVIRQASVDDSREE	0.4781	
Q08013	Ssr3	S	105	1	KEVTRKLSEADNRKM	0.2809	-0.1897
D4A3D9	Stk32c	S	10	2	SGAERRGSSAAAPPG	0.4574	0.0092
D4A3D9	Stk32c	S	18	2	SAAAPPGSPPPGRAR	0.4525	0.0092
P13668	Stmn1	S	16	1	KELEKRASGQAFELI	1.3643	0.0961
P13668	Stmn1	S	31	2	LSPRSKESVPEFPLS	0.4947	
P13668	Stmn1	S	38	2	SVPEFPLSPPKKKDL	0.5087	
A0A0G2JT26	Strip2	S	326	2	VKSMRAASPPSYTLD	0.6614	
G3V7P1	Stx12	S	142	1	ARAGSRLSAEDRQRE	0.3469	-0.0691
Q9WU70	Stxbp5	S	1059	1	LFGGGAQSLDREELF	0.9383	0.0859
D3ZU84	Stxbp5l	S	493	2	SQLPSSRSLSGSTNT	-0.5027	-0.0735
D3ZU84	Stxbp5l	S	497	1	SSRSLSGSTNTVSSE	-0.3126	-0.0733

D3ZU84	Stxbp5l	S	497	2	SSRSLSGSTNTVSSE	-0.4067	-0.1413
D3ZU84	Stxbp5l	T	500	2	SLSGSTNTVSSEGVT	-0.3213	
D3ZU84	Stxbp5l	S	502	2	SGSTNTVSSEGVTKD	-0.3182	-0.1253
D3ZU84	Stxbp5l	S	503	2	GSTNTVSSEGVTKDS	-0.3509	-0.0382
D3ZU84	Stxbp5l	S	675	1	CSSGKRLSSADVSKV	0.5052	0.0447
D3ZSC1	Susd5	S	237	1	EKAQEDASDETPKQD	0.2658	
Q02563	Sv2a	S	42	1	DRVQDEYSRRSYSRF	0.6222	
Q02563	Sv2a	S	45	1	QDEYSRRSYSRFEEE	-0.3599	-0.0408
P09951	Syn1	S	9	1	NYLRRRLSDSNFMAN	0.3192	-0.0788
P09951	Syn1	S	62	1	STAAPVASPAAPSPG	-0.5561	-0.0318
P09951	Syn1	S	62	2	STAAPVASPAAPSPG	-1.4201	0.0531
P09951	Syn1	S	62	3	STAAPVASPAAPSPG	-1.0097	
P09951	Syn1	S	67	2	VASPAAPSPGSSGGG	-1.3581	0.0372
P09951	Syn1	S	67	3	VASPAAPSPGSSGGG	-1.0860	
P09951	Syn1	S	70	2	PAAPSPGSSGGGGFF	-1.1595	0.0202
P09951	Syn1	S	70	3	PAAPSPGSSGGGGFF	-1.1327	
P09951	Syn1	S	71	2	AAPSPGSSGGGGFFS	-1.2159	0.0163
P09951	Syn1	S	71	3	AAPSPGSSGGGGFFS	-1.0399	
P09951	Syn1	S	79	3	GGGGFFSSLSNAVKQ	-0.2704	
P09951	Syn1	S	425	3	LPRQRDASPGRGSHS	-1.0298	-0.1863
P09951	Syn1	S	430	3	DASPGRGSHSQTPSP	-0.5680	-0.1792
P09951	Syn1	S	432	2	SPGRGSHSQTPSPGA	-0.7130	-0.1195
P09951	Syn1	S	432	3	SPGRGSHSQTPSPGA	-0.7759	-0.2208
P09951	Syn1	T	434	2	GRGSHSQTPSPGALP	-0.4780	-0.0788
P09951	Syn1	T	434	3	GRGSHSQTPSPGALP	-0.8073	-0.1732
P09951	Syn1	S	436	1	GSHSQTPSPGALPLG	-0.7530	-0.0951
P09951	Syn1	S	436	2	GSHSQTPSPGALPLG	-0.6050	-0.0617
P09951	Syn1	S	436	3	GSHSQTPSPGALPLG	-0.5554	-0.2015
P09951	Syn1	S	447	1	LPLGRQTSQQPAGPP	1.3955	0.1226
P09951	Syn1	S	500	1	GLGPPAGSPLPQRLP	-0.3305	0.0446
P09951	Syn1	S	508	1	PLPQRLPSPTAAPQQ	-0.9879	-0.0614
P09951	Syn1	T	510	1	PQRLPSPTAAPQQSA	-0.8974	-0.0016
P09951	Syn1	S	549	1	PAARPPASPSPQRQA	-0.6319	0.0417
P09951	Syn1	S	549	2	PAARPPASPSPQRQA	-1.5076	0.1425
P09951	Syn1	T	562	1	QAGPPQATRQASISG	0.8627	
P09951	Syn1	S	566	1	PQATRQASISGPAPP	1.7972	0.1393
P09951	Syn1	S	568	1	ATRQASISGPAPPKV	2.0113	0.1755
P09951	Syn1	S	579	1	PPKVSGASPGGQQRQ	-0.6100	-0.0092
P09951	Syn1	S	603	1	AGPIRQASQAGPGPR	1.5423	0.1331
P09951	Syn1	T	611	1	QAGPGPRTGPPTTQQ	0.4087	-0.0796
P09951	Syn1	T	615	1	GPRTGPPTTQQPRPS	0.3944	-0.1212
P09951	Syn1	S	622	1	TTQQPRPSGPGPAGR	0.4911	
P09951	Syn1	S	664	1	PQLNKSQSLTNAFNL	0.6129	-0.0265
P09951	Syn1	S	697	1	TIRSLRKSFASLFSD	-0.3972	-0.1752

Q63537	Syn2	S	546	1	PQLNKSQSLTNAFSF	0.5257	-0.1399
Q63537	Syn2	S	546	2	PQLNKSQSLTNAFSF	0.7289	-0.0236
Q63537	Syn2	T	548	1	LNKSQSLTNAFSFSE	0.5301	-0.1225
Q63537	Syn2	T	548	2	LNKSQSLTNAFSFSE	1.0623	-0.0048
Q63537	Syn2	S	552	2	QSLTNAFSFSESSFF	0.7680	-0.0813
Q63537	Syn2	S	561	1	SESSFFRSSANEDEA	1.7778	-0.2310
Q63537	Syn2	S	562	1	ESSFFRSSANEDEAK	1.7805	-0.1544
O70441	Syn3	S	418	1	PQTKSAKSPGQGQLG	-1.1508	-0.2370
O70441	Syn3	S	446	1	GGPRQAQSPQPPRSR	-1.0423	0.1327
O70441	Syn3	S	446	2	GGPRQAQSPQPPRSR	-0.6201	0.0504
O70441	Syn3	S	452	1	QSPQPPRSRSPSQQR	-0.4836	0.0018
O70441	Syn3	S	452	2	QSPQPPRSRSPSQQR	-0.9806	-0.0274
O70441	Syn3	S	454	2	PQPPRSRSPSQQRLS	-0.6167	0.0267
O70441	Syn3	S	456	2	PPRSRSPSQQRLSPQ	-0.5685	0.0127
O70441	Syn3	S	469	1	PQGQQPVSPQSGSPQ	-0.3256	0.0555
O70441	Syn3	S	480	1	GSPQQQRSPGSPQLS	-0.6843	-0.0649
O70441	Syn3	S	494	1	SRASGGSSPNQASKP	-0.4893	0.1196
O70441	Syn3	S	519	1	PVQGRSTSQQGEEPQ	1.5310	0.2067
O70441	Syn3	S	540	1	PHLNKSQSLTNSLST	0.3386	0.0337
O70441	Syn3	S	540	2	PHLNKSQSLTNSLST	0.4842	-0.1003
O70441	Syn3	S	544	2	KSQSLTNSLSTSDTS	0.5491	0.0548
O70441	Syn3	S	572	1	TIRNLRKSFASLFSD	-0.3972	-0.2101
Q9QUH6	Syngap1	S	1073	1	PPLQRGKSQQLTVSA	0.2739	0.0222
D4ABN3	Synj1	S	833	1	DLDLLNASFQDESKI	0.8075	0.0036
D4ABN3	Synj1	S	1150	1	GGVGAPPSPGVTRRE	-0.6263	-0.0192
D4ABN3	Synj1	S	1163	1	REMEAPKSPGTARKD	-1.0053	0.1503
O08625	Syt10	T	163	1	ARVQRQTTDPTSSSR	0.3970	0.0102
Q62807	Syt17	S	110	2	YSLTRRISSLDSRRP	0.5948	-0.1017
Q62807	Syt17	S	114	2	RRISSLDSRRPSSPL	0.5948	-0.1017
Q62807	Syt17	S	118	2	SLDSRRPSSPLIDIK	0.4552	-0.0204
Q62807	Syt17	S	119	2	LDSRRPSSPLIDIKP	0.4552	-0.0178
Q62746	Syt6	T	164	1	TKLQRQTTEPASSTR	1.3254	
Q62746	Syt6	S	217	1	PELYKQKSVDGDEAK	0.7705	-0.0306
Q925C0	Syt9	T	159	1	VRVQRQVTEPTPSAR	0.5742	-0.1631
Q925C0	Syt9	S	207	1	PELYKQRSLDNDDGR	0.4633	
Q812E4	Sytl5	S	211	1	AESGRSYSLDLDNQN	1.4037	-0.0106
P37805	Tagln3	S	163	1	QQNRRGFSEEQLRQG	1.7788	-0.1153
A0A0G2K9J0	Tanc2	S	84	2	IMEGVSRSLPSSPLL	-0.4663	-0.0720
A0A0G2K9J0	Tanc2	S	88	2	VSRSLPSSPLLTHQS	-0.4663	-0.0720
D3ZSY8	Tbc1d10b	T	135	2	SPVPGPGTPTRTPSR	-0.4053	
A0A0G2JWM9	Tbc1d22b	S	110	1	YKVIKSSSDAQLSRN	0.2666	0.0153
A0A0G2K5B0	Tbc1d24	S	475	2	CLISHSVSSDPADRL	-0.4576	
A0A0G2K5B0	Tbc1d24	S	476	2	LISHSVSSDPADRLS	-0.4576	
A0A0G2K5B0	Tbc1d24	S	483	2	SDPADRLSPFLAARH	-0.4632	

Q9R1K2	Tenm2	S	142	1	GIKSRRSSGLSSREN	0.3138	
P04177	Th	S	19	1	KGFRRAVSEQDAKQA	1.9169	-0.2432
P04177	Th	S	31	1	KQAEAVTSPRFIGRR	0.2676	-0.1239
Q3ZB99	Tjp2	T	451	2	DITAAGVTEANKEPR	-0.4056	0.1017
Q3ZB99	Tjp2	S	459	2	EANKEPRSQEESPVP	-0.3925	
Q3ZB99	Tjp2	S	463	2	EPRSQEESPVPQPRT	-0.3815	0.1000
D3ZE26	Tmcc2	S	166	1	PSIKRGASLHSSGGS	1.1831	-0.1256
D3ZE26	Tmcc2	S	169	1	KRGASLHSSGGSGGR	0.9653	0.0872
P62329	Tmsb4x	T	23	1	SKLKKTETQEKNPLP	2.6314	
Q52KJ9	Tmx1	S	245	1	EADEEDVSEEETENR	0.3320	
D3ZF26	Tnks1bp1	S	1642	1	KLRSRNRSAEEGEVT	0.3376	
Q5XI21	Tom1	S	376	1	FALTRGSSLADQRKG	0.8166	0.1267
A0A0G2K9L2	Tom1l2	S	160	2	MADLDALSPIHTPQR	-0.5287	0.0281
A0A0G2K9L2	Tom1l2	T	164	2	DALSPIHTPQRSVPE	-0.5287	0.0281
A0A0G2K9L2	Tom1l2	S	394	1	FAQTRGNSLAEQRKT	1.4109	0.1900
Q5PQX1	Tor1aip1	S	157	1	LRDAQSLSEDRGEDE	0.4179	0.1302
A0A0G2K8M7	Tpd52l1	S	132	1	FGDMRSHSIGYSIRH	0.7744	-0.1634
Q6PCT3	Tpd52l2	S	180	1	RNSATFKSFEDRVGT	0.4152	0.2387
A0A0G2K2D6	Tppp	T	32	2	PTKAANKTPPKSPGD	-0.5796	0.1563
A0A0G2K2D6	Tppp	S	36	1	ANKTPPKSPGDPAKA	-0.4514	0.1090
A0A0G2K2D6	Tppp	S	36	2	ANKTPPKSPGDPAKA	-0.5796	0.1563
D3ZE49	Trappc12	S	314	1	EKSPDSTSPSYSTRM	-1.3229	
D3ZQG6	Trim2	S	424	1	FKLKVIRSADVSPTT	0.2932	-0.1190
D3ZQG6	Trim2	S	456	2	KAVKRPASMYSTGKR	-0.4262	
D3ZQG6	Trim2	S	459	2	KRPASMYSTGKRKEN	-0.4262	
F1M0Z1	Trio	T	2432	1	ALGSTSGTSQDGNTK	0.8762	
F1M0Z1	Trio	S	2459	2	KTRPGAVSPLNSPLS	-0.4473	0.0960
F1M0Z1	Trio	S	2463	2	GAVSPLNSPLSTTFP	-0.3520	0.0279
F1M0Z1	Trio	S	2466	2	SPLNSPLSTTFPSPF	-0.3333	0.0459
F1LP64	Trip12	S	1111	1	SGLARAASKDTISNN	0.4878	0.0135
Q9Z136	Tsc1	S	515	1	YRDSLSGSQRKTHSA	0.5402	0.0371
D3ZLW4	Tsc2	T	1383	2	LGDLGDKTDIGRLSP	-0.2735	
D3ZLW4	Tsc2	S	1432	1	LPSSSPRSPSGLRPR	-0.7143	0.0609
D3ZSP7	Ttc3	S	1080	1	EDHNRRNSDSAGPFA	0.4487	-0.0824
P69897	Tubb5	T	285	2	SQQYRALTVPELTQQ	0.5897	
P69897	Tubb5	T	290	2	ALTVPELTQQVFDAK	0.5897	
Q5U300	Uba1	S	820	1	ELQSANASVDDSRLE	0.3938	-0.1507
Q5M7A4	Uba5	S	380	1	VPKKREDSVSEVTVE	0.2857	-0.0599
P0C627	Ubxn2b	S	56	2	STATAFKSPRTPPLR	-1.0543	0.0177
P0C627	Ubxn2b	T	59	2	TAFKSPRTPPLRLYS	-1.0543	0.0177
P0C627	Ubxn2b	S	216	1	RLRFKAFSGEGQKLG	1.2309	-0.0154
A0A0G2K012	Ubxn6	S	119	1	EKTSKGKSPQLALRQ	-0.3633	
A0A0G2K012	Ubxn6	S	161	1	RGPTSQDSIRNQVRK	1.2591	-0.1995
M0R8V0	Uhrf1bp1l	S	443	1	KGTPRTPSVSSQPSK	0.6849	0.0193

D3ZMG0	Ulk1	S	614	2	LPDFLQRSPLPPILG	-1.4063	-0.0388
D3ZMG0	Ulk1	S	622	2	PLPPILGSPTKAGPS	-1.4063	-0.0388
A0A0G2K952	Usp32	S	1452	1	LRLPQIGSKNKLSSS	-0.5960	-0.1154
A0A0G2K952	Usp32	S	1459	1	SKNKLSSSKENLDAS	-0.7847	-0.0541
D3ZVQ0	Usp5	S	785	1	RSAADSISESVPVGP	0.3767	-0.1899
Q8CF97	Vcpip1	S	999	2	RSRESSPSHGLLKLG	-0.3421	
Q8CF97	Vcpip1	S	1030	1	AFQGKGHSLGTASSN	0.3755	0.0891
Q8CF97	Vcpip1	S	1127	1	DKHLRDQSTEQTPSD	0.8465	0.0101
Q8CF97	Vcpip1	T	1128	1	KHLRDQSTEQTPSDL	0.8463	
B1WBS4	Vps26b	T	325	1	TSLGEVRTPGQLSDN	-0.7940	
D3ZP60	Vwa5b1	S	664	1	CSRATTASDPTGTTR	0.3102	-0.2014
D4A7U5	Vwa5b2	S	759	1	ALAGRSLSSPSGRAN	0.4956	-0.1182
M0R7F3	Wasf3	S	235	1	ASSEGSLSPDTRSHT	-0.2794	
D3ZQ02	Wdr37	S	22	1	KQKRKSHSLSIRRTN	1.1715	-0.0608
D3ZQ02	Wdr37	S	24	1	KRKSHSLSIRRTNSS	0.8269	-0.1423
G3V9M3	Wdr47	S	332	1	TSHDKRISDLGNKTS	2.0374	-0.0433
Q9ERH3	Wdr7	T	926	1	TRPPRPGTPDLSKAR	0.3022	-0.1843
Q9ERH3	Wdr7	S	1150	1	KLLTRPRSSSQIPEG	-0.5159	
Q9ERH3	Wdr7	S	1152	1	LTRPRSSSQIPEGFG	-0.3029	0.0833
E9PT53	Wfs1	S	237	1	MLERLVSSESKNYIA	0.9339	
D3ZUD3	Wipf2	S	235	1	PPVKPPPSPVNVRTG	-0.6033	-0.0338
D3ZUD3	Wipf2	S	385	1	LRNGHRDSITTVRSF	0.5466	-0.0444
D3ZMJ7	Wnk2	S	1801	1	HRSSRAGSLGPETPS	0.8352	-0.0836
M0R8P6	Wwc3	S	961	1	CRLYRSDSDSSTLPR	0.5380	
Q5GH59	Xkr4	S	551	1	RSISNNRSVASDRDQ	0.5327	-0.0546
A0A0G2K951	Zfp704	S	11	1	RRLAKRPSLGSRRGG	1.0477	0.0104
Q5PQS2	Znf365	S	139	1	AVDIRADSLDAPRSS	0.2689	
A0A0G2JW65		S	726	2	RLCRKFSSPPPLAVS	0.3923	0.2053
A0A0G2JW65		S	733	2	SPPPLAVSRTSSPVR	0.5924	0.2053
A0A0G2JW65		S	745	2	PVRARKLSLTSSLNS	1.2352	0.0945
A0A0G2JZ27		T	477	2	TEELGARTPGAGGSV	-0.4906	
A0A0G2JZ27		S	483	2	RTPGAGGSVHLLGRG	-0.4906	
A0A0G2K021		T	23	1	SKLKKTETQEKNPLP	2.6314	
M0R970		S	42	3	LLPSSVRSAPSSAPS	-1.2281	
M0R970		S	46	1	SVRSAPSSAPSTPLS	-0.3855	0.0298
M0R970		S	46	2	SVRSAPSSAPSTPLS	-0.6711	0.0310
M0R970		S	46	3	SVRSAPSSAPSTPLS	-1.2388	
M0R970		S	49	3	SAPSSAPSTPLSTDA	-1.2238	
M0R970		T	50	2	APSSAPSTPLSTDAP	-0.6770	
M0R970		T	50	3	APSSAPSTPLSTDAP	-1.2473	
M0R970		S	71	1	KDRPRKKSAPETLTL	-0.7994	
P0CD96		S	28	1	VKDATEDSITEDDKR	0.3519	

Table 8.2: SV-cycling-dependent sites, selection from Suppl. Data 01. *UP.Accession ~ Uniprot accession; Gene.name ~ official gene symbol; AA ~ modified amino acid; Pos ~ position in the protein sequence; Mult ~ multiplicity of phosphorylation (1 – singly phosphorylated, 2 – doubly phosphorylated, 3 – multiply phosphorylated); Seq.window ~ ±7 amino acids flanking phosphorylated residue; CaEGTA ~ log_2 intensity fold change in Ca vs. EGTA experiment, MockBoNT ~ log_2 intensity fold change in Mock vs. BoNT experiment*

UP.Accession	Gene.name	AA	Pos	Mult	Seq.window	CaEGTA	MockBoNT
P0C1X8	Aak1	T	621	2	GQKVGSLTPPSSPKT	-0.4166	0.2843
P0C1X8	Aak1	S	625	2	GSLTPPSSPKTQRAG	-0.425	0.3318
Q63120	Abcc2	T	61	2	RTKRSSITKFYLAKQ		-0.4556
Q63120	Abcc2	Y	64	2	RSSITKFYLAKQVFV		-0.4556
Q9QZM5	Abi1	S	220	1	ARLGSQHSPGRTASL	-0.0489	0.7182
Q9QZM5	Abi1	S	287	2	GTMTRQISRHNSTTS		0.4094
F1LYA6	Abi2	S	150	1	NMAPSQQSPVRTASV	-0.0261	0.311
A0A0G2JTB5	Ablim2	S	413	1	HYTPTSRSPQHYSRP	0.1171	1.5765
A0A0G2JTB5	Ablim2	S	540	1	DADTRTNSPDLDSQS	-0.044	0.282
Q6KC51	Ablim2	S	383	1	HYTPTSRSPQHYSRP	0.0409	1.6334
Q6KC51	Ablim2	S	392	1	QHYSRPGSESGRSTP	-0.1411	1.1417
E9PST5	Acin1	S	216	1	FSEEKGESDDEKPRK		0.5293
P35745	Acyp2	S	42	1	VGWVKNTSKGTVTGQ		-0.3131
D4A3N4	Adcy1	S	397	1	SEKLRNRSSFSTNVV	-0.0711	-0.3943
M0R5U4	Adcy9	S	678	1	KTQNGLLSPPAEEKL		-0.3337
D3ZZ99	Add1	S	353	1	PGKYKAKSRSPGTPA	0.0195	-0.2836
D3ZZ99	Add1	S	355	1	KYKAKSRSPGTPAGE	0.1345	-0.3877
D3ZZ99	Add1	S	572	1	ERTEQTFSPAKSVSF		0.5208
D3ZZ99	Add1	S	632	1	VERKQKGSEENLDET	-0.0875	0.3007
D3ZZ99	Add1	S	646	1	TREQKEKSPPDQSAV	0.0526	-0.3296
D3ZZ99	Add1	S	651	1	EKSPPDQSAVPNTPP	0.0995	-0.2767
Q63028	Add1	S	600	1	TREQKEKSPPDQSAV	0.0526	-0.3296
Q63028	Add1	S	605	1	EKSPPDQSAVPNTPP	0.0995	-0.2767
Q63028	Add1	S	613	2	AVPNTPPSTPVKLEG	-0.2729	0.3956
Q63028	Add1	T	614	2	VPNTPPSTPVKLEGG	-0.2572	0.376
Q05764	Add2	T	612	2	QSPTRAGTKSPAVSP	-0.2254	0.3831
Q05764	Add2	S	614	1	PTRAGTKSPAVSPSK	-0.0329	0.318
Q05764	Add2	S	614	2	PTRAGTKSPAVSPSK	-0.3943	0.5275
Q05764	Add2	S	618	1	GTKSPAVSPSKASED	-0.2495	0.3624
Q05764	Add2	S	618	2	GTKSPAVSPSKASED	-0.4012	0.5318
Q05764	Add2	S	620	1	KSPAVSPSKASEDAK		0.3774
Q05764	Add2	S	620	2	KSPAVSPSKASEDAK	-0.4998	0.4356
Q05764	Add2	S	696	2	GPLSPEGSPSKSPSK	-0.13	0.4278
Q05764	Add2	S	700	2	PEGSPSKSPSKKKKK	-0.1791	0.3976
C0HL12	Adgrb1	S	1253	1	TGTFKRPSLPEEEKM	0.1392	0.2759
C0HL12	Adgrb1	S	1462	1	VATLSVSSLERRKSR		0.5488
A0A0G2K6N2	Adgrb2	S	1469	1	SSAKEKPSPPGGRPG	0.1498	0.4184
D4A831	Adgrb3	S	1411	1	GSTISMSSLERRKSR		0.3928

O88917	Adgrl1	S	1250	2	YNTLIAESVGFNPSS	-0.2419	0.3891
O88917	Adgrl1	S	1263	2	SSPPVFNSPGSYREP	-0.1787	0.3431
Q9Z173	Adgrl3	S	1535	1	PPNKDGASPEGTSKG	-0.2666	0.8795
P22909	Adra2a	S	297	2	ALDLEESSSSEHAER		-0.3294
O35889	Afdn	S	1179	1	KNRADHRSSPNVANQ	0.0209	0.2983
O35889	Afdn	S	1180	1	NRADHRSSPNVANQP	-0.1098	0.3649
O35889	Afdn	S	1180	2	NRADHRSSPNVANQP	-0.2731	0.6676
O35889	Afdn	S	1189	1	NVANQPPSPGGKSPY	-0.0989	0.4754
O35889	Afdn	S	1189	2	NVANQPPSPGGKSPY	-0.4384	0.3518
D3ZQQ1	Aftph	S	619	1	LGTPRTHSVSSAASK		0.2695
Q8CGU4	Agap2	S	650	1	LFANRRGSDSEKRSL	0.3995	1.3185
Q8CGU4	Agap2	S	1171	1	TPSPRRRSSAASLGR	0.3938	0.2865
Q8CGU4	Agap2	S	1175	1	RRRSSAASLGRVDTT	0.1775	0.265
Q4KLH5	Agfg1	S	167	2	LKSLLGESAPALHLN	-0.335	0.3218
Q4KLH5	Agfg1	T	177	2	ALHLNKGTPTQSPVV	-0.1556	0.2633
Q4KLH5	Agfg1	S	181	1	NKGTPTQSPVVGRSQ	-0.157	0.413
Q4KLH5	Agfg1	S	181	2	NKGTPTQSPVVGRSQ	-0.225	0.2785
Q4KLH5	Agfg1	S	293	1	DNFPKSSSADFGSFS	-0.5138	0.2967
G3V8G1	Agtpbp1	S	51	1	KILHLAQSQEKTRRE		-0.337
B5DFN2	Ahcyl1	S	37	1	SAASYTDSSDDEVSP	0.0082	-0.3822
B5DFN2	Ahcyl1	S	38	1	AASYTDSSDDEVSPR	-0.1325	-0.4847
B5DFN2	Ahcyl1	S	38	2	AASYTDSSDDEVSPR		-0.2664
D3ZTF0	Ajm1	S	109	1	SLTTAPASPPVLQRR	0.1982	0.3637
D3ZTF0	Ajm1	S	129	1	RAVRVEGSPCREPSY		0.4908
D3ZTF0	Ajm1	S	509	2	RYAALSLSETSLTEK	-0.2384	0.7389
D3ZTF0	Ajm1	T	511	1	AALSLSETSLTEKGR		0.987
D3ZTF0	Ajm1	S	512	2	ALSLSETSLTEKGRT	-0.2539	0.927
D3ZTF0	Ajm1	S	542	1	ITDNDLRSAERPTAK	0.2587	0.4055
P29410	Ak2	S	151	1	IHPKSGRSYHEEFNP		-0.3554
O88884	Akap1	S	101	1	TRQVRRRSESSGNLP	0.0407	0.2835
F1LPP6	Akap5	S	90	1	LVTHRKPSESAEKQK	0.1454	0.3793
F1LPP6	Akap5	S	223	1	LRMRTPGSEKEAKVI		1.0626
Q9WVC7	Akap6	S	1323	1	TVLTKSLSKDSSFSS		0.3086
P05065	Aldoa	S	100	1	PFPQVIKSKGGVVGI		-0.3353
Q6AY07	Aldoart2	S	100	1	PFPQVIKSKGGVVGI		-0.4312
A0A0G2JWK6	Amer2	S	207	1	RTARRPDSPGQDAPR	0.1457	0.2764
F1LZQ6	Amotl1	S	917	1	LSTAPSNSPVLKHPA		0.9939
F1LZQ6	Amotl1	S	935	1	TVEKQENSPGHGKSS	-0.0381	2.3019
O09178	Ampd3	S	68	1	KELAEQKSVETAKRK		0.4151
D3Z9Z0	Ank1	S	1520	1	VHARITDSPSVRQVL		0.9026
F1M9N9	Ank2	S	1808	1	SAKTERHSPVSPSSK	-0.1284	0.2814
F1M9N9	Ank2	S	1808	2	SAKTERHSPVSPSSK	-0.3732	0.193
F1M9N9	Ank2	S	1820	1	SSKNEKHSPVSPSAK	-0.2626	0.3652
F1M9N9	Ank2	S	1820	2	SSKNEKHSPVSPSAK	-0.4212	0.1747

F1M9N9	Ank2	S	1823	1	NEKHSPVSPSAKAER	-0.27	0.2966
F1M9N9	Ank2	S	1823	2	NEKHSPVSPSAKAER	-0.424	0.179
F1M9N9	Ank2	S	1843	1	SGKPEKHSPGSPSTK	-0.0773	0.3542
F1M9N9	Ank2	T	1909	1	PGAPSIRTPEKQAPG		0.3738
F1M9N9	Ank2	S	1917	1	PEKQAPGSATGKHEK	-0.0109	0.5676
F1M9N9	Ank2	S	1929	1	HEKHLPVSPGKTEKQ	-0.3547	0.2779
F1M9N9	Ank2	S	2373	1	KPQGVIRSPQGLELP	-0.3272	0.4456
F1M9N9	Ank2	S	2630	1	SESRKASSSSESEPE		0.4566
F1M9N9	Ank2	T	3060	1	RTPTEEGTPTSEQNP		0.4022
A0A0G2K1Q7	Ank3	S	1390	1	EKADRRQSFTSLALR	0.2522	0.4187
O70511	Ank3	S	1526	1	KSGSLSSSPSNTPSA		1.0513
O70511	Ank3	S	1676	1	LISSPLKSVVSPTKS	0.2295	1.3718
O70511	Ank3	S	1679	1	SPLKSVVSPTKSAAD	0.2847	1.2892
A0A0G2K2G7	Anks1a	S	557	1	EEEDGSRSRAPPTSK	-0.0162	0.7755
P0C6S7	Anks1b	T	969	2	REPSGNHTPPQLSPS	-0.1997	0.3141
A0A0G2K5K1	Ano8	S	634	1	DGLLEEGSPTMVEKG		0.4784
P62944	Ap2b1	T	2	1	_____MTDSKYFTT	1.6363	-0.4876
B5DFK6	Ap3d1	S	688	1	FYIKSSPSPQKRYQD		0.5064
B5DFK6	Ap3d1	S	1176	1	LLVKKGESSVSVDGK		-0.3163
A0A0G2K8G0	Apc	S	1058	1	QLNSGRQSPSQNERW	-0.334	0.4083
A0A0G2K8G0	Apc	T	1453	1	MPPSRSKTPPPPPPP		0.3195
A0A0G2K8G0	Apc	S	1790	1	TKKKKPTSPVKPMPQ		0.3443
A0A0G2K8G0	Apc	S	2081	1	KGEGERQSPRKVGSV		0.8325
A0A0G2K8G0	Apc	S	2164	2	KSGVSLGSPFHLTPD	-0.3071	0.3523
A0A0G2K8G0	Apc	T	2169	2	LGSPFHLTPDQEEKP	-0.3071	0.3523
A0A0G2K8G0	Apc	S	2262	1	RNSSSSTSPVSKKGP		0.7192
A0A0G2K8G0	Apc	S	2288	1	EGPVATTSPRGTKPA		0.3654
A0A0G2K8G0	Apc	S	2467	1	TFIKEAPSPTLRRKL		0.3413
A0A0G2K8G0	Apc	S	2491	1	SPSSRPDSPTRSQAQ	-0.0715	0.3231
A0A0G2K8G0	Apc	S	2847	1	TESSGAQSPKRHSGS	-0.025	0.6356
A0A0G2JZW4	Apc2	S	2177	1	ALPLRGSSPEDSPAG	-0.0619	0.4015
D4A631	Arfgef1	S	52	1	KVETEKQSPPHGEAK	0.2498	-0.3889
D3ZF86	Arfgef3	S	348	1	RYSESNFSVDDQDLS		-0.3558
D4A6C5	Arhgap1	S	50	1	KSDDSKSSSPEPVTH		-0.515
D4A6C5	Arhgap1	S	50	2	KSDDSKSSSPEPVTH	0.1073	-0.3684
D4A6C5	Arhgap1	S	51	1	SDDSKSSSPEPVTHL	0.0995	-0.4342
D4A6C5	Arhgap1	S	51	2	SDDSKSSSPEPVTHL	0.0885	-0.3749
F1LXQ7	Arhgap21	S	863	1	PLIRRQLSHDQESVG	-0.0131	0.2949
F1LXQ7	Arhgap21	S	863	2	PLIRRQLSHDQESVG	-0.1411	0.3204
F1LXQ7	Arhgap21	S	868	1	QLSHDQESVGPPSLD		0.3498
F1LXQ7	Arhgap21	S	1105	1	PKTQSPHSPKEESER	-0.1403	0.4604
F1LXQ7	Arhgap21	S	1564	1	SSTKKSTSPETRHTE		0.4353
F1MAK3	Arhgap32	S	606	1	PKSLLVSSPSTKLLT		0.955
F1MAK3	Arhgap32	S	720	2	GTLRSAKSEESLTSL	-0.0522	0.8496

F1MAK3	Arhgap32	S	723	2	RSAKSEESLTSLHAV	-0.1294	0.8496
F1MAK3	Arhgap32	S	870	1	TASSEPVSPVQEKLS	-0.1166	0.8862
F1MAK3	Arhgap32	S	966	1	ERDVINRSPTQLGKM	0.0279	1.0432
F1LR18	Arhgap39	S	295	1	IQPRKPSSDSQPSSP	0.502	0.3069
F1LR18	Arhgap39	S	301	1	SSDSQPSSPRYGYEP	-0.6042	0.4461
F1LR18	Arhgap39	S	301	2	SSDSQPSSPRYGYEP	-0.5876	0.0327
A0A0G2K7N9	Arhgap5	S	968	1	SEDVFLPSPRDCFPY		-0.297
D3Z8W6	Arhgef33	S	146	1	ASAPAQGSPFRSINV	-0.057	0.6548
D3Z8W6	Arhgef33	S	692	1	PLPKSATSPASSSGA	0.0522	0.5878
A0A0G2QC21	Arhgef7	S	497	1	LSASPRMSGFIYQGK		-0.3815
D4A3E3	Arid1a	S	90	1	RSHHAPMSPGSSGGG		0.5337
B1WBW4	Armc10	S	43	1	RRLRPSRSAEDLTEG	0.1986	-0.3318
Q642B5	Armcx2	S	46	1	AKPKNRASVGTGTRA	-0.17	0.4169
B4F7F3	Arvcf	S	336	1	PERGSLGSLDRVVRR	0.2414	0.7682
B4F7F3	Arvcf	S	344	2	LDRVVRRSPSVDSTR	0.0188	0.3441
B4F7F3	Arvcf	S	346	2	RVVRRSPSVDSTRKE	-0.0233	0.378
Q1AAU6	Asap1	S	851	1	PGHKRTLSDPPSPLP	0.187	0.4997
Q1AAU6	Asap1	S	851	2	PGHKRTLSDPPSPLP	-0.422	0.0734
P55926	Asic1	S	477	1	QKEAKRSSADKGVAL		-0.3044
A0A0G2JYU3	Astn2	S	445	1	RSKGLLKSPVNKTAL		0.5346
Q3KRE0	Atad3	S	41	1	RGAGDRPSPKDKWSN	0.1656	-0.3219
P06685	Atp1a1	T	226	1	TGESEPQTRSPDFTN	0.1105	-0.3153
P06685	Atp1a1	S	484	1	IVEIPFNSTNKYQLS		-0.5541
P06685	Atp1a1	S	499	1	IHKNPNASEPKHLLV	0.1783	-0.399
P06686	Atp1a2	T	224	1	TGESEPQTRSPEFTH	0.1491	-0.3117
P06686	Atp1a2	T	380	1	SDKTGTLTQNRMTVA		-0.3575
P06686	Atp1a2	S	450	1	RDTAGDASESALLKC	0.1372	-0.4037
P06686	Atp1a2	S	482	1	VAEIPFNSTNKYQLS		-0.3886
P06687	Atp1a3	S	456	1	CIELSSGSVKLMRER		-0.3373
P06687	Atp1a3	S	474	1	VAEIPFNSTNKYQLS		-0.4808
P11505	Atp2b1	S	1126	1	RVVNAFRSSLYEGLE		-0.3588
P11505	Atp2b1	S	1127	1	VVNAFRSSLYEGLEK	0.6029	-0.2675
P11505	Atp2b1	S	1177	1	DAPTKRNSSPPPSPN	0.0681	0.5024
P11505	Atp2b1	S	1178	1	APTKRNSSPPPSPNK	-0.0308	0.4503
P11505	Atp2b1	S	1178	2	APTKRNSSPPPSPNK	-0.0295	0.2883
P11506	Atp2b2	S	1149	1	RVVKAFRSSLYEGLE		-0.3605
P11506	Atp2b2	S	1160	2	EGLEKPESRTSIHNF	0.0489	0.3714
P11506	Atp2b2	T	1162	2	LEKPESRTSIHNFMA	0.0489	0.3986
P11506	Atp2b2	S	1163	2	EKPESRTSIHNFMAH	0.0489	0.3933
P11506	Atp2b2	T	1188	1	HIPLIDDTDLEEDAA	-0.2512	0.3946
P11506	Atp2b2	T	1188	2	HIPLIDDTDLEEDAA	-0.1747	0.7144
P11506	Atp2b2	S	1200	1	DAALKQNSSPPSSLN	-0.2951	0.4472
P11506	Atp2b2	S	1200	2	DAALKQNSSPPSSLN	-0.1841	0.7924
P11506	Atp2b2	S	1201	1	AALKQNSSPPSSLNK	-0.0302	0.3971

P11506	Atp2b2	S	1201	2	AALKQNSSPPSSLNK	-0.1723	0.7622
P11506	Atp2b2	S	1204	2	KQNSSPPSSLNKNNS	-0.0407	1.0315
P11506	Atp2b2	S	1205	2	QNSSPPSSLNKNNSA	-0.0842	0.876
P15999	Atp5f1a	T	236	1	QKRFNDGTDEKKKLY		-0.2968
P15999	Atp5f1a	S	533	1	IRSDGKISEQSDAKL		-0.3436
Q6P503	Atp6v1d	S	216	1	KKIIKEKSEKDLERR		-0.2978
D4A3X6	Atp8a2	S	52	1	DEMSRATSVGDQLEA		-0.2657
A0A0G2JXZ3	Atrx	S	770	1	GKRKRKNSTSGSDFD		0.4591
Q63540	Atxn1	S	213	1	AGLVNPGSPPPTQQN		0.3126
F1M049	Atxn2	S	529	1	LQDQRQNSPAGNKEN		1.4942
A0A0G2JYE0	Atxn2l	S	337	1	RQGSGRESPSLVSRE		0.5694
O70239	Axin1	S	492	1	SPGPGHRSPDSGHVA		0.3119
Q6GMN2	Baiap2	S	324	2	RKAAQPKSLSPPQSQ	-0.0515	0.4707
Q6GMN2	Baiap2	S	326	1	AAQPKSLSPPQSQSK	0.011	0.4687
Q6GMN2	Baiap2	S	326	2	AAQPKSLSPPQSQSK	-0.0515	0.4707
A0A0G2K1L8	Basp1	T	31	1	KKAEGAGTEEEGTQK	0.3282	-0.3434
A0A0G2K1L8	Basp1	T	36	1	AGTEEEGTQKESEPQ	0.2704	-0.2825
A0A0G2K1L8	Basp1	S	40	1	EEGTQKESEPQAAAD	0.2935	-0.3751
A0A0G2K1L8	Basp1	S	91	1	PKAEPEKSEGAAEEQ	0.0254	-0.3736
A0A0G2K1L8	Basp1	S	165	1	AAPAASDSKPSSAEP	0.1208	-0.3252
A0A0G2K1L8	Basp1	S	168	1	AASDSKPSSAEPAPS	0.2988	-0.2913
A0A0G2K1L8	Basp1	S	169	1	ASDSKPSSAEPAPSS		-0.2708
G3V661	Baz1b	S	311	1	TKRKNTGSPDRKPSK		1.3454
Q9QYN5	Bcl10	S	138	1	NNLSRSNSDESNFSE	0.0218	0.3024
B1WC16	Bclaf1	S	263	1	TPSQHSHSIQHSPER	-0.1014	1.9144
B1WC16	Bclaf1	S	267	1	HSHSIQHSPERSGSG	-0.1371	1.5539
B1WC16	Bclaf1	S	496	1	TVKKEVQSPEQVKSE	0.1246	0.528
O88881	Begain	S	213	1	LEKPDPGSLSSRMSD		0.4141
O88881	Begain	S	474	1	GGGGGGGSPGKNAEG	-0.1786	0.8912
O88881	Begain	S	474	2	GGGGGGGSPGKNAEG		1.7859
O88881	Begain	S	484	1	KNAEGRASPLYASYK		0.7657
O88881	Begain	S	484	2	KNAEGRASPLYASYK		1.7194
O88881	Begain	S	521	1	AGGDLSLSPSRSADP	-0.0441	0.9255
Q5U3Z5	Bri3bp	S	51	1	RGTADKNSHRRATSS		-0.2724
Q5U3Z5	Bri3bp	S	250	1	VLENLDRSNEK___	0.1366	-0.2672
B2DD29	Brsk1	S	275	1	VEPEKRLSLEQIQKH		-0.4987
G3V984	Bsn	S	90	1	LGSQRATSPTPKQAS	-1.7085	0.4685
G3V984	Bsn	S	245	1	QLHSPALSPAHSPAK	-0.6205	0.28
G3V984	Bsn	S	245	2	QLHSPALSPAHSPAK	-1.6773	0.0297
G3V984	Bsn	S	245	3	QLHSPALSPAHSPAK	-1.7895	-0.084
G3V984	Bsn	S	548	1	PQRAAGASPLKQKGP	-0.9047	0.3409
G3V984	Bsn	T	1086	1	RRRERSKTPPSNLSP		0.695
G3V984	Bsn	T	1086	2	RRRERSKTPPSNLSP	0.0378	0.383
G3V984	Bsn	T	1086	3	RRRERSKTPPSNLSP	-0.7174	0.3222

G3V984	Bsn	S	1092	3	KTPPSNLSPIEDASP	-0.6794	0.3433
G3V984	Bsn	S	1098	1	LSPIEDASPTEELRQ	0.3503	-0.0204
G3V984	Bsn	S	1098	3	LSPIEDASPTEELRQ	-0.714	0.3634
G3V984	Bsn	T	1100	2	PIEDASPTEELRQAA	0.0072	0.4748
G3V984	Bsn	S	1469	1	YSYFTGSSPPLSPST	0.3313	0.1816
G3V984	Bsn	S	1469	2	YSYFTGSSPPLSPST	-0.2452	0.5949
G3V984	Bsn	S	1469	3	YSYFTGSSPPLSPST	-0.605	0.4956
G3V984	Bsn	S	1473	3	TGSSPPLSPSTPSES	-0.7101	0.4691
G3V984	Bsn	S	1475	3	SSPPLSPSTPSESPT	-0.8634	0.4853
G3V984	Bsn	T	1476	2	SPPLSPSTPSESPTF	-0.1421	0.5702
G3V984	Bsn	T	1476	3	SPPLSPSTPSESPTF	-0.9133	0.1017
G3V984	Bsn	S	1478	2	PLSPSTPSESPTFSP	-0.1754	0.5627
G3V984	Bsn	S	1478	3	PLSPSTPSESPTFSP	-0.6575	
G3V984	Bsn	S	1480	2	SPSTPSESPTFSPSK	-0.2179	0.6476
G3V984	Bsn	S	1480	3	SPSTPSESPTFSPSK	-0.4521	0.5195
G3V984	Bsn	S	2004	1	FQGPGRDSAVDLSSL	-0.6739	-0.2832
G3V984	Bsn	S	2634	1	SRHSDSGSDSKHEAS	0.3301	0.3351
G3V984	Bsn	S	2850	1	LSDPKPLSPTAEESA	-0.552	0.3295
G3V984	Bsn	S	2850	2	LSDPKPLSPTAEESA	-0.6354	0.2229
G3V984	Bsn	S	2850	3	LSDPKPLSPTAEESA	0.4901	
G3V984	Bsn	S	3349	1	LAPAAISSKRSKHRK		-0.3366
A0A0G2K2V4	C2cd2l	S	465	1	VDGKLADSPSRSPSK	0.4169	0.4068
A0A0G2K2V4	C2cd2l	S	465	2	VDGKLADSPSRSPSK	-0.1881	0.5541
A0A0G2K2V4	C2cd2l	S	467	2	GKLADSPSRSPSKVE	-0.1783	0.7078
A0A0G2K2V4	C2cd2l	S	469	2	LADSPSRSPSKVEVT	-0.1976	0.5344
A0A0G2K2V4	C2cd2l	S	471	2	DSPSRSPSKVEVTEK	-0.1654	0.5251
A0A0G2K2V4	C2cd2l	S	641	1	KDHKDNSSPANSSRW	0.1776	1.3209
Q5U2P5	C2cd2l	S	464	2	RVDGKLDSPSRSPSK	-0.024	0.4357
Q5U2P5	C2cd2l	S	468	2	KLDSPSRSPSKVEVT	-0.0441	0.4041
A0A0G2K543	C2cd5	S	260	1	AFLPACNSPSKEMKE		-0.3675
A0A0G2JXK1	Cacna1a	S	462	1	FARASIKSAKLENST		-0.2896
A0A0G2JXK1	Cacna1a	T	1092	1	SNPGPPKTPENSLIV		0.3216
A0A0G2JXK1	Cacna1a	T	2070	1	NLSTISDTSPMKRSA		0.9945
A0A0G2JXK1	Cacna1a	S	2071	1	LSTISDTSPMKRSAS		1.1996
F1LQ87	Cacna1b	S	48	1	QRVLYKQSIAQRART		-0.5709
F1LQ87	Cacna1b	S	2029	1	TQPAPNASPMKRSIS		0.3127
P22002	Cacna1c	S	1720	1	KEAVSAASEDDIFRR		0.5861
P22002	Cacna1c	S	1771	1	NNQADTESPSHEKLV	-0.1062	0.9452
F1LMS1	Cacna1e	S	837	1	ERISRGGSLKGDIGG	0.4629	0.5399
F1LMS1	Cacna1e	S	837	2	ERISRGGSLKGDIGG	-0.3298	0.3979
F1LMS1	Cacna1e	S	854	2	SVLDNQRSPLSLGKR	-0.3185	0.402
F1LMS1	Cacna1e	S	925	2	ASRSRSASQERSLDE	0.2621	0.3112
F1LMS1	Cacna1e	S	929	2	RSASQERSLDEGVSI	0.2507	0.2996
F1LMS1	Cacna1e	S	2036	2	TYKSRRRSYHSSLRL		-0.3036

Q9WUB8	Cacna1g	S	467	1	VRAGLLSSPVARSGQ	0.3392	-0.3373
Q9WUB8	Cacna1g	S	1087	1	AAHHEMKSPPSARSS		0.4983
Q9WUB8	Cacna1g	S	1165	1	SDHRHRGSLEREAKS	0.0252	0.3752
Q9WUB8	Cacna1g	S	1173	1	LEREAKSSFDLPDTL	0.0968	0.4288
Q9WUB8	Cacna1g	S	2268	1	DSTAASPSPKKDTLS		0.3984
D4A055	Cacnb4	S	16	1	GAADGPHSPSSQVAR	-0.0451	0.6545
D4A055	Cacnb4	S	447	1	SNHSTENSPIERRSL	-0.1905	1.5926
D4A055	Cacnb4	S	474	1	RKSRNRLSSSSQHSR	-0.384	0.3269
Q71RJ2	Cacng2	S	243	2	RSRSSSRSTEPSHSR		0.621
Q71RJ2	Cacng2	S	249	2	RSTEPSHSRDASPVG	-0.2552	0.6311
Q71RJ2	Cacng2	S	253	1	PSHSRDASPVGVKGF	0.1258	0.6082
Q71RJ2	Cacng2	S	253	2	PSHSRDASPVGVKGF	-0.2491	0.7494
Q71RJ2	Cacng2	S	310	1	IQKDSKDSLHANTAN	0.0921	0.8288
Q8VHW5	Cacng8	S	290	1	ASPSRDASPGGPGGP	0.0071	0.3539
Q8VHW5	Cacng8	S	357	1	GSERDRGSSAGFLTL		0.3693
F1LLX6	Cadps	S	89	1	AGGGRPSSPSPSVVS	-0.9209	-0.3369
F1LLX6	Cadps	S	89	2	AGGGRPSSPSPSVVS	-1.2942	
P18418	Calr	S	44	1	WVESKHKSDFGKFVL		-0.3521
F1LZG4	Camk2a	S	330	1	GVKESSESTNTTIED	0.4369	-0.3282
F1LZG4	Camk2a	T	334	1	SSESTNTTIEDEDTK	0.382	-0.2993
P11275	Camk2a	S	330	1	KNDGVKESSESTNTT	0.0176	-0.2998
P11275	Camk2a	S	331	1	NDGVKESSESTNTTI	0.0552	-0.3531
P11275	Camk2a	T	334	1	VKESSESTNTTIEDE	0.2713	-0.2704
P11275	Camk2a	T	337	1	SSESTNTTIEDEDTK	0.382	-0.2737
P11275	Camk2a	T	337	3	SSESTNTTIEDEDTK	0.0105	-0.348
F1LNI8	Camk2b	S	71	1	ICRLLKHSNIVRLHD		-0.3379
F1M3F8	Camk2g	S	351	1	GGVKKRKSSSSVHLM	0.1935	0.2825
P11730	Camk2g	S	321	1	FSVGRQSSAPASPAA	0.789	0.3125
P11730	Camk2g	S	321	2	FSVGRQSSAPASPAA	0.2855	0.0337
P11730	Camk2g	S	356	2	GVKKRKSSSSVHLME	0.3179	0.2999
P11730	Camk2g	S	356	3	GVKKRKSSSSVHLME	0.4245	0.0986
P11730	Camk2g	S	357	2	VKKRKSSSSVHLMEP	0.3317	0.2813
P11730	Camk2g	S	357	3	VKKRKSSSSVHLMEP	0.4245	0.115
Q63092	Camkv	T	430	2	PATDRSATPATDGRA	-0.1151	0.5235
Q63092	Camkv	T	438	1	PATDGRATPATEEST	0.1299	0.4969
Q63092	Camkv	T	438	2	PATDGRATPATEEST	-0.0878	0.4049
D4AEC2	Camsap2	S	952	1	SPRPTHPSPQSSTRK		0.3894
P35565	Canx	S	56	2	SDTSTPPSPKVTYKA		-0.3402
Q8VHK2	Caskin1	S	432	1	SESSPGDSPVKPPEG	-0.0285	0.4727
Q8VHK2	Caskin1	S	790	1	PTKAQPGSPQALGGP	-0.2383	0.3081
Q8VHK2	Caskin1	S	1243	1	PVSKIQGSPTPASKK	-0.4762	0.2915
Q8VHK2	Caskin1	S	1258	1	VPLPGPGSPEVKRAH	0.0555	0.3358
Q8VHK2	Caskin1	S	1400	1	DGQGPRPSSIEEKST	0.2598	-0.2716
F1MAS1	Cbarp	S	52	1	SSLDTRGSPKRHHFQ		0.6212

A0A0G2JUY5	Ccdc120	S	253	1	FRAVSGGSPERRAPW	0.1734	0.3017
D4AEK9	Ccdc6	S	410	2	TRPSPRRSSSPDKFK		0.595
D4AEK9	Ccdc6	S	411	2	RPSPRRSSSPDKFKR		0.5461
D3ZMD4	Ccdc85a	T	262	1	HKPRASGTPDHPKAL		0.3389
D3ZMD4	Ccdc85a	S	394	1	RPAQEDSSPHHRNVY		0.5722
Q7TT49	Cdc42bpb	S	1685	2	HSTPSNSSNPSGPPS	-0.245	0.6788
Q7TT49	Cdc42bpb	S	1688	1	PSNSSNPSGPPSPNS		0.5325
Q7TT49	Cdc42bpb	S	1692	2	SNPSGPPSPNSPHRS	-0.224	0.4523
Q7TT49	Cdc42bpb	S	1695	1	SGPPSPNSPHRSQLP	-0.1153	0.9262
Q7TT49	Cdc42bpb	S	1695	2	SGPPSPNSPHRSQLP	-0.2052	0.6635
B1WC33	Cdc42ep4	S	140	1	LPKSLSSSPVKKADT	-0.3445	0.3895
B1WC33	Cdc42ep4	S	154	1	TRDGSPKSPHRNGAT		0.6902
Q63315	Cdh22	S	717	1	ASSSERHSLPRGPSS	0.0405	0.3153
F1M491	Cdk5r2	T	84	1	KKGSKKVTPKPASTG		0.7062
F1LQC8	Cdk7	S	165	1	GLAKSFGSPNRAYTH		-0.2982
D3ZG85	Cdkl5	S	343	1	QTHHRSNSKDIQNLS		0.9937
D3ZG85	Cdkl5	S	407	1	NNIPHLLSPKEAKSK	0.13	1.7226
D3ZG85	Cdkl5	S	691	1	GVYHDPHSDDGTAPK		0.5594
Q5XIM5	Cdv3	S	51	1	SRPGDGGSLGSGARS	0.2791	0.4654
Q9QYP2	Celsr2	S	1854	1	FACSRKPSPDPALTT		-0.289
Q5FVI4	Cend1	S	7	1	_MESRGKSASSPKPD	0.0425	0.4552
Q5FVI4	Cend1	S	7	2	_MESRGKSASSPKPD	0.0837	0.6331
Q5FVI4	Cend1	S	9	2	ESRGKSASSPKPDTK	0.0771	0.6403
Q5FVI4	Cend1	S	10	2	SRGKSASSPKPDTKV	0.0761	0.6452
Q5FVI4	Cend1	T	15	2	ASSPKPDTKVPQATA	0.0853	0.6006
Q5FVI4	Cend1	T	21	1	DTKVPQATAEAKATP		0.4018
B2RZ23	Cenpa	S	15	1	GTPRRRPSSPAPGPS		1.2181
B2RZ23	Cenpa	S	16	1	TPRRRPSSPAPGPSQ		1.0186
B2RZ23	Cenpa	S	41	1	TPTRRPSSPAPGPSR		0.4291
A0A0G2K315	Cep170	S	675	1	DSKALLHSGSNSSKE		0.384
A0A0G2K315	Cep170	S	677	1	KALLHSGSNSSKEKS	0.5197	0.2966
D4A1G8	Cep170b	S	360	1	KHEDGTQSDSEDPLA	-0.0714	0.3794
D4A1G8	Cep170b	S	362	1	EDGTQSDSEDPLAKT	-0.0819	0.4551
D4A1G8	Cep170b	S	862	1	LTFARQESFTKEPTS	0.2803	0.2647
D4A1G8	Cep170b	S	965	1	LSGKNGPSPTTPQTP	-0.1159	0.3807
D4A1G8	Cep170b	T	967	1	GKNGPSPTTPQTPGP	-0.1058	0.4321
D4A1G8	Cep170b	S	1254	1	TSEEEYGSHHSSPKH	-0.0698	1.0695
D4A1G8	Cep170b	S	1257	1	EEYGSHHSSPKHTRS	-0.122	0.9923
D3ZZ61	Cep68	S	416	1	GKNASAGSPQLKTKE	0.0758	1.1451
M0RC65	Cfl2	S	23	1	NDMKVRKSSTQEEIK		-0.328
D3ZUX5	Chchd3	S	46	1	SSPSGSKSQRYSSVY		-0.3045
D4A7N1	Chchd6	S	147	1	TEKHLKASLPKKKAT		-0.3371
D4A7N1	Chchd6	T	179	1	AELSRRDTFYKEQQE		-0.2706
A0A0G2KA92	Chd2	S	1100	1	AQTNDSDSDTESKRQ		0.5401

E9PU01	Chd4	S	1528	1	KKMSQPGSPSPKTPT		-0.2817
O35314	Chgb	S	155	1	KEAKIRHSEERGGKE	0.3859	-0.4208
Q5U2T8	Cir1	S	380	1	KSRSHQHSPERKGSD	0.1408	0.765
Q5U2T8	Cir1	S	426	1	ARSRPHQSPSEEQKG	0.0231	0.5659
E9PSL7	Cit	S	1458	1	FCRDKVSSPGLQSKE	-0.0053	-0.3088
P07335	Ckb	S	309	1	LGKHEKFSEVLKRLR		-0.4259
A0A0G2JZF2	Clip2	S	203	1	SVKTGNESGSNLSDS		-0.3834
A0A0G2JZF2	Clip2	S	205	1	KTGNESGSNLSDSGS		-0.4307
A0A0G2K5Q8	Clk2	S	528	1	VQSSRKLSPAEPKNY	-0.5594	-0.2701
D4A626	Clmn	S	419	1	KDGRRSNSLPVKKSV	0.0946	0.5547
D4A626	Clmn	S	536	1	EKGPSPPSPRDNTIL	0.0769	0.828
D4A626	Clmn	S	722	1	EGLDFKPSPPLSKIS		0.8159
P08081	Clta	S	105	1	SEVDRLQSEPESIRK	0.3735	-0.3541
P11442	Cltc	T	238	1	IEVGTPPTGNQPFPK		-0.3279
P11442	Cltc	S	576	1	ALKNNRPSEGPLQTR	0.0742	-0.4081
D4A1C0	Cnnm1	T	454	2	KAPTTRGTPQTPKDD	-0.1275	0.4618
D4A1C0	Cnnm1	T	457	2	TTRGTPQTPKDDPVL	-0.1335	0.4606
A0A0G2K717	Cnot2	S	165	1	MSSSGLGSPNRSSPS		0.9298
D3ZUV9	Cnot3	S	299	1	TDSEVSQSPAKNGSK	0.212	0.6891
P20272	Cnr1	T	314	2	VRMIQRGTQKSIIIH	1.377	-0.29
P20272	Cnr1	T	322	1	QKSIIIHTSEDGKVQ	1.2867	-0.2432
P20272	Cnr1	T	322	2	QKSIIIHTSEDGKVQ	1.4183	-0.3059
P20272	Cnr1	S	323	2	KSIIIHTSEDGKVQV		-0.3373
D3ZKK3	Cnst	S	356	1	KIVPVEQSPGKKGFP		0.3851
D3ZUI5	Cobl	S	219	1	REMLRKSSLGNDETD		-0.3671
D3ZUI5	Cobl	S	838	1	GKSATHNSPAAVHRN	-0.1341	0.5028
D4ACN6	Col4a3bp	S	380	2	SRSPSMSSIDLVSAS		-0.2663
P22734	Comt	S	260	1	AIYQGPSSPDKS___	0.1362	-0.2711
O35142	Copb2	S	860	1	PDGKPASSPVIMASQ		0.3938
Q920J3	Coro6	S	418	1	LDVRPPASPRRSQSA		0.6628
P10888	Cox4i1	S	26	1	VCLRAHGSVVKSEDY		-0.3241
P10888	Cox4i1	S	58	1	HVKLLSASQKALKEK	0.3069	-0.3512
P63041	Cplx1	S	93	1	MEANSEGSLTRPKKA	0.1562	0.3125
D3ZGN2	Cpne5	S	575	1	PPAAPVQSPPQSPAH		-0.2694
P36201	Crip2	S	104	1	RTEERKTSGPPKGPS		0.5172
Q62950	Crmp1	S	521	2	APAPSAKSSPSKHQP	-0.5016	0.2967
Q8VHF5	Cs	S	225	1	RNLYREGSSIGAIDS		-0.3248
Q8VHF5	Cs	S	226	1	NLYREGSSIGAIDSK		-0.3629
P18395	Csde1	S	514	1	VRLLGRNSNSKRLLG		-0.5896
Q9JJ76	Csnk1e	S	363	1	IQQAGNTSPRAISRA	-0.1775	0.4624
P67874	Csnk2b	S	205	1	QLQLQAASNFKSPVK	0.0096	0.5441
P67874	Csnk2b	S	209	1	QAASNFKSPVKTIR_	-0.0258	0.3192
D4A6H8	Ctnna2	S	462	1	GSQKKHISPVQALSE		0.6749
D3ZZZ9	Ctnnd1	T	310	1	GTARRTGTPSDPRRR		0.411

F1M787	Ctnnd2	S	250	1	PAPPRGGSPLTTTQG	-0.1991	0.5833
F1M787	Ctnnd2	S	250	2	PAPPRGGSPLTTTQG	-0.1388	1.6764
F1M787	Ctnnd2	S	259	1	LTTTQGGSPTKLQRG	-0.1302	0.95
F1M787	Ctnnd2	S	259	2	LTTTQGGSPTKLQRG	-0.1416	1.6852
F1M787	Ctnnd2	T	261	2	TTQGGSPTKLQRGGS		1.0462
F1M787	Ctnnd2	S	282	2	YAAPRGSSPKQSPSR	-0.0146	2.8917
F1M787	Ctnnd2	S	286	2	RGSSPKQSPSRLAKS	-0.0267	2.8538
F1M787	Ctnnd2	S	288	2	SSPKQSPSRLAKSYS	-0.0718	2.3735
F1M787	Ctnnd2	S	310	2	VVSSAGLSPIRVTSP	-0.043	1.2637
F1M787	Ctnnd2	S	316	3	LSPIRVTSPPTVQST		1.2466
F1M787	Ctnnd2	S	343	3	IGTYATLSPTKRLVH	-0.0974	1.2625
F1M787	Ctnnd2	S	444	1	RTSTAPSSPGVDSVP	-0.1597	0.4478
F1M787	Ctnnd2	S	1084	1	RSASAPASPREMISL	0.0068	0.4045
D3ZGE6	Cttn	S	47	1	GAKTVQGSGHQEHIN	-0.0415	0.6655
D3ZGE6	Cttn	S	150	1	GKTEKHASQKDYSSG		0.3057
Q66HL2	Cttn	S	261	1	EKLQLHESQKDYAKG		0.3524
Q2IBD4	Cttnbp2	S	472	1	SPPSRDVSPTSRDNL	0.0231	0.9691
Q2IBD4	Cttnbp2	S	554	1	PGLSQTPSPPHPQLR		0.3173
A0A0G2K652	Cul9	S	939	1	STQGQDGSPESLIRS		-0.8514
Q5EB81	Cyb5r1	S	169	1	NIQPNKKSPPELRVA		-0.2813
Q66H62	Cyld	S	328	1	RGVGDKGSSSHNKPK	0.6781	0.4006
Q66H62	Cyld	S	359	1	FYTLNGSSVDSQQQS		0.3492
Q66H62	Cyld	S	396	1	SSDFGHSSPPPQPPS		0.3815
Q8CJH2	Dab1	S	400	1	TNDSARSSPQSDKPR		0.5227
A0A0G2JTF2	Dab2ip	S	694	1	RSSGVQPSPARSSSY	-0.0335	0.3794
A0A0G2JTF2	Dab2ip	S	950	1	SSSSKGDSPELKPRA	-0.0266	0.4404
M0R4J7	Dact3	S	374	1	RGRSVEQSPPRERPR	0.117	0.2985
Q5YLM1	Dagla	S	733	1	SKSQSEMSLEGFSEG	-0.0799	0.492
Q5YLM1	Dagla	S	808	1	GFRSIRGSPSLHAVL	0.2031	0.5574
Q5YLM1	Dagla	T	1025	1	TDKIRTSTPTGHGAS		1.2612
Q5YLM1	Dagla	T	1025	2	TDKIRTSTPTGHGAS	-0.2622	1.4076
Q5YLM1	Dagla	S	1032	1	TPTGHGASPTKQDDL	-0.1666	1.1749
Q5YLM1	Dagla	S	1032	2	TPTGHGASPTKQDDL	-0.2559	1.3079
A0A0H2UHL9	Dbn1	S	385	1	PIPTRSPSDSSTAST		0.3074
A0A0H2UHL9	Dbn1	S	385	2	PIPTRSPSDSSTAST	-0.3499	
D4A8L4	Dcaf6	S	693	1	DSATRRASDNPELPS	-0.0093	-0.4293
Q9WVP7	Dclk1	S	33	1	PSPTSPGSLRKQRDL	1.0367	-0.2965
Q9ESI7	Dcx	S	306	1	GPMRRSKSPADSGND		0.4896
P49621	Dgkb	S	95	1	SNKFPHSSPNVKSKP	0.1773	0.3436
A0A0G2K1M2	Dlg1	S	143	2	HVSEKSLSEIENVHG	-0.2103	0.7444
A0A0G2K1M2	Dlg1	S	155	1	VHGFVSHSHISPIKP	-0.0082	0.7214
A0A0G2K1M2	Dlg1	S	158	1	FVSHSHISPIKPTEA	-0.0599	0.7082
A0A0G2K1M2	Dlg1	S	158	2	FVSHSHISPIKPTEA	-0.2168	0.7444
Q63622	Dlg2	S	175	1	EALKEAGSIVRLYVR	0.4889	-0.2633

Q63622	Dlg2	T	317	2	NGTLEYKTSLPPISP	-0.7041	0.7973
Q63622	Dlg2	S	323	2	KTSLPPISPGRYSPI	-0.45	0.7773
Q63622	Dlg2	S	328	2	PISPGRYSPIPKHML	-0.5513	0.788
Q63622	Dlg2	S	360	1	KLCDKPASPRHYSPV	0.0378	1.0697
Q63622	Dlg2	S	365	1	PASPRHYSPVECDKS	0.0712	0.5461
Q63622	Dlg2	S	406	1	STATRQPSVTLQRAI	0.1254	0.5397
Q62936	Dlg3	S	632	1	KGVTSNTSDSESSSK	0.1838	0.2989
G3V849	Dlgap1	T	557	1	CITTYKKTPPPVPPR	0.1487	0.2705
G3V849	Dlgap1	S	947	1	APLIRERSLESSQRQ	0.2245	1.5822
P97837	Dlgap2	S	455	2	EESGESDSSPKTSPT	0.2056	0.546
P97837	Dlgap2	S	456	2	ESGESDSSPKTSPTV	-0.1062	0.5503
P97837	Dlgap2	T	459	2	ESDSSPKTSPTVALR		0.6499
P97837	Dlgap2	S	637	1	ISVTAQSSTESTQDA	-0.0628	0.8563
P97837	Dlgap2	S	670	1	GLYNSMDSLDSNKAM		0.4486
P97837	Dlgap2	S	1012	1	FPITREKSLDLPDRQ	0.4817	0.3042
G3V7T8	Dlgap3	S	165	1	APEARSESPSRIRHL		0.7221
G3V7T8	Dlgap3	S	428	1	RFASRRSSSVDTARI	0.1263	0.4894
G3V7T8	Dlgap3	S	559	2	ISITAQSSTDSAHES	-0.1514	0.5736
G3V7T8	Dlgap3	S	562	2	TAQSSTDSAHESFTA	-0.1143	0.3586
G3V927	Dlgap4	S	388	2	GGGSPKPSPKTAARR		0.5816
G3V927	Dlgap4	S	405	1	YLRATQQSLGEQSNP	0.2321	0.3517
G3V927	Dlgap4	S	410	1	QQSLGEQSNPRRSLD	-0.0316	0.4476
G3V927	Dlgap4	S	415	1	EQSNPRRSLDRLDSV	0.0804	0.3018
G3V927	Dlgap4	S	581	2	ISVTVQSSTESAQDT		0.5611
G3V927	Dlgap4	T	582	2	SVTVQSSTESAQDTY		0.5611
G3V927	Dlgap4	S	683	1	PVPKEEPSPATKFQS		0.4703
B2GUY4	Dmtn	S	26	1	RDSSVPGSPSNIVAK	-0.0389	0.5556
B2GUY4	Dmtn	S	152	1	PIYKQRESVGGSPQS	1.525	0.1124
B2GUY4	Dmtn	S	152	2	PIYKQRESVGGSPQS		0.3096
B2GUY4	Dmtn	S	156	1	QRESVGGSPQSKHLI	0.101	0.9248
B2GUY4	Dmtn	S	156	2	QRESVGGSPQSKHLI		0.3096
Q5XIP0	Dnajb4	S	38	1	FHPDKNKSPQAEEKF	0.3709	-0.2913
P60905	Dnajc5	T	27	1	LGLDKNATSDDIKKS		-0.3799
P60905	Dnajc5	S	28	1	GLDKNATSDDIKKSY	0.2311	-0.4726
A0A0G2JY26	Dnajc6	S	687	2	AATSPTGSTHGTPTH	-0.4863	0.6633
A0A0G2JY26	Dnajc6	S	687	3	AATSPTGSTHGTPTH	-0.8134	
A0A0G2JY26	Dnajc6	T	688	2	ATSPTGSTHGTPTHQ	-0.5397	0.6465
A0A0G2JY26	Dnajc6	T	688	3	ATSPTGSTHGTPTHQ	-0.8183	
A0A0G2JY26	Dnajc6	S	795	1	QSDRGKGSTNLEGKQ	0.4131	0.4129
P21575	Dnm1	S	347	1	FEKRIEGSGDQIDTY	-0.1217	-0.3109
Q1LZ53	Dnmt3a	S	102	1	EPQPEEGSPAAGQKG		0.6826
D3ZZW1	Dock1	S	1857	1	KTTRKQTSVDSGIVQ		0.3614
F1M4N6	Dock3	S	1766	1	APSSTRGSPSLPDKY	0.1728	0.7939
F1M4N6	Dock3	S	2049	1	RGLHRKASLPPGSAK	0.391	0.4659

M0R6K4	Dock4	S	1697	1	APSSARASPLLSDKH	0.2314	0.5762
M0R6K4	Dock4	S	1758	1	LSAPEKASPARHTTS		1.381
M0R6K4	Dock4	S	1774	1	SPSPAGRSPLKSSVQ		0.7551
A0A0G2K3H2	Dock7	S	440	1	WSERRNSSLVGRRSL		-0.3789
P47942	Dpysl2	T	521	2	TPASSAKTSPAKQQA	-0.2769	0.3849
P47942	Dpysl2	T	521	3	TPASSAKTSPAKQQA	-0.4307	0.12
P47942	Dpysl2	S	522	2	PASSAKTSPAKQQAP	-0.3987	0.4764
P47942	Dpysl2	S	522	3	PASSAKTSPAKQQAP	-0.5053	0.2483
P18901	Drd1	T	446	1	THSGQHST_____	-0.0244	0.3928
Q9EPA0	Drp2	T	910	1	PREKGQTTPDTEAAD		0.3554
A0A0G2JVM6	Dtnb	S	531	1	QAAQATGSPHTSPTH	0.366	0.1311
A0A0G2JVM6	Dtnb	S	531	2	QAAQATGSPHTSPTH	-0.091	0.7233
A0A0G2JVM6	Dtnb	T	534	2	QATGSPHTSPTHGGG	-0.0532	0.6229
A0A0G2JVM6	Dtnb	S	535	2	ATGSPHTSPTHGGGR	-0.1073	0.7922
Q62698	Dync1li2	S	432	1	KKTGSPGSPSAGGVQ		0.3343
P23965	Eci1	T	249	1	KSMMRKATADNLIKQ		-0.3029
Q68FR9	Eef1d	S	133	1	APQTQHVSPMRQVEP	0.0986	0.355
F1LTW9	Efr3b	S	216	1	EAESRSPSPLQAPEK	0.1502	-0.2942
D4ACF1	Eif4enif1	S	77	1	LYPASGRSSPVESLK		0.8623
D4ACF1	Eif4enif1	S	78	1	YPASGRSSPVESLKK		0.9083
D3ZU13	Eif4g1	S	1185	1	RTPATKRSFSKEVEE		0.3592
A0A0G2JY73	Eif4g3	S	322	1	PEPPRTSSPTTLPPL		0.4022
A0A0G2JY73	Eif4g3	S	526	1	QDKAEAESDGQTEET	0.1311	0.4639
D3ZZ44	Elfn1	S	650	1	SSSGSARSPRTFRAE		1.3782
D3ZH36	Elfn2	S	619	1	HPLQRQLSADAAVTR	0.258	0.5523
D3ZH36	Elfn2	S	747	1	DSTYSQLSPRHYYSG		0.5929
D3ZH36	Elfn2	S	757	2	HYYSGYSSSPEYSSE	-0.2092	0.6845
D3ZH36	Elfn2	S	758	1	YYSGYSSSPEYSSES		0.7351
D3ZH36	Elfn2	S	758	2	YYSGYSSSPEYSSES	-0.2092	0.6845
D4A4R1	Eml3	S	156	1	SDTPRRNSSSSSSPS	-0.0615	0.596
Q5XHX3	Enah	S	430	1	TEQKEDRSEDAEPVT		0.5454
P04764	Eno1	S	419	1	RIEEELGSKAKFAGR	0.2513	-0.3777
D3ZIP3	Epb41	T	60	1	LKASNGDTPTHEDLT		0.9663
D3ZIP3	Epb41	T	62	1	ASNGDTPTHEDLTKN		0.5724
D3ZIP3	Epb41	S	675	1	EIKKHHASISELKKN		0.5452
A0A0G2K0F3	Epb41l1	T	488	1	ELKPEQETTPRHKQE	0.0457	1.3429
A0A0G2K0F3	Epb41l1	T	489	1	LKPEQETTPRHKQEF	0.1911	1.3175
A0A0G2K0F3	Epb41l1	S	544	2	RLPSSPASPSPKGTP	-0.2134	0.4522
A0A0G2K0F3	Epb41l1	S	546	1	PSSPASPSPKGTPEK		0.3303
A0A0G2K0F3	Epb41l1	S	546	2	PSSPASPSPKGTPEK	-0.0964	0.7109
A0A0G2K0F3	Epb41l1	T	550	1	ASPSPKGTPEKASEA		0.3186
A0A0G2K0F3	Epb41l1	T	550	2	ASPSPKGTPEKASEA	0.0431	0.7691
A0A0G2K0F3	Epb41l1	S	915	1	WMGKTEKSPPARRKK		0.5032
A0A0G2K0F3	Epb41l1	S	1223	1	GGRLRFASPPGPQRA		0.5394

Q9WTP0	Epb41l1	S	544	2	RLPSSPASPSPKGTP	-0.2106	0.42
Q9WTP0	Epb41l1	S	546	1	PSSPASPSPKGTPEK		0.3303
Q9WTP0	Epb41l1	S	546	2	PSSPASPSPKGTPEK	-0.0939	0.7109
Q9WTP0	Epb41l1	T	550	1	ASPSPKGTPEKASER		0.3186
Q9WTP0	Epb41l1	T	550	2	ASPSPKGTPEKASER	0.0413	0.6506
G3V874	Epb41l3	Y	82	2	AAAKQLEYQQFEDDK	-0.2417	0.5565
G3V874	Epb41l3	S	91	1	QFEDDKLSQKSSSSK	0.1	0.9216
G3V874	Epb41l3	S	91	2	QFEDDKLSQKSSSSK	-0.2808	0.4869
G3V874	Epb41l3	S	94	2	DDKLSQKSSSSKLSR	-0.2804	0.4771
G3V874	Epb41l3	S	508	1	RHEGKTDSERTDTAA		0.6801
G3V874	Epb41l3	S	578	1	WEKRLSTSPVRLAAR	0.0255	0.8575
A0A0G2JW20	Epb41l4a	S	217	1	KKAKNENSPDPQRSK	0.0184	0.6067
A0A0G2JW20	Epb41l4a	S	356	1	RSRHRSRSRSPDIQA	0.0146	0.6173
A0A0G2JW20	Epb41l4a	S	358	1	RHRSRSRSPDIQAKE	0.0064	0.5379
A0A0G2K3H4	Epb41l4b	S	569	1	SPKIQQVSSPQKSEV	0.037	0.5616
A0A0G2K3H4	Epb41l4b	S	570	1	PKIQQVSSPQKSEVK	0.0087	0.8881
A0A0G2K3H4	Epb41l4b	S	578	1	PQKSEVKSPLSPGAK	0.1702	0.8089
A0A0G2K3H4	Epb41l4b	S	581	1	SEVKSPLSPGAKSPS		0.9305
D3ZZK3	Epha4	S	887	1	KLIRNPNSLKRTGPE		-0.3347
M0R9T2	Erbin	S	377	1	AETNAGNSPVTTNRK	-0.1844	0.9043
D3ZJ32	Esyt2	S	667	1	SSSSLLASPSHIAAK		0.7415
M0R5H1	Etl4	S	187	1	RGSRTRASLPVVRST		-0.3747
M0R5H1	Etl4	S	1856	1	SIASTPLSPQAGRSV	-0.1866	0.3155
M0R5H1	Etl4	S	1881	1	NGSFKFQSPPHAGKG	-0.0731	0.8613
M0R5H1	Etl4	S	1917	1	SSPPSPASPTSLNQG		0.2887
O08719	Evl	S	249	1	PEDASGGSSPSGTSK	-0.0859	0.2846
O08719	Evl	S	250	1	EDASGGSSPSGTSKS	-0.0266	0.3064
Q924K2	Faf1	T	268	1	RLTVGRRTSPVQTRE	0.1308	-0.2732
Q924K2	Faf1	S	269	1	LTVGRRTSPVQTREQ	0.1306	-0.2893
O88407	Faim2	S	7	1	_MTQGKLSVANKAPG		-0.4446
O88407	Faim2	S	37	2	AVPSAPPSYEEATSG		-0.3195
F1M8D5	Fam117b	S	160	1	PGGADKGSNNSSRSQ		0.5954
Q4V7D4	Fam126b	S	294	1	PFDAPDSSQEGQKVL		-0.2878
Q4V7D4	Fam126b	S	398	1	SAIKSNESPRDSVVG	-0.1683	0.2772
F1LUC1	Fam13c	S	562	1	FFKQTGRSPQKEDRM		0.7413
D4A7Y4	Fam171a1	S	793	1	LEGSGRRSGGQLPSL		0.3411
D4AAI7	Fam219a	S	55	1	LKNSSMGSPVNQQPK		0.5469
F1LYQ8	Farp1	S	427	1	LEPGPRQSPALSKSP	0.044	1.0366
P12785	Fasn	S	2191	1	EMSSKAGSDTELAAP	0.1277	-0.2873
D3Z858	Fbrsl1	S	372	1	TRVKENHSPSKEDGA	0.269	0.9251
A0A0G2K9A9	Fbxo41	S	391	1	YAVSRHGSSPSTGAS		0.4889
A0A0G2K9A9	Fbxo41	S	392	1	AVSRHGSSPSTGASS	0.0042	0.6014
A0A0G2K9A9	Fbxo41	S	522	1	SARPEGGSGRGRRME	0.2361	0.9419
A0A0G2K9A9	Fbxo41	S	532	1	GRRMERGSPSRSNEV		0.3033

A0A0G2K7L6	Fgd6	S	382	1	ALTRESNSDRQDSVS		0.3998
A0A0G2K7L6	Fgd6	S	387	1	SNSDRQDSVSSQKAV		0.3571
Q8R5L7	Fgf14	S	210	1	VAMYREPSLHDVGET	0.2267	-0.2903
P84817	Fis1	S	29	1	QSEQAAGSVSKSTQF		-0.2643
Q5U2R3	Frmd8	S	24	2	SHRSSVSSVGARAAD		0.3918
A0A0G2JZZ5	Frs2	S	374	1	VWEARKLSRDEDDNL	-3.00E-04	0.2811
P85845	Fscn1	S	38	1	FKVNASASSLKKKQI		-0.3438
P85845	Fscn1	S	39	1	KVNASASSLKKKQIW	0.1778	-0.419
P19132	Fth1	S	5	1	___MTTASPSQVRQN	0.1511	-0.3871
Q6AY21	G3bp2	S	225	1	LEELEEKSATPPPTE		0.4768
Q6AY21	G3bp2	T	227	1	ELEEKSATPPPTEPA	0.2216	0.6916
A0A0G2JZD5	Gab1	S	445	1	FPSDRSSSLEGFHNQ		0.383
Q9EQH1	Gab2	S	220	1	SQGTRQKSDTAVQKL		0.2723
O88871	Gabbr2	T	762	1	QNRRFQFTQNQKKED	0.9433	-0.3868
P07936	Gap43	T	36	2	DKAHKAATKIQASFR	2.1757	-0.4287
P07936	Gap43	S	41	2	AATKIQASFRGHITR	2.1757	-0.4137
P07936	Gap43	S	110	1	SKAGDAPSEEKKGEG	0.4297	-0.3087
P07936	Gap43	T	131	1	EKAGSAETESAAKAT	0.4235	-0.2704
F1M8X9	Gbf1	S	1786	1	ASSSSPGSPVASSPS		0.3083
Q9JKB7	Gda	S	196	1	KETERFVSEMLQKNY		0.2762
P08050	Gja1	S	328	1	GQAGSTISNSHAQPF	-0.4974	0.3542
P08050	Gja1	S	328	2	GQAGSTISNSHAQPF	-0.339	0.094
P08050	Gja1	S	330	1	AGSTISNSHAQPFDF		0.3293
Q80XF7	Gjc2	S	428	2	RVGSEKGSTGSRDGK	-0.0714	0.4472
Q80XF7	Gjc2	S	431	2	SEKGSTGSRDGKATV	-0.0422	0.4448
G3V8D7	Gjd4	T	355	1	GSAPHLRTKKSEWV_		0.3407
D4ADD7	Glrx5	S	151	1	IDEKDQDSK_____	0.1474	-0.288
P10860	Glud1	Y	193	1	VKINPKNYTDNELEK		-0.3432
P10860	Glud1	T	194	1	KINPKNYTDNELEKI		-0.3695
P10860	Glud1	S	450	1	LKNLNHVSYGRLTFK	0.1651	-0.4203
P10860	Glud1	Y	451	1	KNLNHVSYGRLTFKY	0.2511	-0.3656
A0A0G2JX25	Gmpr2	S	26	1	PKRSTLKSRSEVDLT		-0.2783
P54311	Gnb1	S	136	1	REGNVRVSRELAGHT	0.2705	-0.2875
P00507	Got2	S	306	1	EEAKRVESQLKILIR		-0.3027
Q03555	Gphn	T	278	2	RDTASLSTTPSESPR	-0.1013	0.6838
Q03555	Gphn	T	279	1	DTASLSTTPSESPRA		0.2748
Q03555	Gphn	T	279	2	DTASLSTTPSESPRA	-0.2092	0.4356
Q03555	Gphn	S	281	2	ASLSTTPSESPRAQA	-0.0856	0.5745
Q03555	Gphn	S	283	1	LSTTPSESPRAQATS	-0.0888	0.4123
Q03555	Gphn	S	283	2	LSTTPSESPRAQATS	-0.0699	0.5778
Q6P6V0	Gpi	S	441	1	EALMKGKSPEEARKE	0.3396	-0.2919
A0A0A0MY13	Gpr158	S	806	1	TGRPKEESLKNRVFS	1.0942	-0.3173
A0A0A0MY13	Gpr158	S	1042	1	EVEQNPASFSKEKSH		0.3678
D4AAS1	Gpr162	S	255	1	DTRGKRRSSLDGSES	0.2924	-0.3003

D4AAS1	Gpr162	S	256	1	TRGKRRSSLDGSESA	0.364	-0.2815
Q920R4	Gprasp1	S	345	1	YSDVTSGSVDKNKKD	0.2876	0.3185
Q3KRC4	Gprc5c	S	434	1	GKISQDQSPKNKTRW		0.3891
D3ZF21	Gprin3	S	209	1	RAVRIHSSPSADRPE	-0.0075	0.6179
D3ZF21	Gprin3	S	211	1	VRIHSSPSADRPEGE		1.007
A0A0G2JT06	Gps1	S	275	1	EQRGERDSQTQAILT		-0.2637
Q3KR56	Gramd1a	S	11	1	TTPHSGRSSPSSSPS	0.0398	0.3074
Q3KR56	Gramd1a	S	12	1	TPHSGRSSPSSSPSL		0.3596
D3ZYJ5	Gramd1b	S	174	1	ILRKRSRSPTPQNQD		0.4235
D3ZYJ5	Gramd1b	S	194	1	EKGSDHSSDKSPSTP		0.5058
D3ZYJ5	Gramd1b	T	200	1	SSDKSPSTPEQGVQR	0.0652	0.4058
P0CE43	Grb10	S	50	1	SRGQPQASPRQKMQR	-0.1969	0.5651
Q63226	Grid2	S	861	1	WWSRRKGSRVPSKED		-0.453
Q63226	Grid2	S	865	1	RKGSRVPSKEDDKEI	0.1362	-0.3414
P35439	Grin1	S	897	1	SFKRRRSSKDTSTGG	0.3389	0.5485
Q00959	Grin2a	S	1025	1	MESLRQDSLNQNPVS	0.0237	0.9425
Q00959	Grin2a	S	1198	1	FTLKDKGSPHSEGSD	0.1332	1.1745
Q00959	Grin2a	S	1198	2	FTLKDKGSPHSEGSD	-0.0944	1.3655
Q00959	Grin2a	S	1201	1	KDKGSPHSEGSDRYR	0.285	1.2557
Q00959	Grin2a	S	1201	2	KDKGSPHSEGSDRYR	-0.0351	1.3571
Q00959	Grin2a	S	1204	1	GSPHSEGSDRYRQNS	-0.041	0.4678
Q00959	Grin2a	S	1204	2	GSPHSEGSDRYRQNS	-0.1383	1.3708
Q00959	Grin2a	S	1291	1	LRINRQHSYDNILDK	0.167	0.5227
Q00960	Grin2b	S	1058	2	GHDDLIRSDVSDIST	-0.1746	0.4664
Q00960	Grin2b	S	1061	2	DLIRSDVSDISTHTV	-0.2037	0.4795
Q00960	Grin2b	T	1067	2	VSDISTHTVTYGNIE	-0.2198	0.4625
Q00960	Grin2b	S	1255	2	AGNLYDISEDNSLQE	-0.0801	0.4668
Q00960	Grin2b	S	1259	1	YDISEDNSLQELDQP	-0.0223	0.4291
Q00960	Grin2b	S	1259	2	YDISEDNSLQELDQP	-0.0801	0.4668
Q00960	Grin2b	S	1284	1	SSTKYPQSPTNSKAQ	0.1661	0.3254
P97879	Grip1	S	660	1	IRKDEDNSDEQESSG	0.0218	-0.292
P23385	Grm1	S	973	2	AHFSPPSSPSMVVHR	-0.0922	0.2988
A0A0H2UHW6	Grm5	S	773	1	PAAARPRSPSPISTL		0.85
A0A0H2UHW6	Grm5	S	773	2	PAAARPRSPSPISTL	-0.1019	0.3406
A0A0H2UHW6	Grm5	S	775	1	AARPRSPSPISTLSH	-0.1317	0.8925
A0A0H2UHW6	Grm5	S	778	2	PRSPSPISTLSHLAG	-0.0557	0.4347
A0A0G2JY75	Gtf3c2	S	263	1	PKSPKVSSPTKPKKT		0.652
Q9WVI4	Gucy1a2	S	41	1	LCWNGSRSPPGPPGS	0.077	0.3243
A2RRU1	Gys1	S	698	1	PEWPRRASCSSSTGG		0.645
F1LSH6	Hcn1	T	39	1	AADKRLGTPPGGGAA	0.1947	-0.3718
F1LSH6	Hcn1	S	783	1	PKNEVHKSTQALHNT	-0.4338	0.4701
Q9JKA9	Hcn2	S	834	1	TTRTAAPSPDRRDSA	-0.238	0.3377
D3ZLS5	Hectd1	S	632	1	SALAGPSSDDENEEE		-0.3952
D3ZLS5	Hectd1	S	1571	1	MNLSRSSSDNNTNTL		0.3521

D4ADZ6	Helz	S	1127	1	NSSRQQQSPPKVKSL		0.6081
A0A0G2JTT6	Herc1	S	2718	1	DEVGRRQSLTSPDSQ	0.0721	0.2862
P05708	Hk1	S	337	1	TRGKFNTSDVSAIEK		-0.3745
P17425	Hmgcs1	S	495	2	TATEHIPSPAKKVPR		0.2645
Q66H40	Hmgn3	S	6	1	__MPKRKSPENAEGK	-0.9825	1.3039
P04256	Hnrnpa1	S	2	2	_____MSKSESPKE		-0.3931
P04256	Hnrnpa1	S	6	2	__MSKSESPKEPEQL		-0.449
Q9QX80	Hnrnpab	S	260	1	RNRGNRGSGGGQGST		0.8605
Q8VHV7	Hnrnph1	S	104	1	LKHTGPNSPDTANDG	0.0688	-0.2817
D4ABT8	Hnrnpul2	S	183	1	EQGDDQDSEKSKPAG		1.0485
D4ABT8	Hnrnpul2	S	191	1	EKSKPAGSDGERRGV		0.8338
Q6P747	Hp1bp3	T	51	1	AVNSTRETPPKSKLA		0.6863
P84076	Hpca	S	175	1	EFIRGAKSDPSIVRL	0.2369	-0.2748
G3V8S6	Hrc	S	549	1	RKEDDHSSQEGDEDL	0.147	-0.2956
D4A6D9	Hs1bp3	S	294	1	ESRGPTSSPEHRDAS	-0.0875	0.5874
P34058	Hsp90ab1	S	255	1	PKIEDVGSDEEDDSG	0.1514	-0.4052
P34058	Hsp90ab1	S	261	1	GSDEEDDSGKDKKKK		-0.4754
O88600	Hspa4	S	692	1	IKTRFQESEERPKLF		-0.5763
P63018	Hspa8	S	511	1	TNDKGRLSKEDIERM		-0.3821
P63039	Hspd1	S	232	1	SPYFINTSKGQKCEF		-0.3565
Q66HA8	Hsph1	S	429	1	RNHAAPFSKVLTFLR		-0.3226
Q99NA5	Idh3a	S	193	1	YARNNHRSNVTAVHK	0.2602	-0.3128
F1LY69	Ift140	S	357	1	MWKKVPVSPSGRGAE		-0.2754
D3ZB51	Igsf9b	S	797	1	LRAPSESSDDQGQPA	0.1015	0.3699
D3ZB51	Igsf9b	S	1202	2	VLQPSRLSPLTQSPL	0.0648	0.332
D3ZB51	Igsf9b	S	1207	2	RLSPLTQSPLSSRTG		0.4713
D3ZB51	Igsf9b	S	1258	1	STPSSTGSPSQSSRS	-0.061	0.7262
D3ZB51	Igsf9b	S	1258	2	STPSSTGSPSQSSRS		0.4697
D4A4I9	Il16	S	680	2	GEPRRSASPETPASP		0.6474
D4A4I9	Il16	S	686	2	ASPETPASPGKHPLL	-0.0514	0.5868
Q63257	Il4r	S	335	1	AKTKPLQSPEKAGWY		-0.271
D3ZGJ1	Ildr2	S	560	1	ESNSRGGSLETPSKL	0.1167	1.0006
D3ZGJ1	Ildr2	T	563	1	SRGGSLETPSKLGAQ		1.1005
Q3KR86	Immt	S	34	1	LRPCRRYSTSSSSGV		-0.3302
Q3KR86	Immt	S	106	1	LPKKPIQSGPLKISS		-0.335
Q3KR86	Immt	S	302	1	KKVQAAQSEAKVVSQ		-0.2907
Q5BJY3	Ino80c	S	26	1	NSKKRPASPSHNSSG		0.9074
D3ZKG7	Inpp5f	S	667	1	VSQYQRRSLEDLEKI		-0.3991
Q9JMC1	Inpp5j	S	689	1	KAPSGGPSPSGRESH	-0.0672	-0.2751
D4A4J1	Insyn2	T	107	1	TKSTGVQTSPDLRKC		0.4678
D4A4J1	Insyn2	S	108	1	KSTGVQTSPDLRKCY	0.0482	0.4209
M0R8E8	Ipo11	S	343	1	SKNFEDSSPETLEAH		-0.3202
A0A0G2JUG7	Iqsec1	S	89	1	PRLQHSTSVLRKQAE	0.4161	0.3166
A0A0G2JUG7	Iqsec1	S	399	1	SDRSDRSSLKRQSAY		0.3813

A0A0G2JUG7	Iqsec1	S	416	1	SLGGQQGSPKHGPHG	-0.1883	0.9406
A0A0G2JZX5	Iqsec2	S	918	1	VNGTLARSSLEDTYG	0.1769	0.4169
A0A0G2JZX5	Iqsec2	S	919	1	NGTLARSSLEDTYGA	0.1833	0.4008
Q76M68	Iqsec3	S	131	1	SRVQTPQSPHQHPVA	-0.1201	0.9334
Q76M68	Iqsec3	S	255	1	ERPGAVGSPRAGPLR	0.125	0.5617
Q76M68	Iqsec3	S	1053	1	RLQTFQHSPKLGVER	0.0657	0.7027
D4AAZ8	Irf2bp1	S	384	1	TPRRRKASPEPEGET	0.057	0.7495
D4AAZ8	Irf2bp1	S	436	1	VAEALGHSPKDPGGG		0.2974
Q5EIC4	Irf2bpl	S	534	1	SLRKRKASPEPPDSA		0.6097
P35570	Irs1	S	1077	1	AFTRVNLSPNHNQSA	-0.3393	0.4759
F1MAL5	Irs2	S	1092	1	PEGARVTSPTSGLKR		0.6348
M0R7A6	Itsn2	S	231	1	TASLSGNSPKTGTSE		0.7424
Q6AXU6	JPT1	S	14	1	FKGVDPNSRNSSRVL		0.6165
Q3SWS9	Jakmip1	S	382	1	ASLKRHTSLNDLSLT		-0.2803
F1M065	Jam2	S	236	1	ETSFQKGSPASKATT		-0.2638
D3ZQ55	Jph1	S	475	1	ASPKQSHSPQPSSPK		0.5756
D3ZQ55	Jph1	S	475	2	ASPKQSHSPQPSSPK	0.0904	0.5755
D3ZQ55	Jph1	S	479	2	QSHSPQPSSPKSMKK	0.0892	0.6189
D3ZQ55	Jph1	S	480	2	SHSPQPSSPKSMKKQ	0.0897	0.5649
Q69FB3	Jph4	S	238	1	RAGGRRSSLGSKRGS		0.5123
Q5FWS6	Kazn	S	344	1	STPSDINSPRHRTHS		0.7647
P63142	Kcna2	S	440	1	TSCPKIPSSPDLKKS	0.3699	-0.3181
P63142	Kcna2	S	441	1	SCPKIPSSPDLKKSR	0.3712	-0.3235
P63142	Kcna2	S	447	1	SSPDLKKSRSASTIS		-0.3806
P63142	Kcna2	S	449	1	PDLKKSRSASTISKS	0.1878	-0.3146
P63142	Kcna2	S	449	2	PDLKKSRSASTISKS		-0.3699
P15385	Kcna4	S	82	1	DPQGSRGSREEEATR	0.5451	0.271
P62483	Kcnab2	S	9	1	YPESTTGSPARLSLR	0.086	0.8231
P15387	Kcnb1	S	511	1	FETKEQGSPEKARSS	0.2656	0.6487
P15387	Kcnb1	S	520	1	EKARSSSSPQHLNVQ	-0.1684	0.8552
P15387	Kcnb1	T	732	1	YTTASARTPPRSPEK	0.1278	1.9096
P15387	Kcnb1	T	781	1	PKSLHGSTSPKFSTG	0.2328	1.3851
P15387	Kcnb1	T	803	1	FESSPLPTSPKFLRP		0.8207
P15387	Kcnb1	S	804	1	ESSPLPTSPKFLRPN	0.1213	0.6368
Q63099	Kcnb2	S	520	2	QEVSQKDSHEQLNNT		0.4021
Q63099	Kcnb2	T	725	1	NRGSAPQTPPSTARP	0.2071	0.715
Q63881	Kcnd2	T	154	1	RLQDDADTDNTGESA		-0.2845
Q63881	Kcnd2	T	567	2	QIRCVERTPLSNSRS	-0.2318	0.7884
Q63881	Kcnd2	S	572	1	ERTPLSNSRSSLNAK	0.16	0.3646
Q63881	Kcnd2	S	572	2	ERTPLSNSRSSLNAK	-0.1508	0.6743
Q63881	Kcnd2	S	574	2	TPLSNSRSSLNAKME	-0.1693	0.6477
Q63881	Kcnd2	S	575	2	PLSNSRSSLNAKMEE	-0.2245	0.6417
Q9JIS4	Kcnk10	S	412	1	TGRFKASSQESINNR		0.3617
F1LNC7	Kcnma1	S	1199	1	SRASLSHSSHSSQSS	-0.5141	0.3786

F1LNC7	Kcnma1	S	1199	2	SRASLSHSSHSSQSS	-0.921	
O88943	Kcnq2	S	439	1	VAAKGKGSPQAQTVR		0.445
O88943	Kcnq2	S	454	2	RSPSADQSLDDSPSK	-0.0646	0.3127
D3ZNX0	Kctd3	S	713	1	CAVCERKSPGTEGRC		0.4171
Q99PF5	Khsrp	S	481	1	KLFVIRGSPQQIDHA	0.0546	0.6391
D4A0X3	Kiaa1107	S	340	1	TQGSQGESPHSVKSS	0.2092	0.7452
D4A0X3	Kiaa1107	S	696	1	HQRESPESDTGSATT		0.3869
D4A0X3	Kiaa1107	S	748	1	DFLGRSSSDTSTPEE		0.2633
Q9EQG6	Kidins220	S	1586	1	GVRSNESSPNHSLHN	-0.103	1.0013
O35787	Kif1c	S	1086	1	PRMRRQRSAPDLKES		0.3114
D3ZCG2	Kif21a	S	1217	1	GSISRQPSVSEKKVP	1.0174	0.1144
D3ZCG2	Kif21a	S	1217	2	GSISRQPSVSEKKVP	0.3082	0.4612
Q9WV63	Kif2a	S	139	1	NGSVSDISPVQAAKK	-0.2295	0.2709
A0A0G2JTL4	Kit	S	588	1	EFPRNRLSFGKTLGA		-0.4256
P37285	Klc1	S	162	1	KKYDDDISPSEDKDS	0.313	-0.3568
B2GV74	Klc2	S	589	1	SLNFLNKSVEEPVQP	0.2886	0.2706
B2GV74	Klc2	S	589	2	SLNFLNKSVEEPVQP	0.7237	0.1032
D4A8Q2	Kndc1	S	843	1	KAAASPSSPRGPDGH	0.3051	0.5996
Q56R18	Kpna3	S	60	1	QEESLEDSDVDADFK	0.0986	-0.4449
Q56R16	Kpna5	S	3	1	_____MASPGKDNYR	-0.0323	0.8306
F1LXC7	LOC100362814	S	763	1	RDTAQDGSTIKTAKS	0.0495	0.4493
F1LXC7	LOC100362814	S	1145	1	AVASLRRSTSDIGSK	-0.1365	0.688
F1LXC7	LOC100362814	S	1147	1	ASLRRSTSDIGSKTR	0.0845	0.5212
F1LXC7	LOC100362814	S	1151	1	RSTSDIGSKTRMAES		0.5637
F1LXC7	LOC100362814	S	1263	1	RSRYQQSSPSRLPRQ	0.0903	0.9548
A0A0G2K5L2	LOC100911440	S	95	1	DFFRHQLSKDGQKLT	0.126	-0.3088
D3ZF45	Larp4b	S	718	1	RQPGRRPSPPAAGKR	0.0927	0.8565
D3ZF45	Larp4b	T	732	2	RLNREQNTPPKSP__		1.0525
D3ZF45	Larp4b	S	736	1	EQNTPPKSP_____	0.0411	0.6187
D3ZF45	Larp4b	S	736	2	EQNTPPKSP_____		1.0525
Q99MZ8	Lasp1	S	129	1	YHEEFEKSRMGPSGG	0.1749	-0.2813
E9PTQ0	Ldb2	S	263	1	KRRKRKNSTSSTSNS		1.2455
Q641X2	Leo1	S	642	1	LKAKKLNSDEEGESS	0.2473	0.8283
F1M392	Limch1	S	231	1	GSSDGRGSDSESDLP	-0.0853	0.4377
F1M392	Limch1	T	255	1	DDMSARRTSHGEPKS	0.3128	0.3917
F1M392	Limch1	S	256	1	DMSARRTSHGEPKSA	0.3126	0.4513
F1M392	Limch1	S	523	1	SVAAGTGSPSKTSTP	-3.00E-04	0.3024
F1M392	Limch1	S	603	1	GVATVHGSPVQVKQG		0.5205
P48679	Lmna	T	27	2	PLSPTRITRLQEKED		0.4232
P48679	Lmna	S	407	1	GRASSHSSQSQGGGS		0.8217
P48679	Lmna	S	414	1	SQSQGGGSVTKKRKL		0.4709
A0A0G2K8R3	Lmo7	S	439	1	ITRRKNFSPTPGYRA	0.1371	0.8794
A0A0G2K8R3	Lmo7	S	699	1	KWKDRRKSYTSDLQK	0.1008	1.2291
A0A0G2K8R3	Lmo7	T	1075	1	MRISINQTPGTKHDF		-0.5247

A0A0G2K8R3	Lmo7	S	1231	1	SQFFEQGSSDSVAPD		0.3283
A0A0G2K8R3	Lmo7	S	1632	1	SVKTSPGSPSPRSHS		0.8009
A0A0G2K8R3	Lmo7	S	1639	1	SPSPRSHSPSMSQSG	0.1053	0.7284
A0A0G2K8R3	Lmo7	S	1641	1	SPRSHSPSMSQSGSQ	0.0749	0.2933
A0A0G2K0D3	Lmod1	S	119	1	ALGPRQDSDVGKEPK	0.5695	0.5925
D3ZBH5	Lmtk2	S	756	1	ASPLTEGSPNGPPDS	-0.0234	0.574
A0JN29	Lnpk	S	177	1	TAAQRNLSPAPANSN		0.3444
P0C7J6	Lrfn1	S	576	1	RIKGTSRSPPRVSHV	0.146	-0.3239
P0CC10	Lrrc4b	T	707	1	SKENVQETQI____		0.5626
D3ZXT1	Lrrc4c	S	631	1	PLLIRMNSKDNVQET		0.9182
P70587	Lrrc7	T	848	1	PWQNWTRTPSPFEDR		1.5626
P70587	Lrrc7	S	850	1	QNWTRTPSPFEDRTA	0.0995	1.1023
P70587	Lrrc7	T	864	2	AFPSKLETTPTTSPL		0.9157
P70587	Lrrc7	T	865	2	FPSKLETTPTTSPLP	-0.1933	1.5365
P70587	Lrrc7	T	868	2	KLETTPTTSPLPERK	-0.1452	1.4506
P70587	Lrrc7	S	869	1	LETTPTTSPLPERKD		0.927
P70587	Lrrc7	S	869	2	LETTPTTSPLPERKD	-0.284	1.3311
P70587	Lrrc7	S	933	1	SKSTERLSPLMKDIK		0.8728
P70587	Lrrc7	S	947	2	KSNKFKKSQSIDEID	0.0292	0.6428
P70587	Lrrc7	S	949	2	NKFKKSQSIDEIDVG	0.0761	0.9449
P70587	Lrrc7	T	957	2	IDEIDVGTYKVYNIP	0.0617	0.9874
P70587	Lrrc7	S	977	1	SGSDHLGSHERPDKF	0.1289	0.5473
P70587	Lrrc7	S	1343	1	SQSLQHRSREQQPYE	0.1097	0.6686
Q32Q07	Lrrn1	S	664	1	KRKNYHHSLKKYMQK		-0.3904
B0BNI4	Lsm11	S	15	1	ARSARAGSPASPPSP	0.0866	0.3378
B0BNI4	Lsm11	S	21	1	GSPASPPSPRLDVSS	-0.0346	0.414
B2GV58	Lsm14a	S	182	1	PQLAQGRSSPQLDPL	0.1115	0.5272
B2GV58	Lsm14a	S	183	1	QLAQGRSSPQLDPLR	0.1884	0.6929
B2GV58	Lsm14a	S	183	2	QLAQGRSSPQLDPLR		0.6043
B2GV58	Lsm14a	S	192	2	QLDPLRKSPTMEQAV		0.4288
B2GV58	Lsm14a	T	194	2	DPLRKSPTMEQAVQT		0.6008
B2GV58	Lsm14a	S	216	1	PAPVGRRSPVPARPL	-0.1682	0.7171
Q4QQV6	Lsp1	S	196	1	KLADRTESLNRSIQK		-0.3265
Q9ESV1	Luzp1	S	395	1	KHTSREQSPQHKRER	0.1089	1.2286
Q9ESV1	Luzp1	S	660	1	SGREKPDSDDDLDIE	0.1913	1.0994
Q8CFC9	Lzts1	S	141	1	SGAILHSSPESTNHQ		0.643
G3V8V8	Lzts3	T	678	1	GAAGGSSTPTPQHGE		1.0682
Q4V7D3	Maco1	S	331	1	NASGVVNSSPRSHSA		0.2946
Q4V7D3	Maco1	S	332	1	ASGVVNSSPRSHSAT		0.5973
Q5PPP4	Mageh1	S	31	1	KIQASEASKTPMAAS		-0.449
P34926	Map1a	S	319	1	KIKHRADSKESLKAA	0.2086	0.8289
P34926	Map1a	S	319	2	KIKHRADSKESLKAA	0.0041	0.8811
P34926	Map1a	S	322	1	HRADSKESLKAAPKT	0.1299	2.0976
P34926	Map1a	S	322	2	HRADSKESLKAAPKT	0.0041	0.8811

P34926	Map1a	S	384	1	SERVRGESSEALKAE		0.2635
P34926	Map1a	S	500	2	RGEKELSSEPRTPPA	0.065	1.1628
P34926	Map1a	T	504	1	ELSSEPRTPPAQKGA	0.14	1.227
P34926	Map1a	T	504	2	ELSSEPRTPPAQKGA	0.0544	1.1268
P34926	Map1a	S	526	1	GHRELALSSPEDLTQ	0.3737	0.5571
P34926	Map1a	S	526	2	GHRELALSSPEDLTQ	-0.0882	0.3851
P34926	Map1a	S	527	2	HRELALSSPEDLTQD	-0.0921	0.362
P34926	Map1a	T	532	2	LSSPEDLTQDFEELK	-0.0595	0.3736
P34926	Map1a	S	690	1	TQEALKASPKSREAL	-0.1029	1.0668
P34926	Map1a	S	889	2	QGLDYVPSAGTISPT	-0.0988	0.4177
P34926	Map1a	T	892	2	DYVPSAGTISPTSSL	-0.1153	0.3766
P34926	Map1a	S	897	2	AGTISPTSSLEEDKG	-0.1597	0.4076
P34926	Map1a	S	990	1	DSTVKMASPPPSGPP	0.0378	0.4339
P34926	Map1a	S	990	2	DSTVKMASPPPSGPP	-0.1144	0.3931
P34926	Map1a	T	1002	2	GPPSAAHTPFHQSPV	-0.0628	0.4515
P34926	Map1a	S	1007	2	AHTPFHQSPVEDKSE	-0.0872	0.3761
P34926	Map1a	S	1037	1	PGVSKEDSEEQTVKP	0.3003	0.309
P34926	Map1a	S	1134	3	RFTDQSLSPEDAESL	-0.24	0.2685
P34926	Map1a	S	1140	3	LSPEDAESLSVLSVV		0.2925
P34926	Map1a	S	1145	2	AESLSVLSVVSPDTT	-0.389	0.4073
P34926	Map1a	S	1148	1	LSVLSVVSPDTTKQE		0.4256
P34926	Map1a	S	1148	2	LSVLSVVSPDTTKQE	-0.2953	0.3864
P34926	Map1a	S	1209	1	SKQLSPESLGTLQFG	0.1079	0.513
P34926	Map1a	S	1280	1	LSVDRKHSPGEITGP		0.7194
P34926	Map1a	T	1285	1	KHSPGEITGPGGHFM	-0.2177	0.7951
P34926	Map1a	S	1594	1	RALGLEESPAEGSKA	0.1575	0.3812
P34926	Map1a	S	1622	1	VQGWRETSPTRGEPV	0.1647	0.7525
P34926	Map1a	S	1757	2	EEDKLTRSPFEIISP	-0.1988	0.7932
P34926	Map1a	S	1757	3	EEDKLTRSPFEIISP	-0.2899	0.1386
P34926	Map1a	S	1763	2	RSPFEIISPPASPPE	-0.1393	0.8352
P34926	Map1a	S	1763	3	RSPFEIISPPASPPE	-0.2899	0.1386
P34926	Map1a	S	1767	2	EIISPPASPPEMTGQ	-0.1422	0.8313
P34926	Map1a	S	1767	3	EIISPPASPPEMTGQ	-0.2899	0.1386
P34926	Map1a	S	1895	1	AGAPDSSSFSPKVPE	0.0428	0.5827
P34926	Map1a	S	1897	1	APDSSSFSPKVPEAG	0.0645	0.6665
P34926	Map1a	S	2588	1	PGRAKPASPARRLDI	0.1624	2.3808
P34926	Map1a	S	2600	1	LDIRGKRSPTPGKGP	0.1672	1.915
P34926	Map1a	S	2620	1	RTVPRPRSTPSQVTS		0.471
P34926	Map1a	S	2635	1	AEEKDGHSPMSKGLV	6.00E-04	1.0045
P34926	Map1a	S	2638	1	KDGHSPMSKGLVNGL		1.684
P15205	Map1b	S	825	1	AERSLMSSPEDLTKD		-0.4105
P15205	Map1b	S	1248	2	ERLSPAKSPSLSPSP	-0.8973	0.5216
P15205	Map1b	S	1250	2	LSPAKSPSLSPSPPS	-0.9995	0.3002
P15205	Map1b	S	1250	3	LSPAKSPSLSPSPPS	-0.3374	0.2418

P15205	Map1b	S	1252	2	PAKSPSLSPSPPSPI	-0.3078	0.7224
P15205	Map1b	S	1252	3	PAKSPSLSPSPPSPI	-0.3683	0.2098
P15205	Map1b	S	1254	1	KSPSLSPSPPSPIEK	0.1402	0.3543
P15205	Map1b	S	1254	2	KSPSLSPSPPSPIEK	-0.3868	0.417
P15205	Map1b	S	1254	3	KSPSLSPSPPSPIEK	-0.3923	0.1987
P15205	Map1b	S	1257	1	SLSPSPPSPIEKTPL	0.1246	0.6239
P15205	Map1b	S	1257	2	SLSPSPPSPIEKTPL	-0.3665	0.5831
P15205	Map1b	S	1257	3	SLSPSPPSPIEKTPL	-0.3613	0.214
P15205	Map1b	S	1315	2	EKTLEVVSPSQSVTG	-0.2821	0.39
P15205	Map1b	S	1317	2	TLEVVSPSQSVTGSA	-0.2542	0.3806
P15205	Map1b	S	1317	3	TLEVVSPSQSVTGSA	-0.1496	0.4017
P15205	Map1b	T	1327	2	VTGSAGHTPYYQSPT	-0.2689	
P15205	Map1b	T	1327	3	VTGSAGHTPYYQSPT	-0.1712	0.3592
P15205	Map1b	S	1332	2	GHTPYYQSPTDEKSS	-0.2688	0.3714
P15205	Map1b	S	1432	2	KNGKQGFSDKESPVS	-0.2866	0.3337
P15205	Map1b	S	1436	2	QGFSDKESPVSDLTS	-0.2845	0.3229
P15205	Map1b	S	1439	2	SDKESPVSDLTSDLY		0.306
P15205	Map1b	S	1765	2	LASEKVQSLEGEKLS	0.9949	0.4504
P15205	Map1b	S	1772	1	SLEGEKLSPKSDISP	-0.0931	0.6115
P15205	Map1b	S	1772	2	SLEGEKLSPKSDISP	0.1044	0.7262
P15205	Map1b	S	1772	3	SLEGEKLSPKSDISP	-0.5095	0.3437
P15205	Map1b	S	1775	2	GEKLSPKSDISPLTP	-0.215	0.5987
P15205	Map1b	S	1775	3	GEKLSPKSDISPLTP	-0.5329	0.2574
P15205	Map1b	S	1778	1	LSPKSDISPLTPRES	0.0537	0.6479
P15205	Map1b	S	1778	3	LSPKSDISPLTPRES	-0.4912	0.2399
P15205	Map1b	T	1781	2	KSDISPLTPRESSPT	-0.3642	0.5559
P15205	Map1b	T	1781	3	KSDISPLTPRESSPT	-0.6129	0.1619
P15205	Map1b	S	1786	1	PLTPRESSPTYSPGF	-0.1252	0.5334
P15205	Map1b	S	1786	2	PLTPRESSPTYSPGF	-0.1729	0.5829
P15205	Map1b	T	1788	1	TPRESSPTYSPGFSD	-0.1108	0.4497
P15205	Map1b	Y	1789	2	PRESSPTYSPGFSDS	-0.1014	0.3249
P15205	Map1b	S	1790	2	RESSPTYSPGFSDST	-0.177	0.5903
P15205	Map1b	S	1811	1	TAAYQTSSSPPIDAA	0.0731	0.4688
P15205	Map1b	S	1848	1	SRDLTTSSVEKDNGG	0.4906	0.4713
P15205	Map1b	S	2249	1	GTKTKSSSPVKKGDG		0.9206
P15205	Map1b	S	2264	1	KSKPSAASPKPGALK		0.391
P0C5W1	Map1s	S	686	1	PPPASPGSSDSSARS		0.2829
F1MAQ5	Map2	S	136	2	ETVNLPPSPPPSPAS	-0.0851	0.7255
F1MAQ5	Map2	S	140	2	LPPSPPPSPASEQTA	-0.0878	0.7252
F1MAQ5	Map2	T	146	2	PSPASEQTAALEEAS	-0.083	0.6827
F1MAQ5	Map2	S	217	2	QDMEGEKSPASPFAQ	-0.2969	0.8906
F1MAQ5	Map2	S	220	1	EGEKSPASPFAQTFG	0.162	1.1851
F1MAQ5	Map2	S	220	2	EGEKSPASPFAQTFG	-0.2982	0.8674
F1MAQ5	Map2	T	225	1	PASPFAQTFGTNLED		1.2368

F1MAQ5	Map2	T	225	2	PASPFAQTFGTNLED	-0.3321	1.0293
F1MAQ5	Map2	S	307	2	WEGKQFDSPMPSPFH	-1.0731	0.5945
F1MAQ5	Map2	S	311	1	QFDSPMPSPFHGGSF		0.5853
F1MAQ5	Map2	S	311	2	QFDSPMPSPFHGGSF	-1.0651	0.5939
F1MAQ5	Map2	S	363	1	SATSKESSKDEEPQK	0.4983	0.3211
F1MAQ5	Map2	S	601	1	SRGNAQESLDTVSPK	0.3645	0.7655
F1MAQ5	Map2	S	601	2	SRGNAQESLDTVSPK	-0.0367	0.6826
F1MAQ5	Map2	T	604	1	NAQESLDTVSPKNQQ	0.2868	1.2891
F1MAQ5	Map2	S	606	1	QESLDTVSPKNQQDE	-0.0553	1.3368
F1MAQ5	Map2	S	606	2	QESLDTVSPKNQQDE	-0.0027	0.6826
F1MAQ5	Map2	S	624	1	LAKASQPSPPAHEAG	-0.0181	0.6916
F1MAQ5	Map2	S	624	2	LAKASQPSPPAHEAG	-0.1217	0.7763
F1MAQ5	Map2	S	652	1	SELPEEPSSPQERMF	-0.0174	0.2919
F1MAQ5	Map2	S	652	2	SELPEEPSSPQERMF	-0.1443	0.8909
F1MAQ5	Map2	S	653	1	ELPEEPSSPQERMFT	0.0112	1.4392
F1MAQ5	Map2	S	653	2	ELPEEPSSPQERMFT	-0.1011	0.6293
F1MAQ5	Map2	S	724	2	FGRGHDLSPLASDIL	-0.2709	0.4337
F1MAQ5	Map2	S	724	3	FGRGHDLSPLASDIL	-0.4564	
F1MAQ5	Map2	T	734	2	ASDILTNTSGSMDEG	-0.069	1.0824
F1MAQ5	Map2	S	735	2	SDILTNTSGSMDEGD	-0.0946	1.3404
F1MAQ5	Map2	S	737	1	ILTNTSGSMDEGDDY		1.3672
F1MAQ5	Map2	S	737	2	ILTNTSGSMDEGDDY	-0.0902	1.3262
F1MAQ5	Map2	Y	744	2	SMDEGDDYLPPTTPA	-0.1351	1.6955
F1MAQ5	Map2	S	821	1	GTRSRLASVSADAEV	0.004	0.5763
F1MAQ5	Map2	S	823	1	RSRLASVSADAEVAR		0.75
F1MAQ5	Map2	S	880	1	KYTVPLPSPVQDSEN		0.5487
F1MAQ5	Map2	S	880	2	KYTVPLPSPVQDSEN	-0.304	
F1MAQ5	Map2	S	885	1	LPSPVQDSENLSGES	-0.0477	0.6378
F1MAQ5	Map2	S	889	1	VQDSENLSGESGSFY		0.4883
F1MAQ5	Map2	S	935	1	FTAEKEASPPSSADK	0.1243	0.6756
F1MAQ5	Map2	S	938	1	EKEASPPSSADKSGL	0.017	0.41
F1MAQ5	Map2	S	1064	1	GQMASGMSVDAGKTI	0.1825	0.2911
F1MAQ5	Map2	S	1158	2	DEGKKETSPETSLIQ	-0.4837	0.6873
F1MAQ5	Map2	T	1161	2	KKETSPETSLIQDEV	-0.5437	0.5186
F1MAQ5	Map2	S	1441	1	KTGRGRISTPERKVA		1.8966
F1MAQ5	Map2	T	1442	1	TGRGRISTPERKVAK		2.2479
F1MAQ5	Map2	S	1482	1	KSEVQAHSPSRKLIL	0.0547	2.5098
F1MAQ5	Map2	S	1484	1	EVQAHSPSRKLILKP		2.9912
F1MAQ5	Map2	T	1534	1	DKVTDGITKSPEKRS	0.2384	1.6831
F1MAQ5	Map2	S	1536	1	VTDGITKSPEKRSSL	0.1977	1.7006
F1MAQ5	Map2	S	1542	1	KSPEKRSSLPRPSSI		0.7764
F1MAQ5	Map2	S	1557	1	LPPRRGVSGDREENS		0.664
F1MAQ5	Map2	T	1603	2	TPGSTAITPGTPPSY	-0.2198	0.6952
F1MAQ5	Map2	T	1606	1	STAITPGTPPSYSSR	0.0578	1.15

F1MAQ5	Map2	T	1647	1	KKVAIIRTPPKSPAT	0.3389	1.8782
F1MAQ5	Map2	T	1647	2	KKVAIIRTPPKSPAT	-0.7688	1.3314
F1MAQ5	Map2	T	1647	3	KKVAIIRTPPKSPAT	-0.4699	1.0471
F1MAQ5	Map2	S	1651	2	IIRTPPKSPATPKQL	-0.7783	1.3275
F1MAQ5	Map2	S	1651	3	IIRTPPKSPATPKQL	-0.4699	1.0471
F1MAQ5	Map2	T	1654	2	TPPKSPATPKQLRLI	-0.6769	1.2807
F1MAQ5	Map2	T	1654	3	TPPKSPATPKQLRLI	-0.4699	1.0471
F1MAQ5	Map2	S	1677	1	NVKSKIGSTDNIKYQ		0.3817
F1MAQ5	Map2	T	1678	1	VKSKIGSTDNIKYQP		0.4194
F1MAQ5	Map2	T	1778	1	DHGAEIITQSPSRSS	0.0979	0.4053
F1MAQ5	Map2	S	1780	1	GAEIITQSPSRSSVA	0.2277	0.5734
F1MAQ5	Map2	S	1788	1	PSRSSVASPRRLSNV	0.1705	1.5676
F7FMK8	Map3k13	S	308	1	SKELSDKSTKMSFAG		-0.3227
A0A0G2JW88	Map4	T	1729	2	GKAAVGLTGNDIATP		1.2225
A0A0G2JW88	Map4	T	1735	2	LTGNDIATPPNKELP	-0.1093	1.1903
A0A0G2JW88	Map4	S	1744	1	PNKELPPSPEKKAKP	0.227	0.6645
A0A0G2JW88	Map4	S	1744	2	PNKELPPSPEKKAKP	-0.1093	1.1984
A0A0G2JW88	Map4	S	1837	1	KVAEKRTSPSKPSSA		1.0699
A0A0G2JW88	Map4	S	1862	1	PTISKATSPSTLVST	0.0812	0.5536
A0A0G2JW88	Map4	S	1875	1	STGSSSRSPSTTLPK	-0.0109	1.8811
A0A0G2JW88	Map4	S	1991	1	SVRSKVGSTENMKHQ		0.2856
A0A0G2K7W4	Map4k4	S	547	1	FRKTNHSSPEAQAKQ	-0.0315	0.6377
A0A0G2K7W4	Map4k4	S	683	1	PVLSRRDSPLQGSGQ	0.3996	0.3338
A0A0G2K7W4	Map4k4	S	745	1	HPGSQSGSGERFRVR	-0.3702	0.4629
Q63560	Map6	S	432	1	PAWMVRRSEGHEQTT	0.1363	0.2711
Q63560	Map6	T	438	1	RSEGHEQTTAAHAQG	0.0938	0.3016
Q63560	Map6	S	681	1	PGSLKGQSPTAPGPP	-0.1066	0.5079
Q63560	Map6	T	683	1	SLKGQSPTAPGPPKD	-0.2227	0.3062
D4A644	Map7d1	S	118	1	SQRSSQPSPTAVPAS	0.0152	0.2799
D4A644	Map7d1	S	512	1	KEPAAPASPAPSPVP		0.3677
D4A4L4	Map7d2	S	293	1	VKPTYIGSPVKYYFP		1.1932
D4A1Q2	Mapt	T	420	2	ATRIPAKTTPSPKTP	-0.3579	0.4128
D4A1Q2	Mapt	T	426	2	KTTPSPKTPPGSGEP	-0.2737	0.2633
D4A1Q2	Mapt	S	440	2	PPKSGERSGYSSPGS	-0.2262	0.3952
D4A1Q2	Mapt	S	443	2	SGERSGYSSPGSPGT	-0.1114	0.4426
D4A1Q2	Mapt	S	444	1	GERSGYSSPGSPGTP	0.029	0.264
D4A1Q2	Mapt	S	444	2	GERSGYSSPGSPGTP	-0.0674	0.3581
D4A1Q2	Mapt	S	447	1	SGYSSPGSPGTPGSR	-0.0458	0.3565
D4A1Q2	Mapt	S	447	2	SGYSSPGSPGTPGSR	-0.0858	0.5366
D4A1Q2	Mapt	T	450	2	SSPGSPGTPGSRSRT	0.0047	0.4525
D4A1Q2	Mapt	T	457	2	TPGSRSRTPSLPTPP	0.0359	0.3317
D4A1Q2	Mapt	T	462	1	SRTPSLPTPPTREPK	0.1999	0.2945
D4A1Q2	Mapt	T	462	2	SRTPSLPTPPTREPK	0.0111	0.3661
D4A1Q2	Mapt	T	476	1	KKVAVVRTPPKSPSA	-0.0793	0.395

D4A1Q2	Mapt	T	476	2	KKVAVVRTPPKSPSA	-0.3485	0.4482
D4A1Q2	Mapt	S	480	1	VVRTPPKSPSASKSR	-0.5137	0.0657
D4A1Q2	Mapt	S	480	2	VVRTPPKSPSASKSR	-0.2851	0.4541
D4A1Q2	Mapt	S	482	2	RTPPKSPSASKSRLQ	-0.3706	0.3437
D4A1Q2	Mapt	S	601	1	RVQSKIGSLDNITHV	1.1247	-0.2846
D4A1Q2	Mapt	S	601	2	RVQSKIGSLDNITHV	1.3087	-0.2154
D4A1Q2	Mapt	T	606	1	IGSLDNITHVPGGGN	1.0863	-0.2846
D4A1Q2	Mapt	T	606	2	IGSLDNITHVPGGGN	1.3874	-0.2011
D4A1Q2	Mapt	S	641	2	GAEIVYKSPVVSGDT	-0.0052	0.3144
D4A1Q2	Mapt	S	641	3	GAEIVYKSPVVSGDT	-0.3495	0.2923
D4A1Q2	Mapt	S	645	1	VYKSPVVSGDTSPRH	0.5949	0.2113
D4A1Q2	Mapt	S	645	3	VYKSPVVSGDTSPRH	-0.3889	0.3061
D4A1Q2	Mapt	S	649	2	PVVSGDTSPRHLSNV	-0.2519	0.3945
D4A1Q2	Mapt	S	649	3	PVVSGDTSPRHLSNV	-0.3556	0.2949
D4A1Q2	Mapt	S	661	1	SNVSSTGSIDMVDSP	1.64	0.2673
D4A1Q2	Mapt	S	661	2	SNVSSTGSIDMVDSP	0.7571	0.3422
D4A1Q2	Mapt	S	667	2	GSIDMVDSPQLATLA	0.7323	0.2892
P30009	Marcks	S	163	1	SFKLSGFSFKKSKKE	1.3679	-0.3377
P30009	Marcks	S	163	2	SFKLSGFSFKKSKKE	1.4437	-0.1571
P30009	Marcks	S	163	3	SFKLSGFSFKKSKKE	2.1628	
P30009	Marcks	S	167	2	SGFSFKKSKKEAGEG	1.0535	-0.4045
Q9EPH2	Marcksl1	S	48	1	TPKGEGESPPVNGAD		-0.271
Q9EPH2	Marcksl1	S	104	1	PFKLSGLSFKRNRKE	1.2165	-0.3161
Q8VHF0	Mark3	S	400	1	LSNSTGQSPHHKGQR	-0.0331	0.4364
A0A0G2JTD8	Mark4	S	413	1	NKGQRTSSSTYHRQR		-0.2683
M0R3L1	Mast4	S	1197	1	SPTPQPTSPQRSPSP		0.4528
P43244	Matr3	S	188	1	KRHFRRDSFDDRGPS		0.3433
B0BN72	Mcrip1	S	21	1	KRNSSPRSPTNSSEI	0.0555	0.3154
P04636	Mdh2	T	235	1	GRIQEAGTEVVKAKA		-0.4713
D4A2R5	Mex3c	S	342	1	MKTQRRGSQPSTPRL		0.334
F1M5V7	Mex3d	S	488	1	NTGTRRSSGGGGAAT	-0.0343	0.2662
Q5XIQ4	Mgrn1	S	429	1	KGKTQSKSPDSTLRS	0.0306	0.4694
D3ZGN7	Mical3	S	685	1	AGKRRKTSQSEEEEP	0.0586	0.4214
D3ZGN7	Mical3	S	1152	1	RGPSQVSSPSQPPQK	-0.1209	0.5963
D3ZGN7	Mical3	S	1165	2	QKQAVLFSPAHSPGA	-0.4619	0.5124
D3ZGN7	Mical3	S	1169	1	VLFSPAHSPGAEEAK		0.5516
D3ZGN7	Mical3	S	1169	2	VLFSPAHSPGAEEAK	-0.4619	0.511
D3ZGN7	Mical3	S	1218	1	EEQKTVHSPIRSQPV	0.149	0.5484
A0A0G2KAE6	Miga2	S	111	1	CSSRRVQSPSSKSND	0.2615	0.7271
A0A0G2KAE6	Miga2	S	113	1	SRRVQSPSSKSNDTL		0.6858
A0A0G2KAE6	Miga2	T	206	1	QRGDGGSTPTPGDSL	-0.0036	0.6699
D3ZJ47	Minar1	S	389	1	SFFNRNPSEEKLRYP		0.7683
Q5BJQ2	Mindy1	S	394	1	SHGAEGGSGSPEKQL		-0.3628
Q5BJQ2	Mindy1	S	396	1	GAEGGSGSPEKQLQV	0.3415	-0.2916

F1LN69	Mink1	S	547	1	RMNKQQNSPLAKTKP	0.1088	1.2738
F1LN69	Mink1	S	793	1	ASTKLDSSPVLSPGN		0.9743
D4ABB2	Mlc1	S	207	1	PCKKKKGSISDGTNI	0.2159	-0.3517
A0A096MK47	Mlip	S	442	1	LSQAQPPSPPALASS		0.4385
A0A096MK47	Mlip	S	719	1	PVEHSSDSPSRPSQT		0.6964
Q63327	Mobp	T	73	1	QKTSRRATSPQKPKH		-0.2735
A0A0G2JUR5	Mprip	S	2091	1	YDIMKSKSNPDFLKK	0.1276	-0.3012
A0A0G2JXC5	Mrtfa	S	681	1	QQPAPASSPVKRESS	-0.3274	0.6281
B0BN30	Mtch1	S	61	1	PRPAAQPSARRMDGG	0.2964	0.5915
D4A5D4	Mtcl1	S	1339	1	GGTTPVSSPSRSLRS	0.0841	1.0308
D3ZYM5	Mtss1	S	329	1	SSGSHSHSPSSHYRY	-0.549	1.0083
A0A0G2K4U7	Mtus2	S	329	1	CREERSTSPVDRKEL		0.8352
D3ZNK1	Mtx3	S	283	1	MDGNLRQSPQLLPRK	0.0797	0.3154
D4A2D3	Mycbp2	S	2701	1	ASSPRSSSPQDKNLP		0.6439
Q62812	Myh9	S	1917	1	AMNREVSSLKNKLRR		-0.3914
Q9Z1N3	Myo9a	S	1898	1	FKENKEPSPKAKRKR		0.2973
F1M6E5	Nacad	S	1159	1	ARQRVSLSPHSANPK		0.7176
Q769K2	Napepld	S	27	1	TLRKRQNSVQNSGGS	0.8793	0.4153
D4A5I4	Nav1	S	1039	1	ISLKSIGSPESTPKN		0.9623
D4A5I4	Nav1	S	1042	1	KSIGSPESTPKNQAS	-0.0036	0.7802
D4A5I4	Nav1	S	1456	1	LRIKRQNSSDSISSL	-0.0292	0.469
A0A0G2K0M8	Ncam1	S	903	1	EAATAPASPKSKAPS	-0.0699	0.2801
D3ZXN9	Ncor2	S	2162	1	HSEGGKRSPEPSKTV	-0.0962	0.8452
D3ZXN9	Ncor2	T	2350	1	GRSDHPLTSPGGGGK		0.6664
D3ZXN9	Ncor2	S	2351	1	RSDHPLTSPGGGGKA		0.8226
Q8VBU2	Ndrg2	S	332	3	LSRSRTASLTSAASI	0.0756	0.2964
D3ZS58	Ndufa2	S	76	1	FGQEKNVSLNNLSAA		-0.3524
D4A0T0	Ndufb10	T	24	1	TPAPSPQTSIPNPIT		-0.2828
B5DEL8	Ndufs5	T	93	1	LMKEGKYTPPPHHLG		-0.306
A0A0G2JXP3	Nedd4l	S	617	1	RNNIFEESYRRIMSV		-0.3238
G3V7S2	Nefm	S	30	1	SFSRVSGSPSSGFRS	0.1381	0.556
G3V7S2	Nefm	S	44	1	SQSWSRGSPSTVSSS	0.0568	0.6427
G3V7S2	Nefm	S	501	2	EEPEVEKSPVKSPEA		-0.5221
G3V7S2	Nefm	S	505	2	VEKSPVKSPEAKEEE		-0.5221
G3V7S2	Nefm	S	665	1	PDKKKAESPVKEKAV	0.2273	-0.3141
P97526	Nf1	S	2169	1	SYRDRSFSPGSYERE		-0.4147
P97526	Nf1	S	2798	1	SGRTRHGSASQVQKQ	-0.0797	0.3417
P97685	Nfasc	S	1226	2	EETEGNESSEATSPV	-0.0705	0.2775
P97685	Nfasc	S	1226	3	EETEGNESSEATSPV	-0.1068	0.4249
P97685	Nfasc	S	1227	3	ETEGNESSEATSPVN	-0.1259	0.3693
P97685	Nfasc	T	1230	3	GNESSEATSPVNAIY	-0.1195	0.4132
P97685	Nfasc	S	1231	3	NESSEATSPVNAIYS	-0.1237	0.4114
O70185	Nfib	T	327	1	EKPLFSSTSPQDSSP		0.8925
Q8K1Q0	Nmt1	S	47	1	SHNRGGLSPANDTGA	-0.2121	0.2725

P41777	Nolc1	S	318	1	KKSVGAQSPKKAAAQ		1.0521
A0A0G2K3Q5	Nrcam	S	1299	2	NESSEAPSPVNAMNS	-0.0648	0.2837
D3ZYH3	Nudt10	S	148	1	EKLKLGGSPTNGNSA		-0.2665
D3ZC82	Nufip2	S	212	1	KGADNDGSGSESGYT	0.0839	0.7277
D3ZC82	Nufip2	S	214	1	ADNDGSGSESGYTTP	0.0796	1.0742
Q5XIG4	Ociad1	T	146	1	SGQSSFGTSPAADNI		0.3055
Q5XIG4	Ociad1	S	198	1	EDSPKRKSVTYEELR	0.0034	0.2695
A0A0G2JXN8	Osbpl8	S	341	1	NDQEHDESDNEVLGK	0.244	-0.7943
A0A0G2JXN8	Osbpl8	S	798	1	KVAKGYSSPEPDVQD		-0.4212
A0A0G2JXN8	Osbpl8	S	806	1	PEPDVQDSSGSEAQS	0.0327	-0.2796
A0A0G2JXN8	Osbpl8	S	807	1	EPDVQDSSGSEAQSV	0.1164	-0.3829
A0A0G2JXN8	Osbpl8	S	809	1	DVQDSSGSEAQSVKP		-0.3937
Q5U2R6	P33monox	S	175	2	KHPASAQSSPSSTPH	-0.0226	0.8477
Q5U2R6	P33monox	S	176	2	HPASAQSSPSSTPHS	-0.0741	0.6252
Q5U2R6	P33monox	S	183	1	SPSSTPHSSPKQKSR	0.0647	0.3823
Q5U2R6	P33monox	S	183	2	SPSSTPHSSPKQKSR	-0.1133	0.5283
Q5U2R6	P33monox	S	184	1	PSSTPHSSPKQKSRG	0.1006	0.3976
Q5U2R6	P33monox	S	184	2	PSSTPHSSPKQKSRG	-0.0992	0.3274
O88588	Pacs1	S	18	1	PGGAGGGSSQRGSGV	0.0965	0.4125
O88588	Pacs1	T	44	1	PSQPQQPTPPKLAQA	0.0415	0.2858
O88588	Pacs1	S	493	1	ADLQGSASPSKVEGT	-0.4489	0.3697
O88588	Pacs1	S	493	2	ADLQGSASPSKVEGT	-0.3288	-0.0594
Q62829	Pak3	S	156	1	GYIAAHQSNTKTASE	-0.2857	0.2895
D3ZQ51	Pak6	S	346	1	TGPLPGRSSPAGSPR		0.5311
D3ZQ51	Pak6	S	351	1	GRSSPAGSPRTRHAQ		0.7991
Q920Q0	Palm	S	112	3	PAAPKENSAAPSPIR	-0.0381	0.753
Q920Q0	Palm	S	116	1	KENSAAPSPIRPHST	0.0588	0.5973
Q920Q0	Palm	S	116	2	KENSAAPSPIRPHST	-0.1043	1.3008
Q920Q0	Palm	S	116	3	KENSAAPSPIRPHST	-0.0842	0.8466
Q920Q0	Palm	S	122	2	PSPIRPHSTSPAKEE	-0.1067	0.9557
Q920Q0	Palm	S	122	3	PSPIRPHSTSPAKEE	-0.0675	0.8756
Q920Q0	Palm	T	123	2	SPIRPHSTSPAKEEQ	-0.1005	0.9157
Q920Q0	Palm	T	123	3	SPIRPHSTSPAKEEQ	-0.0657	0.8795
Q920Q0	Palm	S	124	2	PIRPHSTSPAKEEQK	-0.1066	0.9924
Q920Q0	Palm	S	124	3	PIRPHSTSPAKEEQK	-0.0627	0.8887
Q920Q0	Palm	T	141	2	TMVNAQQTPLGTPKE	-0.127	0.5277
Q920Q0	Palm	T	145	1	AQQTPLGTPKENRKS	0.0876	0.4222
Q920Q0	Palm	T	145	2	AQQTPLGTPKENRKS	-0.127	0.5299
Q920Q0	Palm	T	153	2	PKENRKSTPVRSPGG	-0.1521	1.1867
Q920Q0	Palm	S	157	1	RKSTPVRSPGGSTMM	-0.067	0.5122
Q920Q0	Palm	S	157	2	RKSTPVRSPGGSTMM	-0.2534	1.3446
Q920Q0	Palm	S	161	2	PVRSPGGSTMMKAAM	-0.2241	1.2552
Q920Q0	Palm	T	162	2	VRSPGGSTMMKAAMY	-0.2643	1.3414
D4A1J3	Palm3	S	600	1	SGAKDDVSPEEQGKS	0.117	-0.3701

Q4KM62	Palmd	S	371	2	VSPRTELSPSRASPG	-0.1669	1.247
Q4KM62	Palmd	S	373	2	PRTELSPSRASPGKS		1.1199
Q4KM62	Palmd	S	376	2	ELSPSRASPGKSGPQ	-0.1537	1.1186
P14925	Pam	S	961	1	DEDDGTESEEEYSAP		-0.361
A0A0G2QC22	Paxx	S	116	1	FDLSKVPSPEAAPRL		-0.2677
A0A0G2K6T9	Pcdh1	S	852	1	DLYAPKPSGKAAKGS		-0.4479
A0A0G2K6T9	Pcdh1	S	934	1	SIQLQPQSPSASKKH	-0.281	0.3254
A0A0G2K6T9	Pcdh1	S	934	2	SIQLQPQSPSASKKH	-0.6178	
D3ZPN0	Pcdh17	S	1037	1	QEVPSASSSPTKACI		0.3218
D3ZPN0	Pcdh17	S	1080	1	PTDSQYPSPSKQPRD		0.2965
A0A0G2K8I5	Pcdh19	S	1134	1	KEGRDKESPAVKRLK		0.624
Q68HB8	Pcdh7	S	1000	2	ARHYKSSSPLPTVQL	-0.2128	0.5728
Q68HB8	Pcdh7	S	1011	1	TVQLHPQSPTAGKKH	-0.0605	0.5065
Q68HB8	Pcdh7	S	1011	2	TVQLHPQSPTAGKKH	-0.2128	0.5434
F1LS01	Pcdh9	S	941	1	DLAKHYKSASPQPAF		0.3522
F1LS01	Pcdh9	S	943	1	AKHYKSASPQPAFHL		0.4713
F1LS01	Pcdh9	S	943	2	AKHYKSASPQPAFHL	-0.6157	0.1051
Q767H7	Pcdhac2	S	838	1	LTGQSRHSAGNLIIL		-0.363
Q9JKS6	Pclo	S	231	1	EVIQQDSSPKSVSSQ	0.1306	0.3183
Q9JKS6	Pclo	S	617	1	PVPSQQASPKKEPPS	0.1001	0.3134
Q9JKS6	Pclo	S	826	1	TKPVPKGSPTPSGTR	-0.6311	0.3068
Q9JKS6	Pclo	S	924	1	QAPTPSQSPAAQGPA	-0.3338	0.4796
Q9JKS6	Pclo	S	1352	1	FSQESSPSSPSDLAK	-0.3646	0.3483
Q9JKS6	Pclo	S	1352	3	FSQESSPSSPSDLAK	0.3633	
Q9JKS6	Pclo	S	1353	1	SQESSPSSPSDLAKL	-0.4177	0.2906
Q9JKS6	Pclo	S	1353	3	SQESSPSSPSDLAKL	0.4177	
Q9JKS6	Pclo	S	1469	1	DSSESENSPVVRRKR	-0.0645	0.4955
Q9JKS6	Pclo	T	1478	1	VVRRKRRTSIGSSSS		-0.2775
Q9JKS6	Pclo	S	4150	1	DPKMSKFSPIQESRD	-0.0348	-0.3057
Q9JKS6	Pclo	S	4791	2	SSQNSQQSPKPSVIK		-0.2716
Q9JKS6	Pclo	S	4795	2	SQQSPKPSVIKSRSH		-0.2764
A0A0G2K0X1	Pcm1	S	1059	1	WKNHRPVSADGNYRP		0.6117
A0A0G2K0X1	Pcm1	S	1382	1	TFKTRKASAQASLAS		0.5649
A0A0G2K0X1	Pcm1	S	1534	1	DIVSRHISESDEKEG	0.1563	0.2688
A0A0G2K0X1	Pcm1	S	1536	1	VSRHISESDEKEGEN		0.323
D3ZSQ1	Pcnx3	S	287	1	QPLDRRGSGDPLPQK	0.0543	0.5115
D3ZSQ1	Pcnx3	T	370	1	DTVIGAGTPPGQTEP		0.5011
D3ZSQ1	Pcnx3	S	1953	1	GPDGEPASGSPKGGT	-0.0588	0.6739
D3ZSQ1	Pcnx3	S	1955	1	DGEPASGSPKGGTPK	-0.0587	0.5242
D3ZXP8	Pcp2	S	111	1	ALSFRRNSSPQPQTQ	-0.3521	0.3134
P19836	Pcyt1a	S	319	1	QAISPKQSPSSSPTH		0.7063
Q9QYJ6	Pde10a	S	69	1	NKAEDEPSPKEVSRY		-0.3378
Q62920	Pdlim5	S	228	1	AEGQRRGSQGDIKQQ	0.2009	1.037
Q6TRW4	Pds5b	T	1380	1	GRGRPSKTPSPSQPK		0.3828

F1M785	Pdzd2	S	1043	1	TDTQSPRSPENHTSP		0.2648
F1M785	Pdzd2	S	1360	1	SEARLSQSPQKADCR		0.785
F1M785	Pdzd2	S	1763	1	KGVTVPKSPPSRQKS		0.5109
D3ZXY2	Pdzd8	S	518	1	KEETQPLSHSPKRTP	0.0958	0.6704
D4A563	Peak1	S	725	1	RSYSSTHSSPAKIQR		1.0415
D4A563	Peak1	S	726	1	SYSSTHSSPAKIQRP		1.0524
P31044	Pebp1	S	153	1	RGKFKVESFRKKYHL		-0.5176
Q642G4	Pex14	S	271	1	ISPVSNESPSSSPGK		0.3494
P47860	Pfkp	S	156	1	AKNGEIDSDTVKKHA		-0.2923
A0A0G2K8Q4	Phactr2	S	154	1	TGSKASSSPSASSTS	0.0268	0.7899
Q5XIH7	Phb2	S	91	1	RARPRKISSPTGSKD	0.1382	-0.3309
Q5XIH7	Phb2	S	92	1	ARPRKISSPTGSKDL	0.2532	-0.3355
Q5XIH7	Phb2	S	293	1	SFTRGSDSLIKGKK_	0.1982	-0.4209
Q5U2N3	Pitpnm1	S	1203	1	VDFLRKQSQLLRSRG		-0.2683
A0A0U1RRV0	Pja1	S	137	1	EERGKVESPPAARCS	0.0863	1.0583
P11980	Pkm	S	127	1	RTGLIKGSGTAEVEL		-0.3358
F1M2K6	Pkp4	S	220	1	SVPSRAQSPSYVTST	-0.1028	1.2715
F1M2K6	Pkp4	T	225	1	AQSPSYVTSTGVSPS		0.6982
F1M2K6	Pkp4	S	230	1	YVTSTGVSPSRGSLR	0.0038	1.0499
F1M2K6	Pkp4	S	230	2	YVTSTGVSPSRGSLR	-0.1104	0.4883
F1M2K6	Pkp4	S	235	2	GVSPSRGSLRTSLGS	0.0552	0.3575
F1M2K6	Pkp4	S	272	2	LPAQRAASPYSQRPA	-0.5116	0.9758
F1M2K6	Pkp4	Y	274	2	AQRAASPYSQRPASP		0.9204
F1M2K6	Pkp4	S	275	2	QRAASPYSQRPASPT		1.0011
F1M2K6	Pkp4	S	280	1	PYSQRPASPTAVRRV	0.0762	0.7457
F1M2K6	Pkp4	S	280	2	PYSQRPASPTAVRRV	-0.4608	0.9783
F1M2K6	Pkp4	T	282	1	SQRPASPTAVRRVGS		0.7303
F1M2K6	Pkp4	T	282	2	SQRPASPTAVRRVGS	-0.5663	1.0497
F1M2K6	Pkp4	S	326	1	DAQTRVASPSQGQVG		0.4254
F1M2K6	Pkp4	S	326	2	DAQTRVASPSQGQVG	-0.1125	1.3523
F1M2K6	Pkp4	S	328	1	QTRVASPSQGQVGSS		0.343
F1M2K6	Pkp4	S	328	2	QTRVASPSQGQVGSS	-0.0056	1.014
F1M2K6	Pkp4	S	335	1	SQGQVGSSSPKRSGM	-0.0376	0.5921
F1M2K6	Pkp4	S	335	2	SQGQVGSSSPKRSGM	-0.0461	0.8155
F1M2K6	Pkp4	S	336	1	QGQVGSSSPKRSGMT	-0.1325	0.5707
F1M2K6	Pkp4	S	336	2	QGQVGSSSPKRSGMT	-0.0811	1.5788
F1M2K6	Pkp4	S	426	2	YYSPVYRSPNHGTVE	-0.0959	0.425
F1M2K6	Pkp4	S	1090	2	YPGSSKPSPIYISSY	-0.0481	0.8912
F1M2K6	Pkp4	S	1098	1	PIYISSYSSPAREQN		0.6185
F1M2K6	Pkp4	S	1098	2	PIYISSYSSPAREQN	-0.0898	0.8633
F1M2K6	Pkp4	S	1099	1	IYISSYSSPAREQNR		0.8775
F1M2K6	Pkp4	S	1099	2	IYISSYSSPAREQNR	-0.0497	0.9659
D4A8C5	Plcb4	S	901	1	KANVTPQSSSELRPT		0.4779
D4AAX6	Plch2	S	1089	1	SDSSSPDSPGSPKVA		0.883

D4AAX6	Plch2	S	1092	1	SSPDSPGSPKVAPCQ		0.8988
Q6S3A5	Plec	S	4276	1	GFRSRSSSVGSSSSY	-0.0511	0.9176
E9PTG5	Plekha5	S	574	1	TYRSEVSSPIQRGDV		0.5355
E9PTG5	Plekha5	S	1020	1	GVPLRTKSPTPESST		0.7177
E9PTG5	Plekha5	S	1109	1	SPSSVRDSPSRVPQT	0.1383	0.8306
A0A0G2K6Z8	Plekha7	S	827	2	PQLRKVVSPLQSPTK	-0.1439	0.9998
A0A0G2K6Z8	Plekha7	S	831	2	KVVSPLQSPTKATPQ	-0.1398	0.9483
A0A0G2K6Z8	Plekha7	T	833	2	VSPLQSPTKATPQAE	-0.1418	1.0862
D4ACN8	Plgrkt	S	141	1	EKARREQSKFFSDK_		-0.279
P60203	Plp1	S	114	1	TICGKGLSATVTGGQ		-0.3084
P60203	Plp1	T	116	1	CGKGLSATVTGGQKG	0.2759	-0.3338
P60203	Plp1	T	118	1	KGLSATVTGGQKGRG		-0.2985
P60203	Plp1	S	134	1	RGQHQAHSLERVCHC	0.2179	-0.2817
Q66H88	Plpp6	S	24	1	GGSSVPGSPAHGGGG	0.0198	0.3577
Q66H88	Plpp6	S	61	1	ARLRASDSPVHRRGS	0.2864	0.4922
G3V864	Plppr4	S	474	1	DSEPEGQSPPRSIEM		0.465
G3V864	Plppr4	S	547	1	EETQENISTSPKSSS		1.0588
G3V864	Plppr4	T	548	1	ETQENISTSPKSSSA	-0.1218	0.7693
G3V864	Plppr4	S	549	1	TQENISTSPKSSSAR		0.6398
G3V864	Plppr4	S	593	1	KQQGVLQSSPKNAEG	0.2711	0.4085
G3V864	Plppr4	S	594	1	QQGVLQSSPKNAEGS	0.2294	0.3739
D3ZQN3	Pnma8b	S	609	1	TPEKKAGSGASTEDH	0.1397	0.9204
D3ZQN3	Pnma8b	S	612	1	KKAGSGASTEDHAGN		0.968
D3ZQN3	Pnma8b	T	613	1	KAGSGASTEDHAGNN	0.1925	1.1651
O88794	Pnpo	S	164	1	YFHSRPKSSQIGAVV		-0.3642
D3ZGH9	Pom121l2	S	220	1	RSLHAQSSDPKCKRS	1.9696	0.5387
F1M8A4	Ppfia2	S	1125	1	LTTTSGQSRKMTTDV		-0.5336
Q5M821	Ppm1h	S	489	1	KDRGWRISNDRLGSG		-0.3028
Q10728	Ppp1r12a	S	894	1	DSVSRYDSSSTSSSD		-0.2786
A0A0G2K4R1	Ppp1r12c	S	508	1	PSRTEPGSPVKPNVL		0.2732
A0A0G2KB61	Ppp1r13b	S	562	1	DKGSRPQSPRKGPQT		0.4791
D4AA72	Ppp1r16b	S	477	1	WSGFKEQSPQTLLEL		0.2995
D3ZZ26	Ppp1r3d	S	54	2	IIQRRSRSLPTSPER		0.5061
O35867	Ppp1r9a	S	94	1	TRGKGRPSSPQKRMK	0.1146	1.3275
O35867	Ppp1r9a	S	95	1	RGKGRPSSPQKRMKP	0.0408	1.3767
O35867	Ppp1r9a	S	153	1	FERSGHESGQNNRHS	-0.715	0.9538
O35867	Ppp1r9a	S	160	1	SGQNNRHSPKKEKAG	-0.4636	1.0204
O35867	Ppp1r9a	S	929	1	FTFNDDFSPSSTSSA	-0.0939	0.9554
P63329	Ppp3ca	S	462	1	DEAIKGFSPQHKITS	-0.0663	0.5859
A0A0G2JV49	Ppp6r2	S	629	1	GQGRKTGSPTARNVP		0.5263
F1M0J7	Prickle2	S	546	1	TEQTPRGSMESLALS		0.2899
P54645	Prkaa1	S	486	1	DEITEAKSGTATPQR	-0.0098	-0.2748
P68182	Prkacb	S	322	2	FIPKFRGSGDTSNFD	-0.0456	-0.3046
P68182	Prkacb	S	339	2	EEEEIRVSITEKCGK	-0.0561	-0.2979

F1LS42	Prkcb	T	313	1	RAKIGQGTKAPEEKT		-0.4059
Q4V8C7	Prkra	S	18	1	PPLQREDSGTFSLGK		0.8352
Q6AXY7	Prpf38b	S	488	1	EKRKREHSPSREKSR	0.342	-0.3833
O08618	Prpsap2	S	198	1	ASAKRAQSFAERLRL		-0.3605
D3ZPT0	Prr36	S	123	1	AGQGSISSPGRASSG		0.6994
Q6MG48	Prrc2a	S	1007	1	TPAGGNLSPAPRLRR		0.5441
G3V8J5	Psd	S	1010	1	PRAQRPGSEARAGAG	0.0478	0.4836
D3ZUW0	Psd3	S	48	1	ISNSSEFSAKETKAL		-0.3396
D3ZUW0	Psd3	S	58	1	ETKALYNSIKNEKLE		-0.471
Q812D1	Psip1	S	176	1	TASNVKASPKRGRPA		0.7637
O88761	Psmd1	T	311	1	AGAVAGKTPDASPEP	0.5604	-0.3511
O88761	Psmd1	S	315	1	AGKTPDASPEPKDQT		-0.428
G3V6B9	Ptpn4	S	403	1	TPNHRNSSFTQEGTR		0.4841
M0RB22	Ptprd	S	1314	1	ESESRKSSLPNSKEV	0.219	-0.3075
Q64605	Ptprs	S	1292	1	PDSKRKDSEPRTKCL	0.406	-0.2804
D3ZYS1	Purg	S	160	2	RQKHSAPSPPVSVGS	0.0605	0.4403
D3ZYS1	Purg	S	160	3	RQKHSAPSPPVSVGS	0.002	0.5899
D3ZYS1	Purg	S	164	1	SAPSPPVSVGSEEHP		0.3481
D3ZYS1	Purg	S	164	2	SAPSPPVSVGSEEHP	0.1155	0.4158
D3ZYS1	Purg	S	164	3	SAPSPPVSVGSEEHP	0.002	0.5899
D3ZYS1	Purg	S	167	2	SPPVSVGSEEHPHSV	0.0395	0.4379
D3ZYS1	Purg	S	167	3	SPPVSVGSEEHPHSV	0.002	0.619
A0A0G2K4E8	R3hdm2	S	393	1	SILTRGDSIGSSKGG	0.5469	0.4799
A0A0G2K4E8	R3hdm2	S	396	1	TRGDSIGSSKGGSAG		0.4837
D4A3C2	RGD1304884	S	74	1	DQDRRSSSNESFSSN		-0.3188
A0A096MJX5	RGD1305178	S	261	1	EKPEPERSPPNRKRP	-0.091	0.4736
A0A0G2KAX2	RGD1305455	S	495	1	RPLSRKSSPSSPAVR	-0.0333	0.3096
A0A0G2KAX2	RGD1305455	T	541	2	VMERRAITPPVASPV	0.1518	0.2999
A0A0G2KAX2	RGD1305455	S	546	2	AITPPVASPVGRPLY	0.1518	0.2999
D3Z9D0	RGD1306271	S	1470	2	FPVVDDLSSGDTKER	-0.0801	0.4883
D3Z9D0	RGD1306271	S	1471	2	PVVDDLSSGDTKERH	-0.0764	0.4446
D3Z9D0	RGD1306271	S	1830	2	PGLGYPTSSTEDLQP	-0.0906	0.5082
A0A096MJT6	RGD1307100	S	1301	2	QDKSVGQSPLRSPLK		0.5055
A0A096MJT6	RGD1307100	S	1305	2	VGQSPLRSPLKRQAS		0.5055
A0A096MJT6	RGD1307100	S	1355	1	SDENVLDSPKQRRSF	0.1532	0.3258
A0A096MJT6	RGD1307100	S	2368	1	RGSVVQESPVTKSGH		0.2934
D3ZBU7	RGD1310819	S	213	1	PQSPDHMSDASVSSR	-0.0408	0.4542
D3ZBU7	RGD1310819	S	213	2	PQSPDHMSDASVSSR	-0.403	-0.0558
D3ZBU7	RGD1310819	S	484	1	APPERDISPSKDNMS	-0.266	0.269
D3ZBU7	RGD1310819	S	486	1	PERDISPSKDNMSPP		0.3043
D3ZBU7	RGD1310819	S	486	2	PERDISPSKDNMSPP	-0.2146	0.7633
D3ZBU7	RGD1310819	S	491	1	SPSKDNMSPPKRIMA	-0.041	0.3924
D3ZBU7	RGD1310819	S	491	2	SPSKDNMSPPKRIMA	-0.2306	0.708
D3ZBU7	RGD1310819	S	505	1	APPERDKSPSEGDVA	-0.2045	0.4019

D3ZBU7	RGD1310819	S	507	1	PERDKSPSEGDVAPP	-0.1093	0.3525
D3ZBU7	RGD1310819	S	568	1	APPERDKSPSEGDVT	-0.2171	0.425
D3ZBU7	RGD1310819	S	570	1	PERDKSPSEGDVTPP	-0.2244	0.3889
D3ZBU7	RGD1310819	S	570	2	PERDKSPSEGDVTPP		0.6705
D3ZBU7	RGD1310819	T	575	1	SPSEGDVTPPKRIMA	0.0566	0.7534
D3ZBU7	RGD1310819	T	575	2	SPSEGDVTPPKRIMA	-0.1408	0.7054
D3ZBU7	RGD1310819	S	876	1	KLRSTSLSLKYRDSS		-0.3704
D3ZBU7	RGD1310819	S	937	1	QGKGKTRSPEQPGTK		0.2808
D3ZY47	RGD1559896	S	176	1	AQSSRSSSLDALGPA	0.2902	0.4504
D3ZY47	RGD1559896	S	199	1	WKINAERSREGHEAE		0.4914
D3ZQK5	RGD1561149	S	891	1	TEPRSPQSPASKASF		0.4943
A0A0G2K1W1	Rab11fip5	S	152	1	AGRDSIQSPKLLTHK	0.0179	0.2949
A0A0G2K1W1	Rab11fip5	S	163	1	LTHKRTYSDEASQLR	0.1323	0.2971
A0A0G2K1W1	Rab11fip5	S	333	1	NEVGRRGSVGEKGSP	0.4369	0.4866
A0A0G2K1W1	Rab11fip5	S	333	2	NEVGRRGSVGEKGSP		0.6022
A0A0G2K1W1	Rab11fip5	S	333	3	NEVGRRGSVGEKGSP	-0.1	0.646
A0A0G2K1W1	Rab11fip5	S	339	1	GSVGEKGSPSLGASP	0.1151	0.7497
A0A0G2K1W1	Rab11fip5	S	339	2	GSVGEKGSPSLGASP	-0.0031	0.7484
A0A0G2K1W1	Rab11fip5	S	339	3	GSVGEKGSPSLGASP	-0.0967	0.5842
A0A0G2K1W1	Rab11fip5	S	341	1	VGEKGSPSLGASPHH	0.0803	0.8531
A0A0G2K1W1	Rab11fip5	S	341	2	VGEKGSPSLGASPHH	0.0305	0.6426
A0A0G2K1W1	Rab11fip5	S	345	1	GSPSLGASPHHSSTG	-0.0968	1.6046
A0A0G2K1W1	Rab11fip5	S	345	2	GSPSLGASPHHSSTG	-0.0283	0.8233
A0A0G2K1W1	Rab11fip5	S	345	3	GSPSLGASPHHSSTG	-0.0967	0.646
A0A0G2K1W1	Rab11fip5	S	349	2	LGASPHHSSTGEEKA	-0.0228	0.9334
A0A0G2K1W1	Rab11fip5	S	350	2	GASPHHSSTGEEKAK	-0.1915	1.0046
A0A0G2K1W1	Rab11fip5	S	752	1	RLFTPTNSQVEEDKE		0.7316
A0A0G2K1W1	Rab11fip5	S	825	1	DVVGETSSPGSRDCL	0.0169	0.287
A0A0G2K4A0	Rab11fip5	S	521	1	TAAPVEASPDRKQSR		0.7077
O55007	Ralgapa1	S	733	2	QAPMRQRSATTTGSP	0.0563	0.4453
O55007	Ralgapa1	S	739	1	RSATTTGSPGTEKAR	0.1958	0.4503
O55007	Ralgapa1	S	739	2	RSATTTGSPGTEKAR	0.0812	0.351
P86410	Ralgapb	S	414	1	SKVQHQASSTSPLSS		0.2708
F1LV89	Rap1gap	S	526	1	VSTSHSGSFTPNNPD	-0.6723	0.2861
F1LV89	Rap1gap	S	585	1	KKSGPFGSRRSSAIG	-0.6494	-0.3096
A0A0G2JTA7	Rasal2	S	1068	1	QSSSSRESPVPKVRA	-0.063	1.3749
M0R3Z8	Rbm15	S	51	1	TMKGKERSPVKPKRS		1.0201
D3ZRC3	Rbm26	S	127	1	FSRRLNHSPPQSSSR	0.0643	0.7476
F1M1R4	Rbm27	S	120	1	VRKKKYPSPQKSRSE		0.5336
D3ZTA8	Rbm33	S	814	1	DAKAKPLSPGAQPKE		0.5375
P84586	Rbmxrtl	T	163	1	GPPPKRSTPSGPVRS		0.3862
P84586	Rbmxrtl	S	205	1	SRRDVYLSPRDDGYS		0.8208
D3ZL11	Rbsn	T	211	2	ASKDSLSTHTSPSQS		0.3403
D3ZL11	Rbsn	T	213	2	KDSLSTHTSPSQSPN	-0.042	0.3155

D3ZJ01	Relch	S	455	1	SFIPKEKSSDSFPTK	-1.098	-0.4295
A0A0G2K285	Reps2	S	349	1	PSQAAESSPTKKDVP	-0.0531	0.3905
A0A0G2JT77	Rims1	S	908	1	RHIHGESSSKKLQRS	-0.0783	-0.4577
A0A0G2JT77	Rims1	S	1484	1	VEVIRARSLTQKPGS		-0.3284
Q498D5	Rmdn2	S	121	1	RVTVHQVSPQHRARK	0.0596	0.6587
Q66H15	Rmdn3	S	46	1	QRHGRSQSLPNSLDY	0.1008	0.3152
Q3ZAU6	Rnf14	S	30	1	DEFRKAESVQGGETR		-0.302
A0A0G2K6H9	Rnf19b	S	629	1	PRVHGAPSPSAHKSL		0.4807
A0A0G2JZA1	Robo2	S	1393	1	STERKGSSLERQQAA		0.2691
Q62868	Rock2	S	1374	1	MKIQQNQSIRRPSRQ	0.7522	-0.2732
P11250	Rpl34	S	12	1	LTYRRRLSYNTASNK		-0.3626
P19945	Rplp0	S	304	2	KVEAKEESEESDEDM	-0.2591	0.4654
P19945	Rplp0	S	307	2	AKEESEESDEDMGFG	-0.2591	0.4654
P02401	Rplp2	S	102	1	KDEKKEESEESDDDM		-0.2784
P27952	Rps2	S	281	1	VKTHTRVSVQRTQAP		-0.3445
F1M853	Rrbp1	S	135	1	PQEKLASSPKDKKKK		1.0266
F1M853	Rrbp1	S	635	1	QGKKVEGSPNQAKKV	0.1716	0.3228
Q5M9F3	Rrp1	T	24	1	LAGNEQVTRDRALRK		-0.3488
Q9JK11	Rtn4	T	14	1	SSLVSSSTDSPPRPP	0.0238	0.5055
Q9JK11	Rtn4	S	16	1	LVSSSTDSPPRPPPA	0.1238	0.5827
Q9JK11	Rtn4	S	169	1	AAPKRRGSGSVDETL	-0.0347	0.3408
Q9JK11	Rtn4	T	175	2	GSGSVDETLFALPAA	0.0858	0.3396
B0LPN4	Ryr2	S	2353	1	DPSRDGPSPTSGSSK	0.2401	-0.2665
P48303	S1pr1	S	354	1	PGMEFSRSKSDNSSH	-0.3075	0.4039
P48303	S1pr1	S	356	1	MEFSRSKSDNSSHPQ	-0.3917	0.4463
O88453	Safb	S	366	1	RAPTAAPSPEPRDSK		0.4847
Q6AXV4	Samm50	S	253	1	VRKESGHSLKSSLSH		-0.4191
Q6AY30	Sccpdh	S	215	1	GSLRKLRSVSNLKPV		-0.3997
Q6AY30	Sccpdh	S	217	1	LRKLRSVSNLKPVPV		-0.3173
P04774	Scn1a	S	480	1	PSAAGRLSDSSSEAS	0.1632	-0.3171
P04774	Scn1a	S	623	1	ERRNSNLSQTSRSSR		0.6249
F1M9G9	Scn2a	S	599	2	DFADDEHSTFEDNDS	-0.3621	0.3266
F1M9G9	Scn2a	T	1909	1	TDVTPSTTSPPSYDS	0.0261	-0.3357
P54900	Scn2b	T	198	1	LSTDDLKTEEEGKTD	0.0321	-0.4232
P54900	Scn2b	T	204	1	KTEEEGKTDGEGNAE	0.2036	-0.2693
P08104	Scn3a	S	531	1	PKSESEDSVKRRSFL		0.5584
B2RZD1	Sec61b	S	17	1	NVGSSGRSPSKAVAA	-0.0446	0.7379
Q7TP42	Sec62	S	542	1	GDHGPEGSGGERHSD	0.1722	-0.467
D3ZDH8	5-Sep	S	234	1	YQFPECDSDEDEDFK	0.1146	-0.4956
A0A0U1RRT8	6-Sep	S	192	1	KSDAISKSELAKFKI		-0.2783
A0A0G2K7G7	8-Sep	S	194	1	KADTISKSELHKFKI		-0.2682
Q6AXS5	Serbp1	S	327	1	KGFVLHKSKSEEAHA	-0.0046	0.5384
Q6AXS5	Serbp1	S	329	1	FVLHKSKSEEAHAED	-0.067	0.6978
D3ZN16	Sergef	T	300	1	DYGQLGRTLGSPEAQ		-0.2739

D3ZMS1	Sf3b2	S	326	1	PQRVRAASSESSGDR		0.7117
D3ZFJ3	Sh3bp1	S	539	1	SELPKPASPKVSRSP		0.264
D3ZAF9	Sh3pxd2b	S	569	1	SKLRPAKSQEKALLD		0.3694
Q9WV48	Shank1	T	176	1	KQLAKLHTKTGLKKF		-0.483
Q9WV48	Shank1	T	178	1	LAKLHTKTGLKKFLE		-0.3957
Q9WV48	Shank1	S	413	1	DVVPFQESPKYAARR	0.2009	-0.4255
Q9WV48	Shank1	S	540	1	GSGGPGGSLGSRGRR	-0.1501	0.6929
Q9WV48	Shank1	S	1071	1	SPTSGAPSPSHHSSS	-0.1488	0.6168
Q9WV48	Shank1	S	1138	1	GSIPSASSPTSPALP		0.7033
Q9WV48	Shank1	S	1174	1	IKAPSTSSSGRSSQG	0.4313	1.0409
Q9WV48	Shank1	S	1386	1	QPPPRPPSPRYDAPP	-0.2316	1.15
Q9WV48	Shank1	S	1442	1	QEKALTASPPAARRS	0.0029	0.6738
Q9WV48	Shank1	S	1517	1	PAGTRGSSTEDGPGV	0.2059	0.4387
Q9QX74	Shank2	S	67	1	ATSHRSLSPQLLQQT		0.3504
Q9QX74	Shank2	S	648	1	KQSNVEDSPEKTCSI		0.8127
Q9QX74	Shank2	S	666	1	TIIVKEPSTSSSGKS		0.4654
Q9QX74	Shank2	S	1334	2	SGPRRAPSPVVSPTE	-0.6184	0.4954
Q9QX74	Shank2	S	1338	1	RAPSPVVSPTELSKE	0.142	1.2085
Q9QX74	Shank2	S	1338	2	RAPSPVVSPTELSKE	-0.5811	0.4236
Q9QX74	Shank2	T	1340	2	PSPVVSPTELSKEIL	-0.3391	0.2917
Q9JLU4	Shank3	S	986	1	GSFAREPSPTHRGPR		0.9703
Q9JLU4	Shank3	S	1135	1	RSPTPVHSPDADRPG	0.1547	0.7152
Q9JLU4	Shank3	S	1189	1	PTREERKSPEDKKSM	0.6594	1.3883
Q9JLU4	Shank3	S	1511	1	QLNKDTRSLGEEPVG	0.4582	0.5669
D4A4M0	Shisa6	T	284	1	ILSSATQTPTHEKPR		0.3713
D3ZPJ0	Shisa7	S	287	1	NLHYNVNSPKHRAAT		0.3748
A0MZ67	Shtn1	S	381	1	MSMIRKRSHPSGGST	-0.0872	0.5201
A0A0G2KAW2	Sipa1l1	S	1184	1	VSRRSPASIDRQNTQ		0.4437
A0A0G2KAW2	Sipa1l1	S	1249	1	QDPVVHLSPNKQGHS	0.1598	0.4796
A0A0G2KAW2	Sipa1l1	S	1708	2	VQMKSYSSKDSSPTL		0.497
A0A0G2KAW2	Sipa1l1	S	1712	1	SYSSKDSSPTLASKV	-0.0039	0.6222
A0A0G2KAW2	Sipa1l1	S	1712	2	SYSSKDSSPTLASKV		0.4987
O35412	Sipa1l1	S	1752	1	YSSSKDSSPTLASKV	-0.0039	0.638
F1LYG2	Sipa1l3	S	94	1	LREQSNPSPSQDTDG	0.115	1.4359
F1LYG2	Sipa1l3	S	1248	1	QDAAGKDSPNRHSKG	0.2684	1.3602
Q63633	Slc12a5	S	49	1	DGNPKESSPFINSTD	0.1081	0.3706
Q63633	Slc12a5	S	963	1	ITDESRGSIRRKNPA	0.0109	0.3932
Q63633	Slc12a5	S	1045	1	AQKNKGPSPVSSEGI	0.0114	0.4533
G3V6N7	Slc12a6	S	32	1	IPGLSDTSPDLSSRS		0.6532
P53987	Slc16a1	S	210	1	GKVEKLKSKESLQEA	0.1076	-0.2984
P53987	Slc16a1	S	230	1	NTDLIGGSPKGEKLS	0.0376	-0.4259
Q63344	Slc16a7	S	219	1	KSKSKVGSRQDSSTK		-0.3855
G3V6R0	Slc1a2	S	240	1	IEMTKTQSIYDDTKN		0.3606
Q63488	Slc20a2	S	256	1	ESALSRASDESLRKV	0.334	-0.3235

O70594	Slc22a5	S	548	1	TQKDGGESPTVLKST		-0.3112
Q9WTW8	Slc23a2	S	638	1	GKSENRRSSDKDSQA		-0.2762
F1LX07	Slc25a12	S	640	1	LYLPKFKSPGVAAAQ		-0.2891
Q05962	Slc25a4	S	22	1	GGIAAAVSKTAVAPI		-0.4643
Q05962	Slc25a4	S	149	1	AADVGKGSSQREFNG		-0.4036
D3Z9I5	Slc26a6	S	751	1	HRKSGPKSPVLATKL		-0.2687
A0A0G2JYF0	Slc4a10	S	1116	1	SRFPSKSSPS_____		0.8109
P23347	Slc4a2	T	170	2	TDRKAERTSPSPPTQ	-0.0587	0.3886
P23347	Slc4a2	S	171	2	DRKAERTSPSPPTQT	-0.0458	0.2983
P23347	Slc4a2	S	173	2	KAERTSPSPPTQTPH	0.0396	0.2938
P23348	Slc4a3	S	198	1	VGLPSDQSPQRSGSS		0.4417
A0A0H2UHB7	Slc4a4	S	70	2	ERISENYSDKSDVEN	-0.5709	0.3678
A0A0H2UHB7	Slc4a4	S	73	1	SENYSDKSDVENADE	-0.377	0.2654
A0A0H2UHB7	Slc4a4	S	73	2	SENYSDKSDVENADE	-0.5699	0.3697
A0A0H2UHB7	Slc4a4	T	259	2	AMTHRNLTSSSLNDI	-0.5834	-0.2714
A0A0H2UHB7	Slc4a4	S	1031	1	KKKKKKGSLDSDNDD	0.1417	-0.3837
Q08469	Slc6a15	S	701	1	IYRKQSGSPTLDTAP		0.4144
Q9WVR6	Slc7a8	S	23	1	PDRGSDTSPEAEASS	0.1919	-0.3639
Q9WVR6	Slc7a8	S	30	1	SPEAEASSGGGGVAL		-0.276
Q01728	Slc8a1	S	452	1	DGTANAGSDYEFTEG	0.1091	-0.3494
P48768	Slc8a2	S	442	1	DGSAKAGSDYEYSEG	0.1502	-0.3575
P26431	Slc9a1	S	776	1	IRSKEPSSPGTDDVF	-0.7918	0.3181
P26431	Slc9a1	S	776	2	IRSKEPSSPGTDDVF	-0.9138	-0.0871
D4A4W6	Slirp	T	104	1	KVLHGAQTSDEEKDF	0.18	-0.3184
G3V7I8	Slk	T	183	1	VSAKNTRTIQRRDSF	0.0018	-0.2706
A0A0G2K9D6	Smarcc1	S	327	2	NARKRKHSPSPPPPT		0.3434
A0A0G2K9D6	Smarcc1	S	329	2	RKRKHSPSPPPPTAT		0.3434
D4ACJ3	Smg7	S	759	1	VIPALGKSPPHHSGF		0.7575
P60881	Snap25	T	200	1	DEANQRATKMLGSG_	-0.1795	-0.2988
A0A0G2K0B6	Snap91	S	622	2	VDAFAAPSPASTASP	-1.5075	-0.0341
A0A0G2K0B6	Snap91	S	622	3	VDAFAAPSPASTASP	-1.1858	-0.2638
B5DF41	Snph	T	197	2	GVAKEEGTGESAGGS	0.0863	0.4155
B5DF41	Snph	S	200	2	KEEGTGESAGGSPAR		0.4176
B5DF41	Snph	S	204	1	TGESAGGSPARSLTR	0.2067	0.6629
B5DF41	Snph	S	204	2	TGESAGGSPARSLTR	0.105	0.4299
D4A0A1	Soga3	S	759	1	SDAGKKESDDDSRPP	0.2769	0.7951
D4A0A1	Soga3	S	763	1	KKESDDDSRPPHRKR		0.6468
F1M820	Sorbs1	S	55	1	YRETPSSSPVSPQES	-0.2658	
F1M820	Sorbs1	S	55	2	YRETPSSSPVSPQES	-0.1553	0.9709
F1M820	Sorbs1	S	55	3	YRETPSSSPVSPQES	-0.3288	0.2984
F1M820	Sorbs1	S	58	2	TPSSSPVSPQESPKH	-0.2139	0.457
F1M820	Sorbs1	S	58	3	TPSSSPVSPQESPKH	-0.3134	0.3785
F1M820	Sorbs1	S	62	1	SPVSPQESPKHENKS	0.045	0.7486
F1M820	Sorbs1	S	62	2	SPVSPQESPKHENKS	-0.1607	0.8301

F1M820	Sorbs1	S	62	3	SPVSPQESPKHENKS	-0.3228	0.3039
F1M820	Sorbs1	S	470	1	LSGLKRPSSSASTKV	0.185	0.4853
F1M820	Sorbs1	S	794	1	SREGSGGSVHGDFPK	0.1419	0.4102
F1M840	Sorbs1	S	449	1	LSGLKRPSSSASTKD	0.185	0.4853
F1LPM3	Sorbs2	S	254	1	RPLSKSHSDNGTDAF	-0.0452	1.1714
F1LPM3	Sorbs2	S	397	1	FISSSPSSPSRAQGG	-0.0996	0.3464
O35413	Sorbs2	S	254	1	RPLSKSHSDNGTDAF	-0.0452	1.1714
O35413	Sorbs2	S	329	1	RPVSVYQSSIDRSLE	0.1688	0.6405
O35413	Sorbs2	S	330	1	PVSVYQSSIDRSLER	0.2873	0.3921
O35413	Sorbs2	S	354	1	DFRKRRKSEPAVGPP	0.0763	0.8467
O35413	Sorbs2	S	397	1	FISSSPSSPSRAQGG	-0.0996	0.3464
O35413	Sorbs2	S	645	2	LCPKRRFSIESLLEE	-0.0949	0.8274
O35413	Sorbs2	S	648	2	KRRFSIESLLEEETQ	-0.0643	0.8153
O35413	Sorbs2	T	654	2	ESLLEEETQVRHPSQ	-0.0847	0.8444
P27867	Sord	S	169	1	IYACRRGSVSLGNKV		-0.2644
D4A3T0	Sos1	S	1152	1	PESAPAESSPSKIMS	0.2735	0.5802
D4A3T0	Sos1	S	1153	1	ESAPAESSPSKIMSK	0.1023	0.9093
A0A0G2K5D7	Specc1	S	450	1	PFKSSKGSPTGSSPN	0.1357	0.3739
A0A0G2K5D7	Specc1	S	450	2	PFKSSKGSPTGSSPN	-0.3398	0.2655
A0A0G2K5D7	Specc1	T	452	1	KSSKGSPTGSSPNNA	-0.1293	0.3848
A0A0G2K5D7	Specc1	T	452	2	KSSKGSPTGSSPNNA	-0.3292	0.2954
A0A0G2K5D7	Specc1	S	455	1	KGSPTGSSPNNASEL		0.4626
A0A0G2K5D7	Specc1	S	455	2	KGSPTGSSPNNASEL	-0.3125	0.3078
Q63638	Speg	S	439	1	VPLRKARSLEQPKSE	0.2329	0.3141
Q63638	Speg	S	2114	1	PRMARAASSEAAPHH		0.5188
Q63638	Speg	S	2115	1	RMARAASSEAAPHHQ	0.3067	0.5491
A0A0G2K1Y8	Sptan1	S	866	1	EDVKAKLSELNQKWE		-0.3129
A0A140UHX6	Sptb	S	2300	1	SIRVKAQSLPLPSLA		0.4083
A0A0G2K8W9	Sptbn1	T	2153	1	NGAAEQRTSSKESSP		-0.6163
A0A0G2K8W9	Sptbn1	S	2154	1	GAAEQRTSSKESSPV		-0.4493
A0A0G2K8W9	Sptbn1	S	2163	3	KESSPVPSPTSDRKA	-0.2911	0.2973
A0A0G2K8W9	Sptbn1	S	2335	1	VTITSESSPGKREKD	0.0568	1.1886
Q9QWN8	Sptbn2	S	2169	1	NVPEGPGSGTGDESS	-0.0387	0.4445
Q9QWN8	Sptbn2	S	2254	1	YCVLRRGSLGFYKDA		0.556
A0A0G2K677	Sptbn4	S	2268	1	RRPERQESADHEGPH	0.306	0.2645
A0A0G2K677	Sptbn4	S	2301	1	RRIERQESSEQETPT	0.2373	0.6105
A0A0G2K677	Sptbn4	S	2302	1	RIERQESSEQETPTR	0.3234	0.7665
Q9QXY2	Srcin1	S	333	3	TRRLNNLSPASHLAS	-0.1483	0.3618
Q9QXY2	Srcin1	S	336	3	LNNLSPASHLASSSP		0.2941
Q9QXY2	Srcin1	S	341	3	PASHLASSSPPPGLP	-0.172	0.3109
Q9QXY2	Srcin1	S	342	3	ASHLASSSPPPGLPS	-0.172	0.3249
Q9QXY2	Srcin1	S	900	2	DFEIPPPSPPLNLHE	-0.5007	0.2825
Q9QXY2	Srcin1	S	1152	1	AAQGPAGSPDKGKHG	0.0423	1.315
Q66H19	Srfbp1	S	215	1	KAVATPHSPGKPSEK		0.5274

F1M5M9	Srgap3	S	908	1	LSRGRIESPEKRRMA	0.128	0.4347
B0BNJ1	Sri	S	172	1	KLRALTDSFRRRDSG		-0.4264
A0A0G2K2M9	Srrm2	S	332	1	PSTKQSSSPYEDKDK		1.1428
A0A0G2K2M9	Srrm2	S	350	1	SAVRPSPSPERSSTG		0.7735
A0A0G2K2M9	Srrm2	S	881	2	SSTPPRQSPSRSSSP		1.1106
A0A0G2K2M9	Srrm2	S	883	2	TPPRQSPSRSSSPQP		1.1392
A0A0G2K2M9	Srrm2	S	1068	2	PKGGLSRSSSPVTEL		1.2588
A0A0G2K2M9	Srrm2	S	1070	2	GGLSRSSSPVTELTA		1.3986
A0A0G2K2M9	Srrm2	T	1076	2	SSPVTELTARSPVKQ		1.3691
A0A0G2K2M9	Srrm2	S	1096	1	STDPKLKSGMSPEQN		1.4426
A0A0G2K2M9	Srrm2	S	1099	1	PKLKSGMSPEQNKTK	0.0882	1.3542
A0A0G2K2M9	Srrm2	S	1153	1	CVLRDKFSPTQDRPE	0.1319	0.8797
A0A0G2K2M9	Srrm2	S	1181	1	KERSGAGSPPGTRDQ	0.1522	1.036
A0A0G2K2M9	Srrm2	S	1461	2	ARSHSPSSPERNNKS		1.3326
A0A0G2K2M9	Srrm2	S	1524	1	ESDSSPDSKPKARTP		1.3037
A0A0G2K2M9	Srrm2	S	1580	1	AQSGTDSSPEHKIPA		0.6539
A0A0G2K2M9	Srrm2	S	1781	2	RGGSGYHSRSPTRQE	-0.1464	0.4232
A0A0G2K2M9	Srrm2	S	1783	2	GSGYHSRSPTRQESS	-0.1411	0.391
A0A0G2K2M9	Srrm2	T	1785	2	GYHSRSPTRQESSRT		0.4232
A0A0G2K2M9	Srrm2	S	2023	2	RAARGKRSLTRSPPA	-0.0746	0.5968
A0A0G2K2M9	Srrm2	T	2025	2	ARGKRSLTRSPPAIR	-0.0908	0.5629
A0A0G2K2M9	Srrm2	S	2027	2	GKRSLTRSPPAIRRR	-0.0448	0.5852
A0A0G2K2M9	Srrm2	T	2365	1	LDRARSRTPPSAPSQ	-0.0056	0.7931
A0A0G2K2M9	Srrm2	S	2538	1	VALKRVPSPTPVPKE		0.3945
A0A0G2K2M9	Srrm2	S	2659	1	PVERRQPSPQPSPRD	0.0341	0.7066
A0A0G2K2M9	Srrm2	S	2682	2	WRGQRGDSHSPGHKR	0.0546	1.2625
A0A0G2K2M9	Srrm2	S	2684	1	GQRGDSHSPGHKRRK	0.1517	1.7834
A0A0G2K2M9	Srrm2	S	2684	2	GQRGDSHSPGHKRRK	0.0546	1.2625
O35814	Stip1	S	481	1	AQYNRHDSPEDVKRR	0.3348	-0.2802
P32851	Stx1a	S	14	1	ELRTAKDSDDDDDVT	0.2636	-0.457
P32851	Stx1a	T	21	1	SDDDDDVTVTVDRDR	0.1289	-0.4686
P32851	Stx1a	T	23	1	DDDDVTVTVDRDRFM	0.1136	-0.4612
P32851	Stx1a	S	64	1	KHSAILASPNPDEKT	0.1898	-0.2923
P61765	Stxbp1	S	313	1	SLKDFSSSKRMNTGE		-0.2679
P61765	Stxbp1	S	506	1	YPYISTRSSASFSTT	-0.1092	-0.2855
Q9WU70	Stxbp5	S	783	1	FSRSRSSSVTSIDKE	0.1375	-0.3779
D3ZU84	Stxbp5l	S	724	1	YNRSRSSSISSIDKD		-0.3086
D3ZU84	Stxbp5l	S	726	1	RSRSSSISSIDKDSK		-0.2952
D3ZU84	Stxbp5l	S	727	1	SRSSSISSIDKDSKE	0.1187	-0.29
F1LM47	Sucla2	S	281	1	DAKINFDSNSAYRQK		-0.3344
F1LM47	Sucla2	S	283	1	KINFDSNSAYRQKKI		-0.3302
Q68FU8	Sugp1	S	253	1	QAATQKVSPPEDEEA		-0.366
Q63564	Sv2b	S	425	1	FQDEEYKSKMKVFFG		-0.3946
Q9Z2I7	Svop	S	520	1	KGRALQESSHREWGQ	0.1335	-0.3475

F1LUC0	Sybu	S	46	1	QQQQNKVSPASESPF		0.5011
F1LUC0	Sybu	S	199	1	PSHKSGSSPPSPREK		0.913
F1LUC0	Sybu	S	199	2	PSHKSGSSPPSPREK	0.078	0.777
F1LUC0	Sybu	S	202	2	KSGSSPPSPREKDLV	0.0852	0.7439
F1LUC0	Sybu	S	220	1	CRNPLSPSNIHPSYA		0.3372
P09951	Syn1	S	492	1	PQGQQHLSGLGPPAG		0.4578
P09951	Syn1	S	551	1	ARPPASPSPQRQAGP	-0.5697	0.4381
P09951	Syn1	S	551	2	ARPPASPSPQRQAGP	-1.5076	0.1425
P09951	Syn1	S	700	1	SLRKSFASLFSD___	-0.3996	-0.2879
O70441	Syn3	S	575	1	NLRKSFASLFSD___	-0.3996	-0.2879
Q9QUH6	Syngap1	S	109	1	LGRSRRKSVPGGKQY		0.3815
Q9QUH6	Syngap1	S	780	1	MARGLNSSMDMARLP	0.1113	0.6477
Q9QUH6	Syngap1	S	1005	1	ASILHSHSYSDEFGP		0.7916
Q9QUH6	Syngap1	S	1023	1	DFTRRQLSLQDNLQH		0.3034
Q9QUH6	Syngap1	S	1108	2	PARPRQQSLSKEGSI		1.3125
Q9QUH6	Syngap1	S	1114	1	QSLSKEGSIGGSGGS	-0.0058	1.1895
Q9QUH6	Syngap1	S	1114	2	QSLSKEGSIGGSGGS		1.148
Q9QUH6	Syngap1	S	1118	1	KEGSIGGSGGSGGGG	0.0408	1.5074
Q9QUH6	Syngap1	S	1118	2	KEGSIGGSGGSGGGG	-0.1898	1.3935
Q9QUH6	Syngap1	S	1121	1	SIGGSGGSGGGGGGG	-0.0576	2.1683
Q9QUH6	Syngap1	S	1121	2	SIGGSGGSGGGGGGG	-0.1898	1.3935
Q9QUH6	Syngap1	S	1204	1	EYEEEIHSLKERLHM	0.1044	1.0705
D4ABN3	Synj1	S	1215	1	PQSQARVSAGRLTPE		0.2673
Q9Z327	Synpo	S	258	1	RHLEKVASEEEEVPL	0.3631	1.3814
Q9Z327	Synpo	S	537	1	RRLVGQRSPVVERRP	-0.0995	0.6348
Q9Z327	Synpo	S	572	1	SQVRSPPSYSTLYPS	0.0895	1.5041
Q9Z327	Synpo	S	767	1	GFRVASLSPARTPPA	-0.0426	0.3492
Q9Z327	Synpo	S	835	1	TVSPRAASPAKPSSL	-0.1744	2.0667
Q9JKC9	Synrg	S	1090	1	GSHKRSLSLGDKEIS		0.4131
P21707	Syt1	T	201	1	ETKVHRKTLNPVFNE		-0.3867
G3V917	Tanc1	S	1658	1	SSSGSSGSPSSSVKM	-0.0813	0.6321
A0A0G2K9J0	Tanc2	S	1562	1	RSNSSVGSPTRQGYQ	-0.0899	0.3918
A0A0G2K9J0	Tanc2	S	1646	1	IYRSQSGSPVRYQQE	0.0565	0.8037
A0A0G2K9J0	Tanc2	S	1665	1	QLPGRPKSPLSKMAQ		0.2908
A0A0G2K9J0	Tanc2	S	2063	1	DSRQGQTSPIKPKRP	-0.3338	1.0515
I6L9G6	Tardbp	S	183	1	KLPNSKQSPDEPLRS		-0.385
D3ZG21	Tcf20	S	592	1	ASEKAGSSPTQGAQN		0.2705
D4A206	Tcof1	S	1254	1	AAGTSAGSPEKASRT		0.4492
F1LZ38	Tenm4	S	54	1	YTSSSADSEEGKGPQ		0.3268
G3V9L1	Tex2	S	732	1	LPAHSRHSSPSGHLS	-0.2524	0.6628
G3V9L1	Tex2	S	733	1	PAHSRHSSPSGHLSH	-0.107	0.9689
G3V9L1	Tex2	S	733	2	PAHSRHSSPSGHLSH	-0.221	0.4828
G3V9L1	Tex2	S	741	2	PSGHLSHSRSSSKGS	-0.3184	0.4887
G3V9L1	Tex2	S	799	1	PVQSAESSPTAGKKL	0.196	-0.3013

P24155	Thop1	S	634	1	FKQEGVLSPKVGMDY		-0.369
Q5M7V8	Thrap3	S	248	2	DLSPRERSPALKSPL		0.59
A0A0G2K2P5	Tjp1	S	329	1	PSDHSTQSPQQPSNG	-0.0417	0.4571
D3ZE26	Tmcc2	S	119	1	QGLSDQDSPDEKERS	0.0295	0.4392
D3ZE26	Tmcc2	S	126	1	SPDEKERSPEMHRVS		0.6401
F1LYB3	Tmem132c	S	1012	1	PRQEPANSPTSKMKK		0.3471
A9CMA6	Tmem163	S	7	1	_MERAPGSERRSPPG	0.7944	0.3026
A9CMA6	Tmem163	S	56	1	RQPRISESGQFSDGF	0.0511	-0.3009
Q68FV0	Tmem178a	S	291	1	TKIAHLKSGRDSTV_		-0.4927
D3Z9V8	Tmem25	S	275	1	KGPSRRPSLISSDSN		-0.2773
D3ZYW8	Tmem266	T	473	1	TPVGSVQTSPELEHR	0.0815	0.3044
Q5XIP9	Tmem43	S	10	1	ANYSSTGSRKEHVKV	0.1752	-0.2957
F1LUG5	Tmem94	S	517	1	HGRSKHPSGSNVSFS		0.5031
F1LUG5	Tmem94	S	522	1	HPSGSNVSFSRDTEG		0.312
Q62733	Tmpo	S	155	1	LREQGAESRSSTPLP		0.6678
A0A0G2K490	Tnik	S	640	1	VEMPRQNSDPTSENP	-0.0044	0.3816
A0A0G2K490	Tnik	S	688	1	PALARKNSPGNGSAL	-0.0972	1.295
A0A0G2K490	Tnik	S	764	2	RTRVRANSKSEGSPV	0.0626	0.4119
A0A0G2K490	Tnik	S	766	2	RVRANSKSEGSPVLP		0.4305
A0A0G2K490	Tnik	S	769	1	ANSKSEGSPVLPHEP	0.0054	0.3869
A0A0G2K490	Tnik	S	769	2	ANSKSEGSPVLPHEP	0.0599	0.3958
A0A0G2K490	Tnik	S	777	2	PVLPHEPSKVKPEES	0.056	0.3895
D3ZF26	Tnks1bp1	S	1125	1	RVSGAGLSPSRKSGR		0.382
D3ZF26	Tnks1bp1	S	1422	1	PSRCLARSPPSGSQS	-0.156	0.4485
A0A0G2K6R0	Tnrc6b	S	609	1	GSEVGGQSTGSNHKA	-0.0764	0.5212
Q75Q39	Tomm70	T	88	1	KRNSERKTPEGRASP	0.1018	-0.396
B3DMA0	Tp53i11	S	14	1	PPLMKKHSQTDLVSR	0.3236	0.3123
A0A0G2K2D6	Tppp	S	191	1	DTSKFTGSHKERFDQ	1.0396	-0.4102
Q5PPN5	Tppp3	S	134	1	DTSKYTGSHKERFDE		-0.4649
A0A0G2K2H9	Trerf1	S	497	1	DGRAQPGSPESSGQT		0.5101
F1M0Z1	Trio	S	2433	1	LGSTSGTSQDGNTKD	0.8539	0.36
F1LP64	Trip12	S	1049	1	GPRRPKYSPPRDDDK	0.0598	0.3367
F1LP64	Trip12	S	1069	1	KSPTTTQSPKSSFLA	0.2596	0.9591
Q9WUD2	Trpv2	S	82	1	FDRDRLFSVVSRGVP		-0.2877
Q3B8N7	Tsc22d4	T	183	2	PGKAKVETPPLSASP		0.3262
Q3B8N7	Tsc22d4	S	189	2	ETPPLSASPPQQRPP		0.336
D3ZAU7	Ttbk1	T	635	2	SETSQPPTPGSPSHS		0.5114
D3ZAU7	Ttbk1	S	638	1	SQPPTPGSPSHSPLH	0.0454	0.3348
D3ZAU7	Ttbk1	S	1033	1	TKKGTIISPSRHAMP		0.5022
D3ZAU7	Ttbk1	S	1246	1	QSLSRKESSSPSHQA		0.6882
A0A0G2JYZ1	Ttbk2	S	1148	1	SPVVPRRSPSASPRS	-0.051	0.5099
A0A0G2JXJ6	Ttc7b	S	419	1	ALSEVASSLQSSAPK	0.2169	-0.3689
D4ACG4	Ttll7	S	441	1	LQVRKQISQEEHENR	0.1512	0.2649
O88808	Tub	S	209	1	EDENSSSSSQLNSNT		0.3518

Q5XIF6	Tuba4a	T	223	1	NLDIERPTYTNLNRL		-0.2965
Q5XIF6	Tuba4a	Y	224	1	LDIERPTYTNLNRLI		-0.3993
P69897	Tubb5	S	168	2	DRIMNTFSVVPSPKV		-0.4233
P69897	Tubb5	S	172	2	NTFSVVPSPKVSDTV		-0.4233
Q4QQV0	Tubb6	S	172	1	NTFSVMPSPKVSDTV		-0.36
A0A0G2JYC6	Ubap2l	S	467	1	STSAPQMSPGSSDNQ	-0.103	0.9797
A0A0G2JYC6	Ubap2l	S	493	1	KQQKKKTSLTSKIPA		1.0771
A0A0G2JYC6	Ubap2l	S	608	1	RYPSSISSSPQKDLT		1.4308
A0A0G2JYC6	Ubap2l	S	609	1	YPSSISSSPQKDLTQ	0.0451	1.2136
Q5U203	Ube2f	S	26	1	ASASTSDSTRRVSVR		-0.3773
A0A096MJH0	Ube2j1	S	25	1	APKNTSMSPRQRRAQ		0.2901
D3ZNQ6	Ube2m	T	20	1	EEESAGGTKGSSKKA		-0.452
D3ZNQ6	Ube2m	S	23	1	SAGGTKGSSKKASAA		-0.5817
D3ZXV0	Ube2ql1	S	66	1	PGGSGDASPGPGKGK	-0.0595	0.4639
Q9ES53	Ufd1	S	231	1	GFRAFSGSGNRLDGK		0.5986
D3ZMR2	Uhrf1bp1	S	442	1	GKSPLDKSPTQGRQA		-0.2997
M0R8V0	Uhrf1bp1l	S	21	1	SRFTKNLSPDKINLS		-0.4473
D3ZT03	Upf2	S	37	1	PVSSKEKSKDDLKIT		-0.2677
D4ABC7	Uprt	S	25	1	VNSTSSPSPERLLAE	0.0366	0.4071
A0A0G2K8Q8	Uqcr10	S	3	1	_____MASPTVTSRL		-0.28
Q68FY0	Uqcrc1	S	137	1	AYLIKALSKDLPKVV		-0.3509
P20788	Uqcrfs1	S	99	1	RRAEVLDSTKSSKES		-0.2758
Q5U2N2	Usp14	S	393	1	PNANDKNSPPKEIKY	0.1018	-0.2776
D3ZLQ8	Usp20	S	409	2	GHTKLSSSPPRASPV	-0.1821	0.3324
D3ZLQ8	Usp20	S	414	2	SSSPPRASPVRMGPS		0.3324
A0A0G2K2V3	Usp31	S	1040	1	TSTSKPSSPRVNQAR		0.6219
D3ZL57	Usp6nl	S	701	1	RGYGSSGSPKSGKFI	0.0823	0.4119
P63045	Vamp2	S	75	1	DALQAGASQFETSAA	0.3676	-0.3335
Q8CF97	Vcpip1	S	997	1	TTRSRESSPSHGLLK	0.1288	0.9072
Q9Z2L0	Vdac1	S	104	1	LTFDSSFSPNTGKKN	0.2171	-0.4889
P81155	Vdac2	S	252	1	ISAKVNNSSLIGVGY		-0.3346
Q793F9	Vps4a	S	97	1	SEGKGSDSDSEGDNP	0.0858	-0.2931
F1LSG8	Vps50	S	494	1	KFLEQSRSPSVSPSK	0.0656	-0.272
F1LSG8	Vps50	S	561	1	YQDYDSDSDVPEELK		-0.3219
Q80X08	Washc2	S	157	1	LDIKAGNSDSEEEDA		-0.3098
Q80X08	Washc2	S	159	1	IKAGNSDSEEEDANE		-0.3108
Q80X08	Washc2	S	387	1	VSEESPPSPKPGKKI	-0.1085	0.4089
A0A0G2K9M4	Wdfy3	S	3345	1	ARAHPQGSHSHPNPT	-0.0577	0.4726
D3Z9L5	Wdr11	S	1216	1	DLLNELGSPKEEATE	0.2733	-0.3862
A0A0G2KAW5	Wdr48	S	590	1	YLQPHASSGAKTLKK		-0.3924
A0A0G2K1X3	Wdr60	S	63	1	LKAAQSGSPKEEKKL		0.497
E9PT53	Wfs1	S	32	1	ARLNATTSLEQDKIE	0.7501	0.3472
Q810W9	Whrn	S	698	1	GPFPRVQSPPHLKSP	0.033	0.6167
D3ZMJ7	Wnk2	S	1677	1	RGVRDSGSPHKRPGQ	-0.5206	0.4881

D3ZMJ7	Wnk2	S	1677	2	RGVRDSGSPHKRPGQ		0.7641
Q8CG07	Wrnip1	S	153	1	AAAAGSASPRSWDET		0.461
F7EYF1	Wwp2	S	100	1	ATATGEQSPGARNRH		0.5267
Q5GH56	Xkr7	S	154	1	AFRTKEGSPELVPRP	0.2582	-0.2963
D4ABN8	Xrn1	S	1331	1	KLLKRNESPGTSEAQ		0.4878
P62961	Ybx1	S	163	1	YQQNYQNSESGEKNE		0.9245
P62961	Ybx1	S	172	1	SGEKNEGSESAPEGQ		0.9007
P62961	Ybx1	S	174	1	EKNEGSESAPEGQAQ		0.6687
P62260	Ywhae	S	46	1	VEERNLLSVAYKNVI		-0.4141
P61983	Ywhag	S	71	1	SSIEQKTSADGNEKK	-0.0366	-0.2946
P63102	Ywhaz	S	63	1	RSSWRVVSSIEQKTE		-0.4757
Q5S3S9	Zbtb16	S	302	2	LHYGREESGEQLSPP		-0.2652
Q5S3S9	Zbtb16	S	307	2	EESGEQLSPPVEAGQ		-0.2652
A0A0G2K782	Zc2hc1a	S	222	1	GNKPQTLSPSHRALA		0.2855
Q2THW7	Zdhhc5	S	372	1	AAMPHSSSAKLSRGD	-0.1931	0.2845
Q2THW7	Zdhhc5	S	380	1	AKLSRGDSLKEPTSI	0.3274	0.3116
Q2THW7	Zdhhc5	S	694	1	PGQPPLSSPTRGGVK	-0.1021	0.4341
Q2THW6	Zdhhc8	S	335	1	LKTPRPGSAESALSV		0.3482
Q2THW6	Zdhhc8	S	672	1	PARQGLPSPPGTPRS	-0.0516	0.5167
Q2THW6	Zdhhc8	S	679	1	SPPGTPRSPSYSGSK	0.0234	0.8915
D3ZJG8	Zfp592	S	1087	1	VKHAGGHSPQVNHLK		0.9861
D4A069	Zmym4	S	121	1	RRASHHESDNENEIQ		0.2959
Q5PQS2	Znf365	S	370	1	AIHEQAESPREFFRP		0.6991
Q7TM96	Znf622	S	143	1	IKAQPSTSPKKAPFM	0.3419	1.8787
O35986	Zranb2	S	290	1	RDRKRSRSRPSSPAV		0.5467
Q5RK33	Zrsr1	S	418	1	RGREEGSSPGPQSQS	-0.0298	1.2219
A0A0G2JW01		S	51	1	PGSSIPGSPGHTIYA		0.6732
A0A0G2JW01		S	51	2	PGSSIPGSPGHTIYA	-0.3508	0.2072
A0A0G2JW01		S	106	1	EDKQDRQSLGESPRT	0.0642	0.8125
A0A0G2JW01		S	110	1	DRQSLGESPRTLSPT	0.1727	1.424
A0A0G2JW01		S	142	1	TSQGSINSPVYSRHS	0.1219	1.243
A0A0G2JW01		S	289	1	LLASRYDSPLHSASH	0.1056	0.6009
A0A0G2JW01		S	293	1	RYDSPLHSASHAPSS		0.4622
A0A0G2JZ27		S	416	1	QLSSPNHSPSQSPNQ	-0.0629	0.374
A0A0G2JZ27		S	424	1	PSQSPNQSPRIKKRP	0.0211	0.3824
D3ZJK8		T	5	2	___GYEKTDDVSEKT	0.0279	-0.4103
D3ZJK8		S	9	1	YEKTDDVSEKTSLAD		-0.6089
D3ZJK8		S	9	2	YEKTDDVSEKTSLAD		-0.3025
D3ZJK8		T	12	1	TDDVSEKTSLADQEE		-0.5936
D3ZJK8		S	13	1	DDVSEKTSLADQEEV	0.3241	-0.6942
D3ZJK8		S	13	2	DDVSEKTSLADQEEV	0.0469	-0.3796
D3ZZH5		S	98	1	RSISIQTSPSLRKHF		0.3588
M0RDY2		S	36	1	GGAERRGSVPANPGA		-0.2736
O08654		S	270	1	EDKMKIHSPSPHKQV	-0.3446	

O08654		S	270	2	EDKMKIHSPSPHKQV		-0.3365
O08654		S	272	2	KMKIHSPSPHKQVPS		-0.3365
Q63003		S	251	1	IPGQQEESPQQEPSS	0.0547	0.4518
Q63003		S	690	1	HGAINAPSAPDASPP	0.0172	0.3693

Table 8.3: Phosphorylation events from clusters 1 and 2 as presented in Figure 4.2. *UP.Accession ~ Uniprot accession; Gene.name ~ official gene symbol; AA ~ modified amino acid; Pos ~ position in the protein sequence; Mult ~ multiplicity of phosphorylation (1 – singly phosphorylated, 2 – doubly phosphorylated, 3 – multiply phosphorylated); Seq.window ~ ±7 amino acids flanking phosphorylated residue; Correlation ~ Pearson correlation of the two kinetics measuremtns; 0s-180s ~ log_2 intensity fold change relatively to the time point 0 s*

UP.Accession	Gene.name	AA	Pos	Mult	Seq.window	Correlation	Cluster	0s	10s	30s	60s	125s	180s
P0C1X8	Aak1	S	653	1	FGVPASKSTQLLHAA	0.8329	1	0	0.3484	0.9029	0.7033	-0.7212	0.7664
D4ABZ3	Aatk	S	1282	1	VPLRAGHSPDSSAPE	0.6379	1	0	-0.1953	0.2320	0.4731	0.0898	0.5942
O35889	Afdn	S	1208	2	AAKITSVSTGNLCTE	0.6867	1	0	0.5877	0.4401	0.6412	0.0359	0.1327
O35889	Afdn	T	1218	2	NLCTEEQTPPPRPEA	0.7205	1	0	0.6180	0.4817	0.6412	0.0359	0.1577
D3ZTF0	Ajm1	S	109	1	SLTTAPASPPVLQRR	0.9139	1	0	0.1952	0.5913	0.6182	-0.2823	0.4416
O08838	Amph	T	260	1	GPLRIAKTPSPPEEA	0.9762	1	0	0.1017	0.9036	0.9678	-1.3263	0.9902
O08838	Amph	S	268	2	PSPPEEASPLPSPTA	0.9653	1	0	0.1794	0.5000	0.5287	-0.2957	0.6518
O08838	Amph	S	272	2	EEASPLPSPTASPNH	0.9344	1	0	0.2170	0.6283	0.6231	-0.4083	0.7693
O08838	Amph	S	285	2	NHTLAPASPAPVRPR	0.9025	1	0	0.1211	0.5420	0.7015	-0.3835	0.7686
O08838	Amph	S	514	2	TELASSESPQAAELE	0.7890	1	0	0.3489	0.6241	0.6383	-0.2141	0.5301
D3ZKP1	Ankrd34b	S	496	1	KMLLRRQSLQTEQIK	0.9942	1	0	0.0252	0.0910	0.1238	-0.0770	0.9197
O35430	Apba1	S	243	1	LHHYDERSDGESDSP	0.8522	1	0	0.1176	0.3247	0.6128	-0.0579	0.5227
A0A0G2K8G0	Apc	S	2486	2	SFESLSPSSRPDSPT	0.9448	1	0	0.3354	0.6024	0.6341	-0.1940	0.4879
Q3S4A4	Arfgap1	T	135	1	SSPAQNWTPPQPKTL	0.8460	1	0	0.4312	0.7125	0.7249	-0.0523	0.6750
F1LXQ7	Arhgap21	S	863	1	PLIRRQLSHDQESVG	0.6667	1	0	-0.2246	-0.0528	0.1372	-0.0456	0.9882
A0A0G2JZC6	Arhgef11	S	1512	2	KSLGGESSGGTTPVG	0.6319	1	0	0.1685	0.3459	0.3854	0.1082	0.6566
A0A0G2JZC6	Arhgef11	T	1516	2	GESSGGTTPVGSFHT	0.6319	1	0	0.1685	0.3459	0.3854	0.1082	0.6566
F1MAF8	Atg2b	S	918	2	PYDEDSGSEEETLQY	0.9513	1	0	0.2575	0.7401	0.4667	-1.1758	0.3843
F1MAF8	Atg2b	T	922	2	DSGSEEETLQYFSAV	0.9524	1	0	0.3110	0.7598	0.4968	-1.1563	0.4156
P11506	Atp2b2	T	1162	2	LEKPESRTSIHNFMA	0.9794	1	0	0.0918	0.4700	0.3464	-0.6172	0.1886
P11506	Atp2b2	S	1163	2	EKPESRTSIHNFMAH	0.9794	1	0	0.0918	0.4700	0.3464	-0.6172	0.1886
Q9ET45	Bnip3	S	60	1	SKSSHCDSPPRSQTP	0.7248	1	0	-0.1064	0.2760	0.7738	-0.0968	0.5544
G3V984	Bsn	S	2783	2	VSRQPPKSPQVLYSP	0.8756	1	0	0.0330	0.7025	0.3758	-0.6481	0.5464

G3V984	Bsn	S	2795	2	YSPVSPLSPHRLLDT	0.9751	1	0	-0.0765	0.4895	0.3099	-0.6269	0.3473
D4A055	Cacnb4	S	443	1	RMRHSNHSTENSPIE	0.7825	1	0	-0.1095	0.0778	0.2981	0.7322	0.4831
F1M3F8	Camk2g	S	445	1	AGMQPQPSLCSSAMR	0.8362	1	0	0.2348	0.6925	0.7774	-0.1144	0.6306
Q8VHK2	Caskin1	S	648	1	PAAAECQSPKMTTFQ	0.6593	1	0	0.0278	0.5852	0.5210	-0.2237	0.3729
Q5FVI4	Cend1	S	89	2	PTVPAAPSSPDTTSE	0.9695	1	0	0.0477	0.9312	0.8392	-1.8572	0.9093
Q99P82	Cldn11	S	198	1	YYSSGSSSPTHAKSA	0.7909	1	0	-0.4443	0.7533	1.1596	-0.3599	1.6203
D4A1C0	Cnnm1	T	454	2	KAPTTRGTPQTPKDD	0.9496	1	0	0.0704	0.7693	0.5749	-1.0438	0.5889
D4A1C0	Cnnm1	T	457	2	TTRGTPQTPKDDPVL	0.9534	1	0	0.0095	0.6651	0.4538	-0.8450	0.4689
P47875	Csrp1	S	192	1	GAGALVHSE_____	0.8257	1	0	0.3405	0.5804	0.6103	-0.1891	0.5209
Q5YLM1	Dagla	S	808	1	GFRSIRGSPSLHAVL	0.8435	1	0	0.0933	0.4079	0.4848	-0.2582	0.6276
Q6AYH5	Dctn2	T	199	1	GGKSTGGTPPDSSLV	0.8685	1	0	0.0491	0.5790	0.3357	-0.6309	0.1984
Q6AYH5	Dctn2	T	199	2	GGKSTGGTPPDSSLV	0.8737	1	0	0.3587	0.7908	0.6528	-0.6387	0.6465
P60905	Dnajc5	S	12	1	RQRSLSTSGESLYHV	0.8097	1	0	0.0532	0.6908	0.7346	-0.2313	0.9672
A0A0G2JY26	Dnajc6	S	679	3	GFGMGSKSAATSPTG	0.6262	1	0	-0.0750	0.1251	0.0491	0.2764	0.6351
A0A0G2JY26	Dnajc6	T	682	3	MGSKSAATSPTGSTH	0.6262	1	0	-0.0750	0.1251	0.0491	0.2764	0.6351
G3V874	Epb41l3	S	91	1	QFEDDKLSQKSSSSK	0.8119	1	0	0.5162	0.6138	0.6170	-0.1935	0.6839
G3V874	Epb41l3	S	91	2	QFEDDKLSQKSSSSK	0.7330	1	0	0.3859	0.6600	0.6247	-0.1743	0.3462
G3V874	Epb41l3	S	91	3	QFEDDKLSQKSSSSK	0.8004	1	0	0.5118	0.7903	0.7710	-0.2875	0.6256
G3V874	Epb41l3	S	94	3	DDKLSQKSSSSKLSR	0.9071	1	0	0.5813	0.8175	0.8445	-0.2528	0.6595
G3V874	Epb41l3	S	95	2	DKLSQKSSSSKLSRS	0.7370	1	0	0.3592	0.6258	0.5918	-0.0771	0.3364
G3V874	Epb41l3	S	95	3	DKLSQKSSSSKLSRS	0.8004	1	0	0.5118	0.7903	0.7710	-0.2875	0.6256
G3V874	Epb41l3	S	96	2	KLSQKSSSSKLSRSP	0.7169	1	0	0.5210	0.6853	0.6537	-0.0302	0.3195
G3V874	Epb41l3	S	96	3	KLSQKSSSSKLSRSP	0.8004	1	0	0.5118	0.7903	0.7710	-0.2875	0.6256
G3V874	Epb41l3	S	97	3	LSQKSSSSKLSRSPL	0.8509	1	0	0.4932	0.7308	0.7345	-0.3609	0.5650
A0A0G2JZX5	Iqsec2	S	207	1	YFEGKPASLDEGAMA	0.7103	1	0	0.4222	0.6133	0.5836	0.1486	0.6285
F1M9N8	LOC100361087	S	183	1	DGQEDGESERNSDGS	0.6921	1	0	0.5544	1.0945	1.3906	0.5379	1.6896
A0A0G2KA27	Madd	S	861	1	RNHSTSFSLSNLTLP	0.6844	1	0	-0.0435	0.3984	0.5114	0.2270	0.7258
G3V9B3	Mag	S	545	2	RKKNVTESPSFSAGD	0.9004	1	0	0.1837	0.6037	0.2520	-0.3694	0.2542
P34926	Map1a	S	1985	2	SAEKETSSPASPQNL	0.9481	1	0	0.2245	0.8120	0.7608	-0.8020	0.6691

P34926	Map1a	S	1988	1	KETSSPASPQNLQSD	0.8931	1	0	0.3460	0.7460	0.6406	-0.4142	0.5087
P34926	Map1a	S	1988	2	KETSSPASPQNLQSD	0.9471	1	0	0.2412	0.8176	0.7474	-0.8023	0.6915
Q5XII9	Mtfr1l	S	235	1	ISLSKASSFADMMGI	0.7477	1	0	0.3995	0.3029	0.4116	0.7026	0.6264
A0A0G2JXP3	Nedd4l	S	434	2	IRRPRSLSSPTVTLS	0.8255	1	0	0.2138	0.7050	0.4790	-0.4432	0.1724
A0A0G2JXP3	Nedd4l	S	450	2	PLEGAKDSPIRRAVK	0.8255	1	0	0.2138	0.7050	0.4790	-0.4432	0.1724
A1L1I3	Numbl	T	265	2	QPGHVSPTPATTSPG	0.8425	1	0	0.2444	0.2789	0.3519	-0.0086	0.5980
A0A0G2JWR2	Pacsin1	S	326	1	KAEGAALSNATGAVE	0.9539	1	0	0.3398	0.6444	0.4712	-0.0512	0.3711
Q68HB8	Pcdh7	S	1011	1	TVQLHPQSPTAGKKH	0.9322	1	0	0.2198	0.7611	0.6106	-1.2637	0.3971
Q9JKS6	Pclo	S	1659	2	TDSPEDRSRGEGSSS	0.7523	1	0	0.2715	0.6246	0.4655	-0.1147	0.4500
Q01062	Pde2a	S	197	1	PEAVQNTSADPSEDQ	0.8010	1	0	0.2055	0.2712	0.4909	-0.1150	0.5920
P54645	Prkaa1	S	508	1	RSCQRSDSDAEAQGK	0.9979	1	0	0.6305	-0.6284	0.8890	0.7480	0.8301
Q64548	Rtn1	S	68	2	LCSGPARSPPVAMET	0.7357	1	0	0.1837	0.3060	0.1831	0.3386	0.8087
Q9JK11	Rtn4	S	169	1	AAPKRRGSGSVDETL	0.8980	1	0	0.1933	0.6628	0.6875	-0.5328	0.5176
Q9JK11	Rtn4	S	171	1	PKRRGSGSVDETLFA	0.9209	1	0	0.2252	0.8271	0.8122	-0.6394	0.2475
P04774	Scn1a	T	465	2	AQQAAAATASEHSRE	0.7830	1	0	0.4654	0.6093	0.5844	-0.0548	0.7416
P04774	Scn1a	S	467	2	QAAAATASEHSREPS	0.7830	1	0	0.4654	0.6093	0.5844	-0.0548	0.7416
M0RD40	Sik3	S	493	1	GPLGRRASDGGANIQ	0.9804	1	0	-0.0028	0.8718	0.7447	-1.1765	0.7405
A0A0H2UHB7	Slc4a4	S	1060	2	DKIPFLESLGLPSPP	0.9048	1	0	0.3740	0.6947	0.6793	-0.3160	0.6471
A0A0H2UHB7	Slc4a4	S	1069	2	GLPSPPRSPVKVVPQ	0.9050	1	0	0.3636	0.6770	0.6437	-0.3341	0.6403
D4A3T0	Sos1	S	1153	1	ESAPAESSPSKIMSK	0.8570	1	0	0.4358	0.6501	0.6250	-0.0593	0.4472
Q9QXY2	Srcin1	S	374	2	YAGGRPPSYAGSPVH	0.8176	1	0	0.3021	0.7503	0.7556	-0.2259	0.7256
F1M4Q5	Ssh2	S	1223	1	ACRIPHSSSSENIRD	0.6581	1	0	-0.0201	0.1791	0.2180	0.0266	0.5986
P09951	Syn1	S	500	1	GLGPPAGSPLPQRLP	0.8093	1	0	0.5152	0.8583	0.8930	0.0075	0.9500
Q63537	Syn2	S	546	1	PQLNKSQSLTNAFSF	0.6169	1	0	0.4599	0.7096	0.5504	-0.0889	0.5609
Q62807	Syt17	S	118	2	SLDSRRPSSPLIDIK	0.9340	1	0	0.4567	0.7012	0.7921	0.2996	0.5683
Q62807	Syt17	S	119	2	LDSRRPSSPLIDIKP	0.9340	1	0	0.4567	0.7012	0.7921	0.2996	0.5683
A0A0G2K9J0	Tanc2	S	84	2	IMEGVSRSLPSSPLL	0.9406	1	0	0.0729	0.2961	0.4508	-0.0985	0.5962
A0A0G2K9J0	Tanc2	S	88	2	VSRSLPSSPLLTHQS	0.9406	1	0	0.0729	0.2961	0.4508	-0.0985	0.5962
D3ZF26	Tnks1bp1	S	490	2	LGVCRLDSPPPSPIT	0.7181	1	0	0.3871	0.4443	0.6289	0.2932	0.5518

D3ZF26	Tnks1bp1	S	494	2	RLDSPPPSPITEASE	0.7181	1	0	0.3871	0.4443	0.6289	0.2932	0.5518
E9PU02	Trappc9	S	944	1	NFESVPESPGEKGHF	0.8475	1	0	0.6612	0.6897	0.6786	-0.0460	0.6216
D4A383	Ttyh3	S	437	1	GPRQAHDSLYRVHMP	0.6322	1	0	-0.1028	0.3446	0.8376	0.3906	1.0051
A0A0G2K000	Zc3h12c	S	511	1	RGAPKRQSDPSIRTH	0.9450	1	0	-0.0002	0.0512	0.0509	-0.0008	0.6560
B5DF11	Zfand5	S	58	1	GTASGSNSPTSDSAS	0.8544	1	0	-0.0624	0.3242	0.8718	0.0192	1.2072
Q6DTM3	Ahi1	S	26	1	KSQPADDSEDSREKA	0.9880	2	0	0.5789	0.7829	-0.5467	0.0075	-0.5458
Q5QD51	Akap12	S	273	2	TKSPESPSSPVSSET	0.6731	2	0	-0.0612	-0.0910	-0.2931	-0.0314	-0.6088
A0A0G2K8G0	Apc	S	2551	2	HDIARSHSESPSRLP	0.7754	2	0	-0.5053	-0.2958	-0.4793	-0.3209	-0.7193
D3ZGL1	Arhgap25	S	408	2	ASSPDATSPTGPQPG	0.6721	2	0	-0.1057	-0.4202	-0.5942	-0.1234	-0.6589
D4A8B3	Atp2b2	S	1175	1	QDVASLSSPSRVSLS	0.6442	2	0	-0.5265	-0.5766	-0.6347	-0.3806	-1.2591
D3ZML2	Brsk2	S	388	2	RKSMEVLSVTDGGSP	0.6532	2	0	-0.6048	-0.3536	-0.3086	0.0529	-0.2431
P11275	Camk2a	S	333	3	GVKESSESTNTTIED	0.7545	2	0	-0.0381	-0.2130	-0.3703	-0.1333	-0.6004
P11275	Camk2a	T	334	3	VKESSESTNTTIEDE	0.7703	2	0	-0.0488	-0.2102	-0.4497	-0.1588	-0.6697
F1LUE2	Camk2b	S	423	1	LSLVRRGSGAPEAEG	0.7261	2	0	-0.1776	-1.1354	-0.6306	-1.4132	-0.3672
A0A0G2JUY5	Ccdc120	S	283	1	NSVASPTSPTRSLPR	0.6819	2	0	-0.1160	-0.3916	-0.5167	-0.1476	-0.6544
F1LNR0	Clasp1	S	673	2	SQSQRSRSANPAGAG	0.7601	2	0	0.0332	0.0632	-0.0228	0.0630	-0.7764
F1LNR0	Clasp1	S	681	2	ANPAGAGSRSSSPGK	0.7283	2	0	0.0447	0.0021	-0.0103	0.0461	-0.7447
P08081	Clta	S	105	1	SEVDRLQSEPESIRK	0.6899	2	0	-0.2107	-0.3747	-0.7452	0.0473	-0.6814
Q62950	Crmp1	S	521	2	APAPSAKSSPSKHQP	0.6237	2	0	-0.0408	-0.2340	-0.7457	0.1200	-1.1793
Q62950	Crmp1	S	522	2	PAPSAKSSPSKHQPP	0.6179	2	0	-0.0691	-0.2932	-0.7923	0.1376	-1.2614
Q66H62	Cyld	S	341	1	PKVTGSTSDPGSRNR	0.8670	2	0	-0.0716	-0.1060	-0.0837	-0.1382	-0.5869
Q5MPA9	Dclk2	S	359	1	SSSSSPTSPGSFRGL	0.9180	2	0	-0.2518	-0.6886	-0.7391	0.1150	-0.5461
A0A0G2JUI3	Dlgap2	S	558	1	ISVTAQSSTESTQDA	0.6783	2	0	0.1195	-0.0603	-0.3954	-0.0289	-0.6185
G3V7T8	Dlgap3	S	428	1	RFASRRSSSVDTARI	0.6963	2	0	-0.1658	-0.0884	-0.0646	-0.0102	-0.6414
G3V7T8	Dlgap3	S	429	1	FASRRSSSVDTARIN	0.6281	2	0	-0.0946	0.0059	-0.0402	-0.0725	-0.6452
B2GUY4	Dmtn	S	269	1	PIRRKTRSLPDRTPF	0.9480	2	0	-0.1679	-0.1061	-0.2615	-0.0495	-0.6855
F1M3D2	Dmwd	T	453	2	PPLARTRTLPGTPGA	0.6973	2	0	-0.2917	-0.6012	-0.7272	0.1763	-0.5148
F1M3D2	Dmwd	T	461	2	LPGTPGATPPASGGS	0.7015	2	0	-0.2685	-0.5467	-0.6196	0.1561	-0.4719
P47942	Dpysl2	S	522	3	PASSAKTSPAKQQAP	0.7574	2	0	-0.4904	-0.3889	-0.6103	-0.2549	-0.5954

F1M470	Eif4e2	S	2	1	_____MSLKDDDSG	0.7030	2	0	-0.3556	-0.2974	-0.7585	-0.1927	-0.1768
G3V874	Epb41l3	S	743	1	HVMNVHASGDASHTA	0.6517	2	0	-0.0977	-0.3541	-0.5894	-0.0338	-0.3871
M0R5H1	Etl4	S	1914	1	SSSSSPPSPASPTSL	0.6574	2	0	0.0445	-0.1740	-0.2675	-0.2421	-0.6158
P19627	Gnaz	S	25	2	RIDRHLRSESQRQRR	0.6419	2	0	-0.1650	-0.3595	-0.3858	0.0407	-0.6579
P19627	Gnaz	S	27	2	DRHLRSESQRQRREI	0.6419	2	0	-0.1650	-0.3595	-0.3858	0.0407	-0.6579
A0A0A0MY13	Gpr158	S	946	1	RETNRKYSNSDNTET	0.8179	2	0	-0.5831	-1.0844	-1.4053	-0.0650	-0.9936
D3ZEI4	Hepacam	S	378	2	ATGRTHTSPPRAPSS	0.7531	2	0	-0.2588	-0.3967	-0.6362	-0.2011	-1.1869
D3ZEI4	Hepacam	S	385	2	SPPRAPSSPGRSRSS	0.7244	2	0	-0.2753	-0.3881	-0.6857	-0.1720	-1.2058
A0A0G2K427	Ivns1abp	S	322	2	IFLHGRNSPQSSPTS	0.7603	2	0	-0.2699	-0.6448	-0.8064	0.1779	-0.6204
A0A0G2K427	Ivns1abp	S	325	2	HGRNSPQSSPTSTPK	0.7549	2	0	-0.2768	-0.6374	-0.8121	0.1781	-0.6305
P63142	Kcna2	S	447	2	SSPDLKKSRSASTIS	0.7870	2	0	-0.1857	-0.2570	-0.3712	0.1342	-0.5894
B2GV74	Klc2	S	508	1	GRGDRRGSRDVAGGA	0.6632	2	0	-0.3152	-0.1327	-0.2805	-0.0934	-1.0479
M0R439	Klhdc7a	S	344	1	GGTLQVASPQPVPSP	0.6987	2	0	-0.7683	0.2002	-0.1303	0.3033	0.1190
P34926	Map1a	S	898	2	GTISPTSSLEEDKGF	0.8050	2	0	-0.0135	-0.2187	-0.5093	-0.0853	-0.8699
Q3B8Q0	Mapre2	S	222	2	STPSRPSSAKRASSS	0.7942	2	0	0.0804	-0.1081	-0.2622	0.0605	-0.5907
D4A1Q2	Mapt	S	597	2	DFKDRVQSKIGSLDN	0.7760	2	0	-0.3588	-0.3463	-0.3323	0.0230	-0.6621
D4A1Q2	Mapt	S	601	2	RVQSKIGSLDNITHV	0.7760	2	0	-0.3588	-0.3463	-0.3323	0.0230	-0.6621
O55164	Mpdz	S	1802	2	FHSERRPSQSSQVSE	0.7465	2	0	-0.7232	-0.6492	-0.9424	-0.0879	-1.3628
O55164	Mpdz	S	1808	2	PSQSSQVSESSLSSF	0.7111	2	0	-0.3463	-0.2345	-0.4552	0.0880	-0.7732
Q78PB6	Ndel1	S	215	2	SAVQASLSLPATPVG	0.6106	2	0	-0.1845	-0.3153	-0.6464	-0.2417	-0.7313
Q78PB6	Ndel1	T	219	2	ASLSLPATPVGKGTE	0.6106	2	0	-0.1845	-0.3153	-0.6464	-0.2417	-0.7313
Q9Z2L9	Ndrg4	S	304	2	LSGGAVPSASMTRLA	0.8339	2	0	-0.5683	-0.9128	-0.8568	-0.0231	-0.6934
Q9JKS6	Pclo	S	1493	2	DEYKQEDSQGSGEEE	0.7125	2	0	-0.1394	-0.2907	-0.5229	-0.0529	-0.6850
Q9JKS6	Pclo	S	1496	1	KQEDSQGSGEEEDFI	0.9376	2	0	-0.0697	-0.3094	-0.6392	0.0073	-0.7048
Q8VIE2	Pde7b	S	439	1	NQHRRRGSGQDPAGT	0.9585	2	0	-0.2309	-0.9516	-0.9231	0.2477	-0.7538
Q5HZV9	Ppp1r7	S	44	1	GGIVADLSQQSLKDG	0.8220	2	0	-0.3390	-0.8632	-0.9801	0.0288	-0.8236
D3ZFB6	Prrt2	S	242	3	AHGGHPGSPRGSLSR	0.8124	2	0	-0.4686	-0.6362	-0.7668	0.2201	-0.5856
D3ZFB6	Prrt2	S	246	3	HPGSPRGSLSRHPSS	0.7303	2	0	-0.3685	-0.5793	-0.6996	0.1901	-0.4393
D3ZFB6	Prrt2	S	248	3	GSPRGSLSRHPSSQL	0.7303	2	0	-0.3685	-0.5793	-0.6996	0.1901	-0.4393

D3ZWQ0	Prrt3	S	922	2	PWRHGLSSVDSLPLD	0.8150	2	0	-0.2734	-0.6660	-0.2904	0.1071	-0.4665
D3ZWQ0	Prrt3	S	925	2	HGLSSVDSLPLDELP	0.8150	2	0	-0.2734	-0.6660	-0.2904	0.1071	-0.4665
B2RYS6	Prtfdc1	S	4	1	____MAGSSEKAPDS	0.6417	2	0	-0.2360	-0.3810	-0.4887	0.0070	-0.8161
M0RC99	Rab5a	S	193	1	PQNPGANSARGRGVD	0.6130	2	0	-0.0158	-0.2427	-0.5223	-0.2623	-0.6421
D3ZX42	Rabgap1	S	42	1	TPSTNNGSDDEKTGL	0.6013	2	0	-0.3125	-0.4930	-0.8848	-0.1710	-0.7855
Q9JIR3	Rims3	S	104	1	SRVTRQGSRESTDGS	0.8703	2	0	-0.1770	-0.1635	-0.4750	-0.0145	-0.6315
A0A0G2K8W9	Sptbn1	S	2154	2	GAAEQRTSSKESSPV	0.7640	2	0	-0.0760	-0.3884	-0.5853	-0.0334	-0.7279
F1M5M9	Srgap3	S	868	2	AAIPRRRSGGDTHSP	0.9202	2	0	-0.3753	-0.2930	-0.5677	-0.1765	-0.9100
F1M5M9	Srgap3	S	874	2	RSGGDTHSPPRGLGP	0.9253	2	0	-0.4110	-0.2464	-0.4878	-0.2985	-2.1900
P09951	Syn1	S	549	2	PAARPPASPSPQRQA	0.8239	2	0	-0.0428	-0.2003	-0.4153	-0.0721	-0.7641
P09951	Syn1	S	551	1	ARPPASPSPQRQAGP	0.6980	2	0	-0.0511	-0.1973	-0.4142	-0.1319	-0.7201
P09951	Syn1	S	551	2	ARPPASPSPQRQAGP	0.8239	2	0	-0.0428	-0.2003	-0.4153	-0.0721	-0.7641
Q75Q39	Tomm70	S	84	2	ASGLKRNSERKTPEG	0.6673	2	0	0.0415	-0.2841	-0.5373	-0.0863	-0.6836
Q75Q39	Tomm70	T	88	1	KRNSERKTPEGRASP	0.7021	2	0	-0.3184	-0.5587	-0.8622	-0.2392	-1.4362
Q75Q39	Tomm70	T	88	2	KRNSERKTPEGRASP	0.6636	2	0	0.0350	-0.2850	-0.5355	-0.0859	-0.6760
Q6PCT3	Tpd52l2	S	175	2	SMPVMRNSATFKSFE	0.8708	2	0	-0.1138	-0.2171	-0.3164	-0.2647	-0.6551
D3ZAU7	Ttbk1	S	433	2	RGVGVPSSPVRAPPD	0.6075	2	0	-0.2771	-0.3465	-0.5729	-0.0980	-0.6538
Q499N6	Ubxn1	S	188	2	GTVGSRSSPPATDPG	0.8777	2	0	-0.5727	-0.9535	-1.0804	-0.1067	-0.9013
Q499N6	Ubxn1	S	200	2	DPGPVPSSPRQEPPT	0.8635	2	0	-0.5093	-0.8739	-0.9821	-0.0902	-0.8259
A0A0G2JX77	Wdr44	S	567	2	YNTEGRVSPSPSQES	0.7470	2	0	-0.1132	-0.1857	-0.2768	0.0670	-0.5854
P62961	Ybx1	S	172	1	SGEKNEGSESAPEGQ	0.7897	2	0	-0.1406	-0.2921	-0.7509	-0.3135	-1.0044
D3ZTR5	Zbed5	S	46	1	AAPSAVGSPAAAPRQ	0.7487	2	0	0.0040	-0.5867	-0.3639	0.1331	-0.4413
F1LWK7		S	412	2	PGSSIPGSPGHTIYA	0.6644	2	0	-0.2834	-0.2378	-0.6225	-0.0130	-0.7902